Biogeochemistry of Selenium in different aquatic sytems (Lakes and estuaries)

Andréa Romero Rama

THÈSE

UNIVERSITE DE PAY ET DES PAYS DE L'ADOUR

École doctorale des sciences exactes et de leurs applications

Présentée et soutenue le 11 décembre 2020

par **Andrea ROMERO RAMA**

pour obtenir le grade de docteur

de l'Université de Pau et des Pays de l'Adour

Spécialité : Chimie Analytique et Environnement

BIOGÉOCHIMIE DU SÉLÉNIUM DANS DIFFÉRENTS MILIEUX AQUATIQUES (LACS ET ESTUAIRE)

Biogeochemistry of Selenium in different aquatic sytems (Lakes and estuaries)

DIRECTEUR DE THÈSE :

David Amouroux

ENCADRANT DE THÈSE :

Maïté Bueno

RAPPORTEURS :

Oleg Pokrovski / Directeur de recherche CNRS – Géosciences Environnement Toulouse

Corinne Casiot-Marouani / Directeur de recherche CNRS – HydroSciences Montpellier

EXAMINATEURS :

Yaron Be'eri-Shlevin / Chercheur – Israel Oceanographic and Limnological Research Institut

Lenny Winkel / Professeur – ETH Zurich, EAWAG

Florence Pannier / Professeur IPREM, UPPA

UNIVERSITÉ DE PAU ET DES PAYS DE L'ADOUR

Remerciements

Je tiens tout d'abord à remercier tous ceux qui ont rendu possible la réalisation de cette thèse et la participation des membres du jury pour l'évaluation des travaux.

Je remercie à l'École Doctoral (ED 211) de l'Université de Pau and Pays de l'Adour ainsi que à Institut des Sciences Analytiques et de Physico-Chimie pour l'Environnement et les Matériaux (IPREM) pour le co-financement de ce projet de thèse.

J'adresse en suite mes remerciements à mon directeur de thèse, David Amouroux et à Maïte Bueno en tant qu'encadrante de ce project. Merci de m'avoir donnée l'opportunité de réaliser ce projet et de m'acueilleur dans le group de recherche. Merci pour votres conseilles, pour les discussions et pour le temps que vous avez dédié pour améliorer mon travail et me guider dans le cours de ces quatre années. Et surtout, merci pour la patience !!

J'aimerai bien remercier aussi à Emmanuel Tessier pour le temps passée au terrain et pour l'apprentissage qui m'a apportée et pour l'aide dans la réalization des analyses des composés volatiles. También quiero agraderce a ti Javi por toda la ayuda y los consejos que me has dado sobre el icp y por las charlas y los momentos pasados en el laboratorio.

En suite, je voudrais remercier l'ensemble du group de chimie analytique ce soit pour l'aide au laboratoire et les moments passées ensemble. Je remercie en especial à Bastien et Sandrine pour les bons moments passés au terrain et au labo ainsi que pour les cafés et discussions qui on était un soutien important pendant ce periode. De plus, j'aimerai bien remercier à Marine qui c'était la personne qui m'a plus integré dans le group à mon arrivée, merci pour l'effort de comunication faite au début, j'ai apris beaucoup de ton courage et ton optimisme. Je ne peux pas m'oublié non plus des autres doctorant/es avec lesquel j'ai passée de très bons moments, en particulier à Manue, Paulina, Mathieu, Dimitri, Maxime, Javi, Robin, Jéremy, Larissa, etc…, qui on été fondamentaux pour supporter les nombreuses heures de travail. Pero sobretodo gracias a Nagore por la ayuda que me brindaste al llegar al laboratorio, a Marina por las horas que hemos pasado juntas y a Mari Carmen por tantos buenos momentos.

No me puedo olvidar tampoco de todas las personas que he conocido en Pau, incluyendo a Sol, Úrsula, Oriol, Javi Toledo, Gonzalo, Laura, Laia, Jesús, Iris, Chiti, Diego, Sara, Aralar, Izar y un

largo etcétera que no se acabaría nunca. Gracias por haber sido un pilar fundamental y las personas que habéis hecho de mi estancia en Pau uno de los mejores períodos de mi vida.

Y hablando de buenos momentos, quiero agradecer al equipo de Gaby por el enorme cariño que recibí de todos vosotros en Chile. No podía haber ido a una ciudad más bonita ni a un grupo mejor ensamblado. Gracias.

También quiero agradecer al grupo de Alberto en Bilbao por los buenos momentos pasados en los Pirineos, algunos días fueron duros pero hubieron momentos maravillosos. Gracias en especial a Alberto, Luís Ángel, Olaya, Leire, Kepa y a Mireia, quién en un refugio perdido en medio de la montaá encontró una velita para que la pudiese soplar en mi cumpleaños ☺.

No em puc oblidar de les les noies del Nucli, perque passen els anys i la vida ens canvia pero l'amistat perdura tot i que estem desperdigades per mig món. Bueno y los chicos de la pantalla, ojalá pasemos tan buenos ratos en el futuro como hemos pasado hasta ahora.

De la misma manera quiero agradecer a mi familia el apoyo recibido durante este período. A mi abuelo por su humor hasta en los peores momentos, a mi madre por los consejos que no siempre escucho y a mi padre por acogerme durante este último período, cajas de mudanza incluidas. Y a mi hermano porque aunque me escriba poco sé que se preocupa por mi. También a mis tíos y primos, os quiero un montón. No me olvido de mi familia política, en especial Miriam, Coni, Amalia, el Bolita, Jacho y Marlon que os habéis convertido en personas muy importantes de un tiempo a esta parte.

Hablando de familia quisiera incluir a Baldric y Eva, y por tanto también al Abadiano, sois personas que quiero tener en mi vida para siempre.

Por último pero no por ello menos importante a Thamy, para ti no tengo palabras, me has dado todo el apoyo del mundo en este período y además has sido la persona más paciente del mundo conmigo, sin ti esto no hubiese sido posible. T'estimo.

Résumé

Le sélénium (Se) existe dans les systèmes aquatiques sous différents états d'oxydation (VI, IV, 0, -II) et sous formes inorganiques et organiques. Le sélénate et le sélénite sont généralement mesurés et quantifiés dans des eaux naturelles, mais ne représentent généralement pas la teneur totale en Se, du fait de la co-existence de formes réduites de Se non identifiés. En raison de son rôle essentiel pour les organismes vivants, la caractérisation de ses composés est nécessaire pour mieux comprendre les transformations biotiques et abiotiques de Se et son devenir dans les systèmes aquatiques. Le sélénium étant présent à l'état de traces dans la plupart des milieux aquatiques, le développement de méthodes analytiques sensibles est nécessaire pour atteindre cet objectif. Les travaux dédiés à l'étude du cycle de Se dans les milieux aquatiques non pollués considérant l'ensemble de ses formes dissoutes (volatiles et non-volatiles) sont encore peu nombreuses justifiant davantage de recherches dans cette thématique.

Dans ce travail, l'optimisation d'une séparation chromatographique à l'aide d'une phase stationnaire en mode mixte combinant phase inverse et échange anionique a permis la séparation simultanée de six composés inorganiques et organiques du sélenium. La méthode développée ainsi qu'une méthode sensible pour la détermination des composés volatils de Se, ont été appliquées en parallèle pour la première fois à l'étude du cycle de Se dans différents systèmes aquatiques en fonction des variations biogéochimiques et saisonnières. Dans un lac eutrophe stratifié (lac Kinneret, Israël), l'existence de Se réduit et plus probablement de composés organosélénié produits par le phytoplancton et précurseurs de la volatilisation du Se a été mise en évidence. En conditions d'anaérobie, une diminution de la teneur en Se dissous suggère une réduction des espèces oxydées de Se vers ses formes réduites et son tranfert vers les sédiments. Dans les lacs oligotrophes de haute altitude (lacs des Pyrénées, France – Espagne), le séléniate a été la seule forme détectée dans l'eau représentant 63 % de Se total. Dans l'estuaire de l'Adour, l'influence de l'utilisation de fertilisants contenant Se sur les terrains agricoles du bassin versant a été démontrée par une corrélation positive des concentrations de Se et des ions nitrate dans l'eau, tandis que la transformation du sélénium en composés réduits et volatils semble favorisée du côté océanique pendant les périodes de production plus chaudes.

Mots clés : Sélénium, Spéciation, HPLC-ICP-MS, Cycle biogéochimique, Eau douce.

Abstract

Selenium (Se) exists in aquatic systems in multiple oxidation states (VI, IV, 0, -II) in a wide variety of species. Selenate and selenite are generally found in natural waters but may not account for total Se content indicating the co-existence of unidentified reduced Se compounds. Due to the role of Se as a micro-nutrient for living organisms, the characterization of Se compounds must be done to better constrain Se biotic and abiotic transformations and fate in aquatic systems. Selenium occurring in trace amounts in most aquatic environments, sensitive analytical methods are required to achieve this goal. In addition, the number of studies reporting on selenium speciation and cycling in non-polluted aquatic environments is still limited claiming for more field investigations.

In this work, the optimization of chromatographic separation based on mixed-mode stationary phase combining reverse phase and anionic exchange allowed the simultaneous separation of six inorganic and organic compounds. The developed method together with a sensitive method for the determination of volatile Se compounds, were applied in parallel for the first time to provide new insights on the Se cycle in different aquatic systems as function of biogeochemical and seasonal variations. In a stratified eutrophic lake (Lake Kinneret, Israel), the existence of reduced and most probably organic Se containing compound actively produced by phytoplankton was revealed and suggested as a precursor for Se volatilization. Meanwhile under anaerobic conditions, the reduction of oxidized Se species to reduced forms could result in Se removal to sediments. In oligotrophic alpine lakes (Pyrenees lakes, France - Spain), selenate was the major compound in water and represented 63% of total Se. Downstream in the Adour estuary, the influence of agricultural land use on Se inputs was demonstrated with a clear relationship between Se and nitrates water concentrations, while selenium uptake and transformation to reduced and volatile compounds was promoted seaward during warmer productive periods.

Keywords: Selenium, Speciation, HPLC-ICP-MS, Biogeochemical cycling, freshwaters.

Table of Contents

List of Figures

CHAPTER 1

CHAPTER 2

Article II

Article III

List of Tables

CHAPTER 1

CHAPTER 2

CHAPTER 3

Article I

Article III

Glossary

AAS	atomic absorption spectroscopy
AC	activated carbon
AEC	anionic exchange columns
AES	atomic emission spectroscopy
AFS	atomic fluorescence spectroscopy
CE	capillary electrophoresis
CPE-ETV	selective cloud point extraction - electrothermal vaporization
CR/C	collision/reaction cell
CRM	certified reference material
CSV	cathodic stripping voltammetry
CT	cryo-trapping
DCP	direct current plasma
DLLME	dispersive liquid-liquid micro-extraction
DP-CSV	differential pulse cathodic stripping voltammetry
ED	electrodeposition
ETAAS	electrothermal atomizer atomic absorption spectroscopy
GC	gas chromatography
HFBA	heptafluorobutyric acid
HG	hydride generation
HHPN	hydraulic high pressure nebulization
HPLC	high pressure liquid chromatography

HS-LPME	head-space liquid phase microextraction
FAAS	flame atomic absorption spectroscopy
FI	flow injection
FID	flame ionization detector
ICP	inductively coupled plasma
MS	mass spectrometry
MW	microwave oven
PGC	porous graphitic carbon
PVG	photochemical vapor generation
RF	radiofrequency
RP	reverse phase
SWV	square-wave voltammetry
SPME	solid phase micro-extraction
TBAH	tetrabutylammonium salt
TFA	trifluoroacetic acid
USAEME	ultrasound assisted emulsification micro-extraction
UV-VG	ultraviolet (chemical) vapor generation

Chapter 1: Introduction

The study of selenium biogeochemical cycling in aquatic ecosystems is a subject of interest for several disciplines (i.e. biogeochemistry, aquatic chemistry, ecotoxicology). It requires the comprehension of the different processes occurring not only in the water but also in other environmental compartments (soil, atmosphere). The objective of this chapter is to present the state of the art of the actual knowledge of selenium biogeochemistry in the environment, identifying the gaps of knowledge at the different environmental compartments.

This chapter begins with a general description of selenium physicochemical properties, followed by a review of the sources and content of selenium in the different environmental compartments. Afterwards, the global selenium cycle is described in order to have a global vision of selenium processes that take place in the environment. Then, the chapter focus on selenium speciation in aquatic environments. In this part, the dynamics of selenium speciation in different aquatic systems (freshwaters and marine waters) is reviewed.

Thereafter, an assessment of the existing analytical techniques is presented in order to show the strengths and weakness of the different techniques that can be used for Se speciation analysis of natural water samples.

A synthesis of the actual knowledge of selenium cycling in the aquatic environment is presented, together with a review of the most suitable analytical methods for selenium speciation in waters. At the end of this chapter, the objectives and questions to which this thesis aims to answer are presented.

1.1. Selenium Generalities and Cycling in the Environment

1.1.1. Selenium Discovery and Physicochemical Properties

Jöns Jacob Berzelius and his assistant, Johan Gottlieb Gahn, first discovered selenium (Se) in 1817. They observed a reddish sludge occurring in a sulfuric acid production plant that used the lead chamber process. The sludge was initially believed to be an arsenic derivative, but the first's chemical analyses discarded this hypothesis and indicated the possible presence of tellurium. Initially, Berzelius identified the compound as tellurium but further experiments concluded that the sludge contained a new element. Due to its similarities with tellurium (that received its name in reference to the Earth), Berzelius named this new element selenium, in reference to the Moon (Reich & Hondal, 2016; Weeks, 1932).

Selenium is a non-metallic element with atomic number 34 and atomic mass 78.96 (Coplen et al., 2017). It belongs to the chalcogen group and it's located between sulfur (S) and tellurium and shows similar properties to these elements (Trofast, 2011). Selenium has six stable isotopes: ^{74}Se, ^{76}Se, ^{77}Se, ^{78}Se, ^{80}Se and ^{82}Se. ^{78}Se and ^{80}Se are the most abundant. ^{82}Se is radioactive with a relatively long half-life (9×10^{19} years) (Holden et al., 2018). Atomic masses and natural abundances of Se isotopes are presented in Table C1.1.

Table C1.1. Atomic Masses and Natural Abundances of Selenium Isotopes (Holden et al., 2018).

Isotope	Atomic Mass	Natural Abundance (%)
^{74}Se	73.922	0.86
^{76}Se	75.919	9.23
^{77}Se	76.920	7.60
^{78}Se	77.917	23.69
^{80}Se	79.917	49.80
^{82}Se	81.917	8.82

Se is an essential micronutrient for animals, but it presents a narrow range between deficiency and toxicity levels. Selenium exerts its biological functions through selenoproteins (Kurokawa & Berry, 2013). In the environment, selenium is commonly found in four oxidation states, selenate (Se(VI)), selenite (Se(IV)), elemental Se (Se(0)) and several forms of reduced

selenium (Se(-II)). However, in specific organic compounds, Se may exist in the form of Se(-I) such as the Se amino acid seleno-cystine or the volatile dimethyldiselenide.

Selenate and selenite are highly soluble, mobile and bioavailable, especially selenate. In opposition, the elemental Se is considered a non-soluble species and inorganic selenides that show limited solubility, are considered as non-bioavailable (Séby et al., 2001).

In natural waters, with pH generally between 5.0 - 9.0, oxidizing processes will be a driving factor controlling Se mobilization meanwhile reduction processes will promote Se precipitation and its unavailability (Sharma et al., 2014). The potential-pH diagram for inorganic Se in water is presented in Figure C1.1.

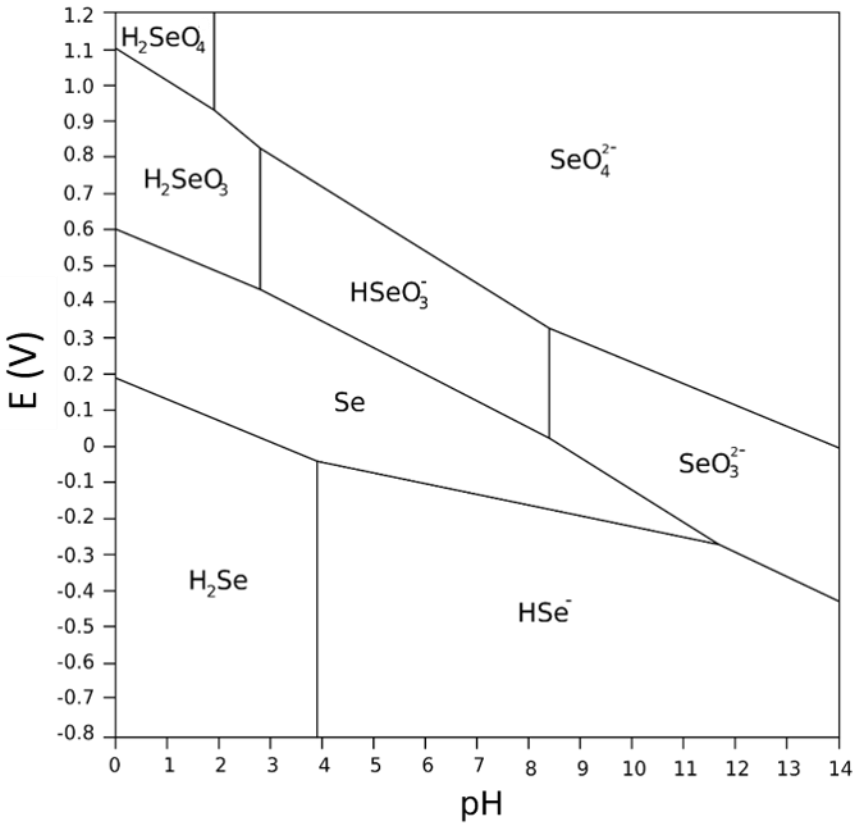

Figure C1.1. Selenium potential-pH diagram at 25 ºC and 1 bar pressure for dissolved Se activity of 10^{-7} mol L^{-1} (Séby et al., 1998).

In real systems, the thermodynamic scheme is useful but not sufficient to describe Se species distribution. For example, under strong oxidizing conditions only selenate would be expected, however, Se(IV) is found under unstable thermodynamic conditions due to slow kinetic of the oxidation reaction (Cutter & Bruland, 1984).

Aside from kinetics, it is important not to forget the biological processes occurring in the media. Se is known to be essential for bacteria and animals (Reich & Hondal, 2016). In waters, the presence of microorganisms, plants and animals will affect Se speciation either by modifying the redox conditions of the water (i.e. producing or consuming oxygen) or by the uptake, transformation and further release of Se to the water.

1.1.2. Selenium sources and content in the different environmental compartments (soil, water, atmosphere)

1.1.2.1. Natural and anthropogenic selenium sources

Selenium in the different environmental compartments – soil, water, atmosphere – originates from both natural and anthropogenic sources. Natural sources of Se to the environment include volcanic activity, wildfires, weathering and leaching from rocks and soils and, volatilization from water bodies – mainly oceans – and plants (Floor & Román-Ross, 2012; Janz, 2011). Anthropogenic activities include but are not limited to: mining, fossil fuels burning, agriculture (use of fertilizers and intensive irrigation); industrial and manufacturing processes (Lemly, 2004).

Rocks are the main source of Se to terrestrial ecosystems, representing 40% of total Se present in the Earth's crust (Fernández-Martínez & Charlet, 2009). Natural processes such as leaching and weathering processes transport Se from rocks to soil and, afterwards to water. The anthropogenic sources of Se to soil and water are derived from industrial activities and the use of Se-fertilizers in agriculture. In addition, wet and dry deposition derived from natural and anthropogenic sources are a non-negligible Se source to soils (Winkel et al., 2015) and recent a recent model has shown that atmospheric Se deposition is a source of Se to the oceans (Feinberg et al., 2020).

Ross (1985) estimated that only 20–30% of total atmospheric Se emissions derived from natural sources. Meanwhile, Mosher & Duce (1987) suggested that natural Se emissions corresponded to 60% of total Se emissions. Wen & Carignan (2007) compared both values and stated that most probably, the results of Ross (1985) were overestimating the contribution of anthropogenic emissions since their studies were only focused on the north hemisphere.

Table C1.2. Estimated global flux of atmospheric Se emission from natural and anthropogenic sources in 10^3 tonnes of Se yr^{-1}. This estimation is based on the experimental data collected by Mosher & Duce (1987), Nriagu (1989) and Nriagu & Pacyna (1988). The table has been adapted from Wen & Carignan (2007).

	Mosher and Duce (1987)	**Nriagu and Pacyna (1988), Nriagu (1989)**
Natural sources (10^3 t yr^{-1})		
Crustal weathering	0.003 – 0.025	0.01 – 0.035
Sea salt spray	0.04 – 0.4	0 – 1.1
Volcanoes	0.4 – 1.2	0.1 – 1.8
Marine biosphere	5.0 – 8.0	0.4 – 9
Continent biosphere	0.7 – 3.6	0.15 – 5.25
Wild forest fires		0 – 0.52
Total annual flux (mean values)	6.1 – 13.2 (9.65)	0.66 – 17.7 (9.2)
Anthropogenic sources (10^3 t yr^{-1})		
Combustion		
Coal	3	1.8275[a]
Oil	0.51	0.4845[a]
Refuse incineration	0.21	0.0655[a]
Other biomass	0.37	
Non-ferrous metal production	1.713	1.4155[a]
Manufacturing	0.2441	0.0015
Total annual flux	6.047	3.7945[a] / 6.3241[b]
Total annual emissions	**15.7**	**15.5**
Natural Se contribution	**62.5%**	**59.4%**
Anthropogenic Se contribution	**37.5%**	**40.6%**

[a]Particulate Se, [b]Total volatile Se

Therefore, the source of Se emissions may differ substantially depending on the study site (Wen & Carignan, 2007). The model presented by Feinberg et al., (2020) establishes marine emissions (32 – 50%) and anthropogenic (30 – 42%) as major Se sources to the atmosphere, followed by volcanic (6 – 22%) and terrestrial sources (5 – 18%); in agreement to previous studies where natural Se emissions contributed to around 60% of total Se emissions over anthropogenic emissions (~40%) (Mosher & Duce, 1987; Nriagu, 1989; Nriagu & Pacyna,

1988). Both terrestrial ecosystems and the atmosphere are sources of Se to the aquatic systems.

Se easily replaces sulfur in some minerals such as pyrite, chalcopyrite, pyrrhotite and pentlandite (Lahermo et al., 1998), and it is extracted as a byproduct from sulfuric acid production plants and copper refinery industries (ATSDR, 1997). The estimated industrial production of Se is estimated to be about 3000 tons per year (Naumov, 2010). The United States Geological Survey published in 2014 estimated that every year 1200 tons of Se are dedicated to metallurgy (40%), 750 tons to glass manufacturing (25%), 900 tons are used for agriculture (10%), chemicals and pigments (10%) and electronics (10%), the remaining 5% being exploited for other applications (Anderson, 2014). Metal refining and coal combustion are the main anthropogenic sources of Se to the atmosphere with an estimated contribution between 83 and 90% of total atmospheric anthropogenic Se emissions (Mosher & Duce, 1987). In fact, only coal combustion represents around 50% of non-natural total Se emissions to the atmosphere (Table C1.2). Concentrations in coal and oil usually range from 0.47 to 8.1 mg Se kg^{-1} and from 2.4 to 7.5 mg Se kg^{-1}, respectively (Alexander, 2015; Raptis et al., 1983), but levels of selenium up to 84 g kg^{-1} have been found in coal in China; considered as the source of local soil contamination (Alexander, 2015).

1.1.2.2. Selenium content in the different environmental compartments

Selenium occurs in the Earth's crust at concentrations from 0.05 to 0.09 mg kg^{-1} (Hall, 2018; Plant et al., 2013). The average Se content in some selected environmental compartments is presented in Table C1.3.

Selenium is unevenly distributed worldwide and can be found in rocks and soils at trace levels, usually between 0.01 and 2 mg kg^{-1} (Fernández-Martínez & Charlet, 2009). It is commonly found as selenite, selenate and, selenides associated with sulfide minerals (Davis & Hall, 2017; NRC, 1983). Nevertheless, high concentrations of Se have been reported in Cretaceous marine sedimentary rocks, coal and other fossil fuel deposits (Casey, 2000). High selenium concentrations may be present in extrusive volcanic rocks (120 mg kg^{-1}). In opposition, other volcanic rocks such as basalt and rhyolites may contain lower concentrations. Specific sedimentary rocks are well known for containing elevated Se amount such as shales, sandstone uranium deposits (1000 mg kg^{-1}), and some carbonate rocks (30 mg kg^{-1}) (Alexander, 2015).

Table C1.3. World average selenium concentrations in selected environmental compartments. Adapted from Fernández-Martínez & Charlet (2009) and Fordyce (2006).

Material	Total Se (mg kg^{-1})
Igneous rocks	0.35
Volcanic rocks	0.35
Limestone	0.03 – 0.08
Shale	0.05 – 0.06
Shales (USA)	1 – 675
Granite	0.01 – 0.05
Soil	0.4
Se-deficient (China)	0.004 – 0.48
Seleniferous (China)	1.49 – 59.4
Seleniferous soils (Ireland)	1 – 1200
World freshwater (μg L^{-1})	0.02
Air (ng m^{-3})	0.00006 – 30
Atmospheric dust	0.05 – 10

Chapman et al., (2010) indicated that ancient organic enriched depositional marine basins are linked to the actual global distribution of Se source rocks, the composition of these deposits suggested bioaccumulation as the major mechanism for Se enrichment of ancient sediments. In particular, geologically rich Se areas with arid or semi-arid climate are known for their tendency to accumulate Se. Two examples are Northwestern China and western United States regions (Han, 2007), with Se content up to 1200 mg Se kg^{-1} (Fordyce, 2013; Ohlendorf, 2003).

In freshwater systems, Se content is highly variable and depends on multiple factors, such as biogeochemical conditions of each specific area and Se soil content. Aquatic systems containing total Se concentrations above 200 ng Se L^{-1} are considered polluted (Luoma & Rainbow, 2008). In most fresh natural (unpolluted) waters, selenium is present at trace or ultratrace levels in the range from <0.1 to 400 μg L^{-1} and, in most cases, concentrations are below 3 μg L^{-1} (Fordyce, 2013; Plant et al., 2013; WHO, 2011).

In general, groundwaters contain higher selenium concentrations than surface waters due to longer contact times of rock-water interactions (Fordyce, 2013; Hem, 1985). Therefore, Se content in surface water systems may increase if they receive groundwater or water from

ponds and/or reservoirs. Se in groundwaters vary from very low concentrations, for example in Australia, Belgium or Finland (<1 μg L^{-1} (Alfthan et al., 1995; Dall'Aglio et al., 1978; Robberecht et al., 1983)) up to extremely high values in seleniferous areas (i.e. USA, 1400 μg Se L^{-1} (Bailey, 2017)). In drinking waters, Se concentration is generally below 10 μg L^{-1} (the recommended value for drinking waters (Barron et al., 2009)); thus, far from 40 μg L^{-1}, which is the maximum tolerable value recommended by the World Health Organization (2011). Only waters from specific seleniferous areas, such as Punjab, India (up to 35.6 μg L^{-1}, (Dhillon & Dhillon, 2016)) or some regions of China (up to 159 μg L^{-1}, (Fordyce et al., 2000; Yang et al., 1989)) show greater Se content.

The typical total Se concentrations in temperate and tropical European and Asian lake waters ranges from 30 - 1520 ng Se L^{-1} (Conde & Sanz Alaejos, 1997). While in temperate lakes of North America, Se concentrations are between 200 and 500 ng L^{-1} (Brandt et al., 2017). In lakes of southern Norway, Se levels range from 20 to 60 ng L^{-1} (Økelsrud et al., 2016); Finish (Wang et al., 1994) and Canadian (Nriagu & Wong, 1983) lakes also have concentrations below 100 ng Se L^{-1}. And, in western Siberian lakes and rivers total Se ranged from 20 to 100 ng L^{-1} (Pokrovsky et al., 2018). Pokrovsky et al. (2018), observed large variability (2- to 5-fold increase of Se concentration) due to evaporation during prolonged heating periods, and freezing in confined space afterwards. Western Siberian rivers exhibited total Se concentrations ~40 ± 20 ng L^{-1}, lower or similar to that measured in organic-rich rivers in Sweden (30–400 ng L^{-1}) (Lidman et al., 2011) and Finland (~100 ng Se L^{-1}) (Wang et al., 1994). And greater values were found in industrially affected European, American, and Asian rivers, ranging from 100 - 1000 ng Se L^{-1} (Conde & Sanz Alaejos, 1997).

The ocean is by far the largest global sink for primary Se emissions (Mason et al., 2018). Inputs of Se to oceanic waters include riverine discharge and mainly atmospheric depositions (Winkel et al., 2015; Cutter, 1993; Mosher & Duce, 1987; Wen & Carignan, 2007). However, limited data about oceanic Se distribution worldwide exist in the literature. Cutter & Bruland (1984) measurements established total Se content of Pacific Ocean to be between 80 – 185 ng Se L^{-1}. In the same ocean, recent experimental data indicated slightly lower values of around 47 ng Se L^{-1} (Mason et al., 2018). Lower Se concentration was found in the North Atlantic Ocean, of around 31 ng Se L^{-1} (Measures & Burton, 1980a). Oceans act at the same time as a source of Se to other environmental compartments through air-sea exchange (Amouroux & Donard, 1996; Amouroux et al., 2001; Mason et al., 2018; Tessier et al., 2002b; Wen &

Carignan, 2007). In non-volcanic areas atmospheric Se in estimated to be in the range between 0.1 to 1 ng Se m^{-3} (Fordyce, 2013; Haygarth, 1994).

1.2. Selenium biogeochemical cycling

The study of the global Se cycling is of vital importance due to the role of Se as micro-nutrient and potential toxicant for living organisms. In this section, a review of the actual knowledge about Se cycle is presented in order to identify what is known, what is missing and what should be addressed in future research concerning Se transformations in the environment. An overview of the global Se processes transporting Se among the environmental compartments is presented in Figure C1.2.

Selenium content in soil depends on many environmental features, for example, the type of parent rock and the intensity of processes such as leaching and weathering, sorption processes and biological activity (Brodowska et al., 2016; Rovira et al., 2008). Despite the non-negligible contribution of atmospheric deposition, weathering of rocks is the major primary source of environmental Se (El-Ramady et al., 2014; Wen & Carignan, 2007). The chemical forms in which Se is present in soils depends on pH, redox potential, free oxygen concentration and moisture content (Brodowska et al., 2016; Wang & Gao, 2001).

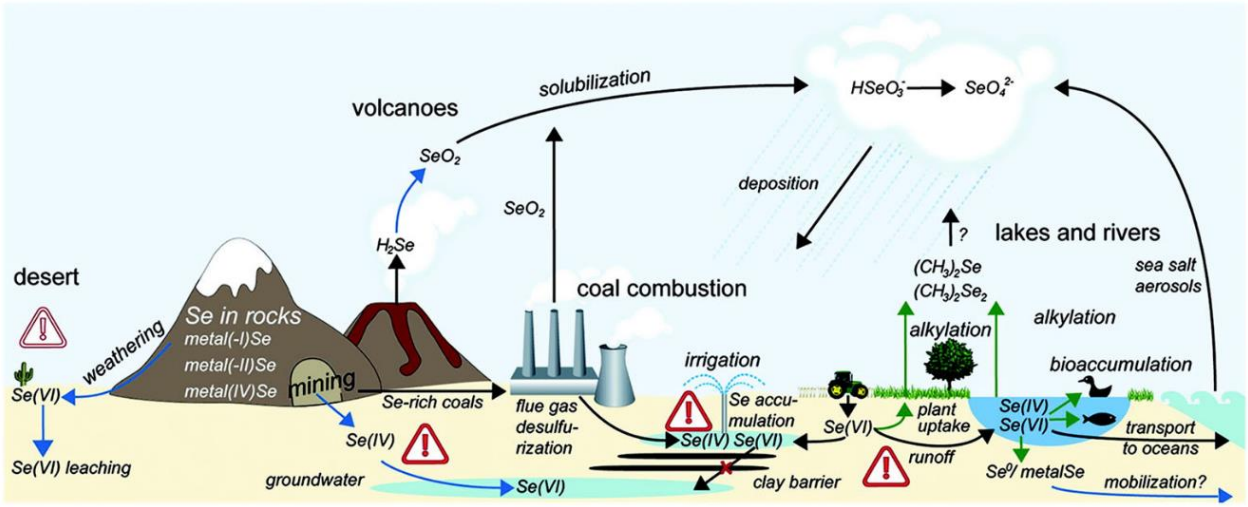

Figure C1.2. Selenium emissions and transport through the environmental compartments (Sharma et al., 2014).

The key processes that contribute to the transformation, immobilization and/or transport of Se to other environmental compartments are schematized in Figure C1.3. Three processes are particularly important: reduction/oxidation, sorption to minerals and the interaction with organic matter (Winkel et al., 2015).

The oxyanions present higher solubility than elemental Se and selenides (Séby et al., 1998; 2001). The reduction of Se(VI) to Se(IV) may induce the immobilization of selenium, especially due to the sorption of selenite to manganese, aluminum and iron oxy-hydroxides (Rovira et al., 2008; Saeki et al., 1995; Söderlund et al., 2016). In general, the reduction of oxyanions to elemental Se or Se(-II) is a way to decrease the mobility and bioavailability of Se. As illustrated in Figure C1.3., reduced Se may interact with minerals, resulting in a co-precipitation, and it may also be assimilated by microorganisms and incorporated into organic matter. The water acts as a carrier and is essential for the transport of Se from the solid phase into the biological tissues of the living organisms (Shahid et al., 2018; Winkel et al., 2015).

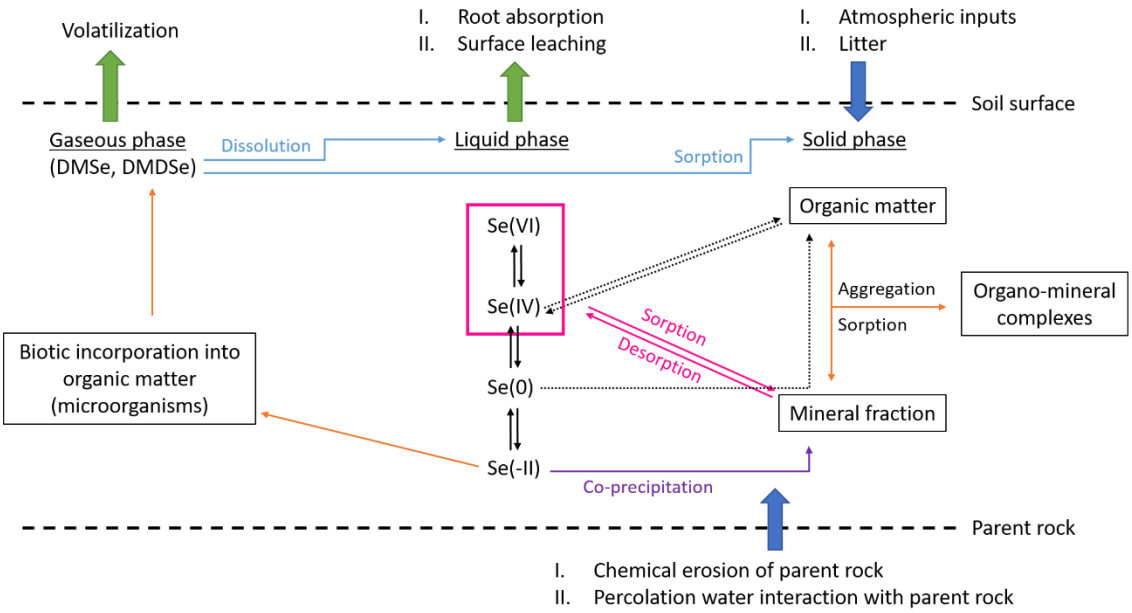

Figure C1.3. Biogeochemical cycling of selenium in soils. Adapted from (Tolu, 2012; Di Tullo, 2015).

It has been reported that plant Se concentration depends significantly on the soluble fraction of soil Se, instead of the total Se soil content. Therefore, the uptake of Se by plants may not necessarily depend on the Se concentration of soils but on speciation. Hawaiian soils are an example: despite a content between 6–15 mg Se kg^{-1}, limited vegetation uptake decreases Se

toxicity. The opposite case is observed for soils of South Dakota and Kansas containing <1 mg Se kg^{-1} but poisoning vegetation (Meyer & Burau, 1995; Wang & Gao, 2001).

Selenium is incorporated into aquatic systems from either soils or the atmosphere. The increase of water-irrigated farm lands increases the lability of selenium becoming a non-negligible input to water (Han, 2007). Natural weathering is also accelerated by mining activities that expose ores and waste rocks to oxidation. Oxidized Se easily leaches to surface and ground waters and it is transported to ponds, reservoirs, rivers and lakes (Chapman et al., 2010). Oceans are a major reservoir for Se. Oceans are of vital importance due to its dual role as sink and source of Se to the atmosphere and soils through the formation of aerosols and biomethylation and, further atmospheric transport and deposition.

Few studies have focused on Se transport and transformations in the atmosphere, Wen & Carignan (2007) proposed the schema presented in Figure C1.4. From left to right, anthropogenic emissions, Se transformations and biogenic Se species emitted and their transformations are described.

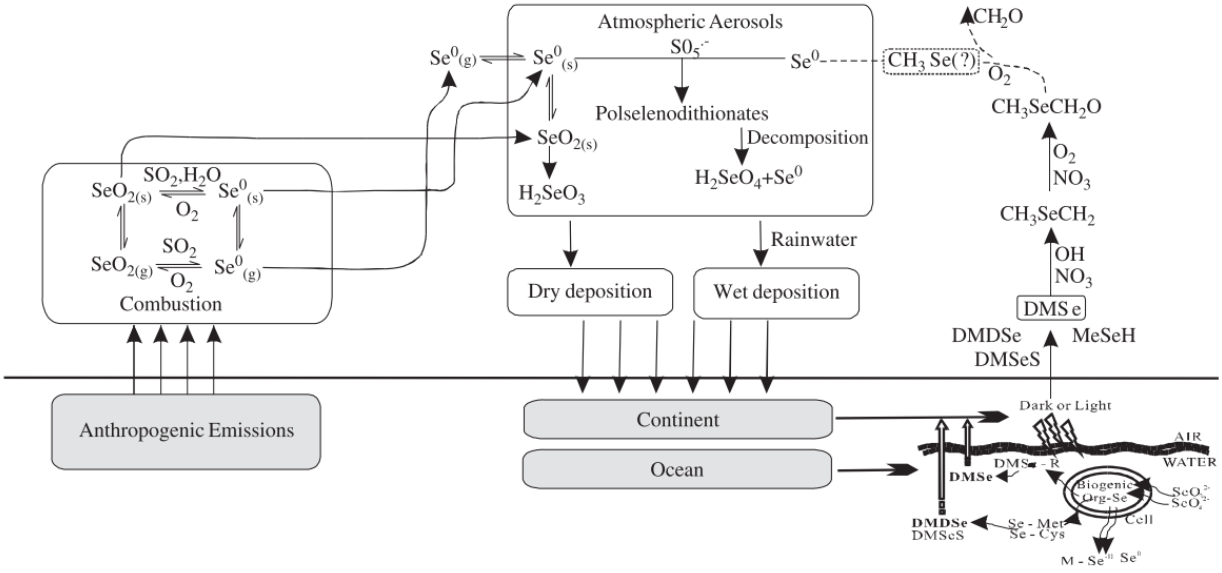

Figure C1.4. Se species and transformations in the environment, special focus in the air compartment. From (Wen & Carignan, 2007) and based on the cycle proposed by Ross (1984) and the speciation data from (David Amouroux et al., 2001).

The residence time of volatile organic Se is relatively short (e.g. DMSe residence time is 6 h (Atkinson et al., 1990)) and similar residence times have been predicted for volatile inorganic Se (reviewed by Wen & Carignan, 2007). The latest estimations suggest Se lifetime in the

atmosphere to be around 5 days (Feinberg et al., 2020). In addition, 96% of total atmospheric Se in the aerosol phase. Atmospheric Se removal is associated with wet deposition (81%) and dry deposition (19%). Over the oceans wet atmospheric Se deposition have a higher incidence (87%) than in land areas (74%) (Feinberg et al., 2020). Therefore, the transport of volatile Se species will be limited to short or medium distances. However, the exposure of gaseous Se to physicochemical and photochemical atmospheric conditions will transform it to particulate Se. Thus, the smaller Se particles will potentially be transported through longer distances up to 1000 km (Wen & Carignan, 2007).

Atmospheric Se exists in a wide range of compounds that can be divided in three categories: non-volatile particulate Se (elemental Se), volatile inorganic Se (hydrogen selenide, selenium dioxide and elemental Se), and volatile organic Se (methylselenol, MeSeH; dimethylselenide, DMSe; dimethyldiselenide, DMDSe; dimethylselenide sulphide, DMSeS; etc.) (David Amouroux et al., 2001; Wen & Carignan, 2007). Volatile inorganic Se has rarely been measured experimentally due to the short lifetime and instability, these species rapidly transform to particulate phases. Volatile organic Se species are mainly released as the result of biomethylation processes carried out by microorganisms and plants (Amouroux & Donard, 1997; 2001; Wen & Carignan, 2007). Even though, the mechanisms for Se biomethylation and volatilization are still not well understood. Thus, more biogeochemical studies are necessary to better understand Se cycling, especially in regards to reduced Se species, which is the case of main volatile Se species.

1.2.1. Processes involved in Se species formation and transformation in aquatic systems

As part of global Se cycle, the understanding of the behavior of Se in aquatic systems and their interfaces is necessary. As previously highlighted, selenium is incorporated into aquatic systems from either soils or the atmosphere. Due to the higher mobility of selenate over selenite, elemental Se and reduced Se species, this species is more easily lixiviated from soils, thus selenate is the main species in which Se is transported from soils to the dissolved aqueous phase (Table C1.5).

In aquatic systems, physicochemical and biological processes take place. Physicochemical processes include lixiviation, weathering, sorption, redox processes, photoreactivity, complexation and precipitation (Masscheleyn & Patrick Jr, 1993; Sharma et al., 2014). Physicochemical processes, driven by pH, redox conditions, organic matter content and the

presence of competitive ions are well known. Biological processes leading to alkylation and de-alkylation, are much less understood (Sharma et al., 2014). Actual knowledge of main processes occurring for Se in surface water systems and interface environmental compartments is presented in Figure C1.5.

Some aquatic systems, in particular deep lakes, oceans and some estuaries present stratification. This fact is of particular importance for Se cycling due to substantial differences concerning Se reactions in oxidizing compared to reducing waters. While estuaries present salinity stratification, deep lakes and oceans present thermal stratification that can be a permanent or temporal condition. In general, the surface water layer (epilimnion) is well aerated in thanks to the gas exchange with the atmosphere. In addition, solar radiation may enhance photochemical reactions and biological processes, in this case carried out by algae. Radiation and air temperature substantially modify the water temperature; while wind speed increases surface water mixing. Seasonal fluctuation of temperature and dissolved oxygen highly influence Se speciation, especially in temperate lakes that present seasonal stratification (Boehrer & Schultze, 2008; Horne & Goldman, 1994). The bottom water layer (hypolimnion) becomes isolated during stratification periods, which results in oxygen depletion due to biological activity and limited vertical transport (Boehrer & Schultze, 2008). The more reducing conditions of hypolimnion can affect Se oxyanions species and stabilize the presence of reduced Se species, that would be fast re-oxidated under oxic conditions (Nishri, Brenner, Hall, & Taylor, 1999). Therefore, stratification and seasonal variations are crucial factor to take into account when a system is studied.

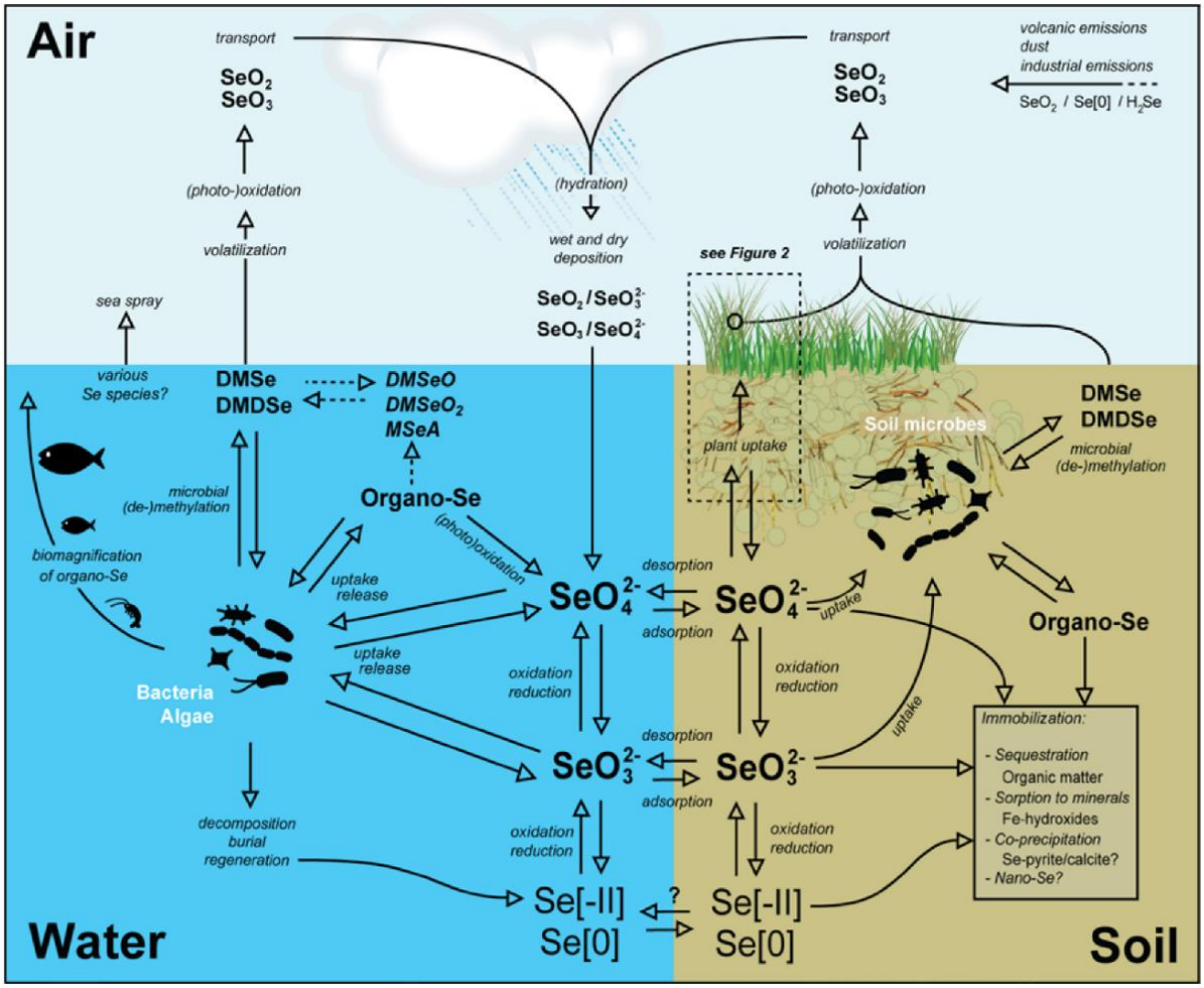

Figure C1.5. Overview of Se species, pathways and transformations in soil, water, atmosphere and their interfaces. Abiotic and biotic transformations are indicated in italics at the corresponding arrows. Potential immobilization processes in soils are listed in the frame-inset. From (Winkel et al., 2015).

Oceans are the perfect example of how the concentrations of total Se and Se species change with depth. Several studies have shown the nutrient type distribution of Se in oceanic waters (Aono et al., 1991; Cutter & Bruland, 1984; Mason et al., 2018; Measures et al., 1983; Takayanagi & Wong, 1984). The authors found that selenite behavior correlated well with phosphate and nitrate anions (R^2=0.8-0.9); meanwhile, selenate and reduced Se fraction were poorly correlated with nutrients in the water column (R= 0.4-0.7). Cutter & Bruland (1984) found significant amounts of reduced Se, assumed to be organic selenide, at oxic and suboxic depths. As selenite and selenate were spotted in the suboxic and anoxic zones, authors suggested that particulate organic selenide (via sinking detritus) was a possible source of these species in anoxic waters. Mason et al. (2018), in agreement to previous studies, also

observed the characteristic nutrient type profile for Se. However, the authors recognized that long storage times resulted, most probably, in organic Se oxidation and an overestimation of Se(IV) concentration. Despite the evidenced Se speciation variations among the water column in marine waters, most of the studies of freshwater systems are limited to the study of Se speciation surface or subsurface waters.

The presence of reduced Se species is non-negligible in most aquatic systems, representing up to 80% of total Se in marine (Cutter & Bruland, 1984) and lake waters (Wang et al., 1995). However, the identification of species that conform the reduced Se pool has not been yet accomplished. The mechanisms involved in the production of reduced Se species are usually associated to the biological activity of the aquatic system. However, those mechanisms remain unknown. In order to better comprehend the mechanisms driving Se transformation in aquatic systems, it is thus necessary to develop new analytical strategies that allow the identification of reduced and most probably organically bound Se. Environmental studies in freshwater systems including Se speciation along the water column, in particular for stratified systems, should help to better understand dissolved selenium behavior in aquatic systems as a function of depth and seasonal variations.

1.3. Selenium speciation in aquatic environments

This section intends to review Se speciation in aquatic systems (freshwaters and marine waters) in order to show the variability among systems in terms of total Se concentration and Se speciation, including Se speciation for volatile species.

1.3.1. Selenium speciation in freshwater systems

Groundwaters and drinking waters. Data concerning Se speciation for these types of waters are scarce. However, the few presented in Table C1.4 show the predominance of selenate in both drinking and groundwaters.

Drinking waters undergo chemical treatments including aeration and disinfection processes (oxidation); selenate is therefore expected to be the main species detected. For example, Wang et al. (2001), observed that 85% of Se present in tap water (subjected to disinfection, i.e. oxidation) was in the form of selenate. The predominance of selenate in groundwaters is consistent with the higher solubility and mobility of selenate from bedrock. The predominance of selenate has been documented also in groundwaters from Kesterson reservoirs in California (White et al., 1991).

Table C1.4. Se total concentrations and speciation in drinking and groundwaters worldwide (µg Se L^{-1} except * in µg Se kg^{-1}).

Site	Total Se	Se(IV)	Se(VI)	Reference
Groundwaters				
India				
Chennai city pre-monsoon		0.15–0.43	0.16–4.73	Kumar & Riyazuddin, (2011)
Chennai city post-monsoon		0.15–1.25	0.58–10.37	Kumar & Riyazuddin, (2011)
Punjab	0.01–35.6			Dhillon & Dhillon, 2016)
Finland				
Oripää, (South)	0.215–0.220	0.002	0.194	
Hämeelina, (South)	0.81–0.84			(Alfthan et al., 1995)
Joutsa (Central)	0.50 - 0.59			
Germany				
Rottenacker	4.1–29.4*			Grober et al., (1988)
Rottenacker	4.8–17.36*	0.19–0.40*	4.0–15.64*	(Heumann & Grober, 1989)
Gravel aquifer	1.8*	0.13*	1.63*	(Tanzer & Heumann, 1991)
Karst aquifer	13.7–15.6*	0.60–1.29*	12.3–15.1*	(Tanzer & Heumann, 1991)
Other Countries				
Ukraine	0.07–4			Fordyce (2013)
France	1.11–15.40			Cary et al., (2014)
Sicily, Italy	0.6–66.8			Aiuppa et al., (2000)
Belgium	<0.05–0.84	<0.04–0.28	<0.05–0.84	Robberecht et al., (1983)
Belgium	0.13–0.38	<0.02–0.05		Neve et al., (1980)
Colorado, USA	<0.5–4070			Mills et al., (2016)
USA	2–1400			Bailey (2017)
Australia	0.008–0.330			Dall'Aglio et al., (1978)
Nigeria	7.33–46.3			Etim (2017)

Table C1.4. (Continued)

Site	Total Se	Se(IV)	Se(VI)	Reference
		Drinking waters		
		China		
Seleniferous areas	5–159			(G. Yang et al., 1989)
Enshi District	0.168–32.6			(Fordyce et al., 2000)
Beijing	0.2	0.02	0.17	(Wang et al., 2001)
		Other Countries		
Sri Lanka	0.06–0.24			(Fordyce et al., 2000)
Belgium	<0.05–0.84*	0.04–0.28	0.05–0.84	(Robberecht et al., 1983)
France	<2–10			(Montiel, 1981)
Moscow, Russia	0.125	0.05	0.075	(Nazarenko & Kislova, 1978)
Venezuela	0.186–0.204			(Jaffe et al., 1972)
Turkey	0.002–0.825			(YanardaĞ & Orak, 2001)
Punjab, India	0.01–35.6			(Dhillon & Dhillon, 2016)
Croatia	0.001–2.68			(Ćurković et al., 2016)
USA	0.0–0.01			(Fordyce, 2013)
Bulgaria	<2			
Sweden	0.06			
Germany	1.6–5.3			
Reggio, Italy	7–9			
Greece	0.05–0.70			

Despite the importance of groundwaters as a source of Se for lakes, rivers and human consumption, few studies have addressed the seasonal variations of Se in groundwaters. Kumar & Riyazuddin (2011) studied the Se speciation in India. Their observations showed higher selenite and selenate concentrations in the post-monsoon period than in the pre-monsoon period. Authors found more pronounced oxidizing conditions in the post-monsoon period; which would increase the mobility of Se-oxyanions from rocks to groundwaters (A. Ramesh Kumar & Riyazuddin, 2011).

Rain. Selenium content and speciation in rainwaters has rarely been investigated. A review of existing data is presented in Table C1.5. In general, rain samples present a range from tens to hundreds of ng Se L^{-1}.

Table C1.5. Se total concentrations (in ng L^{-1}) and speciation (%) in rainwater. Adapted from *Wallschläger & London (2004)* and *Conde & Sanz Alaejos (1997)*.

Site	Total Se	Se(IV) (%)	Se(VI) (%)	Reference
Tokyo, Japan	5-118	5-104		Suzuki et al. (1981)
Belgium	<50–250	~80	<20	Robberecht et al. (1983)
Delaware, USA	174			Cutter & Church (1986)
The Netherlands	54–212			Woittiez & Nieuwendijk (1987)
Canada	12–62			Milley & Chatt (1987)
Greece	100–200·10^3			Bratakos et al. (1988)
Helsinki, Finland	44–222	60	34	Wang et al. (1993;1994)
Ireland	74			Cutter & Cutter (1998)
Beijing, China	540	~40	~40	Wang et al. (2001)
Chile	7–1310	42–78	22–58	De Gregori et al. (2002)
Etna Volcano, Italy	1100		67	Floor et al. (2011)
Bermuda, USA	30			Lawson & Mason (2001)
Maryland, USA	80-1579			
Sweden	5–830			Lidman et al. (2011)
Finland	120			
Jungfraujoch, Switzerland	16		65	Suess et al. (2019)
Pic du Midi, France	51		84	

Rivers, lakes. Like rain, these aquatic systems become Se sources for other environments. Table C1.6 gives an overview of the experimental values for total Se and its species in lake and river waters. Se speciation in wetlands has been much less studied in unpolluted waters (natural wetlands not impacted by anthropogenic activities) and these systems are out of the scope of this project. Instead, the focus will be on rivers and lakes. Data presented on Table C1.6 reflect the high variability of Se concentrations in these systems depending on their geographic location and the anthropogenic activities occurring nearby. In polluted areas

(>200 ng Se L^{-1}), dominant species tends to be selenate with the exception of Italian Rivers and Belgium lakes where selenite showed greater values than selenate (Luoma & Rainbow, 2008).

Selenite predominates in Belgium lakes (Robberecht et al., 1983), lakes from Canadian metal smelters area (Dominic E. Ponton & Hare, 2013) and Moorland Lake in Germany (Tanzer & Heumann, 1991). Meanwhile, selenate is the major species in Erken Lake in Sweden (Lindström, 1983); in coal mining areas from Germany (Tanzer & Heumann, 1991); in Japan rivers, containing up to 171 ng Se L^{-1} of selenate at a maximum total Se concentration of 231ng L^{-1} (Suzuki et al., 1981; Uchida et al., 1980)); China rivers (Dunhu et al., 1989) or in the Goddard Marsh in Canada (Martin et al., 2011). The case of China is particularly extreme with values two orders of magnitude above the rest; being Se(VI) the main species detected in waters close to mining sites. Oxyanions predominance (>50%) is the common characteristic of polluted aquatic ecosystems, and may also predominates in unpolluted systems.

Concentration of reduced Se fraction (calculated as the difference between total Se and oxyanions concentrations) is not significant in polluted surface water systems. In opposition, in unpolluted fresh waters, this fraction, including Se(-II) and/or elemental Se, may be present in a significant amount (Nakaguchi & Hiraki, 1993; Nishri et al., 1999). The importance of this pool was observed in lake water samples from Finland in which more than half of the total Se was reduced organic Se (Wang et al., 1995; Wang et al., 1994). In lentic fresh water environments, in particular lakes, the seasonal variations of physico-chemical parameters (temperature, dissolved oxygen, pH…) and biological events in the water column may influence the total dissolved Se concentration and its speciation (Simmons & Wallschläger, 2005).

Table C1.6. Se total concentrations (mean or range) and speciation in lake and river surface waters (in ng L^{-1}). Reduced Se (Red.Se) is calculated value (Red.Se = TDSe – Se(IV) – Se(VI)).

Site	Total Se	Se(IV)	Se(VI)	Red. Se	Ref.
Lakes					
Belgium					
Belgium	<50–230	<40–150	<50–80		Robberecht et al. (1983)
Campus L.	230	150			Jiang et al. (1983)
Germany					
Artificial L.	190	30	171		Tanzer & Heumann (1991)
Coal mining area	830	46	805		
Moorland L.	210–240	27–141	35–47		
Finland					
Valkea-Kotinenjärvi	58	4	5	37	Wang et al. (1994, 1995)
Iso-Hietajärvi L.	34	4	4		Wang et al. (1995)
Pääjärvi L.	143	10	17		
Pesosjärvi L.	89	7	7		
Pyhäjärvi L.	81	6	5		
Other Countries					
Arrowhead L., USA		17.7	<5		Cutter (1978)
Sutton, USA	1900				Brandt et al. (2017)
Mayo, USA	700				
Erken L., Sweden	65–200	10–40	30–160		Lindström (1983)
Kinneret L., Israel*	50–184	<5–78	31–103	<5–50	Nishri et al. (1999)
Pszczewski Landscape Park Lakes, Poland	<150–740				Niedzielski et al. (2002)
Metal smelters area, Canada	35–3063	<21–1616	<21–918	<21–528	Ponton & Hare (2013)
Subartic ponds, Canada	18–107				Lanceleur et al. (2019)
Khanymey Lakes, Siberia	20–100				Pokrovsky et al. (2018)

Table C1.6. (Continued)

Site	Total Se	Se(IV)	Se(VI)	Red. Se	Ref.
			Rivers		
			China		
China Rivers	60–284	9–37	23–275		Dunhu et al. (1989)
Mining zone Rivers	1–30,600	80–4920	610–19900	90–4800	Zhang et al. (2013)
Yodo R.		16 - 30	2–19	6–32	Nakaguchi & Hiraki (1993)
			Other Countries		
Japan Rivers	16–231	<2 - 17	3 - 171	5–12	Suzuki et al. (1981); Uchida et al. (1980)
Italian Rivers	25–77·10^3	8–56·10^3	7.8–41·10^3	3–6·10^3	Orvini & Gallorini (1982)
Venezuela Rivers	17–58	<2–13			Yee et al. (1987)
Finland Rivers	71–217	9–14	13–68		Wang et al. (1994)
Siberia	19–111				Pokrovsky et al. (2018)
San Joaquin R., USA	<2–9000	<2–900	<2–6450		Cooke & Bruland (1987)

*Data concerning Se value at different depths of the water column.

Field and laboratory studies investigating volatile Se speciation and corresponding fluxes to the atmosphere from Se-deficient environments are scarce (Vriens et al., 2014). Specifically in fresh water systems, data concerning volatile Se speciation is almost inexistent. Existing data is summarized Table C1.7 that includes data from three polluted locations in the Unites States (Great Salt Lake) with total volatile Se (TVSe) concentrations from 40 to 22,700 pg L^{-1} (Diaz et al., 2009); Kesterson Reservoir ponds presenting TVSe in the range between 3.8 to 34 ng L^{-1} (Cooke & Bruland, 1987); from a minerotrophic peatland located at Gola di Lago, where Vriens et al. (2014) estimated volatile Se concentration around 0.8 pg Se L^{-1}, mainly as dimethylselenide (DMSe); lakes from Bolivia with TVSe in the range between 42 to 1740 pg Se L^{-1}; Tulare Lake with TVSe concentrations up to 108,995 pg Se L^{-1} (data extracted from Lanceleur et al., (2019)); and from Canadian Subarctic permafrost, where Lanceleur et al. (2019) where TVSe concentrations were in the range from 1 to 32 pg L^{-1}, with DMSe accounting for 96%, dimethylselenide sulfide (DMSeS) contributed for 4% and dimethyldiselenide (DMDSe) was not detected.

Table C1.7. Dissolved volatile Se total concentrations (in pg L^{-1}) and speciation (%). n.d.: non detected.

Site	TVSe	DMSe	DMSeS	DMDSe	Ref.
Gola di Lago, CH[1]	~0.8	≥99.8			Vriens et al. (2014)
Great Salt Lake, USA	40–22,700				Diaz et al. (2009)
Kesterson Reservoir, USA	(3.8–34)·10^3	99.8		0.1–0.2	Cooke & Bruland (1987)
Tulare Lake, USA	(11–109)·10^3	80	13	6	Lanceleur et al. (2019)
Kuujjuarapik, Canada	1–32	96	4	n.d.	
Poopo Lake, Bolivia	1,038–1,740	60	37	1	
Uru Uru Lake, Bolivia	42–1,679	49	41	7	

[1]CH is the abbreviation of Switzerland

1.3.2. Selenium speciation in marine and coastal systems

The input of dissolved Se to the estuaries and, afterwards to the ocean most typically results from riverine discharge and dissolution of suspended and sedimentary selenium (Cutter & San Diego-McGlone, 1990). Estuaries are semi-enclosed mixing zones for fresh and saline waters. Thus, intense physical, chemical and biological interactions, together with high impact of industrial and municipal wastewater sources, must be expected (Cochran & Brook, 2014). For example, Cutter (1989) found that major input of Se to the San Francisco Bay came from oil refineries and sewage treatment plants effluents. Several authors have reported a conservative profile of total Se in different estuaries among seasons (Guan & Martin, 1991; Measures & Burton, 1978; Takayanagi & Wong, 1984) despite the non-conservative profiles of its species. In the Bohai bay, significant differences between spring and autumn periods were observed where inorganic Se averaged 112 ng L^{-1} with 56% Se(IV) and, 103 ng L^{-1} with 30 % Se(IV) for spring and autumn respectively (Yao & Zhang, 2005). A compilation of existing data for oceanic and estuarine systems is presented in Table C1.8.

Oceanic waters are characterized by long residence times (several years), in opposition to fresh water systems (rivers and lakes). Probably, the Pacific Ocean has been the most extensively studied. Experimental measurements show total Se concentration in the range between 38 to 208 ng Se L^{-1}, selenite concentration in the range from 2 to 89 ng Se L^{-1} and selenate concentration in the range between 11 – 129 ng Se L^{-1} (Aono et al., 1991; Cutter & Bruland, 1984; Mason et al., 2018). Total Se increased with depth alongside with selenite and selenate concentrations (Cutter & Bruland, 1984). However, maximum total Se values

reported depend on the geographical area studied. Cutter & Bruland (1984) sample site was close to the Mexican coast. This region is located on a cretaceous black shale bedrock (Tuttle et al., 2014) enriched in Se. Meanwhile, Aono et al. (1991) samples proceed from a point close to Hawaii, a different tectonic plate with, apparently different rock composition leading to lesser Se content at high depth. Reduced Se pool was estimated by subtraction of Se oxyanions concentration from total Se. Concentrations of this pool of reduced compounds were in the range between 1 to 81 ng Se L^{-1} (Aono et al., 1991; Cutter & Bruland, 1984). Cutter & Bruland (1984) suggested that major part of reduced Se was presumably particulate organic selenides forming colloidal aggregates. Despite analytical advancements since these studies, the chemical composition of reduced Se pool remain unidentified nowadays, which in turn, makes it difficult the understanding of aquatic Se processes.

Measures et al. (1983) compared the concentrations of selenium and its inorganic speciation in Pacific, Indian and Atlantic oceans. Results showed that Atlantic Se concentrations were 30–40% lower than in Pacific and Indian oceans. Species distribution was similar for the three oceans with maximum total Se concentration in the subsurface region and lower concentrations that remain almost constant in deeper zones. Total dissolved Se concentration in deep waters from Mediterranean Sea (63 to 68 ng L^{-1}) were lower than in the Atlantic (79–118 ng L^{-1}) and Pacific (158–181 ng L^{-1}) oceans (Guan & Martin, 1991). Studies on the Mediterranean Sea reported low surface concentrations for selenite and selenate (14 and 11 ng L^{-1} respectively). Inorganic Se concentrations increased with depth to values around 27 and 20 ng Se L^{-1} for selenite and selenate respectively (Guan & Martin, 1991). Reduced Se was operationally defined in the range between 4 – 24 ng Se L^{-1}.

Table C1.8. Ranges of Se total concentrations and speciation (in ng Se L^{-1}) in marine and coastal waters.

Site	Total Se	Se(IV)	Se(VI)	Red. Se	References
Oceanic waters					
North Atlantic	28–138	≤2–35	26–103		Measures & Burton (1980)
South Atlantic	32–134	<8–47	<8–63	<40–55	Cutter & Cutter (1995)
Japan Sea	33–67	<2–32	18–51	<2–6	Uchida et al. (1980)
Pacific, California	45–184	4–65	41–119		Conde & Sanz Alaejos (1997)
East Tropical Pacific	83–208	2–89	11–129	1–81	Cutter & Bruland (1984)
Pacific, Alaska	62–131	21–57	11–58	7–55	Aono et al. (1991)
Pacific	39–152	3–56	18–60	7–53	Aono et al. (1991)
Pacific, Hawaii to Samoa	38–61		21–48		Mason et al. (2018)
Mediterranean Sea	40–76	5–29	8–41	4–24	Guan & Martin (1991)
Seawaters, New Zealand	49–75	9–18	24–52	6–25	Sherrard et al. (2004)
Bohai Sea, China	37–195	18–54	24–85		Yao & Zhang (2005)

Table C1.8. (Continued)

Site	Total Se	Se(IV)	Se(VI)	Red. Se	References
			Estuarine waters		
San Francisco Bay, USA	48–358	16–133	<1–218	<1–196	Cutter (1989); Cutter & San Diego-McGlone (1990)
San Francisco Bay, USA	72–161	10–17	47–135	1.6–35	Yao et al. (2006)
Chesapeake Bay, USA	71–151	43–136	15–28		Takayanagi & Wong (1984)
KrKa, Croatia	9–204				Seyler & Martin (1991)
Rhône, France	58–190	5–76	23–92		Guan & Martin (1991)
Kaoping, Taiwan	47–95	<5–22	13–67	5–50	Hung & Shy (1995)
Erhjen, Taiwan	63–83	<5–75	<5–24	<5–40	Hung & Shy (1995)
Zhujiang, China	63–392	22–225	47–257		Yao et al. (2006)
Changjiang, China	28–375	25–90	42–76		Wu et al. (2014) Chang et al. (2016)

Several authors have stated the importance of marine environments as major sources of Se to the atmosphere via biomethylation (David Amouroux & Donard, 1996; David Amouroux et al., 2001; Mosher & Duce, 1987). However, there is few experimental data available in the literature. Table C1.9 compiles the existing data, this table has been adapted from Lanceleur et al. (2019) and includes estuarine, coastal bays and oceanic data. Total volatile Se is in the range between 22–2,423 pg L^{-1} in the Rhine and Gironde estuaries while the range for Seine estuary varies from 317 to 4,855 pg L^{-1} and, at Scheldt estuary values from 51 to 8,067 pg L^{-1} were reported (Amouroux & Donard, 1997; Tessier et al., 2002). Seine estuary is known to be considerably influenced by human activities (Billen et al., 2001) while the Scheldt estuary is a well known industrial impacted area (Robberecht et al., 1983; Van Ael et a., 2017).

In the two coastal bays presented in Table C1.9, the total volatile Se ranges from 12 to 426 pg L^{-1}, *i.e.* lower values than those measured in estuaries. Finally, concentration levels found in the North Atlantic Ocean and in the Eastern Mediterranean Sea are between 20–417 pg L^{-1}, what is similar to the values reported in coastal bays. The high biological activity in the estuaries (Kennish, 2019; Kennish, 2017) together with the higher potential influx of selenium from urban and industrial areas, may explain higher levels of volatile Se in estuaries compared to coastal bays and oceans (Stewart et al., 2013).

The main component of volatile Se fraction appears to be DMSe in all studies except for the North Atlantic measurements, where the presence of the Se-S mixed compound DMSeS accounts for 56% (David Amouroux et al., 2001). The volatile methylated Se compounds in estuarine and seawaters occur mainly as DMSe, DMDSe and DMSeS with relative contributions depending on the marine environment. Compared to terrestrial ecosystems where DMSe is dominant, the marine biosphere appears to be more complex with variable ratios between methylated Se species (see Table C1.9) (Wen & Carignan, 2007).

Table C1.9. Dissolved volatile Se total concentrations (in pg L^{-1}) and speciation (%) in estuarine systems and seawaters.

Site	TVSe	DMSe	DMSeS	DMDSe	References
Oceanic and Sea waters					
N. Atlantic	37–417	44	56	n.d.	(David Amouroux et al., 2001)
Mediterranean	20–75	64	36	n.d.	(David Amouroux & Donard, 1996)
Estuarine waters					
Rhine	37–2,423	73	23	4	Amouroux & Donard (1997); Tessier et al. (2002b)
Scheldt	51–8,067	84	12	4	
Gironde	22–1351	82	13	5	
Seine*	317–4,855	94	4	3	Lanceleur et al. (2019)
Coastal Bay					
Arcachon Bay*	30–426	81	14	5	Lanceleur et al. (2019)
Norway*	12–156	79	21	n.d.	

*Unpublished data from Tessier & Amouroux. extracted from *Lanceleur et al. (2019)*

1.5. Analytical methods for total selenium and speciation analysis at trace or ultratrace levels in waters

1.5.1. General aspects of the analysis of selenium in aquatic samples

Nowadays, the analysis of total Se is frequently achieved in the range of dozen ng L^{-1} while speciation determination remains complicated task due to low concentrations close to quantification limits and matrix interferences (Santos et al., 2015). To overcome these difficulties many methods have been investigated. Traditional techniques, such as atomic absorption spectroscopy and atomic fluorescence spectroscopy have been commonly coupled to hydride generation introduction system which has limited these methods to the detection of selenite. Total Se concentration is then measured after pre-treating the sample to transform all Se species to selenite. Nowadays, the use of inductively coupled plasma mass spectrometry (ICP–MS) has become the most powerful technique to detect Se, in thanks to the low sample required for the analysis and low detection limits of recent instruments.

In recent years, hyphenated techniques that combine a separation step with a sensitive and selective detector have decreased the limits of detection (LoD) and increased the number of species identified (Santos et al., 2015). The objective of this chapter is to review the existing techniques to determine total Se and its species, and expose critically the advantages and weaknesses of each method with specific attention to environmental aqueous matrices.

The development of methodologies to determine Se speciation must take into account the detection limit needed, the physicochemical properties of the matrix and its potential interferences (Santos et al., 2015). Secondly, an accurate quantification of Se species is subjected to adequate preservation and storage of the sample to avoid Se transformation processes (e.g. reduction or oxidation, volatilization, etc.) during or prior to the analysis. These processes depend on sample characteristics (pH, biota, salinity, etc.) storage conditions, i.e. temperature and light exposure, selenium concentration and container material among other factors (Conde & Sanz Alaejos, 1997; Palacios & Lobinski, 2007). In many studies, the samples are preserved in acidic media (Conde & Sanz Alaejos, 1997). When samples are preserved in acidic media for long time, selenite and reduced Se species are susceptible to oxidation (Mason et al., 2018). Selenate is more stable than selenite in aqueous solutions and less dependent on the acidic conditions of the sample. The stability of the samples must be tested for each environmental matrix and conditions. Some authors have reported that the optimum temperature at which there is no significant risk of inorganic selenium losses at 10 and 50 µg

Se L^{-1} concentration levels over 12 months is -20 ºC, however the water samples generally present lower concentration and are rarely conserved at this temperature (Palacios & Lobinski, 2007; Pyrzynska, 1996). Samples preserved at -20 ºC do not need to be acidified, which is an advantage to prevent redox transformations of oxyanions. However, little is known about the stability of reduced Se species in acidic conditions. In addition, acidified samples may require sample dilution for some detection methods, e.g. hydride generation (Pyrzynska, 1996) and may affect the pH of the mobile phase when using chromatographic techniques.

Nowadays, the performance of analytical Se speciation has improved significantly, providing both good separation of inorganic Se species and detection levels in the low ng Se L^{-1} range (Pettine et al., 2015). Whilst, the quantitative evaluation of reduced and elemental selenium is still problematic (Chen et al., 2006; Lenz et al., 2008; Oram et al., 2008). Due to its insolubility, elemental Se (Se(0)) is commonly found in colloidal form. Moreover, the composition of reduced Se species is still unknown in most cases. Gao et al., (2000) suggested that Se(0) may be one of the largest pool of Se in aquatic systems, accounting for about 30 – 60% of total Se in sediments. The identification of certain Se species, in particular reduced Se forms, is difficult due to the unavailability of certified reference materials (Pettine et al., 2015). Instead, some authors provided an indirect estimation of the reduced Se fraction based on the subtraction of inorganic Se oxyanions from total Se: Red. Se = TDSe – Se(IV) – Se(VI) (Cutter & Bruland, 1984; Nishri et al., 1999; Velinsky & Cutter, 1991). Therefore, from now on, when Red. Se is mentioned in the text, it will refer to this estimation.

1.5.2. The detection of Se using ICP-MS

Since its commercialization in 1983, ICP-MS has become the most powerful technique for Se detection thanks to the low detection limits (in the low range of ng Se L^{-1}) and faster analysis times compared to other detectors. In this section, the principle of the instrument and an overview of its limitation for Se analysis is presented.

1.5.2.1. The principles of ICP-MS

ICP–MS systems are composed of a nebulizer, spray chamber, plasma torch, interface cones, vacuum chamber, ion optics, mass discriminator and, finally a mass spectrometer as detector (Figure C1.7). Liquid samples can be directly pumped to the ICP–MS using a peristaltic pump at variable flow rates, typically up to 1 mL min^{-1} (Thomas, 2013). The nebulizer turns the liquid sample into an aerosol and droplets are carried to the torch by the cooling gas, which is

a constant Ar stream at about 15 mL min^{-1} (Thomas, 2013). Only a small fraction of the injected sample enters the torch (1-2% of the injected volume). After larger droplets removal at spray chamber, fine aerosol droplets are vaporized, atomized and ionized in the plasma torch, which works at temperatures ~10,000 K. Such temperature is generated by radiofrequency (RF) generator and produces positively charged ions. The ions are extracted through a pair of interface cones and focused by the extraction lenses (also called ion optics) in an ion beam to reach the mass spectrometer (MS). This interface is set up to eliminate photons and neutral species, avoiding potential interferences and background noise (Thomas, 2013).

The MS detector is always composed by a quadrupole to discriminate the mass to charge ratios (m/z) of selected ions. To avoid ions path scatter, it works at high vacuum (10^{-6} torr). The quadrupole serves as mass discriminator and can be adjusted to monitor multiple masses to charge ratios in the same analysis. Selenium isotopes may suffer interferences associated to the formation of $^{40}Ar–^{40}Ar^{+}$ or $^{40}Ar–^{38}Cl^{+}$ and other dimers as detailed in Table C1.10. In order to decrease such interferences, some instruments add a collision/reaction cell (C/RC), consisting of hexa- or octopole to reduce polyatomic spectral interferences using He as collision gas and H_2 as reaction cell gas (Darrouzès et al., 2005b).

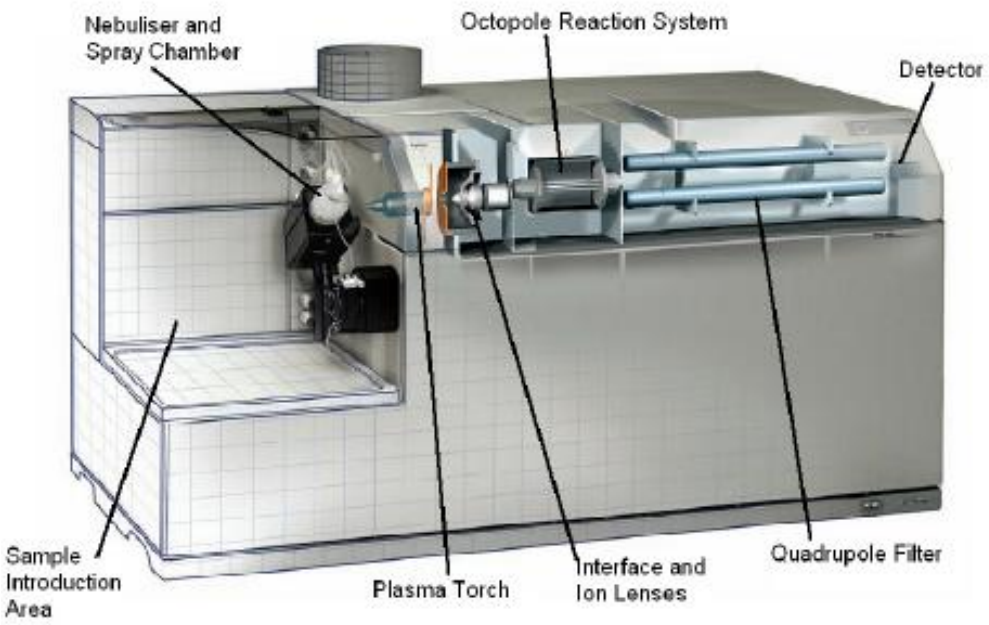

Figure C1.6. Overview of an Agilent 7500cx ICP-MS system equipped with an octopole collision/reaction cell, image from *(Aries, 2011)*.

1.5.2.2. Limitations of ICP-MS

The main drawback of the ICP–MS for Se detection in the unavoidable use of argon as carrier and plasma gas resulting in polyatomic interferences, the $^{40}Ar–^{40}Ar^{+}$ dimer, directly interfering with the most abundant Se isotope. In addition, selenium has a high first ionization potential compared to Ar which complicates Se ionization. Other common ions present in the sample (*i.e.* waters), such as chlorine, calcium or potassium can also become problematic due to the formation of polyatomic spectral interferents (Tolu, 2012). A complete list of the spectral interferences for Se is shown in Table C1.10. These interferences are quantitatively reduced with the use of C/RC with operating conditions appropriately optimized for specific matrix. Darrouzès et al., (2005a), demonstrated for an Agilent 7500c ICP–MS that the use of H_2 resulted in a better sensitivity than the use of He, the most common collision cell gas. The use of H_2 decreased the signal intensities of analyte Se ions. Helium did not allow a quantitative elimination of ^{80}Se interferences, but it kept constant the signal intensity of intermediate to high m/z species, probably due to thermalization and focalization effects (Darrouzès et al., 2005a). Other potential interferences, mainly caused by the formation of oxides (from Ni and Zn) or doubly charged (from lanthanides) ions are much less common in waters.

1.5.3. Non-chromatographic methods for Se speciation

In this section, a review of the main off-line and on-line non-chromatographic methods that exist for Se speciation analysis in water samples is presented. The aim is to show the main features of off-line methods (*i.e.* low detection limits but time consuming sample pre-treatment) versus the existing on-line non-chromatographic methods that typically reduce the analysis time, but present higher detection limits. At the end of this section, a summary of the analytical non-chromatographic methods is presented at Table C1.11.

1.5.3.1. Sequential hydride generation followed by atomic absorption or atomic fluorescence spectroscopy

Probably hydride generation (HG) is the most widely applied non-chromatographic method for Se speciation. HG is a relatively cheap and easy sample introduction technique. Because of this, it is still a widely used technique despite its limitations. It profits that only Se(IV) forms volatile SeH_2 in the presence of borohydride (BH_4^-) (Cutter, 1978; D'Ulivo et al., 2005). The fact that HG is able to volatilize only selenite means that Se species must be pre-treated to transform them into Se(IV) which is a considerable drawback. Using HG, selenite, selenite +

selenate, and total Se are the typical fractions quantified following different sample pre-treatments.

Table C1.10. Spectral interferences for Se isotopes divided by type of interference (isobaric, polyatomic and oxides). Extracted from Darrouzès et al., (2005) and Tolu (2012).

	^{74}Se	**^{76}Se**	**^{77}Se**	**^{78}Se**	**^{80}Se**	**^{82}Se**
			Isobaric			
	$^{74}Ge^{+}$	$^{76}Ge^{+}$		^{78}Kr	^{80}Kr	^{82}Kr
			Polyatomic (due to Ar)			
	$^{36}Ar^{38}Ar^{+}$	$^{38}Ar^{38}Ar^{+}$	$^{36}Ar^{40}Ar^{1}H^{+}$	$^{38}Ar^{40}Ar^{+}$	$^{40}Ar^{40}Ar^{+}$	$^{40}Ar_2{}^{1}H^{2+}$
	$^{38}Ar^{36}S^{+}$	$^{40}Ar^{36}Ar^{+}$	$^{40}ArCl^{37+}$	$^{38}Ar^{40}Ca^{+}$	$^{40}Ar^{40}Ca^{+}$	$^{38}Ar^{44}Ca^{+}$
	$^{40}Ar^{34}S^{+}$	$^{40}Ar^{36}S^{+}$	$^{41}K^{36}Ar^{+}$	$^{40}Ar^{37}Cl^{1}H^{+}$		$^{40}Ar^{42}Ca^{+}$
		$^{42}Ar^{34}S^{+}$	$^{38}Ar_2{}^{1}H^{+}$			
		$^{40}Ca^{36}Ar^{+}$	$^{39}K^{38}Ar^{+}$			
			Polyatomic (non-related to Ar)			
	$^{37}Cl^{37}Cl^{+}$	$^{64}Zn^{12}C^{+}$	$^{42}Ca^{35}Cl^{+}$	$^{44}Ca^{34}S^{+}$	$^{32}S^{16}O^{3+}$	$^{12}C^{35}Cl^{2+}$
		$^{39}K^{37}Cl^{+}$	$^{40}Ca^{37}Cl^{+}$	$^{66}Zn^{12}C^{+}$	$^{68}Zn^{12}C^{+}$	$^{34}S^{16}O^{3+}$
		$^{40}Ca^{36}S^{+}$	$^{65}Cu^{12}C^{+}$	$^{41}K^{37}Cl^{+}$	$^{79}Br^{1}H^{+}$	$^{81}Br^{1}H^{+}$
		$^{42}Ca^{34}S^{+}$	$^{63}Cu^{14}N^{+}$	$^{64}Ni^{14}N^{+}$		$^{68}Zn^{14}N^{+}$
		$^{41}K^{35}Cl^{+}$		$^{64}Zn^{14}N^{+}$		$^{12}C^{35}Cl^{2+}$
		$^{31}P_2{}^{14}N^{+}$		$^{63}Cu^{14}N^{1}H^{+}$		
				$^{31}P_2{}^{16}O^{+}$		
			Oxides			
		$^{60}Ni^{16}O^{+}$	$^{61}Ni^{16}O^{+}$	$^{62}Ni^{16}O^{+}$	$^{64}Ni^{16}O^{+}$	$^{62}Zn^{16}O^{+}$
					$^{64}Zn^{16}O^{+}$	
Doubly charged	$^{148}Nd^{++}$ $^{148}Sm^{++}$	$^{152}Sm^{++}$ $^{152}Eu^{++}$	$^{154}Sm^{++}$ $^{142}Gd^{++}$	$^{156}Gd^{++}$ $^{156}Dy^{++}$	$^{160}Gd^{++}$ $^{160}Dy^{++}$	$^{160}Dy^{++}$ $^{162}Er^{++}$

In brief, selenite can be directly analyzed without any treatment in samples acidified to pH 2 with HCl (Zhang et al., 1999). The fraction Se(IV) + Se(VI) can be obtained after the reduction of Se(VI) to Se(IV) by reaction with HBr, HBr/$KBrO_3$, HCl or HCl/KBr at high temperature (80 – 100 ºC)(Pettine et al., 2015). UV photolysis in alkaline or acid solution can be also used for the same purpose. Moreover, an alternative approach consists on heating the sample with 2 –

6 M HCl in a microwave oven at 90–100 ºC for 20 – 45 min. If samples contain reduced Se species, their oxidation to selenite, can be carried out with 0.04 M potassium peroxodisulfate solution in HCl. Total Se requires a first step in which the quantitative oxidation of all selenite compounds to selenate is achieved. For that, strong oxidants such as H_2O_2 or persulfate ($K_2S_2O_8$ or $(NH_4)_2S_2O_8$) are employed. Thereafter, selenate must be converted into selenite for the analysis, employing the method already presented above (Zhang et al., 1999). A schematic overview of the hydride generation coupled to AAS is shown in Figure C1.7.

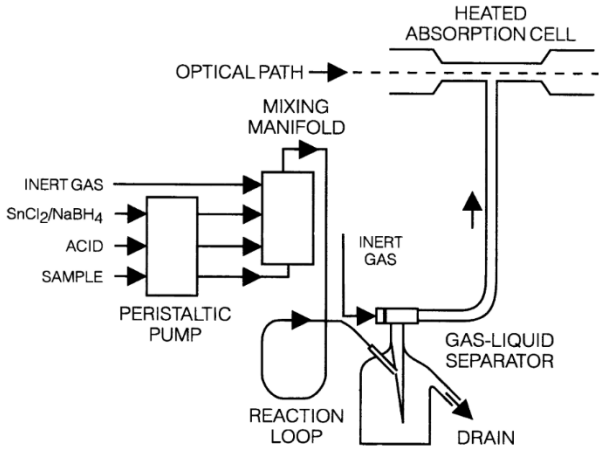

Figure C1.7. Left: Schematic diagram of a continuous flow injection (FI) coupled to hydrige generation atomic absorption spectroscopy (HG-AAS) system (Kumar & Riyazuddin, 2006). Right: Example of the signal obtained from FI-HG-AAS for several Se species. The reagents introduced consisted in 0.3% sodium borohydride in 0.1% sodium hydroxide with 3 M HCl and SnCl2 as solid catalizer; sample volume 500 mL.

Using HG methods for sample introduction, reduced Se fraction is operationally defined as the difference between total Se and (Se(IV)+Se(VI)) determinations, as a consequence, the Red.Se fraction includes elemental Se and Se(-II) but it cannot be described in further detail (Cutter & Cutter, 2004). Furthermore, conventional HG techniques can suffer serious liquid phase interference from several transition metal ions (such as Cu^{2+}, Ni^{2+} and Co^{2+}). This interference is most probably caused by the interaction of the Se hydride with either reduced metals or metal borides (formed after reaction with $NaBH_4$) (Tao & Sturgeon, 1999). Additionally, such types of analyses are vulnerable to overestimation of some fractions as they assume that only specific Se species are reactive to the applied method, which can result in systematic over- or under-estimation of the real content of Se in some fractions (LeBlanc et al., 2018; Pettine et al., 2015). For example, a significant error during Se analysis using hydride generation is the potential overestimation of Se(IV) caused by the presence of volatile Se compounds, in

particular DMSe (Moreno et al., 2003), or other organic Se compounds that can react with $NaBH_4$. Most publications using HG methods, do not take in consideration the volatile fraction that could potentially be quantified with selenite.

HG is typically coupled to Flameless atomic absorption spectroscopy or to Atomic fluorescence spectroscopy, however it has been also used coupled to inductively coupled plasma mass spectrometry (Hall & Pelchat, 1997; Nishri et al., 1999; Olson et a., 1995). Herein, a description and comparison of the most common detector performances is presented.

Flame atomic absorption spectroscopy (FAAS). Two configurations are the most common (D'Ulivo et al., 2002; Pettine et al., 2015): hydride generation with quartz tube atomization (HG-AAS) and hydride generation with in situ trapping in an electrothermal atomizer (graphite furnace) (HG-ETAAS). The couplings HG-AAS and HG-ETAAS offer reduced chemical interferences compared to ETAAS. However HG-AAS and HG-ETAAS require larger sample volumes than ETAAS (Stripeikis et al., 2004).

HG-ETAAS allows preconcentration and better control of interferences both in the liquid phase and in the atomization step compared to HG-AAS (D'Ulivo et al., 2002; Pettine et al., 2015). The use of a graphite furnace reduces sample volume required for the analysis and the limit of detection. Therefore, despite the longer analysis time of HG-ETAAS in comparison to HG-AAS, when the sample volume is limited or the concentration of Se species is very low, the coupling of ETAAS seems the most convenient detector after hydride generation.

Sample pre-treatment is typically the most time consuming step of methods using hydride generation. To minimize the sample pre-treatment and reduce analysis time, several online methods exist. An example is flow injection (FI) system coupled to HG-AAS presented in Figure C1.7. However, a sample containing a mixture of Se amino acid species would require a previous separation step, for example using high pressure liquid chromatography (Chatterjee & Irgolic, 1998). Flow injection, BH_4^- is added online to the sample and it reacts to form the corresponding hydrides in a mixing loop. If needed, a pre-reduction of Se(VI) to Se(IV) can be achieved adding a heated and acidified mixing loop (Wallschläger & Bloom, 2001) or an online microwave digestion process (Moreno, 2000). These online methods are widely applied, mostly for inorganic Se speciation. When coupled with a flow injection (FI) technique, HG-ETAAS Se speciation presents detection limits of hundreds of ng Se L^{-1} (Gallignani et al., 2000; Kumar & Riyazuddin, 2006).

Atomic fluorescence spectroscopy (AFS). AFS is well suited for coupling with HG using small hydrogen-argon diffusion flames as atomizers. In 2005, Chen et al., (2005) developed an off-line speciation method for Se(IV) and Se(IV) + Red. Se. The proposed methodology consisted in a direct measurement of selenite in 3M HCl, and selenite + Red. Se was measured after UV irradiation for 2.5 h in an acidic solution (0.154 M of HNO_3), while total selenium was measured after UV irradiation in 3M HCl. This method presented a LoD of 5 ng Se L^{-1}, however large sample volume would be required considering a flow rate of 9 mL min^{-1} and 60 minutes to complete the analysis in the case of selenite. In order to reduce the time of sample pre-treatment, Tyson & Palmer (2009) have described the use of a flow-injection system in which Se(VI) is reduced to Se(IV) by using either microwave-assisted reduction with hydrochloric acid at 6M or 12M without the need of microwave radiation (Tyson & Palmer, 2009). Once converted to the gaseous hydrides, selenite and selenate were determined in AFS system. An example of the system is presented in Figure C1.8.

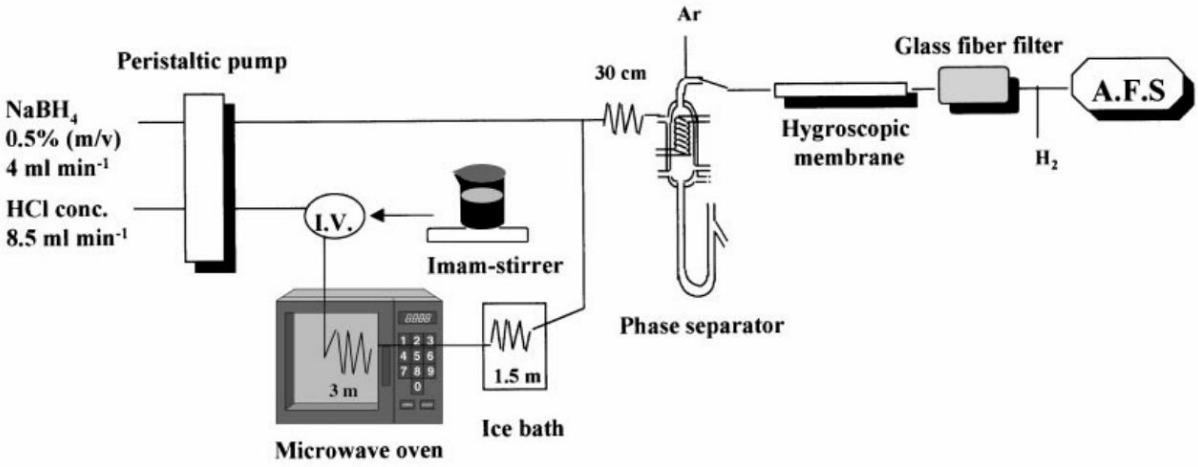

Figure C1.8. Schematic overview of an on-line microwave assisted digestion system coupled to FI-HG-AFS. Extracted from (Moreno et al., 2000).

Table C1.11. Compilation of analytical methods used since the 70's decade to analyze selenium speciation. Data are classified in different categories: HG-AAS, HG-AFS, other techniques separating off- and on-line speciation. These methods only detect Se(IV); therefore, other species were previously converted to Se(IV) or calculated operationally. Detection limits are presented in ng Se L^{-1}. †ng Se kg^{-1}. n.d.=not determined.

Method	LoD	Matrix	Reference
		Off-line speciation	
HG–AAS	5	Lake, Seawater California, USA	Cutter (1978)
HG–AAS	0.79	Saanich fjord, Canada	Cutter (1982)
HG–AAS	0.79†	Pacific Ocean	Cutter & Bruland (1984)
HG–AAS	0.79†	San Francisco Bay, USA	Cutter (1989)
HG–AAS	1.58	San Joaquin Valley, USA	Cooke & Bruland (1987)
HG–AAS	1.58	San Francisco Bay, USA	Cutter & Cutter (2004)
ETAAS	30	Tap and mineral waters, Turkey	Tuzen et al. (2006)
ETAAS	10	Tap and Sea water, Turkey	Saygi et al. (2006)
ETAAS	0.79	Seawater, New Zealand	Sherrard et al. (2004)
ETAAS	4.6	Tap and mineral water, Turkey	Panhwar et al. (2017)
		On-line speciation	
FI–HG–AAS	250 – 300	Standards	Gallignani et al. (2000)
FI–HG–AAS	150	Groundwaters, India	Kumar & Riyazuddin (2006, 2011)
ED[a]–ETAAS	1000	River, tap and seawater, Iran	Najafi et al. (2010)

Table C1.11. (Continued)

Method	LoD	Matrix	Reference
HG–AFS	4.7 – 7.1	Bohai Bay, China	Yao & Zhang (2005)
HG–AFS	6.3	Bohai Bay, China	Duan et al. (2010)
HG–AFS	5	Standards	Chen et al. (2005)
HG–AFS	10.5	Canadian Lakes	Ponton & Hare (2013)
HG–AFS	20	Mining wastewaters, China	Zhang et al. (2014)
TiO_2-HG-AFS	24 – 42	River waters, China	Fu et al. (2012)
FI-HG-AFS	n.d.	Waste water	Moreno et al. (2000)
		Other techniques	
HG-ICP-MS	5	Kinneret Lake, Israel	Nishri et al. (1999)
CPE-ETV[b]-AAS	2.5	Tap and ground waters	Sounderajan et al. (2010)
HS-LPME[c]-ETV-AAS	5 – 6	Spiked river, sea and waste waters	Ghasemi et al. (2012)
CE-HG-AFS	$(25 – 30) \cdot 10^3$	River water	Lu and Yan (2005)
CE-ICP-MS	1270 – 2310	Groundwater	Liu et al. (2014)

[a]ED: Electrodeposition

[b]CPE-ETV: selective cloud point extraction - electrothermal vaporization

[c]HS-LPME: Head-space liquid phase microextraction

Considering the low Se concentration in some environments, preconcentration seems a good addition to HG-AFS. For example, Fu et al. (2012) presented a method to preconcentrate selenite and selenate based on the use of nano-sized TiO_2 colloid as selective adsorbent for Se(IV) and Se(VI). The range of pH between 6.0 – 7.0 allows the selective adsorption of selenite. Coupled to HG-AFS, the colloid with adorbed Se can be directly measured, thereby desorption step is no longer necessary. The detection limit of this method was 24 and 42 ng Se L^{-1} for selenite and selenate respectively for 100 mL sample. (Fu et al., 2012; Gallignani et al., 2000; Kumar & Riyazuddin, 2006, 2011).

In conclusion, hydride generation coupled to atomic absorption detectors is a low cost technique that can be useful for the detection of inorganic Se species. However, HG requires large sample volumes and several pre-treatments for the identification of Se species. Moreover, the reduced Se fraction cannot be analyzed directly and it is required an oxidation process to convert reduced compound(s) into selenite, which precludes the identification of reduced Se species. The development of on-line procedures has reduced the pre-treatment time required for each analysis; however, it has a cost in term of detection limits that are much higher for on-line procedures compared to off-line ones. In order to reduce the limit of detection, atomic fluorescence spectroscopy detectors can be used. Nowadays, the limits of detection of HG-AAS or HG-AFS are good enough for selenium speciation quantification in real water samples (Table C1.11). Nevertheless, these techniques cannot be used to identify the composition of the reduced Se species present in the environment.

1.5.3.2. Photochemical vapor generation

Ultraviolet (chemical) vapor generation (UV-VG), also known as photochemical vapor generation (PVG), is based in the selective production of volatile Se species from selenite. Se(IV) can be converted into volatile Se hydride, selenium carbonyl, dimethyl selenide and diethyl selenide in the presence of formic, acetic, propionic and malonic acids respectively. These methods require pre-treatments to convert Se species into selenite prior to the analysis. Such conversion can be carried out applying the same procedures detailed for hydride generation. Therefore, PVG presents the same limitations when the objective is the identification of reduced Se species. The production of volatile Se compounds is achieved introducing selenite samples containing low amounts of acid in the photochemical reactor. After a 2 minutes irradiation, sample is pumped to the head of the cryogenic trap for its preconcentration prior to the analysis (Guo et al., 2003). The schematic overview of the coupling of UV photochemical reactor to AAS, ICP-MS and GC-MS is presented in Figure C1.9.

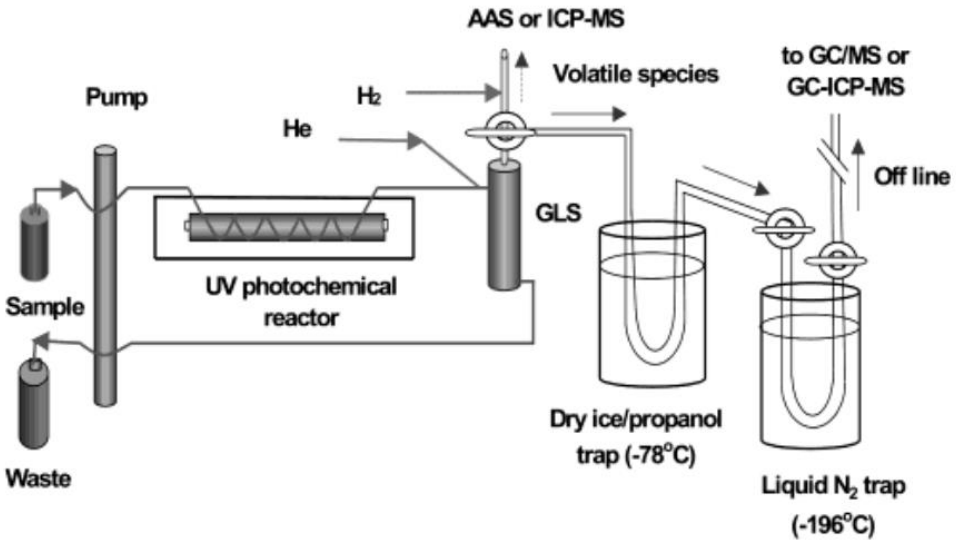

Figure C1.9. Schematic view of an UV-PVG system coupled to AAS or ICP-MS for non-volatile Se speciation and coupled to a cryogenic trap followed by an GC-MS or GC-ICP-MS for volatile Se speciation. (Guo et al., 2003).

Wang et al., (2004) developed the on-line reduction of selenate obtaining a detection limit of 13 ng Se L^{-1} when using PVG coupled to AFS as detector. It consisted in a glass fiber coated with nano-TiO_2 fixed in a quartz capillary to achieve the on-line reduction of Se(VI) under UV-irradiation in a flow system. Zheng et al. (2008) studied the water boiling bath conditions using nano-TiO_2 as catalyst for the determination of both selenite and selenate. Limits of detection were in the range between 20-100 ng Se L^{-1} depending on the detector and the organic acid employed. The lowest limit of detection was achieved coupling PVG to ICP-MS.

As happened with HG system, PVG considers that volatile Se compounds will proceed exclusively from Se(IV), not considering the potential reactivity of reduced Se that may cause important interferences. In addition, this technique is as limited as HG for the identification of reduced Se species. Moreover, some organic Se compounds such as SeMet, MeSeCys, $SeCys_2$ or Se-urea are susceptible to photo-oxidation under UV light in aqueous matrices (Amouroux et al., 2000; Chen et al., 2005). Therefore, it is possible that some studies using this technique (Wang et al., 2004) may have potentially overestimated the inorganic Se content in aqueous samples (LeBlanc et al., 2018).

1.2.3.3. Voltammetry

Even if voltammetry methods are not the most common method for Se analysis, they have been applied by several authors to study total Se and Se(IV) content in natural waters (do Nascimento et al., 2009; Grabarczyk & Korolczuk, 2010; Long & Nagaosa, 2007; Mattsson et al., 1995). Cathodic stripping voltammetry (CSV) is sensitive to Se(IV). The reduction of Se(VI) to Se(IV) requires a very positive standard potential. which means that selenate quantification using CSV requires sample pre-treatment to reduce Se(VI) to Se(IV) (Pettine et al., 2015).

Cathodic stripping voltammetry (CSV) with a hanging mercury drop electrode (HMDE) or a thin mercury film electrode as the working electrode is often used for selenium preconcentration (Stará & Kopanica, 1988). Despite the potential of this technique for preconcentration of Se species, the methodology requires having Se in the form of selenite. Therefore, quantification of selenate requires a pre-reduction of Se(VI) to Se(IV). Moreover, most studies do not consider the study of reduced Se species for total Se, quantifying total Se as the sum of inorganic Se species (Pettine et al., 2015; Stará & Kopanica, 1988).

Cathodic stripping voltammetry consist on the transformation of Se(IV) into an hydrophobic chelate using the 3,3'-diaminobenzidine on a Hg electrode. It involves the formation of HgSe at a deposition potential between +0.05 V and -0.35 V, followed by the reduction of HgSe during the cathodic polarization of the electrode. Selenium is accumulated by electro-reduction either in the form of HgSe (Kovaleva et al., 2006; Rubinskaya et al., 2003; Stará & Kopanica, 1988) or as intermetallic compounds, such as copper-selenium and rhodium–selenium, if Cu or Rh are used as reagents (Pettine et al., 2015). Grabarczyk & Korolczuk (2010) used $Cu(NO_3)_2$ at 0.4 mM and 0.1M of $HClO_4$ to achieve the reduction of Se(IV) to Se(-II) in the form of Cu_2Se. The procedure consisted in a first step of deoxygenation with nitrogen for 5 min and simultaneous removal of the organic matter present in the sample by adsorption on Amberlite XAD-7 resin to reduce organic matter and surfactant interferences. Second step consisted in the accumulation of Cu_2Se in the surface of a mercury electrode decreasing at –0.35 V for 30 s. Se(IV) detection limit was about 62 ng Se L^{-1} (Grabarczyk & Korolczuk, 2010). Therefore, CSV can be useful for the determination of inorganic Se species (Stará & Kopanica, 1988) but it is not suitable for reduced Se species determination (Table C1.12).

Table C1.12. Vapor generation, voltammetry and other non-chromatographic methods for Se speciation. All methods presented in this table are sensitive to selenite; thereby other species are calculated operationally or transformed prior to the detection. Limits of detection are in ng Se L^{-1}.

Method	Species	LoD	Matrix	Reference
(On-line) Vapor generation				
TiO_2-UV-VG-AAS	Se(IV)	2500	Ottawa River and seawaters	Guo et al. (2003)
TiO2-UV-VG-AFS	Se(IV)	13	Artificial sample	Wang et al. (2004)
TiO_2-VG-AFS TiO_2-VG-ICP-MS	Se(IV) Se(VI)	20-100 20	Water CRM[a], mineral, tap and waste waters	Zheng et al. (2008)
Voltammetry				
DPCSV[b]	Se(IV)	400	Standards	Stará & Kopanica (1988)
Hg-film ED[c]-CSV	Se(IV)	100	Spiked waters	Rubinskaya et al. (2003)
AC[d]-SWV[e]	Se(IV) Se(VI)	10	(Unspecified) water samples	Bertolino et al. (2006)
Plated Bi-film ED-CSV	Se(IV)	25	Kuzury River and coastal water (Japan)	Long & Nagaosa (2007)
UV-CSV	Se(IV) Se(VI)	30	Seawater	do Nascimento et al. (2009)
DPCSV[b]	Se(IV) Se(VI)	0.37	Caspian Sea and saline lakes	Ashournia & Aliakbar (2009, 2010)

Table C1.12 (Continued)

Method	Species	LoD	Matrix	Reference
ED-DPCSV	Se(IV)	62	Bystrzyca River and Zemborzyce Lake (Poland)	Grabarczyk & Korolczuk (2010)
ED-CSV	Se(IV) Se(VI)	65-210	Spiked tap water	Merino et al. (2019)

[a]CRM: certified reference material

[b]DP-CSV: Differential pulse cathodic stripping voltammetry

[c]ED: Electro-deposition

[d]AC: Activated carbon

[e]SWV: Square-wave voltammetry

As reviewed by Pettine et al. (2015), Ashournia & Aliakbar (2009, 2010) developed a method to improve selenite adsorption on the Hg electrode. The method optimized the adsorption efficiency by accumulation of SeI_2 and 5-nitropiazselenol on a thin mercury film electrode without applying potential, which minimized the interferences. After self-accumulation of piazselenol, stripping was carried out in a 10 mL separate deaerated solution of 0.05 M HCl and quantified by differential pulse CSV. Natural waters are 10 times preconcentrated using this method, giving detection limits of 60 ng L^{-1} (Ashournia & Aliakbar, 2010).

Methods using voltammetry may be useful in some cases. However, they require multiple steps sample pre-treatment and analysis. Long time analysis drastically reduces the attractiveness of these methods considering that there are other alternatives.

1.5.4 Chromatographic methods

1.5.4.1. Liquid Chromatography

High pressure liquid chromatography (HPLC) is nowadays the most powerful separation method for the purpose of selenium speciation. HPLC offers great versatility in thanks to the wide variety of chromatographic columns in the market. HPLC is very easily coupled to other techniques such as ICP-MS (Thomas et al., 1998). Due to the presence of Se oxyanions in almost all water types, the most common chromatographic columns employed are anionic exchange columns (AEC). Reversed phase (RP) chromatography has also been widely used for Se speciation, but it is more frequently used in biological matrices. Other stationary phases such as porous graphitic carbon (PGC) (Dauthieu et al., 2006) or mixed-mode columns (Vriens et al., 2014) have been also proposed in much lesser amount.

HPLC can be easily coupled to different detectors such as ETAAS, atomic emission spectroscopy (AES) or ICP–MS among others. Due to the low concentration of total Se and its species in non-polluted waters, very low detection limits are required for Se analysis, which turns ICP-MS into the most suitable detector for Se species at trace or ultra-trace levels (Table C1.13.). In addition, the coupling of HPLC to ICP–MS is generally direct and much easier than for other sampling introduction methods, such as HG. A schematic example of an on-line Se speciation system by HPLC-UV-HG-ICP is presented here below (Figure C1.10). It corresponds to the method developed by Darrouzès et al. (2008) and consisted in the use of a Hamilton PRP-X100 anionic exchange column (AEC) column to separate the Se species, followed by an online UV-HG system to improve the detection limit and eliminate the bromine interferences, and coupled to an ICP-MS as detector (see Figure C1.10).

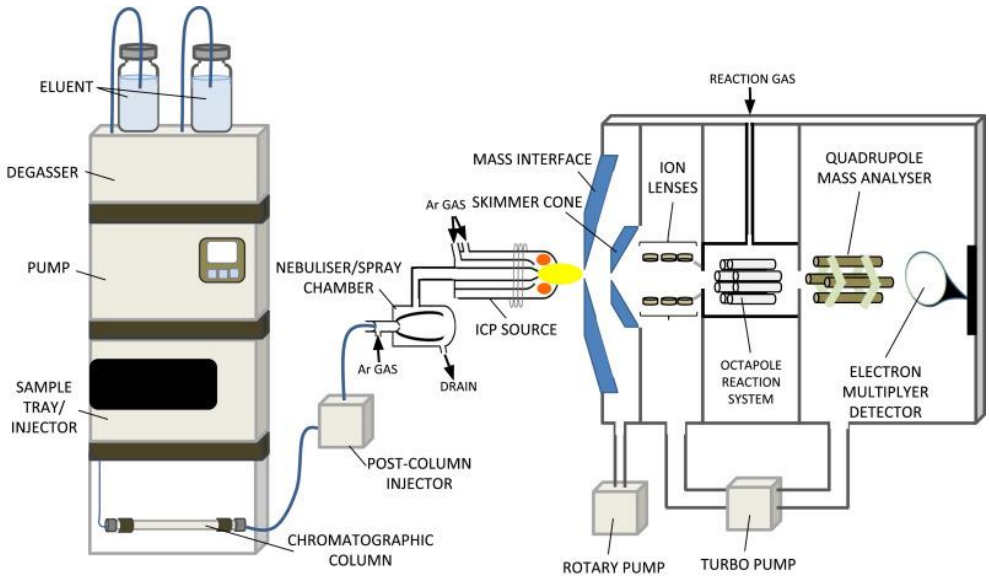

Figure C1.10. Example of an online HPLC–ICP–MS equipped with an octopole reaction system. Image extracted from Delafiori et al., (2016).

Reversed phase chromatography (RP). Reversed phase chromatography columns consist in a hydrophobic stationary phase, typically a silica-bonded octyl (C_8) or octadecyl carbon chain (C_{18}). The principle of RP chromatography is simple: the most hydrophobic the analytes are, the more retained they will be in the stationary phase (Neue, 2007). Typical mobile phase contains a tetrabutylammonium salt (TBAH) in isocratic water-methanol solution. The use of TBAH as ion-pairing agent allowed most authors to separate inorganic Se species, thus Se(IV) and Se(VI), in less than 10 minutes, being selenate the most retained Se compound (Guerin et al., 1999). As can be seen in Table C1.13., limits of detection vary depending on the chromatographic column size, the mobile phase conditions and the detector. In general, methods coupled to ICP-MS present the lowest LoD compared to other detectors with similar separation conditions.

Anionic exchange chromatography (AEC). In this type of chromatography, the higher negatively charged compounds will present larger retention times. AEC is very effective for selenium oxyanions; however, organo-selenium compounds (including SeMet) exhibit poor retention and resolution (LeBlanc et al., 2012). Hamilton PRP-X100 has been widely used in different matrices including water (Cai et al., 1995; Cobo-Fernandez et al., 1995). Most authors developed isocratic methods using phosphate, carbonate, citrate or phthalate anions as eluents; being Se(IV) and Se(VI) the main target species in most cases (Guerin et al., 1999) together with some seleno-amino acids, $TMSe^+$ and $SeCN^-$ (Bueno et al., 2005; Darrouzès et al., 2008; Leblanc & Wallschläger, 2016; Wallschläger & Bloom, 2001; Wallschläger & London,

2004) as it is shown in Table C1.13. The separation is generally achieved in less than 10 minutes (Cai et al., 1995; Chandrasekaran et al., 2009; Cobo-Fernandez et al., 1995; Laborda et al., 1993) or 15 minutes in other cases (Quijano et al., 1996; Wallschläger & London, 2004). Typically selenate is the higher retained species, only surpassed by selenocyanate (Wallschläger & Bloom, 2001; Wallschläger & London, 2004); meanwhile $TMSe^+$ is not retained using AEC and typically elutes in or very close to the void volume (Guerin et al., 1999).

Alternative chromatographic strategies. Few other stationary phases have been successfully applied to Se speciation in waters. Lindemann & Hintelmann (2002) achieved the separation of five Se amino acids (MeSeCys, SeMet, SeEt, SeCys and selenocystamine) within 16 minutes using a porous graphitic carbon. Authors applied a gradient using the ion-pairing agent heptafluorobutyric acid (HFBA) and MeOH as organic solvent (Table C1.13.). The use of HFBA increased retention times of Se amino acids while reducing peak width compared to pure water.

To our knowledge, only two methods found in the literature have addressed the analysis of real water samples using alternative stationary phases. They correspond to the use of a porous graphitic carbon (PGC) coupled to a ICP-MS (Dauthieu et al., 2006) and the mixed mode Omnipac PAX-500 column proposed by Vriens et al. (2014). The PGC stationary phase exhibits both hydrophobic and electronic interactions. Dauthieu et al. (2006) achieved the on-line preconcentration and speciation of selenite, selenate, SeMet, SeCys and SeEt in less than 10 minutes. This method was applied to mineral waters detecting only the presence of Se(VI). The Omnipac PAX-500 is a mixed-mode column that combines strong anionic exchange and reversed phase characteristics (ThermoScientific). Omnipac PAX-500 was recently employed in a minerotrophic peatland to study Se speciation in a minerotrophic peatland for the study of inorganic Se and methylseleninic acid (MeSeA), which was considered to be a reaction product of the volatile dimethyl diselenide directly detected in the aqueous samples (Vriens et al., 2014). Vriens et al. (2014) achieved the separation of methylseleninic acid (MeSeA), Se(IV) and Se(VI) in around 15 minutes in spiked waters and natural waters using a gradient between two mobile phases: a) H_2O at pH 8.4 and b) 30 mM NH_4NO_3 + 1% MeOH at pH 7.5. Considering the equilibration time of the column between analyses, the run time was about 25 minutes. This methodology showed detection limits between 100-170 ng Se L^{-1}.

Table C1.13. Reversed phase, anionic exchange and other chromatographic methods for Se speciation analysis. Limits of detection (LoD) are presented in ng Se L^{-1}, except for those marked with * absolute detection limit (ng Se) . Retention time (Rt) is given in minutes.

Method	Column details	Mobile Phase	Species (Rt)	LoD	Matrix	Reference
Reversed Phase						
RP[a]-ETAAS	C18 Altex Lichrosorb RP-1 10 µm (250 x 4.6 mm)	Gradient: A) 1mM TBAH B) MeOH, pH=7	Se(IV) (3.0) Se(VI) (16)	25*	Spiked synthetic river water	Guerin et al. (1999)
RP-DCP[b]-AES	C18 Waters µBondpak 10µm (150 x 3.9 mm)	2.5mM TBAH + 10mM K2HPO4 + 10mM KH2PO4, pH=6.55	Se(IV) (4.0) Se(VI) (6.0)	50*	Spiked waters	Guerin et al. (1999)
RP-ICP-AES	C18 Alltech Kromasil 10 µm (250 x 4.6 mm)	5mM TBAH phosphate buffer, pH=3.4 + 50% MeOH (v/v)	Se(IV) (3.3) Se(VI) (4.9)	Unspecified	Spiked tap water	Yang et al. (1996)
RP-ICP-MS	C18 Spherisorb ODS 5 µm (250 x 4.6 mm)	5mM TBAH phosphate buffer, pH=3.4 + 5% MeOH (v/v)	Se(IV) (<10) Se(VI) (<10)	1.25 2.00	Spiked waters	Cai et al. (1995)
RP-HHPN[c]-ICP-MS	C18 Eurospher RP 100 5 µm (60 x 4.6 mm)	10mM TBAH + 40% MeOH	Se(IV) (1.5) Se(VI) (2.7)	0.028	Spiked tap water	Jakubowski et al. (1996)

Table C1.13. (Continued)

Method	Column details	Mobile Phase	Species (Rt)	LoD	Matrix	Reference
			Anionic exchange			
AEC-AAS	ESA Anion III 10 µm (250 x 4 mm)	Gradient: potassium hydrogen phthalate A) 2mM, pH=9 B) 12mM, pH=9 + 20% MeOH (v/v)	TMSe (1.1) SeCys (1.6) Se(IV) (2.5) SeMet (3.9) Se(VI) (7.2) SeEt (8.3)	~10*	Standards	Guerin et al. (1999)
AEC-MW^{d}-HG-AAS	PBHamilton PRP-X100 10µm (250 x 4.1 mm)	0.1M phosphate buffer, pH=6.8	TMSe (1.8) Se(IV) (2.5) Se(VI) (4.3)	1.1* 1.4* 2.2*	Spiked tap water	Cobo-Fernandez et al. (1995)
AEC-ETAAS	SBNucleosil 100-SB 10µm (50 x 2 mm)	Gradient: 10mM ammonium citrate A) pH=3 B) pH=7	TMSe (1.2) Se(IV) (5.2) Se(VI) (8.8)	1.67 1.27 0.76	Spiked water	Laborda et al. (1993)

Table C1.13. (Continued)

Method	Column details	Mobile Phase	Species (Rt)	LoD	Matrix	Reference
AEC-ICP-MS	PBHamilton PRP-X100 10µm (250 x 4.6 mm)	80mM $(NH_4)_2CO_3$ / 80mM NH_4HCO_3	Se(IV) (3.3) Se(VI) (5.9)	0.40 0.42	Spiked water	Cai et al. (1995)
AEC-FI^e-ICP-MS	SBSpherisorb 5 ODS-AMINO 5µm (250 x 4.6 mm)	Gradient: A) 3.5mM and B) 7mM phosphate buffer pH=6	SeCys (3) SeMet (4.2) Se(IV) (6.3) Se(VI) (12.2)	0.20 0.10 0.16 0.12	Certified water for Se(IV) and Se(VI)	Quijano et al. (1996)
AEC-HG-AFS	AS-16, Dionex, Thermo	Gradient: NaOH A) 17.5mM B) 100mM C) 17.5mM	Se(IV) (6.5) Se(VI) (8.2) SeCN (12.7)	26 33 34	Gold mine waste water	Wallschläger & Bloom (2001)
AEC-HG-ICP-CR/C-MS	IonPac AS-16, Dionex, Thermo	Gradient: NaOH A) 10mM B) 100mM C) 10mM	Se(IV) (11.4) Se(VI) (14.9) SeCN (25.7)	0.15 0.17 0.19	Sea water and rain water	Wallschläger & London, (2004)
AEC-HG-AAS	Supelco LC-SAX1 5µm (250 x 4.6 mm)	Phosphate buffer, 5mM Na_2HPO_4, KH_2PO_4, pH=5.40	Se(IV) (1.7) Se(VI) (3.1)	2400 18600	Polluted groundwaters	Niedzielski (2005)

Table C1.13. (Continued)

Method	Column details	Mobile Phase	Species (Rt)	LoD	Matrix	Reference
AEC-HG-ICP-MS	IonPac AS17, Dionex (250 x 4mm)	18.8mM NaOH	Se(IV) (4.8) Se(VI) (9.7)	300 - 800	Well water, Punjab, India	Chandrasekaran et al. (2009)
AEC-ICP-CR/C-MS	IonPac AS-16, Dionex	Gradient: NaOH + 2% MeOH A) 100mM B) 10mM	SeMet (~15) Se(IV) (~33) Se(VI) (~36)	5	Standards and Porcupine River waters	LeBlanc et al. (2016)
AEC-ICP-ESI-MS/MS	IonPac AS-16, Dionex	Gradient: A) KOH + 5% MeOH B) H_2O + 5% MeOH				
Other stationary phases						
PGC-ICP-MS/MS	PGC Thermo Hypercarb 5 µm (100 x 2.1 mm)	Gradient: A) 7.5 mM HFBA, pH=3.5 B) MeOH	MeSeCys SeMet SeEt SeCys Se-cystamine	2100 2300 3100 2400 3400	Standards	Lindemann & Hintelmann (2002)

Table C1.13. (Continued)

Method	Column details	Mobile Phase	Species (Rt)	LoD	Matrix	Reference
PGC-ICP-CR/C-MS	PGC Thermo Hypercarb 5 µm (100 x 4.6 mm)	240mM HCOOH + 1% MeOH (v/v), pH=2.6	Se(IV) (3.2) Se(VI) (3.6) SeMet (5.3) SeCys (5.9) SeEt (8.2)	2 – 8	Commercial mineral waters	Dauthieu et al., (2006)
Mixed-mode HPLC-(HR)-ICP-MS	Omnipac PAX-500 (250 x 4mm)	Gradient: A) 30mM NH4NO3 + 1% MeOH, pH=7.5 B) H2O, pH=8.4	MeSeA (8.5) Se(IV) (9.5) Se(VI) (15)	150 100 170	Minerotrophic peatland waters	Vriens et al., (2014)

[a]RP: reversed phase

[b]DCP: direct current plasma

[c]HHPN: hydraulic high pressure nebulization

[d]MW: microwave oven

[e]FI: flow injection

1.5.4.2. Gas chromatography

Gas chromatography has been mainly applied for the study of volatile Se species, especially for DMSe, DMDSe, MeSeH and DMSeS. Few studies exist in the literature, they are presented in Table C1.14. Among the studies listed, it is necessary to remark that Thompson-Eagle et al., (1989) and Ghasemi & Farahani (2012) injected directly the head-space of the water samples, thus obtaining limits of detection much higher than other methods.

The major part of the methods proposed are based on the collection and purge of 1 liter of sample, bubbled with He or N_2 to degas the sample. A moisture trap at -20 ºC is subsequently connected to the system to dry the sample before in order to avoid potential interferences. Se compounds are typically trapped in the head of a silanized wool column immersed in liquid nitrogen. The compounds are trapped and preconcentrated at –190 ºC and sequentially desorbed increasing the temperature up to 200 or 300 ºC, depending on the method (Amouroux & Donard, 1996; Cooke & Bruland, 1987; Pécheyran et al., 1998; Tessier et al., 2002). A schematic overview of the system has been introduced in Figure C1.9.

In some cases, when it is not possible to purge and analyze on line the sample, a carbotrap may be used after the moisture trap instead of cryogenic trapping, in order to preconcentrate the Se compounds until the analysis. The carbotrap consists in a glass column filled with 1 cm^3 of activated charcoal. In that case, the compounds are thermally desorbed and collected in the head of the chromatographic column (Lanceleur et al., 2019).

Since volatile Se is present in natural waters in the range of pg Se L^{-1}, or in some cases, low ng Se L^{-1}, low detection limits are imperative (Wen & Carignan, 2007). Because of this, the preferred detector is ICP-MS. The described method based on purge trapping of 1L of sample followed by cryotrapping (PT-CT) coupled to ICP-MS has demonstrated detection limits between 0.1 - 0.5 pg Se L^{-1} (Lanceleur et al., 2019). Other detectors, such as AAS or AFS have also been employed, however detection limits were higher, from 71 to 158 pg Se L^{-1} for 2L sample purged using AAS and from 8 to 47 pg Se L^{-1} for 1L using AFS (Amouroux & Donard, 1996, 1997).

Gas chromatography has rarely been proposed to study Se oxyanions at it requires a previous derivatization process to transform Se(IV) into piazselenol. Gómez-Ariza et al., 1999, used 5 ml of 0.1% 4-chloro-*o*-phenilendiamine in 0.1 M HCl heated at 75 ºC for 7 minutes to quantitatively transform selenite into piazselenol. The solution was subsequently dried under

N_2 stream and dissolved in 50 µL of hexane. For quantification of selenate, a previous reduction must be done in order to transform Se(VI) into selenite. Other methodologies have been proposed for extraction of the piazselenol from the organic solvent. Ultrasound-assisted emulsification micro-extraction (USAEME) and dispersive liquid–liquid micro-extraction (DLLME) coupled to gas chromatography-flame ionization detection (GC-FID) was optimized by Najafi et al., 2012. Nevertheless, detection limits of 50 and 110 ng Se L^{-1} are much higher than those obtained using other techniques like HPLC-ICP-MS. Moreover, derivatization process implies not only pre-treatment but the need of multiple analyses for the speciation of inorganic Se species.

Table C1.14. Gas chromatographic methods applied to obtain volatile Se speciation in environmental waters. PT: purge trapping. CT: cryo-trapping. *Absolute detection limit (ρg Se).

Method	Column details	Ramp (º C)	Species	LoD (ρg Se L^{-1})	Matrix	Reference
CT-GC-AAS	5% OV on Chromosorb WHP (25 cm, 80-100 mesh)	−196 to 100	TVSe	100*	Surface water Kesterson reservoir, USA	Cooke & Bruland, (1987)
GC-HG-FID	Stainless steel column (10 m, 2.2 mm i.d.); liquid phase, 10% Carbowax 1000; solid support, Chrom W-AW; (mesh 60/80)	58 to 105	DMSe	$10 \cdot 10^6$	Head-space injection from surface water, USA	Thompson-Eagle & Frankenberger, (1991); Thompson-Eagle et al., (1989)
PT-CT-GC-AFS	Silanized glass packed column (U-tube 13 to 40 cm length, 6mm i.d., Chromosorb WHP, Supelco 60-80) coated with SP2100 10%	−190 to 300	DMSe DMDSe MeSeH	8 - 47	Seawater and estuarine waters	Amouroux & Donard, (1996, 1997); Pécheyran et al., (1998)
CT-GC-ICP-MS	Silanized glass packed column (U-tube 13 to 40 cm length, 6mm i.d., Chromosorb WHP, Supelco 60-80) coated with SP2100 10%	−190 to 300	DMSe DMDSe DMSeS	0.79 - 1.18	Gironde, Scheldt and Rhine estuarine surface waters (1-3m depth)	Amouroux et al., (1998); Tessier et al., (2002a; 2002b)
CT-GC-ICP-MS	Silanized glass packed column (U-tube 13 to 40 cm length, 6mm i.d., Chromosorb WHP, Supelco 60-80) coated with SP2100 10%	−190 to 300	DMSe DMDSe DMSeS	0.1 - 0.5	Thermokarst ponds, Canada	(Lanceleur et al., (2019)

Table C1.14. (Continued)

Method	Column details	Ramp (º C)	Species	LoD (ρg Se L^{-1})	Matrix	Reference
TiO_2-UV-VG-GC-ICP-MS	DB1 capillary column, J&W Scientific (1% phenyl, 99% poly(dimethylsiloxane)		DMSe DEt-Se SeCO	2500	Ottawa River and seawaters	Guo et al., (2003)
[a]USAEME-GC-FID [b]DLLME-GC-FID	30 m BP-5, fused-silica capillary column (0.32 mm i.d. and 0.5 µm film thickness, SGE)	100 to 260	Se(IV) Se(VI)	50,000 - 110,000	Caspian Sea, Haraz and Tajan Rivers, tap, drinking and waste water	Najafi et al., (2012)
HS-SPME-GC–MS	DB-624 fused silica capillary column (60 m × 0.25 mm i.d. × 1.40 µm film thickness)	50 to 250	DMSe DMDSe	11,000 - 16,000	Well, river, tap, waste waters (head-space air injection)	Ghasemi & Farahani, (2012)

[a]USAEME: ultrasound assisted emulsification micro-extraction

[b]DLLME: dispersive liquid-liquid micro-extraction

1.6. Objectives and presentation of the work

Selenium is an essential micronutrient for animal life and the growth of microorganisms. It is well known that algae and bacteria are responsible of the uptake and biotransformation of Se, however most mechanisms and species released to water remain unknown. In aquatic systems, selenium can be present in multiple oxidation states (VI, IV, 0, –II) in a wide variety of chemical forms that include selenate, selenite, elemental selenium and a great variety of reduced Se species that contain Se(–II), including organically bound Se species such as selenomethionine, selenocystine, trimethylselenonium ion and others species that have not been identified yet. In addition, the presence of volatile Se species, as dimethylselenide, dimethylselenide sulfide and dimethyldiselenide has been reported as well in aquatic systems, typically in the range of hundreds of pg Se L^{-1}. In fact, the presence of reduced Se species, that may include organically bound Se, has been reported as a non-negligible fraction of total Se in most aquatic systems. The literature review showed the lack of suitable methods able to identify reduced Se species at ultra-trace concentration levels. In fact, in most environmental studies, only selenite and selenate are identified and quantified. Afterwards, the concentration of reduced Se species is operationally estimated as the difference between the total dissolved Se and Se(IV) and Se(VI) contents. However, it has not yet been possible to identify which species compose the reduced Se fraction and in what proportion. This is why the development of methods allowing to obtain low detection limits, in the low range of ng Se L^{-1}, with operating conditions appropriate to pH value of natural waters is essential to improve the knowledge of biogeochemical Se processes that occur in the environment. In this regard, the use of HPLC-ICP/MS offers low detection limits while allowing the simultaneous analysis of more than one species.

Based on this knowledge and in order to obtain more insights on the biogeochemical cycle of Se in different aquatic ecosystems, this doctoral research work has the following objectives:

I. Develop a complementary, fast and robust analytical strategy that allows the simultaneous analysis of reduced and oxidized selenium species in different water matrices.

II. Expand current knowledge concerning the biogeochemical cycle of Se in aquatic systems based on two factors:

II.a. The evolution of the physicochemical and biological conditions of the water column driven by specific ecosystems functioning such as in eutrophic or oligotrophic lakes and in estuarine waters.

II.b. The evolution of Se speciation based on the detection of inorganic, organic/reduced and volatile Se compounds as a function of seasonal variations in such different aquatic ecosystems.

To achieve these objectives, this work is articulated in two parallel and complementary axes. First, the development of the analytical method carried out during this project is presented (Chapter 2). The originality of this analytical approach is based on the use of a mixed-mode stationary phase that combines reversed phase and anionic exchange. Second, three environmental studies have been carried out in parallel to the analytical method development to study the origin and fate of Se in real freshwater systems. This chapter is divided in three sections:

Chapter 3.1. presents the results of a three years survey carried out at the eutrophic Lake Kinneret (Israel). The seasonal and interannual variability of physicochemical parameters and hydrobiological settings of this lake are well-monitored among the water column. This high quality information is used in this work to determine Se biogeochemical processes driving its speciation that occur under oxic and suboxic to anoxic conditions as a function of the lake physicochemical and phytoplankton dynamics throughout seasons.

Chapter 3.2. presents the study carried out in alpine lakes from the central and western Pyrenees located along the French–Spanish border. The data obtained are providing new insights on the total Se content and Se speciation of these oligotrophic remote and high altitude lakes. It allows to better constrain Se sources in Pyrenees lakes and Se background concentrations in head-waters aquatic environments.

Chapter 3.3. presents the studies carried out in the Adour estuary (Bay of Biscay, SW France). This study was designed to follow Se speciation in different water bodies from the estuarine systems, such as upstream river inputs, downstream mixed estuarine water and various urban and wastewater effluent inputs. This study also contribute to better understand the land use impacts on Se inputs and speciation in river watershed as well as the potential contribution of estuarine urban effluents and biological activity in downstream estuarine waters.

Chapter 2: Optimization of mixed mode chromatography coupled to ICP-MS for simultaneous separation of organic and inorganic selenium non-volatile species in natural waters

2.1. Introduction

The development of new methodologies for Se speciation has received considerable attention in the last years. Different environmental studies have reported the presence of Se in different chemical forms. Selenate (Se(VI)) and selenite (Se(IV)) ubiquitously in natural waters (Conde & Sanz Alaejos, 1997). Oyamada & Ishizaki, 1986 and Tanzer & Heumann, 1991 proved the presence of trimethylselenonium ion ($TMSe^+$) in lake waters. More recently selenocyanate ($SeCN^-$) was found in industrial waste waters (Wallschläger & Bloom, 2001) and algae growing media (Leblanc & Wallschläger, 2016). Selenomethionine has been identified in high ionic strength water samples (LeBlanc et al., 2016). Despite these advancements, a fraction of Se in natural waters still unidentified. This fraction is presumably composed by elemental Se and/or more reduced Se species containing Se(–II). The reduced Se fraction, including elemental Se, can represent up to 80% of total Se in some freshwater samples (Table C1.6).

The presence of this non-negligible amount of reduced, and probably organically bound selenium, reflects the need of new strategies for Se speciation at ultra-trace levels. The most widely applied technique for Se speciation analysis in water samples is hydride generation (HG) coupled to different detectors. However, as previously highlighted in section 1.5.3.1. HG is not suitable for the identification of reduced Se species. In thanks to its capacity for the analysis of more than one species simultaneously when standard compounds are available (B'Hymer & Caruso, 2006), the use of high-pressure liquid chromatography has extended in recent years. Moreover, the use of HPLC avoid the need of sample pre-treatments, thus decreasing the possibility of element loss, contamination by reagents and/or species interconversion.

Among the different types of stationary phases, anionic exchange has been probably the most commonly applied for Se analysis in water. Inorganic anionic Se forms, *i.e*. selenite and selenate, are easily separated using anion exchange columns like the Hamilton PRP-X100 or the Dionex AS-16 (Chen & Belzile, 2010). Using the Dionex ionPac AS11, selenocyanate was identified in petroleum refinery wastewater (Wallschläger & Bloom, 2001). While using the Hamilton PRP-X100, selenocystine ($SeCys_2$), SeMet, Se(IV) and Se(VI) were identified in spiked waters. Alternative stationary phase as porous graphitic carbon made possible the separation of selenite, selenate, SeMet, selenoethionine (SeEt) and $SeCys_2$ in a single run with detection limits in the range between 2 – 8 ng L^{-1} (Dauthieu et al., 2006) (Table C1.13). The use of reversed-phase (RP) columns for Se speciation in waters is limited due to poor

retention of anions. To overcome this problem and obtain better resolution for organically-bound Se compounds, the use of ion-pairing agents is a good option. For example, Afton et al., (2008) optimized a methodology using tetrabutylammonium hydroxide (TBAH) for aqueous samples achieving the separation of selenocystine, selenomethionine, selenite and selenate in spiked river waters. Trifluoroacetic acid (TFA), and other perfluorinated compounds such as or heptafluorobutyric acid (HFBA), are also used for other matrices (Kotrebai et al., 2000).

In addition to simultaneous species separation, high-pressure liquid chromatography presents an important advantage over other introduction sample, due to easy coupling (on-line analysis) to inductively coupled plasma mass spectrometry (ICP–MS), which has proven to be one of the most sensitive detector for simultaneous multi-element analysis (Pettine et al., 2015) (Table C1.11 and C1.13.).

The need of new methodologies to better understand Se species distribution in natural waters and its behavior in the aquatic environment is clear. Therefore, our objective was to optimize the separation of inorganic and organic selenium species using a mixed mode stationary phase combining anionic exchange and reversed phase mechanisms and evaluate its applicability at concentrations levels representative of natural waters. Selection of eluent nature and pH of the mobile phase, solvent effect, the use of co-eluent and the maximum injectable sample volume are described and optimized for this mixed-mode column. The analytical performance using standards and real water samples was evaluated as well. The main goal was to obtain appropriate separation (resolution) and low detection limits (in the low range of ng Se L^{-1}) for the larger number of Se compounds in the pH range of natural waters while maintaining a reasonable analysis time.

2.2. Material and Methods

2.2.1. Reagents

Sodium selenite (Se(IV)), selenate (Se(VI)) (Spectracer), selenocyanate ($SeCN^-$), DL-selenomethionine (SeMet), L-Selenocystine ($SeCys_2$), methylselenocysteine (MeSeCys), methylseleninic acid (MeSeA) (Sigma) and lab-made trimethylselenonium ion ($TMSe^+$) were used without further purification. Stock standard solutions containing 1000 mg Se L^{-1} of each compound (except selenate 100 mg L^{-1}) in Milli-Q water (Millipore, 18.2MΩ) were stored in the dark at 4 ºC. Formic acid, citric acid (monobasic), ammonium phosphate dibasic, ammonium nitrate, trifluoroacetic acid, heptafluorobutyric acid, p-hydroxybenzoic acid

(Aldrich), and methanol, isopropanol and acetonitrile (Prolabo) were used for mobile phases preparation. The pH was adjusted by addition of 30% ammonia solution (Merck). Chromatographic conditions were optimized with solutions containing standards, individual or mixed, at 100 ng Se L^{-1}. Working standard solutions were prepared daily by dilution in Milli-Q water.

2.2.2. Instrumentation

Chromatographic separation was carried with an Agilent 1200 HPLC pump hyphenated to an Agilent 7900x Series inductively coupled plasma mass spectrometer (ICP-MS) system (Agilent Technologies, Tokyo, Japan) equipped with an octopole reaction cell, concentric nebulizer and a Scott double pass spray chamber cooled to 2 °C. Argon-based polyatomic interferences were reduced by using H_2 as cell gas at a flow rate of 5 mL min^{-1}. The parameters settings were as follow: Ar plasma gas flow, 15 L min^{-1}; Ar auxiliary gas flow, 0.86 L min^{-1}; Ar nebulizer gas flow, 1–1.1 L min^{-1}; radio frequency (RF) forward power, 1550 W; m/z monitored ratios were 77 and 78. The chromatographic column was an Omnipac PAX-500 (Thermo Scientific) (4 x 250 mm, p.s. 8.5 µm) connected to an Omnipac PAX-500 guard column (4 x 50 mm).

2.2.3. Chromatographic parameters

The following characteristics have been used to evaluate the quality of the separation:

A) Retention (capacity) factor (k). The retention (or capacity) factor (k) is a mean of measuring the retention of an analyte on the stationary phase. Retention factor is calculated as the ratio of retention time (Rt) of the analyte to the hold-up time or dead time (t_M) (Equation 1) (Barnes, 1992). We fixed 60 minutes as the maximum run time at 1 mL min^{-1} flow rate. Dead time for the Omnipac column and its guard column was 2.4 minutes; thus, k factors over 25 (k>25) indicates the no elution of the corresponding standard in 60 minutes analysis time.

$$k = \frac{(Rt - t_M)}{t_M} \quad (1)$$

B) Peak resolution (R_{AB}). Resolution is calculated by dividing the difference in the retention times of two adjacent peaks by the average peaks width at the base (ω). A resolution value of 1.5 or greater between two peaks is considered enough for the baseline separation of two compounds enabling quantitative analysis (Barnes, 1992).

$$R_{AB} = \frac{(Rt_B - Rt_A)}{\frac{1}{2}(\omega_A + \omega_B)} \quad (2)$$

C) Plate number (N). The efficiency of a chromatographic column is a measure of the dispersion of the analyte band during its movement through the chromatographic system and column. Due to dispersion effects, analyte peaks take a 'Gaussian' shape. The plate number (N) is a measure of this peak dispersion (Equation 3). The plate number depends on the column length and can be used to compare different columns dividing the column length by N, thus obtaining the height equivalent to a theoretical plate (HETP).

$$N = 16\left(\frac{Rt}{\omega}\right)^2 \quad (3)$$

2.2.4. Analytical performance

The analytical performance has been evaluated calculating the limits of detection and quantification and the repeatability (RSD).

D) Detection and quantification limits

The IUPAC defines the detection limit $x_i = x_b + 3\sigma_b$ where x_i is the analyte signal intensity (counts), x_b is the baseline signal and σ_b is the standard deviation of the blanc. Following the IUPAC recommendation (Long & Winefordner, 1983), the limit of detection (LoD) can be calculated as:

$$LoD = \frac{t \cdot \sigma_b}{S_c} \quad (4)$$

where t is the student coefficient (t=3 for a confidence interval of 99.86% (Dauthieu et al., 2006)), σ_b corresponds to the standard deviation of the baseline of 10 replicates of the blank. S_c is the slope of the calibration curve calculated using peak height vs concentration in ng Se L^{-1}.

The limit of quantification, stablished as $x_i = x_b + 10\sigma_b$, can be calculated using Equation 4 with t=10 (Long & Winefordner, 1983).

F) Repeatability:

The repeatability (RSD) of peak height and area is calculated from a triplicate injection of the standard, using Equation 5:

$$RSD\ (\%) = \frac{SD_{sample}}{\bar{x}} \quad (5)$$

Where SD_{sample} is the standard deviation of the mean sample height ($\bar{x}$).

2.3. Results

2.3.1. Mobile phase selection and pH optimization

Based on published methodologies applied for Se speciation (Table C1.13.), sometimes in different matrices, we selected five potential compounds as mobile phase eluent: ammonium formate, ammonium citrate (monobasic), ammonium phosphate (dibasic), ammonium nitrate and p-hydroxybenzoic acid (Peachey et al., 2009). It is well known that the presence of a certain amount of organic carbon has a signal enhancement effect for Se (Larsen & Stürup, 1994). For Se analysis, the most common solvent added to mobile phase is methanol, it was used in the first step of mobile phases testing at 1 – 2% (v/v) addition.

Ammonium citrate monobasic (5 – 10 mM, pH=8.0) and ammonium phosphate dibasic (10 mM, pH=8.0) mobile phases resulted in poor separation of early eluting peaks preventing Se compounds separation. Despite the wide use of these mobile phases, especially for the commonly used Hamilton PRP-X100 column; they were not adapted in the case of Omnipac PAX–500 column that may be due to their different anionic exchange capacities (0,319 meq for 4.6×250 mm PRP-X100 column and 40 µeq for 4×250 mm Omnipac PAX-500 column). In addition, the column required a cleaning procedure after these tests due to column binding sites blockage. This happened most probably because those mobile phases had a higher affinity for the stationary phase than our compound and less exchange capacity as previously highlighted; therefore, both, ammonium citrate and ammonium phosphate mobile phases were discarded.

Ammonium formate eluent was tested in the range between 15 – 50 mM, pH between 6.0 and 8.5, and with 1–2 % methanol (MeOH) addition. The 50 mM ammonium formate at pH=8.0 mobile phase did not elute selenate in 60 minutes chromatographic run. p-hydroxybenzoic acid mobile phase was tested at concentrations of 0.72 and 1.45 mM at pH=8.5 and with 2% MeOH. At 0.72 mM, however long retention times were observed for selenate and selenocyanate (Rt~60min) (Table C2.1). The increase of concentration to 1.45 mM significantly reduced retention times for selenium compounds. However, this mobile phase

was discarded due to poor resolution (*i.e.* co-elution) of $SeCys_2$ and MeSeCys, and selenite and $TMSe^+$.

Table C2.1. Retention times and retention factor (k) for the mobile phases composed of 0.72 and 1.45 mM of p-hydroxybenzoic acid + 2% MeOH, at pH=8.5. Compounds are listed in each case by elution order.

$[C_7H_6O_3]$ = 0.72 mM			$[C_7H_6O_3]$ = 1.45 mM		
Species	**Rt (min)**	**R**	**Species**	**Rt (min)**	**R**
MeSeA	2.0		MeSeA	2.0	
		2.8			2.2
MeSeCys	3.1		SeCys	3.0	
		1.2			0.2
SeCys	3.6		MeSeCys	3.1	
		2.9			3.6
SeMet	4.8		SeMet	4.9	
		4.0			3.2
$TMSe^+$	10.0		Se (IV)	6.8	
		1.6			0.4
Se (IV)	12.7		$TMSe^+$	7.2	
		13.1			15.0
$SeCN^-$	57.8		Se (VI)	22.9	
		0.3			6.5
Se (VI)	59.4		$SeCN^-$	38.8	

Ammonium nitrate eluent was tested in the range between 5 – 30 mM with 2% of MeOH in the pH range between 6.0 and 8.5. A recent study using the Omnipac PAX-500 for water analysis achieved the separation of methylseleninic acid (MeSeA), selenite and selenate using a gradient of water (pH=8.4) as first eluent, followed by a 30 mM NH_4NO_3 + 1% MeOH at pH=7.5 mobile phase in 25 minutes (Vriens et al., 2014). Our results showed decreasing retention times with increasing salt concentration for anionic species. Despite the fast elution of selenate using 30 mM of NH_4NO_3 at pH 8.5 (selenate Rt=10.8 min), this mobile phase was not suitable for routine analysis due to salt precipitation observed in the sampler cone and potential signal decrease with time. Therefore, regarding the compromise between selectivity and fast run time, 20 mM of NH_4NO_3 was selected for further analysis.

Certain species, in this case selenite, selenate and the Se amino acids present variable charge depending on pH. This is dependent on the pK_a values and regulates the charge of the species and, in consequence the interaction with the stationary phase. To explain the different capacity of the species to interact with the stationary phase, the apparent charge is commonly used. The apparent charge establishes the evolution of species average charge as function of the pH and the acidity constant of the species. It is calculated using Equation 6:

$$AC = \frac{\sum(z_i \cdot ion\ i\ concentration)}{total\ concentration} \quad (6)$$

Where z_i is the ionic charge of a species. AC was calculated for Se(VI) with pKa_2=1.8; Se(IV) with pKa_1=2.7 and pKa_2=8.54 (Seby et al., 2001); SeCys with pKa_1= 1.68, pKa_2=2.15, pKa_3=8.07 and pKa_4=8.95; and for SeMet with pK_{a1}=2.19 and pK_{a2}=9.05 (Olivas et al., 1996). No pK_a data was found for MeSeCys. The calculation of the AC of selected species as function of pH is represented in Figure C2.1.

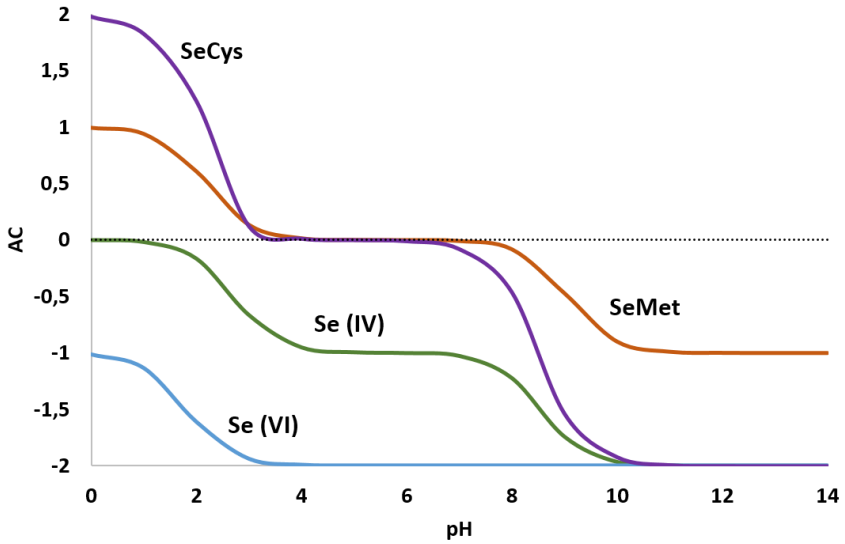

Figure C2.1. Apparent charge versus pH for selected Se species: selenite, selenate, selenomethionine and selenocystine.

The zwitterionic character of SeMet and $SeCys_2$ is reflected in the pH range between 4 and 7.5. SeMet and $SeCys_2$ carry thus an average positive charge at pH<4, and negative one over pH 8.0. Therefore, SeMet and $SeCys_2$ are expected to interact by reversed phase mecanism in the range of pH between 4 and 7.5, and with the anionic exchange phase over pH 8 but their carbon-based part can also affect their retention on mixed mode column in this pH range.

Our results for the analysis of Se amino acids at pH 8.5 (Figure C2.2) show two peaks for SeMet, $SeCys_2$ and MeSeCys. Peak areas integration showed that unretained peak represented around 20% of the sum of both peak areas which, according to their pK_a, may indicate that unretained peak may correspond to negatively charged SeMet and to doubly negatively charged $SeCys_2$.

A decrease of pH mobile phase should therefore allow to reduce the peak area of unretained SeMet and $SeCys_2$. However, this alternative was not adopted as the retention of selenite, with pK_a values of 2.35 and 7.94, was increased at 8.5 compared to lower pH achieving a better

separation between Se amino acids (eluting before 6 minutes) and selenite (Rt=8.1 min) at pH 8.5 (Fig. C2.2.). Therefore, pH 8.5 was selected for further tests.

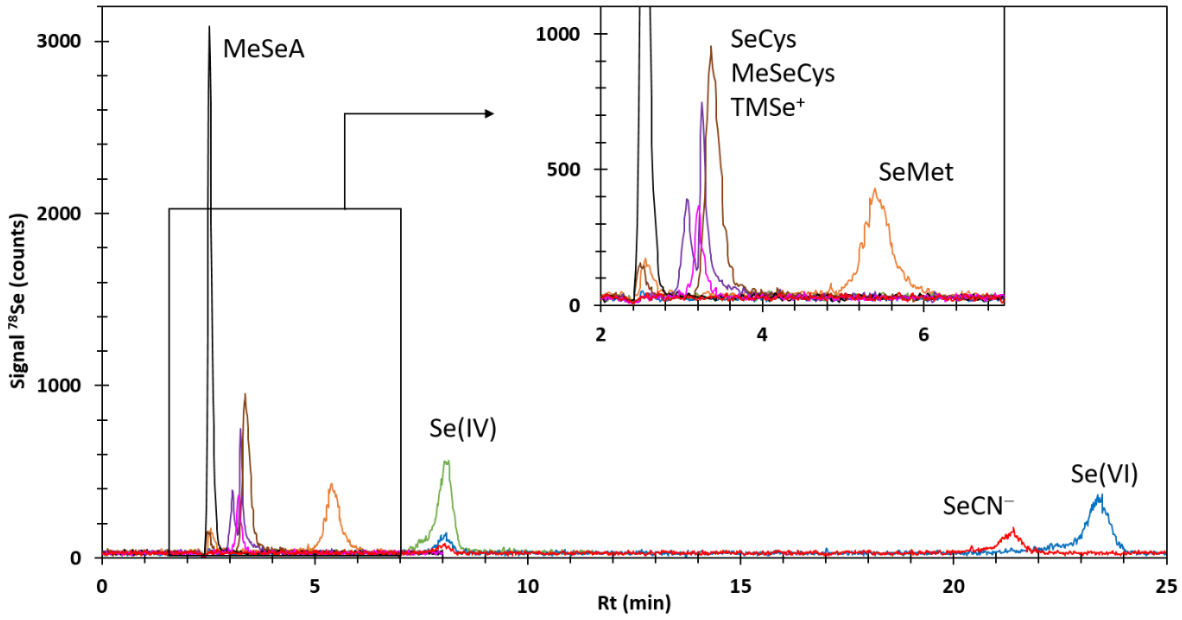

Figure C2.2. Example chromatogram obtained for standards: MeSeA (black), $SeCys_2$ (purple), MeSeCys (brown) and $TMSe^+$ (pink) (co-eluted), SeMet (orange), Se(IV) (green), $SeCN^-$ (red) and Se(VI) (blue). Mobile phase was 20 mM NH_4NO_3 + 2% MeOH at pH=8.5, flow rate of 1mL min^{-1}. All standards were injected at 100 ng Se L^{-1}, injection volume was 100 µL.

A summary of corresponding chromatographic parameters using 20mM NH_4NO_3 + 2% MeOH at pH 8.5 is presented in Table C2.2. These conditions appear not suitable for the separation of selenocystine, methylselenocysteine and $TMSe^+$, presenting resolution poor resolution. The elution of selenate in less than 25 minutes was an improvement compared to the first tests where this species did not elute before 60 minutes. In order to improve the sensitivity of the method for selenate, which using this mobile phase presents a broad peak shape (Figure C2.2.) further tests were carried out to optimize the solvent effect in peak height.

Table C2.2. Chromatographic parameters for 20 mM NH_4NO_3 + 2% MeOH at pH=8.5 injecting 100 µL at 100 ng Se L^{-1}.

Species	Rt (min)	h_{max} (counts)	k	R	N
MeSeA	2.5	3175	0.1		1120
				2.0	
$TMSe^+$	3.2	395	0.3		1037
				0.2	
SeCys	3.3	765	0.4		388
				0.1	
MeSeCys	3.4	980	0.4		789
				3.1	
SeMet	5.4	442	1.2		721
				3.1	
Se (IV)	8.1	580	2.4		1128
				11.5	
$SeCN^-$	21.4	205	7.9		3904
				1.4	
Se (VI)	23.4	390	8.7		4399

2.3.2. Solvent effect

Keeping the mobile phase chosen in the previous section (20 mM NH_4NO_3 at pH = 8.5), the effect of MeOH, acetonitrile (ACN) and isopropanol (ipa) addition was compared in the range 0.5 – 5%. Methanol was first used due to its capacity to enhance Se signal, adding between 1 – 2% of MeOH to the mobile phase. It is well known that solvating power and hydrophobicity of the organic solvent can influence the retention mechanisms (Rabin & Stillian, 1994). Previous studies have shown that higher MeOH concentrations (>5%) no longer show any enhancement effect on Se signal (Larsen & Stürup, 1994). Using the Dionex ionPac AS11, Rabin & Stillian (1994), reported better resolution (*i.e.* narrower peak shape) for analytes strongly retained, in our case selenate and selenocyanate, when the mobile phase contained 16% of MeOH. We tested the effect of 10 and 20 % MeOH but results showed higher noise and poor sensitivity without improvement of resolution between SeVI and selenocyanate. Therefore, 5% (v/v) of organic solvent was selected as maximum solvent for further tests. Acetonitrile (ACN) is also a common solvent used in reverse phase HPLC and presents lower polarity (relative polarity ACN=0.46) than MeOH (0.76) (Reichardt & Welton, 2010). Isopropanol is an intermediate polarity solvent, between the weak polarity of acetonitrile and the stronger polarity of methanol, was selected (Reichardt, 1979). Solvent effect was compared in terms of retention time, peak height, peak width at half maximum, and plate number (Table C2.3.).

Table C2.3. Retention time (min), retention factor (k), resolution (R) and plate number (N) as function of the solvent type: acetonitrile (ACN, 0.5 – 1%), isopropanol (IPA, 0.5 – 5%) and methanol (MeOH, 1 – 2 %). Data includes: selenite (Se(IV)), selenate (Se(VI)), selenomethionine (SeMet), selenocysteine ($SeCys_2$), Methylselenocysteine (MeSeCys), methylseleninic acid (MeSeA), trimethylselenonium ion ($TMSe^+$) and selenocyanate ($SeCN^-$) listed by retention time for each condition. All compounds were tested using the following mobile phase: 20 mM NH_4NO_3 + the corresponding solvent adjusting the pH to 8.5 using ammonia. All standards were injected at 100 ng Se L^{-1} at 1 mL min^{-1} of flow rate.. Note that for the same conditions at 2% of MeOH the results have been shown in Table C2.2.

Species	Rt (min)	k	R	N	Species	Rt (min)	k	R	N
0.5% ACN					1% ACN				
MeSeA	2.5	0.1		406	MeSeA	2.5	0.1		581
			1.1					0.7	
$TMSe^+$	3.2	0.3		393	MeSeCys	3.1	0.3		97
			0.3					0.1	
MeSeCys	3.4	0.4		329	$TMSe^+$	3.2	0.3		312
			1.4					1.3	
$SeCys_2$	5.0	1.1		166	SeMet	4.5	0.9		216
			<0.1					<0.1	
SeMet	5.0	1.1		196	$SeCys_2$	4.5	0.9		605
			5.0					5.9	
Se(IV)	11.7	3.9		1424	Se(IV)	10.9	3.6		897
			5.7					7.5	
Se(VI)	21.8	8.1		1413	$SeCN^-$	22.1	8.2		3464
			0.4					0.5	
$SeCN^-$	22.4	8.3		5403	Se(VI)	22.8	8.5		2492
1% MeOH					*2% MeOH*				
MeSeA	2.5	<0.1		886	MeSeA	2.5	0.1	2.0	1120
$TMSe^+$	3.2	0.1	1.9	1135	TMSe+	3.2	0.3	0.2	1037
MeSeCys	3.6	0.1	0.9	900	SeCys	3.3	0.4		388
SeCys	4.3	0.4	1.3	850	MeSeCys	3.4	0.4	0.1	789
SeMet	5.9	1.0	2.2	733	SeMet	5.4	1.2	3.1	721
Se(IV)	10.3	3.7	3.8	807	Se(IV)	8.1	2.4	3.1	1128
$SeCN^-$	not tested*		8.6		SeCN–	21.4	7.9	11.5	3904
Se(VI)	22.9	7.7		3880	Se(VI)	23.4	8.7	1.4	4399

Table C2.3. (Continued)

Species	Rt (min)	k	R	N	Species	Rt (min)	k	R	N
0.5% ipa					*1% ipa*				
MeSeA	2.6	0.1		720	MeSeA	2.5	0.1		445
			0.9					0.7	
$TMSe^+$	3.0	0.3		331	$TMSe^+$	2.9	0.2		498
			0.4					0.4	
MeSeCys	3.3	0.4		286	MeSeCys	3.1	0.3		457
			1.6					1.1	
$SeCys_2$	4.6	0.9		491	$SeCys_2$	3.9	0.6		307
			0.3					0.6	
SeMet	4.9	1.0		398	SeMet	4.4	0.8		500
			7.4					7.9	
Se(IV)	11.2	3.7		3760	Se(IV)	10.7	3.5		2724
			11.7					11.8	
Se(VI)	21.9	8.1		6342	Se(VI)	22.1	8.2		6331
			0.6					0.3	
$SeCN^-$	22.6	8.4		5006	$SeCN^-$	22.4	8.3		5844
2% ipa					*5% ipa*				
MeSeA	2.5	<0.1		1361	MeSeA	2.5	<0.1		790
			1.0					0.6	
$TMSe^+$	2.8	0.2		929	$TMSe^+$	2.7	0.1		784
			0.2					0.1	
MeSeCys	2.9	0.2		521	MeSeCys	2.7	0.1		260
			1.4					0.9	
SeMet	3.8	0.6		411	SeMet	3.4	0.4		262
			1.2					1.6	
$SeCys_2$	4.7	1.0		626	$SeCys_2$	4.7	1.0		581
			9.0					8.6	
Se(IV)	11.1	3.6		4392	Se(IV)	11.4	3.7		3400
			12.9					7.5	
$SeCN^-$	21.4	7.9		8496	$SeCN^-$	20.8	7.7		2293
			0.7					2.0	
Se(VI)	22.2	8.2		6993	Se(VI)	23.8	8.9		5889

*SeCN standard was not available at the moment analysis

Acetonitrile was not tested above 1% due to low peak height and plate number observed for all compounds (Table C2.3.). Methanol and isopropanol were compared at 1 and 2%. In general, at equal percentage, isopropanol showed higher plate number than methanol for all compounds at the same conditions and similar retention times, which indicates narrower peaks, thus higher signal intensity and lower detection limits. Therefore, isopropanol was selected for further tests. This solvent was tested in the same conditions at 0.5 and 5%, however the best performance was obtained at 2% in terms of plate number.

2.3.3. Addition of anionic co-eluent

The method obtained using 20 mM NH_4NO_3 + 2% ipa at pH = 8.5 had one main drawback, a poor separation between $TMSe^+$ and MeSeCys (R=0.20) and selenate and selenocyanate (R=0.73). In general, ion-pairing agents are added the mobile phase to improve the separation

between species. Considering the literature and the availability at the laboratory, two ion-pairing agents were proposed: heptafluorobutyric acid (HFBA) (Kotrebai et al., 2000) and p-hydroxybenzoic acid (Mehra & Frankenberger, 1988). Ion pairing agents used are anionic, which means that they can act both as ion pairs for $TMSe^+$ using reverse phase properties of the stationary phase and as "eluent strength enhancer" (co-eluent) for anions using the anionic exchange sites of the stationary phase.

The first co-eluent tested was 1% of trifluoroacetic acid (TFA), following the procedure of Peachey et al., (2009) for the Acclaim WAX-1 mixed-mode column, however it did not improved peak resolution. A range between 1.0 – 2.5 mM of HFBA was tested. The addition of 1.0 mM of HFBA did not improve resolution, plate numbers nor decreased significantly run time. Our results showed baseline increase when adding HFBA to the mobile phase, from less than 25 counts for ^{78}Se in average without HFBA to around 50 – 60 counts (^{78}Se) at 1.0 mM and over 100 counts (^{78}Se) at 2.5 mM. Higher noise can potentially affect sensitivity and therefore, the use of HFBA was rejected. The last compound tested was p-hydroxybenzoic acid. Our observations testing it as mobile phase showed its capacity for eluting strongly retained anions. The addition of 1 and 2 mM of p-hydroxybenzoic acid was compared and results are shown in Figure C2.3. and Table C2.4.

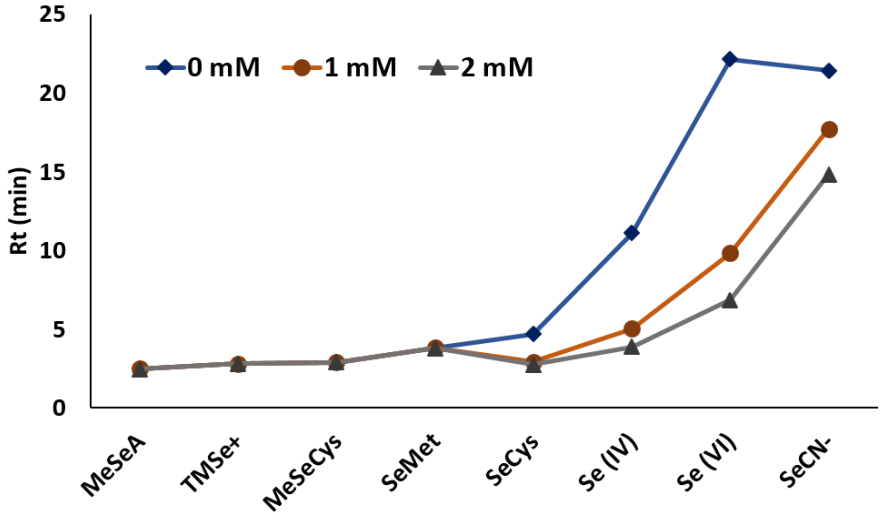

Figure C2.3. Evolution of retention times for the different concentrations of the co-eluent p-hydroxybenzoic acid tested.

Table C2.4. Retention times and resolution (R) for different concentrations of p-hydroxybenzoic acid.

0 mM			1 mM			2 mM		
Species	**Rt (min)**	**R**	**Species**	**Rt (min)**	**R**	**Species**	**Rt (min)**	**R**
MeSeA	2.5	1.0	MeSeA	2.5	1.1	MeSeA	2.5	0.7
$TMSe^+$	2.8	0.2	$TMSe^+$	2.8	0.1	SeCys	2.8	0.1
MeSeCys	2.9	1.4	MeSeCys	2.9	0.1	$TMSe^+$	2.8	0.1
SeMet	3.8	1.2	SeCys	2.9	1.1	MeSeCys	2.9	1.4
SeCys	4.7	9.0	SeMet	3.8	1.6	SeMet	3.8	0.1
Se(IV)	11.1	12.9	Se(IV)	5.0	7.5	Se(IV)	3.9	4.3
$SeCN^-$	21.4	0.7	Se(VI)	9.8	10.6	Se(VI)	6.9	10.0
Se(VI)	22.2		$SeCN^-$	17.7		$SeCN^-$	14.8	

Results of adding 1 mM of p-hydroxybenzoic agent to the mobile phase showed a significant decrease in the retention time of selenate, allowing its complete separation from selenocyanate and improving the sensitivity for this analyte (Figure C2.4). However, trimethylselenonium ion still co-eluted at the same retention time of SeCys and MeSeCys. An additional test using 2 mM of ion pairing agent produced a co-elution of selenite and SeMet and was therefore discarded. The addition of 1 mM of p-hydroxybenzoic acid as co-eluent the mobile phase composed of 20 mM NH_4NO_3 + 2% isopropanol at pH=8.5 was finally selected due to its effect on the eluent strength of the ammonium nitrate mobile phase and the improvement of resolution (Figure C2.4). Figure C2.4 presents an example of a chromatogram of standards obtained with selected conditions, allowing the separation of selenomethionine, selenite, selenate and selenocyanate, which are species reported in natural waters.

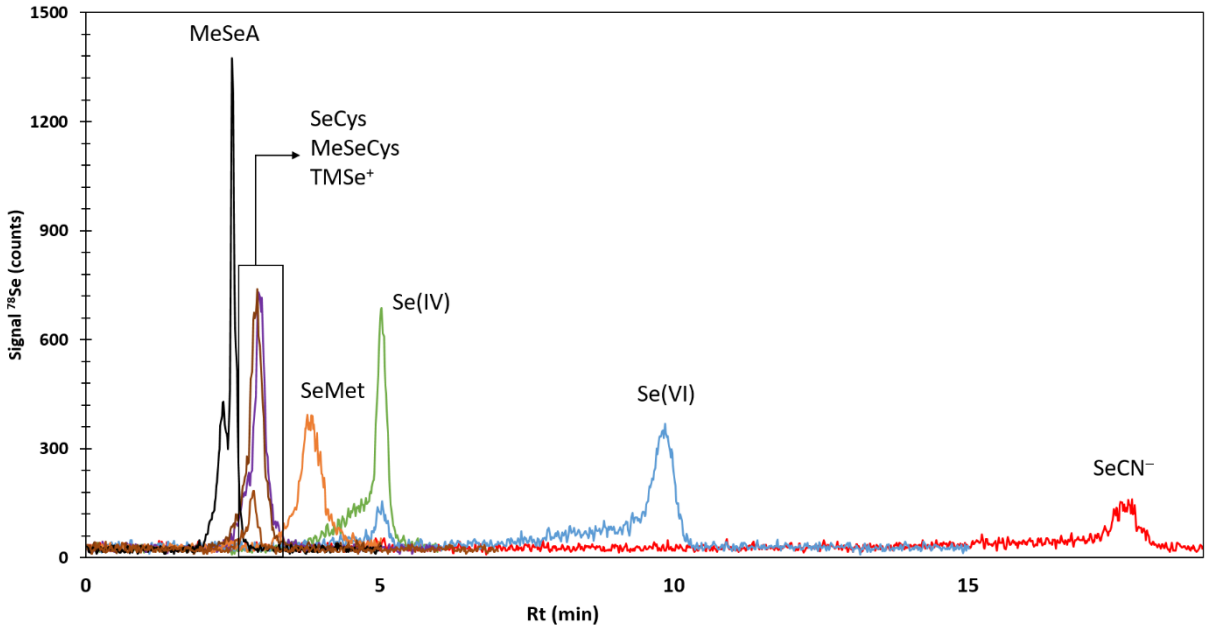

Figure C2.4. Example chromatogram obtained for standards with final mobile phase composed of 20mM NH_4NO_3 + 1.0 mM p-hydroxybenzoic acid + 2% isopropanol at pH=8.5 (1 ml min^{-1}). The chromatogram shows the Se^{78} isotope. Standards tested were: methylseleninic acid (MeSeA), trimethylselenonium ion (TMSe), DL-selenocysteine ($SeCys_2$), DL-selenomethionine (SeMet), selenite (Se(IV)), selenate (Se(VI)) and selenocyanate (SeCN). All standards were injected separately at 100 ng Se L^{-1} injecting 100 µL of each compound.

2.3.4. Determination of maximum injectable volume and analytical performance

The optimization of the maximum injectable volume main goal is to increase the sensitivity without degrading the peak quality. The higher the injected volume, the longer the time of injection and the potential peak broadening. To minimize this effect, the draw and eject speed was set up to 500 µL min^{-1}. The maximum injectable volume was determined on the basis of peak height versus peak area for injected volumes of individual standard solution at 100 ng Se L^{-1} of 100, 200, 300, 400 and 500 µL (Figure C2.5.).

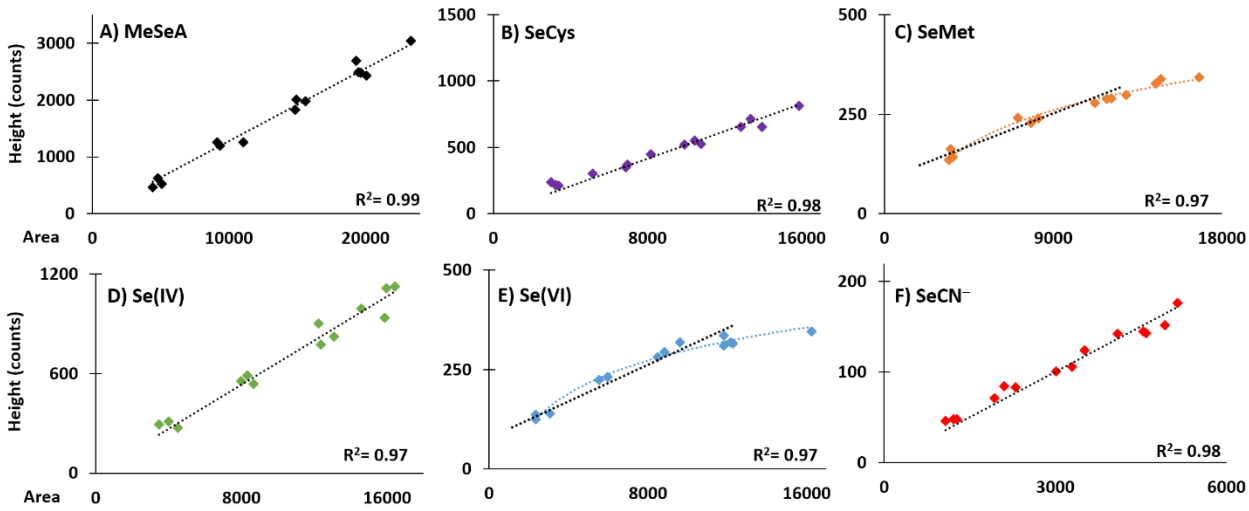

Figure C2.5. Peak height (counts) vs peak Area for injection volumes between 100 to 500 µL. All standards were injected in triplicate at 100 ng Se L^{-1}. Regression lines (dotted black lines) and R^2 is given for the range 100 – 400 µL Colored dotted lines correspond to the logarithmic regression lines in the range between 100 – 500 µL to show the loss of linearity for SeMet and Se(VI) at 500 µL of injection volume.

The regression lines show that, in general, linearity is maintained in the injection volume range between 100 and 500 µL (Figure C2.5). Only two analytes, SeMet and SeVI, showed linearity no longer than injection volume of 300 µL. Therefore, the maximum injection volume was determined as 300 µL.

The proposed methodology allows the simultaneous separation and quantification of methylseleninic acid, selenomethionine, selenite, selenate and selenocyanate in less than 20 minutes, which allows the application of this methodology to different water types being able to separate reduced Se species simultaneously to Se oxyanions and selenocyanate.

2.3.5. Application to natural waters and method intercomparison

The injection volume of 300 µL implies the injection of larger quantity of species but it can increase matrix effect, especially in fresh waters. We have tested this methodology in three different water types: oligotrophic freshwater mountain lakes (Pyrenean lakes, France), eutrophic/mesotrophic freshwater lake (Lake Kinneret, Israel) and river-dominated upstream estuarine waters (Adour river estuary, France). These studies sites are detailed in Chapter 3. An example of the chromatograms obtained is presented in Figure C2.6.

For validation and intercomparison, the same samples were analyzed using a porous graphitic carbon phase (100 mm x 4.6 mm i.d., 5 µm particle size) applying the method developed by Dauthieu et al., (2006) that consisted in a mobile phase of 240 mM formic acid + 1% MeOH at pH=2.4 adjusted with ammonia.

Up to three Se-containing chromatographic peaks were detected in investigated samples including selenate and selenite species and a peak of unknown composition. Despite the no identification of this compound, it elutes with similar retention times of Se amino acids with both columns used that suggests similar retention mechanisms and probably organic nature of Se-containing compound.

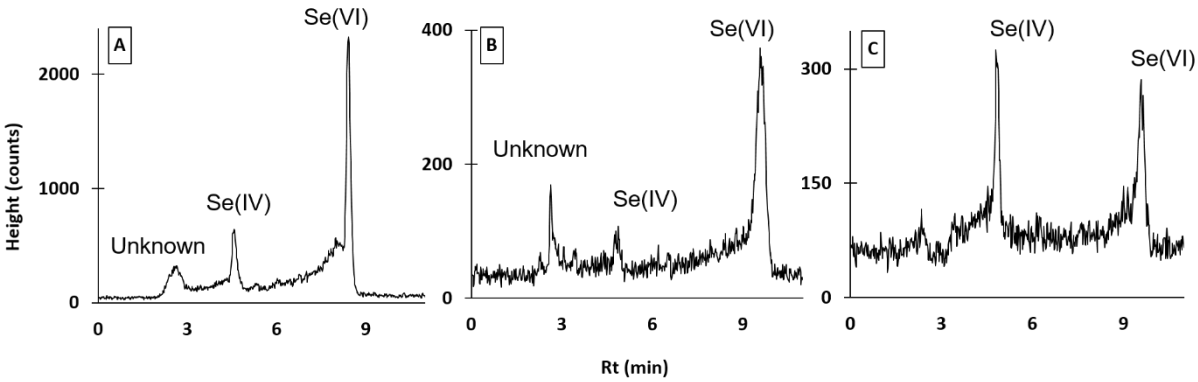

Figure C2.6. Example of practical application of optimized method to natural waters analysis. ^{78}Se isotope was used for quantification. Fig. C2.6.A corresponds to a Lake Kinneret sample containing an unknown compound (Rt = 2.6 min), selenite (Rt = 4.6 min; 11 ± 1 ng Se L^{-1}) and selenate (Rt=8.4 min, 70 ± 13 ng Se L^{-1}). Fig. C2.6.B corresponds to a pristine lake sample from the Arratille Pyrenean Lake. In this case only Se(VI) was quantified (Rt = 9.6 min; 33 ± 4 ng Se L^{-1}), selenite concentration was between the LoD and LoQ (Rt = 4.8 min, 2.5 ± 0.1 ng Se L^{-1}). Fig. C2.6.C corresponds to a sample from Adour estuary. Selenite (Rt = 4.9 min, 27 ± 1 ng Se L^{-1}) and selenate were quantified (Rt = 9.6 min, 65 ± 10 ng Se L^{-1}). Injection volume was 300 µL. Mobile phase: 20mM NH_4NO_3 + 2% isopropanol + 1.0 mM p-hydroxybenzoic acid at pH=8.5 was pumped at 1 m min^{-1}.

The detection limits obtained with developed mixed mode chromatography were calculated for standards solutions for selenite and selenate, the compounds detected in real samples and were 1.5 ng Se L^{-1} for selenite and 3.6 ng Se L^{-1} for selenate. The limits of quantification were 5 ng Se L^{-1} for selenite and 12 ng Se L^{-1} for selenate. Retention times varied from 5.32 min for

selenite standard in MQ water to 4.6 min and tailing increased with increasing spike concentration. Selenate retention time varied and was around 10.0 min in Pyrenean lakes and around 8.4 min for fresh waters from Lake Kinneret (Israel). The waters from Lake Kinneret present much higher conductivity values, in other words anionic species such as Cl^-, SO_4^-, NO_3^-, etc., than Pyrenean lakes. Thus, the decrease of retention time can be associated to the binding site competition between anions and anionic Se species, *i.e.* selenite and selenate.

Results of selenite and selenate quantification with both columns are shown in Figure C2.7. This interomparison indicates that selenate was equally quantified using both methods (y=1.02x) while for selenite the PGC column quantified slightly higher concentrations of the analyte (y=0.85x).

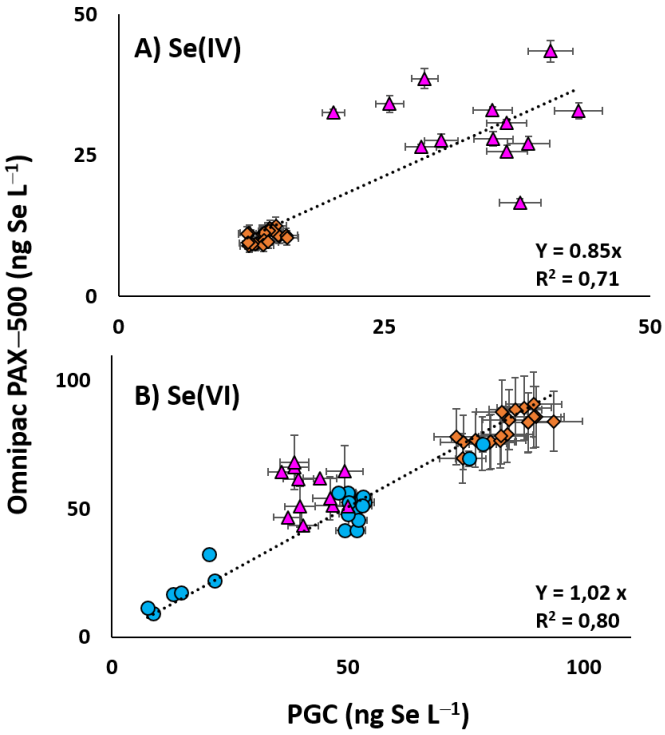

Figure C2.7. Intercomparison between Omnipac PAX-500 and PGC hypercarb columns for the analytes: A) selenite and B) selenate. The results obtained correspond to samples from Lake Kinneret (orange), Pyrenees lakes (blue) and Adour estuary (pink).

2.4. Conclusion

The combination of reversed-phase and anionic exchange offers a good alternative for the simultaneous separation of Se amino acids and inorganic selenium species in a single analysis in less than 20 minutes. Isocratic separation was achieved for six selenium compounds:

methylseleninic acid, selenocystine, selenomethionine, selenite, selenate and selenocyanate; using a mobile phase composed of 20 mM NH_4NO_3 + 2% of isopropanol + 1.0 mM p-hydroxybenzoic acid at pH 8.5 pumped at 1 mL min^{-1}. Optimization was conducted at pH value similar to that of natural waters samples, in order to ensure the species preservation during analysis. This method was successfully applied to natural freshwater samples detecting selenite, selenate and an unknown Se compound eluting at similar retention times than the Se amino acids. The occurrence of such unknown Se compound was also determined using the PGC column. The concentration of Se species quantified was similar to the ones obtained with chromatography based on porous graphitic carbon stationary phase in the case of selenate, while for selenite the concentration measured using the mixed-mode stationary phase was slightly lower (76%) for the three sampling sites studied in this work and presented in detail in Chapter 3.

Chapter 3: Study of the Biogeochemistry of Selenium compounds in the water column of lacustrine and estuarine systems

3.1. Introduction

The bioavailability of Se in aquatic systems is regulated by its speciation, which, in turns depends on the physicochemical characteristics of the water and the biological activity. The study of selenium speciation in aquatic systems is a subject of interest due to the important role of Se for living organisms. However, most studies have only focused on total Se and/or Se speciation determination in subsurface samples, thereby overlooking the potential differences that may exist among the water column.

This chapter presents for the first time the simultaneous study of volatile and non-volatile Se speciation in the water column of a eutrophic lake (Lake Kinneret, Israel) and several oligotrophic high mountain lakes from the Pyrenees (Adour and Ebro watersheds, France – Spain). The aim is to understand which are the sources and fate of Se in lakes and how its speciation is affected as function of seasonal lakes dynamics in the water column. Both study sites present very different characteristics. With semi-arid warm climate and low annual precipitation, Lake Kinneret is surrounded by populated areas, receiving high nutrient load and presenting important algae blooms during spring and summer periods. Remote high altitude lakes are ice-covered for around the half of the year, receive high amounts of precipitation and low levels of nutrients. Both studies are thus complementary to investigate Se biogeochemical processes occurring in lake waters.

For the study of Lake Kinneret, four seasonal sampling were carried out every year in January, April, September and November for the period between 2015 and 2017. Samples were collected at different depths of the water column with special regard on the oxic/anoxic water interface (metalimnion). The results of this study demonstrate how phytoplankton dynamics control Se speciation and the capability of certain algae to produce reduced and most probably organically bound Se species. In addition, the lake water column dynamics, in particular the evolution of suboxic to anoxic conditions in the hypolimnion support that bacteria respiration transforms selenate and selenite into reduced Se forms, most probably as elemental Se. This work was supported by the Israeli Water Authority.

For the study of Pyrenean lakes, bi-annual samples were collected at different lakes, including depth and diurnal profiles at selected lakes. The results have shown that Se originates from geogenic sources (60%). Our results demonstrate the important contribution of wet deposition (40% in average) to lake waters Se concentration. At Pyrenean lakes, selenium is mostly in the form of selenate without remarkable seasonal variations. However, the study of

stratified lakes revealed the predominance of reduced Se species over selenium oxyanions under oxygen depleted conditions. This work is a contribution to the REPLIM-OPCC project and has been partially supported (65%) by the FEDER funds through the INTERREG V-A Spain-France-Andorra (POCTEFA 2014-2020) (REPLIM project, ref. EFA056/15).

With the aim to better constrain how Se evolves from mountain headwaters towards the river end-member, a third study focused on the Adour estuary (Bay of Biscay, France), following the course of Pyrenean lake waters. The Adour estuary is subjected to important seasonal variations due to higher riverine discharge in winter flood periods. Three sampling campaigns were implemented in May and September 2017 and January 2018, to monitor the seasonal estuarine dynamics. The results have shown an increase of total Se in the waters entering the estuary compared to total Se concentrations observed at the Pyrenees. This seems to be the consequence of farmlands in the course of two rivers arriving to the estuary. The impact of human activities related to industrial activities and high density population resulted in higher dissolved Se and volatile Se production at certain points of the estuary. This work has been possible in thank to the Micropolit research program « État et évolution de la qualité du milieu littoral Sud Aquitain » is co-financed by the European Union and l'Agence de l'Eau Adour Garonne. Europe is involved in Nouvelle Aquitaine with the European Regional Development Funds.

In addition, the author aknowledge the Aquitaine Region (AQUITRACES project n° 20131206001-13010973) and ANR IA RSNR (AMORAD project n°ANR-11-RSNR-0002) for equipment fundings. The financial support of the Doctoral School (ED 211), the Université de Pau and Pays de l'Adour and the Institut des Sciences Analytiques et de Physico-chimie pour l'Environnement et les Matériaux (IPREM) given as a pre-doctoral fellowship is aknowledged.

3.2. Article I <<Biogeochemistry of Selenium compounds in the water column of the warm, monomictic, Lake Kinneret>>

Biogeochemistry of Selenium compounds in the water column of the warm, monomictic, Lake Kinneret

Andrea Romero-Rama[1], Maïté Bueno[1], Emmanuel Tessier[1], Yaron Be'eri-Shlevin[2], Assaf Sukenik[2], Tamar Zohary[2], David Amouroux[1]

1 - Université de Pau et des Pays de l'Adour, E2S UPPA, CNRS, Institute of Analytical Sciences and Physical-Chemistry for the Environment and Materials - IPREM, Pau, France

2 - The Kinneret Limnological Laboratory, Israel Oceanographic and Limnological Research, Migdal 14950, Israel

Abstract

The speciation and biogeochemistry of dissolved selenium (Se), a trace micronutrient, was investigated over three years (2015-2017) in the warm subtropical monomictic and meso-eutrophic Lake Kinneret (*Sea of Galilee*, Israel). The study covered seasonal variations and vertical distribution of aqueous phase total Se (T.Se), inorganic oxyanions (Se(IV) & Se(VI)), reduced Se fraction (Red.Se), organic (Org.Se) and volatile Se compounds. The Org.Se form was ubiquitous and is probably organic Se metabolite(s) released by the phytoplanktonic activity and the most feasibly precursor of volatile Se species.

Measured concentrations of dissolved T.Se components, Se(IV) ranged between null (< 2) and 84 ng Se L^{-1}, Se(VI) between < 2 and 90 ng Se L^{-1}, Org.Se between <LoD and 84 ng Se L^{-1}. Selenium distribution exhibited large seasonal variations concomitant with the lake stratification dynamics. During holomixis, depth profiles of Se species were uniform whereas variations became evident during summer-fall stratification. Dissolved T.Se decreased during stratification, especially in the hypolimnion, due to anoxic conditions and reduction of soluble oxyanions to insoluble Se forms (i.e: Se(0) and Se(-II)). In the hypolimnion, production of Red.Se tripled the concentration of previous studies (Nishri et al., 1999) seems to be associated with organic matter degradation and Se(VI) and Se(IV) depletion and was apparently enhanced during dry years.

Org.Se was detected mainly at the epilimnion during spring and summer. Strong correlations (R^2=0.95 in 2015 and 2016 and R^2=0.94 in 2017, P<0.01) were found between Org.Se and Chl-*a* during the spring algal bloom, followed by accumulation of volatile Se compounds during summer-fall, probably as a result of microbial-mediated degradation in the metalimnion. Organic Se produced in the photic zone during the spring bloom was degraded during late summer/fall, producing volatile Se species close to the chemocline. Volatile Se included mainly dimethyl diselenide (DMDSe) and dimethyl selenide sulphide (DMSeS) and, in a lesser amount, dimethyl selenide (DMSe).

We conclude that in stratified productive lakes such as Lake Kinneret, Se cycling is highly dependent on dynamic along seasons, exhibiting significant biotic transformations under both oxic and anoxic conditions to form organic and inorganic reduced compounds having both importance for Se removal and cycling in the water column.

1. Introduction

Selenium (Se) can be found in water bodies in different oxidation states ((-II), (0), (IV) and (VI)). Selenite (IV) and selenate (VI) occur in aquatic systems together with reduced and probably organically bound Se species (Conde & Sanz Alaejos, 1997; Cooke & Bruland, 1987; Cutter & Bruland, 1984; Nakaguchi & Hiraki, 1993; Nishri, et al., 1999). Transformations between different Se forms can be caused by the physicochemical characteristics of the water (mainly Eh, pH and dissolved oxygen) or mediated by microorganisms, including the formation of elemental Se(0) and reduced Se (-II) species. Reduced Se species include: inorganic, organically bound and volatile Se compounds such as: dimethylselenide (DMSe), dimethyl diselenide (DMDSe) and dimethyl selenide sulphide (DMSeS) (Amouroux & Donard, 1997; Amouroux et al., 2001). Elemental Se, (Se(0)) is present as non-soluble colloids and considered as non-bioavailable (Guo et al., 1999; Velinsky & Cutter, 1990; Winkel et al., 2012; Zhang et al., 2004).

It is well established that selenium is an essential micronutrient in both oceanic and fresh water bodies (Measures & Burton 1980, Lindstom et al. 1983), with a key role as growth limiting factor for phytoplankton (Harrison et al. 1988, Duan et al. 2010). However, there is no consensus if a specific chemical form of Se is preferentially uptaken by microorganisms in natural aquatic systems. Selenium compounds bioavailability can be driven by the potential energy required to the reductive uptake of more oxidized form (e.g. Se(VI)) or the competition with other aquatic constituents such as sulphur analogues (David Amouroux et al., 2001; Ivanenko, 2018). In the Bohai Bay, Duan et al. (2010) showed a correlation between the decrease of Se(IV) and the presence of dinoflagellates in contrast with the presence of selenate that was associated with the biological oxidation of Se(IV) to Se(VI) carried out by diatoms. Laboratory experiments suggest that planktonic green algae assimilate preferentially Se(VI) over Se(IV) (Neumann et al., 2003; Simmons & Wallschläger, 2011). In contrast, Nishri et al., (1999) reported important removal of dissolved Se in Lake Kinneret that can be explained by the preferential uptake of Se(IV) by phytoplankton, as it was demonstrated in previous experimental studies (Hu et al., 1997; Wrench & Measures, 1982). Recent studies carried out using the chlorophyte (Chlamydomonas reinhardtii) showed that the uptake of selenite was five times higher at pH 9 than at pH 7 (Ponton et al., 2018). In contrast, 15-50% decrease of Se(IV) uptake was observed with increasing phosphate concentration from 100 to 450 µM (Vriens et al., 2016). The same species showed a decrease by half of selenate uptake in the presence of 1 µM of sulfate (Ponton et al., 2018). Several authors agree on the faster uptake of

organic Se over inorganic species (Ponton et al., 2018; Vriens et al., 2016; Winkel et al., 2015). Therefore, Se uptake highly depends on the bioavailability of each species, the type of microorganisms present in the water, and the concentration of different anions in the case of Se oxyanions.

The current knowledge on Se biotransformations has been reviewed by Chasteen & Bentley (2003) and Lenz & Lens (2009) but the mechanisms of the processes underlying Se biotransformations remain unclear. Since aquatic microorganisms mediate several oxidation/reduction and alkylation/dealkylation processes that release Se(0) and reduce Se species to the water, Se cycling is affected by phytoplankton, and bacteria.

The most important potential removal pathways proposed for dissolved Se are: sorption of selenite into Fe, Mn and Al oxy-hydroxides (Balistrieri & Chao, 1987; Y. M. Nakamaru & Altansuvd, 2014), scavenging and deposition of Se-enriched organic matter (Weres et al., 1990; Weres et al., 1989), reduction of Se oxyanions to either insoluble Se(0) (Nancharaiah & Lens, 2015) and/or to Se(-II), including volatile compounds (Amouroux & Donard, 1996, 1997; Amouroux et al., 2001; Chau et al., 1976; Cooke & Bruland, 1987). The chemical analogy between sulfur (S) and Se are well known (Fernández-Martínez & Charlet, 2009) and similar biogeochemical pathways for both elements have been reported in marine, estuarine and wetland environments (Mehdi et al., 2013; Winkel et al., 2015). Nevertheless, while many studies focused on volatile S, only few have been carried out to study volatile Se speciation in lake waters (Cooke & Bruland, 1987; Diaz et al., 2009; Lanceleur et al., 2019). In aquatic environments, the production of volatile S and Se compounds has been strongly linked to microbial processes suggesting biological mediated processes to be an important removal pathway for dissolved Se (Amouroux et al., 2001; Mason et al., 2018; Wen & Carignan, 2007). Therefore, the study and characterization of the volatile Se fraction in lake water is necessary to complete our understanding of the Se biogeochemical cycling in such ecosystems (Diaz et al., 2009).

Lake Kinneret can be considered as a remarkable site to study Se aquatic biogeochemistry due to (i) the current understanding of its sulfur biogeochemistry (Ginzburg et al., 1999; Knossow et al., 2015; Sela-Adler et al., 2016); (ii) the typical seasonal alternation between oxic (winter) and anoxic (summer-fall) conditions in its hypolimnion and; (iii) because its physical, chemical and biological features are well described and monitored routinely (Zohary et al., 2014a). Oxygen depletion in the hypolimnion together with H2S production are linked to the

activity of sulfate reducing bacteria (SRB) (Hadas & Pinkas, 1995). Oremland et al. (1989) described the potential reduction of Se oxyanions by SRB, whereas Nishri et al. (1999) suggested that the removal of Se(IV) was due to chemical reactivity with H2S. The present study is based on a 3-years survey conducted in Lake Kinneret, Israel, consisting of simultaneous depth profile monitoring of volatile and non-volatile dissolved Se species. This warm monomictic lake is characterized by high biological activity and strong seasonal stratification, with anoxic sulfide-rich hypolimnion in late summer (Zohary et al., 2014a). Our main goal was to investigate the speciation and fate of dissolved selenium in Lake Kinneret at seasonal and interannual time scales in the water column. A comparison with past data presented by Nishri et al. (1999) is given to overview the main changes in terms of Se concentration and speciation over the last decades.

2. Materials and Methods

2.1. Site Description

Lake Kinneret (Fig. Art.1.1) is a warm, monomictic, meso-eutrophic freshwater lake located at the northeast of Israel (32º50'N; 35º35'E). The lake has an area of 170 km^2, mean depth of 25 m and maximum depth of 42 m (Berman et al. 2014). Lake Kinneret is stratified 8-9 months per year, from March-April until November-December, and is homothermal during the remaining months. The stratified period is characterized by a strong separation and low exchange of water between the warmer top (epilimnion) and cooler bottom (hypolimnion) layers, with resulting strong vertical gradients of physicochemical and biological parameters along the water column. Primary production is limited to the illuminated, well-oxygenated and warm epilimnion (18-30 ºC). The cooler, dark hypolimnion becomes anoxic within a few weeks after the onset of thermal stratification and maintains a constant temperature (~15-16 ºC) (Berman et al., 2014). The interphase layer (metalimnion) is located at 15-20 m during the summer. Nitrate (NO_3^-) accumulates in the well-mixed water column in winter due to riverine inflows and nitrification of ammonium (NH_4^+) previously accumulated in the hypolimnion. Once stratification begins, the NO_3^- concentration decreases in both the epilimnion and hypolimnion as a consequence of biological uptake and denitrification, respectively (Berman et al., 2014). Sulfate presents a conservative behavior in the epilimnion, meanwhile reducing conditions at the hypolimnion lead to the production of hydrogen sulfide (HS^-) during stratification (Berman et al., 2014; Ginzburg et al., 1999).

Figure Art.1.1. Lake Kinneret (Israel). St. A indicates the sampling point located in the center of the lake. Additional samples were taken before and after the Hula Valley at Joseph Bridge (Joseph B.) and Huri Bridge (Huri B.).

Hypolimnetic reducing conditions are associated to organic matter degradation by anaerobic microorganisms, in particular, to methanogenesis in sediments and sulphate reduction both in sediments and water leading to the accumulation of CH_4 and H_2S in the hypolimnion (Eckert & Conrad, 2007).

The Jordan river (annual inflow ~ 350 10^6 m^3; (Rom et al., 2014)), is the largest source of freshwater flowing into Lake Kinneret, supplying ~65% of the incoming water, while direct precipitation contributes only ~10% of the total water input to the lake (Rimmer & Gal, 2003). Notably, during the three years of this study, the annual minimum lake water level dropped by 1.34 m as a result of continuous drought, with below average annual rainfall. Evaporation (~230 × 10^6 m^3 $year^{-1}$) and water withdrawal (~375 × 10^6 m^3 $year^{-1}$) for agricultural and human consumption are usually the main water outflows (Ostrovsky et al., 2013; Rimmer & Givati, 2014), although during the years of this study (2015-2017), water pumping out of the lake was reduced drastically due to sever draught conditions. The Jordan River is also the main external source of Se loading into the lake, mainly as inorganic Se (selenite and selenate) originating from the Hula Valley (Nishri et al., 1999).

Lake Kinneret has been subjected to major man-made hydrological and other changes during the last decades (Berman et al. 2014). One dramatic hydrological change was the draining in the 1950s of Lake Hula and its associated wetlands. Lake Hula, a natural shallow lake in the Hula basin, to the north of Lake Kinneret through which the Jordan River used to flow before reaching Lake Kinneret, acted as a natural filter to Lake Kinneret (Hambright & Zohary, 1998) (Fig. Art.1.1). In an attempt to alleviate some of the ecological damages to the Hula Valley caused by the drainage, a small shallow water body, Lake Agmon, was created in 1994 on part of the historical site of Lake Hula (Hambright & Zohary, 1998). With its creation, most water from the Hula Valley is being diverted for agricultural use and no longer reaches Lake Kinneret (Berman et al., 2014). In addition to the water required for agriculture, municipal and domestic demands for water in the Lake Kinneret catchment have increased during the last decades resulting in lower annual inflows into Lake Kinneret compared to previous decades (Rimmer & Givati, 2014). The effects of these changes on Lake Kinneret microbiota and thus, on Se cycling are still not well understood. The stress over Lake Kinneret ecosystem has been shown to affect the phytoplankton dynamics (Zohary, 2004; Zohary et al., 2014b). For example, the predicted annual bloom of the dinoflagellate Peridinium gatunense was gradually vanished and replaced by winter-spring bloom of cyanobacteria (mainly Microcystis). A loss of species diversity together with the appearance and establishment of N2-fixing cyanobacteria has also been observed since the mid 90's, especially Chrysosporum (formerly Aphanizomenon) ovalisporum and Cylindrospermopsis raciborskii (Sukenik et al., 2014). Cyanobacteria not only represents a major concern for water quality, it also has the ability to uptake and transform Se and it may have an impact in Se cycle (Bender et al., 1991; Chouhan & Banerjee, 2010).

2.2. Sampling, transport and samples storage

Sampling was carried out four times a year during 2015-2017, at Station A (Fig. Art.1.1), using a 5 L vertical point water sampler (Aquatic Research Instruments, Hope, ID, USA). For dissolved Se (Total Se and species), water samples were collected during January (winter holomixis), April (early spring when stratification commences at 10-12 m), September (summer with thermocline around 15 m), and November (late fall, when the thermocline deepens to ~25-30 m). For each sampling campaign at Station A, water samples were collected from discrete depths, representing the epilimnion (samples from 1, 3, 5 and 10 m), hypolimnion (25, 30 and 35 m samples) and metalimnion (intermediate-depth samples) in correlation with depths sampled for the routine weekly monitoring of the lake. Samples were

stored in cool conditions until arriving to the lab where they were filtered (cellulose acetate 0.45 µm filter, Sartorius) and sealed with no headspace in 120 ml glass vials, pre-cleaned with nitric acid and deionized water. For volatile Se, the sampling was concurrent to dissolved Se sampling. One liter, pre-cleaned glass bottles were filled directly from the water sampler on board without filtering, ensuring via overflow minimum contact with atmosphere and sealing the bottles without any air bubbles. The samples for volatile Se and dissolved Se were stored at 4º C, under dark conditions up to two weeks until shipping for Se analysis at the IPREM laboratory, Pau, France.

Accompanying physical, geo-chemical and biological parameters used in this study were obtained from the Lake Kinneret Database (LKDB) of the Kinneret Limnological Laboratory, Israel Oceanographic and Limnological Research, and based on the long-term monitoring program on the lake (Sukenik et al., 2014). In general, these include sampling of the water column at station A and other stations at weekly (physical and geo-chemical) or biweekly/monthly intervals (biological parameters). Sampling for Se in this study was usually made concurrently with the sampling for the routine monitoring, from the same times, depths and sampling bottles at Station A.

2.4. Reagents

Ultrapure water (18.2 Ωcm) was obtained from a Milli-Q System (Millipore Co., Bedford, MA, USA). Commercial chemicals of analytical reagent grade were used without further purification. DL-selenomethionine (Sigma), sodium selenite and sodium selenate (Merck) were used. Stock standards solution of 1000 mg (Se) L^{-1} were prepared in ultrapure water and stored at 4ºC in the dark. Working standard solutions were prepared daily by dilution in ultrapure water.

2.5. Total Selenium Analysis

Total Se was determined with Agilent 7500ce or 7900 ICP-MS instruments (Agilent Technologies, Tokyo, Japan) both equipped with octopole collision/reaction cell (CRC), concentric nebulizer and a Scott double pass spray chamber cooled to 2°C. Argon-based polyatomic interferences were reduced by using H_2 as cell gas at a flow rate of 5 ml min^{-1}. Acquisition parameters were: integration time, 200 ms per isotope; 10 (7900) or 15 (7500ce) replicates; monitored m/z 77 and 78. External calibration (single element Se standard 1000 mg L^{-1} SCP Science) was performed. The instrumental detection limits of Se (based on ^{78}Se) were in the range 1.6-13 ng L^{-1} depending on the instrument. Typical analytical precision was

<5% (relative standard deviation, 10 to 15 replicates) (Darrouzès et al., 2008; Pokrovsky et al., 2018).

2.6. Selenium Speciation Analysis

2.6.1. Non-Volatile Dissolve Se Analysis

The chromatographic system consisted of an Agilent 1100 or 1200 series HPLC pump, equipped with autosampler and variable volume sample loop. The HPLC-ICPMS interface was made up of a polyetheretherketone (PEEK) tube. Chromatographic separation was carried out on porous graphitic carbon stationary phase (Hypercarb, Thermo Fisher Scientific, 100 × 4.6 mm i.d, part. size 5 µm) with formic acid mobile phase (240 mmol L^{-1}, 1% methanol and pH 2.4 adjusted with ammonia) delivered at 1 mL min^{-1} flow rate (Dauthieu et al., 2006). The injection volume varied from 100 to 300 µL. Species quantification was achieved by standard addition with limit of detection (LoQ) around 2 ng L^{-1} for Se(IV) and Se(VI).

The chromatographic conditions used allowed the simultaneous separation of inorganic (selenite and selenate) and organic (trimethylselenonium ion, methane seleninic acid, selenomethione and selenocystine) species. Some selenium-containing compounds (up to 3) were detected in the samples. However, their retention times did not match any of the organic Se standards available. A particular compound eluting between Se(VI) and selenomethionine (SeMet) was detected in most samples. This uncharacterized Se containing compound is referred here as Organic Se (Org.Se) (see Fig. Art.1.SI 1). Its concentration was estimated using the standard addition slope of Se(VI) as its retention time was between those of Se(VI) and SeMet and, corresponding slopes were similar (12% difference). This compound was part of a reduced Se pool that was defined as the difference between Total Se (T.Se) and inorganic Se (Se(IV)+Se(VI)) concentrations and calculated as follow: Red.Se =T.Se - Se(IV) - Se(VI).

2.6.2. Volatile Se Analysis

Volatile Se analysis was carried out by a cryo-trapping system coupled to a GC-ICP/MS. The low concentration of the volatile species required the use of a preconcentration procedure. For this purpose a purge system followed by a moisture trap and an activated carbon trap described elsewhere (Lanceleur et al., 2019; Tessier et al., 2002) were used. Carbon traps were pre-cleaned by heating three times at 250°C for 2 min, under argon flow (100 mL min^{-1}). After cooling the traps in a laminar flow hood, they were closed with caps until analysis. For preconcentration in the carbon traps, 1 L of sample was purged and dried applying a constant He flow (between 400 to 500 mL min^{-1}) for 90 minutes. The moisture trap consisted of an

acid-washed silanized glass kept at -20°C with an acetone/ice bath. Volatile Se compounds were trapped in activated carbon solid phase. For analysis, the carbon trap was desorbed for 2 min at 250 ºC and analytes were cryofocused in the head of a U-shaped glass trap filled with acid-cleaned silanized glass wool (Chromosorb SP2100) and immersed in liquid nitrogen (–196 °C). This procedure concentrates and stabilizes the analytes for their further sequential desorption by heating the column for 6 min up to 300 ºC. Thermodesorption efficiency was controlled by carrying out two consecutive analyses of the activated charcoal trap. Volatile species quantification was performed by external calibration. Analyses of purge blanks were done to estimate the efficiency of the sample treatment procedure. Three selenium species (dimethylselenide (DMSe), dimethylselenide sulphide (DMSeS) and dimethyldiselenide (DMDSe)) were detected, with limit of detection of 0.1-0.5 pg Se L^{-1}, and quantified. Total dissolved volatile Se (TVSe) was calculated as the sum of detected species.

An estimation of the annual Se emission at the water-air interface was made using the Cole & Caraco (1998) model adapted for volatile Se compounds (Lanceleur et al., 2019) and providing flux densities for total dissolved volatile Se (Table Art.1.SI 6).

2.6.3. Volatilization fluxes estimation

The volatile emission fluxes across the air-water interface were calculated using an adapted version of the lake gas exchange equation from Cole & Caraco (1998) using the total volatile Se data (TVSe; Table Art.1.SI 5) from sub–surface samples (1m depth). The model was originally used to estimate the gas transfer velocity of CO_2 as function of wind speed. In our case the adaptation consisted in using the atmospheric data of DMSe and calculations were carried out using weak wind speed (3 m s^{-1}) and strong wind speed (10 m s^{-1}). The same model adaptation has been used by several authors for the same purpose (Lanceleur et al., 2019; Tessier et al., 2002)

2.6.4. Stability of Se compounds during sample storage

The time elapsed from the sampling to the analysis for dissolved non-volatile Se speciation was between 1 week and 1 month in most (over 80%) sampling campaigns but, January 2015, April 2015 and January 2016 samples were analyzed 2 months after sampling (Table Art.1.SI 7). To assure the quality of the results for Se speciation, a stability assay was conducted including two stability tests, among the 12 sampling campaigns. Stability tests are particularly important due to the potential oxidation/reduction of species during storage. The first test was conducted to check the influence of sample acidification after sampling; samples were

then analyzed once after a 1 week storage duration. The difference between acidified (0.2% HNO_3) and non-acidified samples (n=6) was less than 6, 4 and 3% for Se(IV), Se(VI) and T.Se determinations respectively, indicating that samples acidification for transport and short-term storage was not necessary which also allows a better preservation of other organic Se compounds (*i.e.* hydrolysis). The second test was conducted to evaluate the maximum error range for species determination due to longer time storage at 4 ± 1 ºC in the worst conditions of this study, *i.e.* 1 month storage in the presence of headspace at 4ºC in the dark. In this case, differences in Se(IV) species quantification in the same sample (35 ng L^{-1} concentration level) within a month were 18% and 10% for non-acidified and acidified samples (n=4) respectively. Reduced stability of Se(IV) was thus observed in non-acidified samples and poor storage conditions. This maximum uncertainty of 18% was thus applied to selenite concentrations in samples stored more than 1 month. For Se(VI) at ca. 50 ng L^{-1} concentration level, differences in species quantification was much lower: 3 and 4% in non-acidified and acidified samples (n=4) respectively, suggesting a greater stability for this species even under poor storage conditions and a negligible effect of acidification.

Volatile Se samples were stored at 4ºC in the dark prior to analysis. Generally, analyses were performed less than 15 days after sampling, but longer storage were unavoidable in April 2015 (45 days), April 2016 (22 days) and September 2016 (36 days). Stability tests were carried out to study the TVSe and speciation alterations due to long storages. In November 2016, a triplicate of 1 m and 25 m depth samples were stored for 4, 18 and 37 days from sampling to purge and analysis. At 1 m depth, the TVSe concentration after 18 days was ten times higher than the concentration at 4 days. TVSe increase after 18 days corresponds mainly to the production of DMSeS and, and to a lesser extent, to the production of DMDSe (Amouroux et al., 2000). The concentration of DMSe at 1m of depth was constant for the first 18 days and decreased by ca. 45% after 37 days. At 25 m the concentration the TVSe difference after 18 and 37 days was below 7%. However, in this case, the speciation varied, with an increase of DMSe (74%) and a slight decrease of DMSeS and DMDSe after 18 days. After 37 days, DMDSe ca. increase was around 13% compared to fresh sample analysis. The results of this stability test indicate that for long storage times (> 2 weeks), DMSeS and DMDSe concentrations may be overestimated mainly in some epilimnion samples as well as DMSe concentration in hypolimnion samples. So far, the largest volatile Se compounds concentrations observed in this study never corresponded to the sampling campaigns for which sample storage was the longest.

2.6.5. Stock and depth integrated Se concentration calculation

Stock of total Se or Se compounds as calculated by weighting sample measured concentration by its vertical size, following Eq(1) :

$$(1)\ Se_{stock}\ (ng \text{ or } \mu g\ Se\ m^{-2}) = \sum \frac{C_i + C_{i+1}}{2} \times (h_{i+1} - h_i)$$

where i = 1,…,12 the number of the depth level; h_i = depth in meters of the i-th level; C_i = selenium concentration of the i-th level (pg L^{-1} for volatile Se; ng L^{-1} for non-volatile Se).

Depth-integrated average Se concentration ($[Se]_{dia}$ was then calculated by dividing Se_{stock} for a considered vertical layer depth by the corresponding integration depth (Eq(2)). Values are given in pg or ng of Se per liter, assuming water density as 1 kg L^{-1}. Depth-integrated average value gives a representative value of average Se concentration considering entire or given water column depth allowing to take into account interseasonal depth variability which is necessary for interseasonal comparisons.

$$(2)\ [Se]_{dia}\ (pg \text{ or } ng\ Se\ L^{-1}) = \frac{Se_{stock}}{h}$$

Stocks and depth-integrated average concentrations were also calculated for the physico-chemical (T, pH, turbidity, dissolved oxygen and conductivity) and biological parameters (chlorophyll a, primary production, phytoplankton taxa).

Stocks and depth-integrated average concentrations were calculated considering either the entire depth of the water column (0-35 m) or epilimnion (0-10 m) or hypolimmion (25-35 m) depths except for primary production (PP) and chlorophyll (Chl-a) data obtained from LKDB that were integrated from the surface to 15 m depth regardless of thermocline depth.

Oxygen saturation ratio (% Ox. Sat.) was calculated by dividing the measured dissolved oxygen concentration (DO) by the theoretical concentration at 100% saturation for the corresponding temperature (Mortimer, 1981).

2.6.6. Statistical analysis

Statistical analyses were performed to compare seasonal and interannual selenium concentration variations. Shapiro–Wilk normality test was applied to average concentrations. Results show that non-volatile dissolved Se concentrations were normally distributed while volatile Se and biological data were not. A Student's t-test (2-tail and 1-tail) was then used to compare non-volatile Se species concentrations and, Mann-Whitney (MW, 2-tail and 1-tail) test was performed to compare non-volatile Se values with other data sets, *i.e.* volatile Se and

biological parameters. Note that whenever 1-tail t-test if given, samples were previously tested positive for 2-tail t-test. Pearson's correlation was used for linear regression analysis. All tests were conducted at a confidence level of 95% using Origin8 (OriginLab Corporation).

3. Results and Discussion

3.1. Seasonal and annual variabilities of hydrobiological characteristics in the water column

The seasonal variations of Se are inherent to the water column characteristics and changes during the year. Here we describe the main dynamics of the lake in stratified (late spring – fall) and non-stratified periods (winter – early spring) with special focus on Chlorophyll-a and primary productivity, conductivity, temperature, pH, turbidity and oxygen saturation (Fig. Art.1.2, Fig. Art.1.3. and Fig. Art.1.SI 3).

Physical parameters (T, conductivity, pH & DO)

Epilimnetic temperature gradually increased from around 15 – 16 ºC at winter to ~30 ºC at September each year (Fig. Art.1.SI 2). Hypolimnetic temperatures remained relatively stable for the three years studied (~16 ºC). At spring periods, lake surface water had higher pH and was oxygen-supersaturated due to the increase of PP and weak winds that limit water-air gas exchange (Fig. Art.1.2, Fig. Art.1.3, Fig. Art.1.SI 3 and Table Art.1.SI 1). After the spring phytoplankton development (see next section), epilimnetic DO levels remained around 100% saturation (Fig. Art.1.SI 3). In the hypolimnion, oxygen level decreased progressively as stratification developed and, by June, it became anoxic. This situation was maintained until December or January as previously reported by (Berman et al., 2014). Conductivity (Cond.) values increased during the period monitored (Table Art.1.1) from 1235 in April 2015 to 1376 $\mu S\ cm^{-1}$ in November 2017, representing an increase in salinity, as a result of declining inflows but continued inflow of saline springs during those draught years.

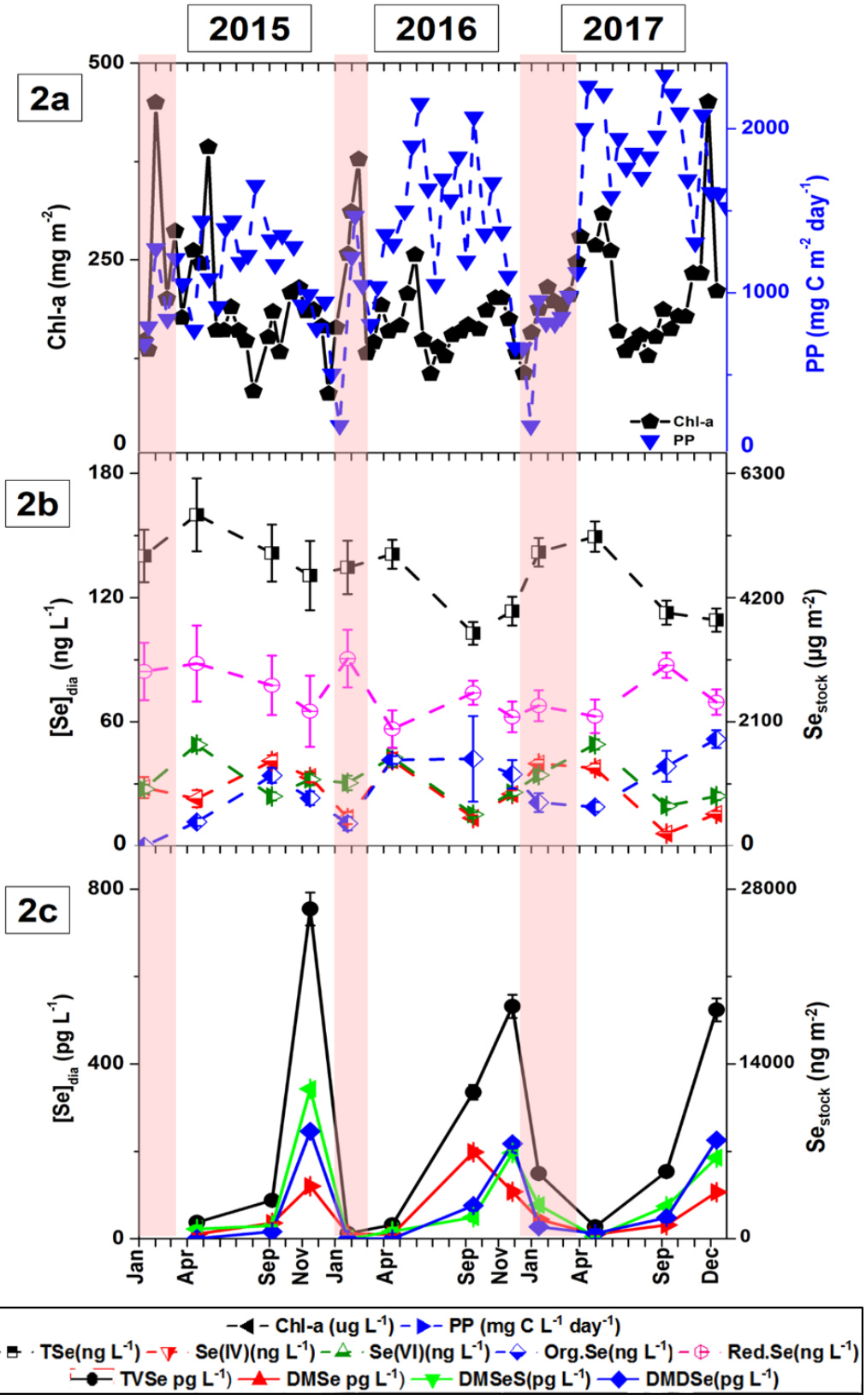

Figure Art.1.2. Temporal variations in various limnological parameters in Lake Kinneret during 2015-2017: (a) chlorophyll-a (Chl-a), and primary production (PP) stocks (0-15 m depth); (b, c) stocks and depth-integrated concentrations for total selenium and selenium species. 2b includes: Total Se (T.Se), selenite (Se(IV)), selenate (Se(VI)), estimated organic Se

(Org.Se) and reduced Se (Red.Se). 2c includes: total volatile Se (TVSe), dimethylselenide (DMSe), dimethylselenide sulphide (DMSeS) and dimethyldiselenide (DMDSe). Vertical red-shaded rectangle indicates holomixis period. Se data correspond to the average concentrations in the water column. For more detail, Se data in Table Art.1.SI 5. Source of Chl-a and PP data: Tamar Zohary, Lake Kinneret database, Kinneret Limnological Laboratory, Israel Oceanographic & Limnological Research.

Chlorophyll a and Primary Productivity

Chl-a maximum values were observed during January and February in 2015 (450 mg m^{-2}) and 2016 (378 mg m^{-2}), with another peak in May of both years (Fig. Art.1.2a). In 2017 the early year peak was missing, a spring peak was noticed, and an unusual peak, the highest value of the year, was observed in November (451 mg m^{-2}) (Fig. Art.1.2a). Statistically, 1-tail Mann-Whitney test did not show interannual significant variations ($P<0.05$). Previous studies reported a typical annual pattern with maximum values of Chl-*a* in spring (Yacobi et al., 2014). This annual pattern continues to be typical of high rainfall years with *Peridinium* blooms, but in drought years, different patterns were reported (Zohary et al. 2012).

In contrast to Chl-a, primary productivity (PP) followed similar annual patterns for the 3 years studied (Fig. Art.1.2a). Annual minimum values occurred around the time of overturn, late December or early January, followed by a sharp increase in the following weeks. It then remained high (with fluctuations) until the end of summer, declining again to the December minimum values. Despite interannual similarities, the annual average values increased from 1108 ± 265 mg C m^{-2} day^{-1} at 2015 to 1272 ± 413 and 1635± 464 mg C m^{-2} day^{-1} at 2016 and 2017 respectively.

In summary, the increase of major elements concentration in water due to evaporation increased the conductivity as consequence of the dry period recorded during the 3 years studied. In these conditions, Chl-a peaked earlier than previously reported suggesting that the lake biological productivity was activated earlier. Figure Art.1.4 shows the main phytoplankton species present in the water (0 – 15m). Similar dynamics were observed for the three years. At the beginning of stratification, dinophyta and chlorophyta increased and were predominant species. During late summer and fall, bacillariophyta and cyanophyte increased and became the main species.

Table Art.1.1. Depth-integrated average concentrations (entire depth of the water column 0-35 m) for non-volatile and volatile dissolved Se (total dissolved Se (T.Se), Se(IV), Se(VI), organic Se (Org.Se) and reduced Se pool (Red.Se) in ng L–1; total volatile Se (TVSe) in pg L–1) and, for the main physicochemical parameters (monthly means if n>1): % of oxygen saturation (Ox. Sat), pH, temperature (T), conductivity (Cond.) and turbidity (Turb). For detailed data see tables SI 3, SI 4 and SI 5. Confidence interval is indicated in brackets and in italics. Source of Chl-a and PP data: Tamar Zohary and Yaron Be'eri-Shlevin, Lake Kinneret database, Kinneret Limnological Laboratory, Israel Oceanographic & Limnological Research. <LoD: below detection limit, n.d. means no data.

Sample name & date	**Jan 15** **11/01/15**	**Apr 15** **19/04/15**	**Sep 15** **06/09/15**	**Nov 15** **16/11/15**	**Jan 16** **25/01/16**	**Apr 16** **17/04/16**	**Sep 16** **15/09/16**	**Nov 16** **27/11/16**	**Jan 17** **15/01/17**	**Apr 17** **30/04/17**	**Sep 17** **10/09/17**	**Nov 17** **12/12/17**
T.Se (ng L^{-1})	140 (*13*)	160 (*18*)	141 (*14*)	131 (*17*)	135 (*13*)	141 (*7*)	103 (*6*)	113 (*7*)	142 (*7*)	149 (*7*)	113 (*6*)	109 (*6*)
Se(IV) (ng L^{-1})	28 (*5*)	23 (*4*)	41 (*3*)	33 (*2*)	14 (*3*)	42 (*3*)	14 (*1*)	25 (*2*)	40 (*2*)	38 (*2*)	6 (*1*)	16 (*1*)
Se(VI) (ng L^{-1})	28 (*2*)	49 (*3*)	24 (*2*)	32 (*3*)	31 (*3*)	43 (*4*)	15 (*1*)	26 (*2*)	34 (*2*)	49 (*2*)	19 (*1*)	24 (*2*)
Org.Se (ng L^{-1})	< LoD	12 (*2*)	34 (*4*)	23 (*3*)	11 (*3*)	42 (*2*)	42 (*21*)	35 (*7*)	21 (*5*)	19 (*2*)	39 (*7*)	52 (*4*)
Red.Se (ng L^{-1})	84 (*14*)	88 (*18*)	78 (*14*)	65 (*17*)	91 (*14*)	57 (*9*)	74 (*6*)	62 (*7*)	68 (*7*)	63 (*8*)	87 (*6*)	70 (*6*)
TVSe (pg L^{-1})	n.d.	37 (*2*)	88 (*4*)	755 (*38*)	12 (*1*)	32 (*2*)	335 (*17*)	532 (*27*)	149 (*7*)	28 (*1*)	154 (*8*)	524 (*26*)
O_2 Sat (%)	85 (*9*)	63 (*5*)	43 (*6*)	57 (*4*)	76 (*9*)	63	47 (*4*)	59 (*7*)	88 (*5*)	87 (*1*)	37 (*5*)	53 (*9*)
pH	8.1 (*0.1*)	8.1 (*0.1*)	8.0 (*0.1*)	7.9 (*0.1*)	7.9 (*0.1*)	8.1 (*0.1*)	8.0 (*0.1*)	8.0 (*0.1*)	8.1 (*0.1*)	8.3 (*0.1*)	8.0 (*0.1*)	8.0 (*0.1*)
T (°C)	16.5 (*0.9*)	17.2 (*0.3*)	23.3 (*0.3*)	20.8 (*0.7*)	16.7 (*0.3*)	17.6	23.3 (*0.1*)	20.9 (*1.1*)	15.5 (*0.5*)	17.0 (*0.8*)	22.8 (*0.3*)	20.3 (*0.7*)
Cond (µS cm^{-1})	1259 (*5*)	1235 (*7*)	1248 (*5*)	1271 (*6*)	1280 (*3*)	1277 (*5*)	1310 (*3*)	1337 (*4*)	1335 (*6*)	1319 (*2*)	1357 (*3*)	1376 (*5*)
Turb (NTU)	2.0 (*1.7*)	1.3 (*0.2*)	1.9 (*1.1*)	1.4 (*0.3*)	1.6 (*0.6*)	1.5 (*0.6*)	2.5 (*0.7*)	1.9 (*0.6*)	1.7 (*0.4*)	2.4 (*0.3*)	3.7 (*1.7*)	3.8 (*2.1*)

3.2. Selenium speciation in the entire water column (0 – 35m) among seasons

3.2.1. Dissolved total Se and inorganic Se(IV) and Se(VI)

During the three years studied, depth-integrated average total Se ($TSe_{dia\ (0\ -\ 35m)}$) concentration ranged from 103 ± 6 to 160 ± 18 ng Se L^{-1} (Table Art.1.SI 5) and showed an overall declining trend from April to the end of the year, each year (Fig. Art.1.2b). An increase of T.Se for the entire depth-integrated concentration occurred between January and April corresponding to the end of holomixis–beginning of stratification each year (135 - 160 ng Se L^{-1}), more markedly in 2015 and 2017. From then and until the end of stratification these concentrations decreased by 18 to 27% to reach a minimum in September (2016) or November (2015, 2017) (Table Art.1.1).

Depth integrated average concentrations of Se(IV) in the water column ranged from 14 ± 3 to 42 ± 3 ng Se L^{-1} during the 2015-2017 period with an exceptional low value of 6 ± 1 ng Se L^{-1} in September 2017 (Fig. Art.1.2b, Table Art.1.1). The t-tests do not show significant differences among selenite seasonal concentrations integrating the entire depth of the water column. Although no statistically significant differences were found, $[Se(IV)]_{dia\ (0-35m)}$ increased during stratification in 2015, by 80% from April to September (Fig. Art.1.2b), whereas in 2016-2017, during the same period Se(IV) exhibited opposite trend with 67-84% decrease.

The seasonal pattern for Se(VI) was similar to the one of Se(IV) described above (Fig. Art.1.2b). Higher average concentrations values were found in April, followed by 50-60% decrease in September and November. Statistically significant differences were found, comparing seasonal $Se(VI)_{dia\ (0\ -\ 35m)}$ ca. April > January (1–tail t–test: t= 5.7, P<0.003) ≈ November (t=6.1, P<0.002) ≈ September (t= 8.4, P<0.001).

3.2.2. Dissolved Reduced Species

Reduced Se depth-integrated average (0 – 35m) concentrations ranged from 57 ± 9 to 91 ± 14 ng L^{-1} (Fig. Art.1.2b, Table Art.1.1). No interannual significant differences were statistically found. For seasons, Red.Se concentration only proved to be statistically higher in September than in November (t=3.1, P<0.02). However, a more detailed view of $Red.Se_{dia\ (0-35m)}$ showed relatively stable concentrations of Red.Se in 2015 with a decrease in November compared to other seasons. In 2016, January showed the highest annual Red.Se concentration (Table Art.1.1), it decreased in April (57 ± 9 ng Se L^{-1}) and increased again in September (74 ± 6 ng Se L^{-1}). From November to April of 2017, concentration were between 62 – 68 ng Se L^{-1} and

increased in September to 87 ± 6 ng Se L^{-1} with a subsequent decrease in November to 70 ± 6 ng Se L^{-1}. Additionally, depth profiles for Red.Se (Fig. Art.1.3 and Fig. Art.1.SI 4) show its predominance in the hypolimnion during anoxic periods.

A Se-containing compound whose retention time did not match any of the organic Se standards available was detected ubiquitously during the three years studied except in January 2015. This compound that is referred to here as Org.Se showed a repeated trend each year with lower values occurring in January and increased concentrations in spring and fall. Concentrations of $Org.Se_{dia\ (0-35m)}$ were in the range of <LoD – 21 ± 5 ng Se L^{-1} in January while the concentration of other seasons was between 12 ± 2 to 52 ± 4 ng Se L^{-1} (Table Art.1.1). Despite the difference were not statistically significant, the trend observed indicates an increase during (late) spring and summer that occurred mainly at epilimnion. A strong correlation was observed between Chl-a (µg L^{-1}) and Org.Se (ng L^{-1}) at water column in spring for the three years studied (Fig. Art.1.SI 5, R^2 values between 0.946 and 0.983 ($P<0.01$)). It is worth noting that during spring, dinophyta and chlorophyta were dominant species. No evidence of correlation was found in other seasons.

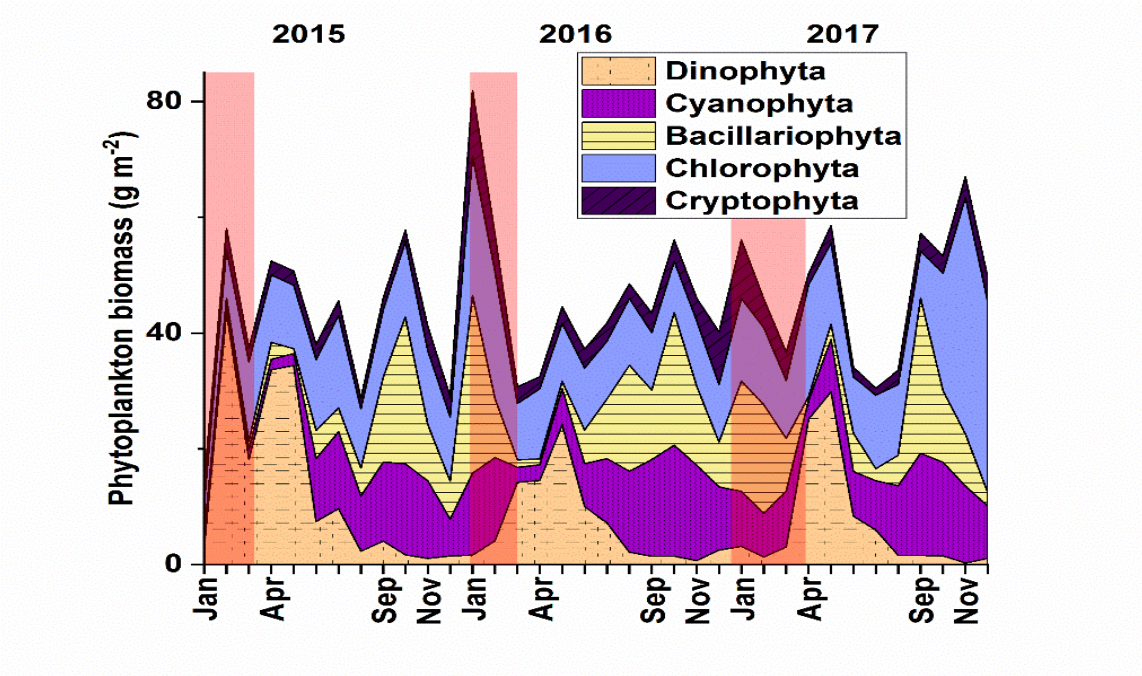

Figure Art1.3.2 Temporal dynamics of depth-integrated (0-15 m) wet-weight biomass, in g m^{-2}, of the major Phytoplankton taxa, (Dinophyta, Cyanophyta, Bacilariophyta, Chorophyta and Cryptophyta), 2015-2017. Vertical pink-shaded rectangle correspond to holomixis period. Source of data: Tamar Zohary, Lake Kinneret database, Kinneret Limnological Laboratory, Israel Oceanographic & Limnological Research.

As suggested by Nishri et al., (1999) increase of total selenium during winter seems to be associated with the oxidation of reduced Se species to Se(IV) and Se(VI). This seems to be a common process for water column and for the sediments as the deepening of the thermocline reached oxygen depleted zones. In addition, Se(VI) or Se(IV)+Se(VI) decrease coincided with an increase of Org.Se and/or Red.Se pool (Fig. Art.1.2b). The variation of Org.Se seems to be associated in parallel with phytoplankton growth, increased concentrations being observed during spring or summer when phytoplankton primary production rates are high. However, in 2016, lower Chl-a concentrations (that may result from lower amount of dynophyta, Fig. Art.1. 3) compared to other years resulted in a higher slope of the regression Org.Se vs Chl-a (Fig. 4). This could be caused by different assimilation, production and release Se rates of the different species, and could indicate that dynophyta would not be the main producer in the lake nowadays.

The behavior of Red.Se pool is somehow different; it accounted between 40-60% of total selenium during holomixis period until April. From April to the end of stratification, as oxyanions concentration decreased, this fraction became the main component of T.Se, representing about 80% under anoxic conditions at hypolimnion (25-35 m depth). Selenate and selenite reduction in the hypolimnion is most probably due to oxygen deficient conditions as long as stratification evolves. The trends observed indicates an inversely proportional relation between Red.Se fraction and Se(IV) ($R = -0.497$, $P<0.01$) during the three years of this study.

Table Art.1.2 shows that the lack of information for reduced Se species in lake waters. Comparing our results to those published for other lakes (Table Art.1.2) similar ranges of concentrations for T.Se, Se(IV) and Se(VI) were obtained, as long as we exclude lakes impacted by mining activities. Notably, despite the physical variations in the Hula Basin, in the drainage basin of Lake Kinneret (Fig. 1) and more than 20 years that elapsed since the study of Nishri et al. (1999) the T.Se concentration remained very similar. However, while total Se lake reservoir remain the same speciation has changed. The range of total selenium and Se(IV) measured in our study (2015-2017 period) was similar to that reported by Nishri et al. (1999) for the period 1993-1995. In those years T.Se values oscillated in the range of 50 - 184 ng Se L^{-1}, Se (IV) between <5 to 78 ng Se L^{-1} (Table Art.1.2) and Se(VI) ranged between 31 - 103 ng Se L^{-1}, slightly higher than in the present work. Likewise, the concentration range of the Red.Se oscillated at the beginning of the 90's between <5 – 50 ng Se L^{-1} , while in the present work, concentration of Red.Se was three times higher (Table Art.1.2).

3.2.3. Volatile Dissolved Selenium

Depth integrated total volatile Se concentration ranged from 12 ± 1 to 755 ± 38 pg Se L^{-1}. Total volatile Se concentration was higher in late summer and fall (Table 3) than in winter-spring seasons, especially at epilimnetic depths close to thermocline (Fig. Art.1.3 and Fig. Art.1.SI 4, Table Art.1.SI 1). Concentrations of $TVSe_{dia\ (0-35m)}$ oscillated between 12 ± 1 and 149 ± 7 pg Se L^{-1} during winter-spring seasons; while in summer-fall the concentrations were between 88 ± 4 and 755 ± 38 pg L^{-1} (Table Art.1.3). Three volatile Se compounds were identified in the water column: dimethyl diselenide (DMDSe) and the mixed S-Se compound dimethyl selenide sulphide (DMSeS) as the dominant species and, DMSe in lower concentration except in Sep 2016. In brief, during stable thermal stratification $DMSe_{dia\ (0-35m)}$ ranged from 31 ± 2 to 198 ± 10 pg Se L^{-1} (30% of TVSe in average), $DMSeS_{dia\ (0-35m)}$ from 30 ± 2 to 343 ± 7 pg Se L^{-1} (36% of TVSe) and $DMDSe_{dia\ (0-35m)}$ from 16 ± 2 to 246 ± 6 pg Se L^{-1} (32% of TVSe) (Table Art.1.3). In contrast, concentration during holomixis was usually close or below the detection limit (<0.5 pg Se L^{-1}). During winter and spring seasons $DMSe_{dia\ (0-35m)}$ range was 10 ± 1 – 45 ± 2 pg Se L^{-1}, $DMSeS_{dia\ (0-35m)}$ <LoD – 77 ±2 and $DMDSe_{dia\ (0-35m)}$ <LoD – 27 ± 2 pg Se L^{-1} (Table Art.1.3). The production of volatile Se compounds has been found to be inherent to the biodegradation of organic matter in estuarine environments (Amouroux & Donard, 1997; Tessier et al., 2002).

Only few studies reported volatile Se measurement values in similar environments (Table Art.1.2). Compiled data include lakes with high total Se contents, which are encountered when lakes are affected by mining activities or contain large geogenic sulfate and inorganic Se enrichments (Diaz et al., 2009; Domagalski et al., 1989). To the best of our knowledge, only Lanceleur et al., (2019) reported TVSe concentrations in non-polluted freshwater lakes, and these are one order of magnitude lower than in the present study. For further comparison, measurements of volatile Se compounds in European estuaries surface waters (Tessier et al. 2002; Amouroux & Donard 1997) are reported in Table Art.1.2. Despite the differences between tidal estuaries and the freshwater lake in this study, TVSe in Lake Kinneret is in the same range of concentrations measured in 3 estuaries (Gironde: 22 – 1350 pg Se L^{-1}, Rhine: 37 – 2423 pg Se L^{-1} , Scheldt 51– 8067 pg Se L^{-1}) (Amouroux & Donard, 1997; Tessier et al., 2002). There are however, some differences in the speciation of volatile Se compounds. In the studied estuaries, DMSe was the main compound while DMSeS and DMDSe were frequently detected but were residual in comparison to DMSe. We observed, in Lake Kinneret, the opposite with DMDSe and DMSeS the dominant species, whereas DMSe was usually detected

in lower amounts. In a recent study, Luxem et al., (2017) showed that a mixture culture of algae and bacteria exposed to Se(IV) produced greater concentration of volatile Se than the algae alone. Vriens et al. (2016) observed that DMDSe was produced 3.5 and 10 times more than DMSe when exposing the chlorophyte *Chlamydomonas reinhardtii* to selenate and selenite respectively. They suggested that under high Se concentration, DMDSe containing two Se atoms would be a more efficient detoxification product as it happens in hyperaccumulator plants (Pilon-Smits & Quinn, 2010).

Table Art.1.2. Bibliographic data for Se speciation in lake waters. Data for non-volatile Se speciation and T.Se in expressed in ng L^{-1}. TVSe is expressed in pg L^{-1} and volatile speciation is given as a percentage of TVSe.

Site	Description	T.Se	Se(IV)	Se(VI)	Red. Se	TVSe	References
		ng Se L^{-1}	ng Se L^{-1}	ng Se L^{-1}	ng Se L^{-1}	pg Se L^{-1}	
North America							
Great Salt Lake, USA	Salt Lake	500				40-22,700	Diaz et al. (2009)
Mining area, Canada		35 - 3063	<21 - 1616	<21 - 918	<21 - 528		Ponton & Hare (2013)
Kuujjuarapik, Canada	Artic Thaw ponds	35 - 63				1 - 32	Lanceleur et al. (2019)
Europe							
Gola di Lago, Switzerland	Minerotrophic Peatland	500 - 1500				10,000	Vriens et al. (2014)
Belgium		<50 - 230	<40 - 150	<50 - 80			Cutter (1978)
Campus Lake, Belgium		230[a]	150[a]	80[a]			Robberecht et al. (1983)
Artificial L., Germany		190	30	171			
Coal mining area, Germany		830	46	805			Tanzer & Heumann (1991)
Moorland L., Germany		210 - 240	27 - 141	35 - 47			
Valkea-Kotinenjärvi, Finland		58	4	5	37		Wang et al. (1994; 1995)
Iso-Hietajärvi L., Finland		34	4	4			
Pääjärvi L., Finland		143	10	17			Wang et al. (1995)
Pesosjärvi L., Finland		89	7	7			
Pyhäjärvi L., Finland		81	6	5			
Pszczewski Landscape, Poland Park Lakes, Poland		<150 - 740					Niedzielski et al. (2002)
Erken L., Sweden		65 - 200[a]	10 - 40[a]	30 - 160[a]			Lindström (1983b)
Asia							
Kinneret L., Israel		50 - 184	<5 - 78	31 - 103	<5 - 50		Nishri et al. (1999)
		74 - 203	<1 - 84	<1 - 90	34 - 147	28 - 755	This study

Table Art.1.3. Dissolved volatile selenium depth-integrated average concentrations in the entire depth of the water column 0-35 m, epilimnion (0-10 m) and hypolymnion (25-35 m) and confidence interval. Concentrations are reported in pg L^{-1}.

Month	n	Water column				Epilimnion				Hypolimnion			
		TVSe	DMSe	DMSeS	DMDSe	TVSe	DMSeS	DMSeS	DMDSe	TVSe	DMSeS	DMSeS	DMDSe
		(pg Se L^{-1})				(pg Se L^{-1})				(pg Se L^{-1})			
Apr15	3	37 ± 2	11 ± 1	22 ± 1	0.9 ± 0.6	15 ± 1	<LoD	12 ± 0.1	1 ± 0.003	54 ± 3	19 ± 1	30 ± 1	1 ± 1
Sep15	5	88 ± 4	36 ± 2	30 ± 2	16 ± 2	122 ± 6	38 ± 2	60 ± 2	24 ± 2	22 ± 1	8 ± 0.4	3 ± 0.4	5 ± 0.4
Nov15	5	755 ± 38	120 ± 6	343 ± 7	246 ± 6	965 ± 48	65 ± 3	674 ± 7	193 ± 4	610 ± 30	140 ± 7	147 ± 7	278 ± 7
Jan16	4	12 ± 1	11 ± 1	<LoD	<LoD	14 ± 1	13 ± 1	<LoD	<LoD	10 ± 1	10 ± 0.5	<LoD	<LoD
Apr16	4	32 ± 2	10 ± 0.5	17 ± 0.5	<LoD	19 ± 1	1 ± 0.1	11 ± 0.1	<LoD	61 ± 3	25 ± 1	30 ± 1	<LoD
Sep16	6	335 ± 17	198 ± 10	49 ± 10	76 ± 10	260 ± 13	226 ± 11	27 ± 11	6 ± 11	135 ± 7	20 ± 1	38 ± 1	60 ± 1
Nov16	5	532 ± 27	108 ± 5	196 ± 5	217 ± 5	551 ± 28	126 ± 6	184 ± 7	235 ± 6	259 ± 13	45 ± 2	142 ± 2	62 ± 2
Jan17	5	149 ± 7	45 ± 2	77 ± 2	27 ± 2	134 ± 7	44 ± 2	64 ± 2	25 ± 2	<LoD	<LoD	<LoD	<LoD
Apr17	6	28 ± 1	10 ± 1	5 ± 1	12 ± 0.5	14 ± 1	7 ± 0.4	5 ± 0.4	2 ± 0.3	49 ± 2	16 ± 1	4 ± 1	29 ± 1
Sep17	5	154 ± 8	31 ± 2	74 ± 2	48 ± 2	198 ± 10	39 ± 2	92 ± 2	67 ± 2	21 ± 1	11 ± 1	3 ± 1	7 ± 1
Nov17	5	524 ± 26	107 ± 5	185 ± 5	226 ± 5	455 ± 23	107 ± 5	162 ± 5	187 ± 5	583 ± 29	74 ± 4	238 ± 4	247 ± 4

3.2.4. Selenium compounds biogeochemistry along with water column stratification

3.2.4.1. Epilimnetic Selenium (0 – 10m)

During winter-spring periods, relatively homogeneous profiles were observed in the water column compared to stratified periods (Fig. Art.1.3, Fig. Art.1.SI 4 and Table Art.1.SI 1). Nishri et al., (1999) obtained similar vertical profiles in the 90's when holomixis exposed sediments to oxidizing conditions. In September, T.Se concentration decreased with respect to April with marked minimum (around minus 30-35% compared to 1 m depth) in the thermocline region. Total dissolved Se regeneration occurred together with holomixis in January. Se(IV) and Se(VI) concentrations also increased from fall to winter however in 2016, Se(IV) regeneration was observed later on.

Org.Se depth-integrated average (0 – 10m) concentration in winter-spring were between <LoD and 27 ± 2 ng L^{-1} except in 2016 where they reached 55 ± 1 ng L^{-1}, similar to the maximum values found in late summer (and fall of 2017) that were between 62 ± 10 and 67 ± 7 ng L^{-1}. Org.Se values in fall of 2015 and 2016 decreased to approximately half of those observed in summer. The production of Org.Se increased after a Chl-a maximum at late winter or early spring. Org.Se appeared together or just before the maximum PP of the corresponding year (Fig. Art.1.2).

In general, the maximum production of volatile Se was detected between 10-15 m matching with thermocline depth. The maximum production of volatile Se in this region coincided with maximum turbidity values (Table Art.1.SI 3). In estuarine systems high turbidity zones associated with an intense heterotrophic activity leading to organic matter degradation, consequently produced significant amounts of volatile Se compounds (Amouroux & Donard, 1997; Lanceleur et al., 2019; Tessier et al., 2002). An estimation of the volatilization flux was made resulting in annual emissions of TVSe between 6.5 and 9.6 kg Se $year^{-1}$. Compared to the annual T.Se input, ~110 kg Se yr^{-1} in the 90's from Nishri et al. (1999), volatilization cannot be neglected as an important Se removal pathway in lake Kinneret. However, this value must be taken with caution as it was estimated minimizing other processes removing volatile Se compounds from surface waters such as photo-degradation (Mason et al., 2018).

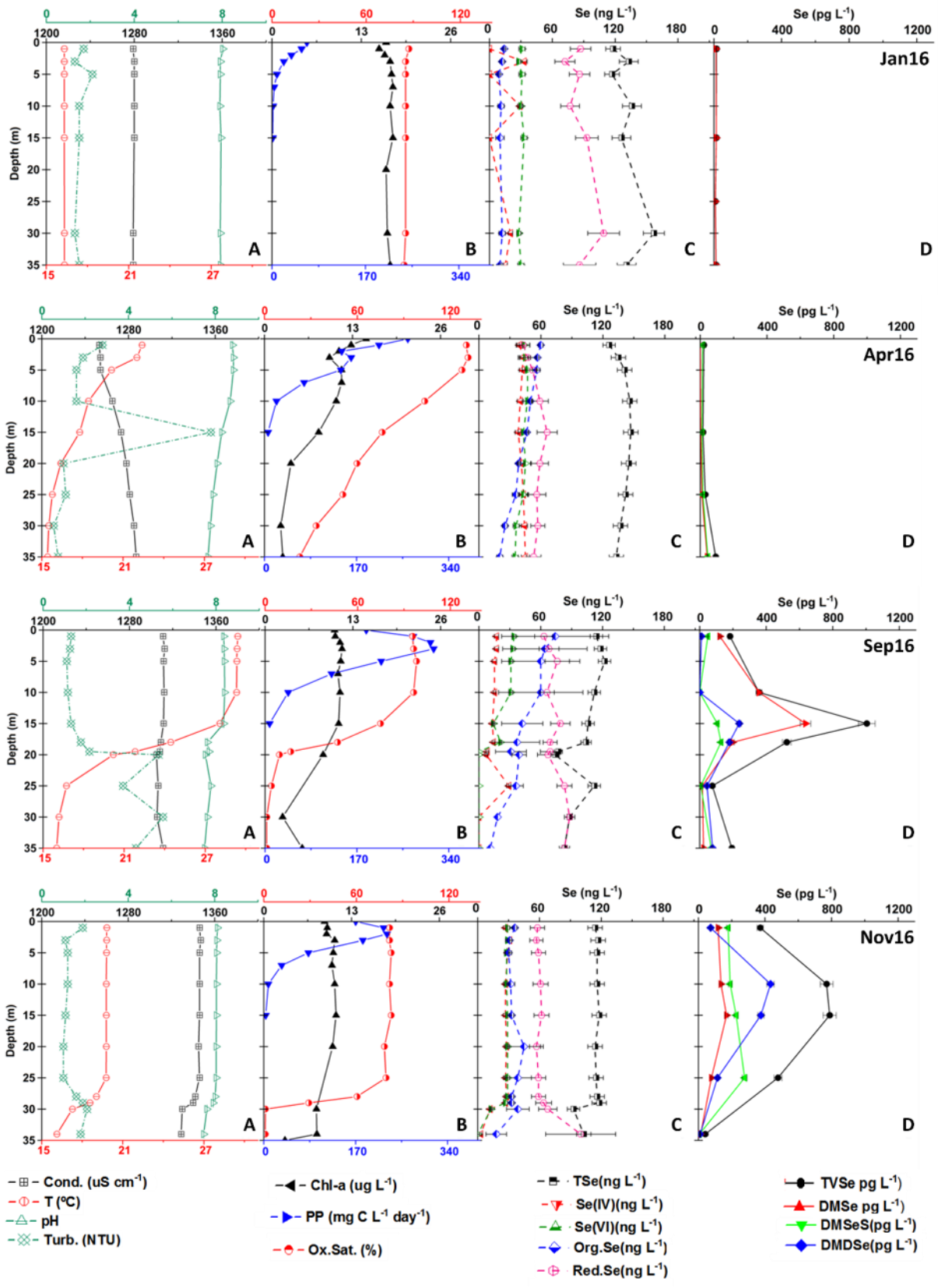

Figure Art.1.4. Depth profiles of physical and chemical parameters from Lake Kinneret for 2016. Each row presents data for the month in 2016 indicated in the top right corner of the last panel to the right. Column A: Conductivity (µS cm-1), Temperature (ºC), pH and Turbidity (NTU). Column B: Chl-a (µg L–1), PP (µg C L–1 day-1), oxygen saturation (%). Column C: T.Se,

Se(IV), Se(VI), Org.Se and Red.Se in ng L−1. Column D: TVSe, DMSe, DMSeS and DMDSe in pg L^{-1}. Abbreviations as in the tex. Source of Conductivity, temperature, pH, Turbidity, Chl-a, PP, oxygen data: Lake Kinneret database, Kinneret Limnological Laboratory, Israel Oceanographic & Limnological Research.

Luxem et al. (2017) observed that marine bacteria contributed significantly to the algal production of volatile Se. The data presented here revealed a direct link between metalimnion biological turnover and the production of volatile species. The decrease of Org.Se concentration may not only be due to dilution but partially caused by the abiotic decomposition of the dissolved Org.Se. The mechanisms for these processes remains unclear. The lack of data for Se forces the comparison with sulfur. Hu et al., (2007) observed in a monomictic lake that dimethyl sulfide (DMS) showed its maximum at the interface between oxic/anoxic layers. In addition, previous studies on Lake Kinneret reported the production of DMS in the metalimnion and suggested that *Peridinium gatunense* produced DMDS and oligosulfides, in particular dimethylsulfopropionate (DMSP), the precursor of DMS in natural waters (Ginzburg et al., 1998; Ginzburg et al., 1999; Knossow et al., 2015; Sela-Adler et al., 2016). We suggest that the similarities between sulfur and selenium, allow assuming that phytoplankton and bacteria responsible for organic matter degradation, produce not only DMSP but also selenonium compounds during high productive seasons as suggested previously (Cooke and Bruland, 1987; Amouroux et al, 2000). Although further molecular identification is required, such precursor of volatile Se compounds could presumably correspond to the Org.Se compound detected in our study in Lake Kinneret. Cyanobacteria (quantified as cyanophyta) and bacillariophyta are the main species present between September and November (Fig. Art.1.3). In cyanophyte cultures in agricultural drainage waters, the production of volatile Se from oxyanions has been demonstrated (Fan et al., 1998). The precursors (CH_3-Se-Met and CH_3-Se-Cys) were also characterized by Fan et al., (1998). Some of these precursors could be composing the Red.Se fraction and potentially the Org.Se detected and could eventually be converted to the corresponding volatile Se compounds detected in this study. Therefore, the key processes occurring in the epilimnion are the production of organically bound Se as a function of plankton dynamics and its depletion associated with dilution and conversion into volatile species during late summer and fall. The presence of organic matter degrading bacteria and the subsequent production of volatile species seems to be an important removal pathway of dissolved Se to the atmosphere.

3.2.4.2. Hypolimnetic Selenium (25 – 35m)

During late stratification, hypolimnetic concentration of T.Se decreased compared to winter-spring period (Table Art.1.SI 2). In addition, a sharp depletion of oxyanions was observed in September, especially for Se(VI) but also for Se(IV) in 2016 and 2017. According to Winkel et al., (2012), the reduction of dissolved Se oxyanions to Se(0) is mediated by microbial reduction processes and represents an efficient removal pathway for dissolved Se in anoxic waters. In Lake Kinneret, the sulfate reducing bacteria are, most probably, the Se(VI) reducing organisms (Oremland et al., 1989). In fact, when oxygen and SO_4^{2-} are consumed in late summer (Fig. Art.1.SI 2), there is a total Se and selenate depletion. As suggested by Nancharaiah & Lens (2015), selenate and selenite can act as electron acceptors and reduce soluble selenate and selenite to insoluble elemental selenium via dissimilatory reduction under anaerobic conditions.

In late summer, a maximum of Se(IV) is observed below the thermocline (25 m depth), which rapidly decreases at a greater depth (Fig. Art.1.3 and Fig. Art.1.SI 4). It is possible that selenite observed in this region is related to organic matter degradation and that selenite disappearance at greater depths is a consequence of i) a potential complexation with dissolved or particulate organic matter (Mcneal & Balistrieri, 1989) or ii) its reduction due to anoxic conditions.

Organic Se concentration were lower at hypolimnion compared to epilimnion during the study (1-tail t-test: $t=2.95$, $P<0.01$). The difference of Org.Se concentration between epilimnion and hypolimnion was greater during stratification, with average epilimnetic concentration of 64 ± 2 ng Se L^{-1} versus 16 ± 7 Se L^{-1} at hypolimnion in September. At April and November hypolimnetic $Org.Se_{dia\ (25\ –\ 35m)}$ concentration was the half compared to the same period for epilimnion. We suggest that the residual concentrations of Org.Se in the hypolimnion may have their origin at epilimnion, where Org.Se is produced. Red.Se concentration in the hypolimnion increased in summer and subsequently decreased in fall because of the thermocline deepening and the dilution effect in the water column. T.Se concentration decreased with time during this study. The presence of Fe, Al and Mn (Hadas & Pinkas, 1995; Shaked et al., 2004) among other metals in the waters and sediments, suggests the scavenging of Red.Se into sediments as a key process for Se sink in Lake Kinneret, as it happens in Canadian thermokarst ponds (Lanceleur et al., 2019) and Siberian lakes (Pokrovsky et al., 2018). In addition, the presence of Red.Se during holomixis periods (around

40-60% of total selenium) suggests that reduced Se is not completely recycled (*i.e.* oxidized) every year.

Hypolimnetic TVSe production is limited. Low production rates have been observed during spring at 35 m, in the water-sediment interface (Fig. Art.1.3). In September 2016 and November 2017 some production or accumulation was observed as well close to the water-sediment interface (Fig. Art.1.3 and Fig. Art.1.SI 4), although, the maximum concentration of volatile species was detected close to the thermocline as described previously.

Volatile Se production near the sediments may be due to microbial production at this location linked to organic matter degradation as observed in heterotrophic and reducing waters of upper European estuaries (Tessier et al., 2002) or in permafrost lakes (Lanceleur et al., 2019). In our study, the mixed Se-S compounds (DMSeS and DMDSe) were the dominant species. In the literature, it is common to found DMSe as the dominant component of TVSe. Nevertheless, studies carried out at Gironde estuary (France) and Mediterranean Sea showed a significant concentration of DMDSe (David Amouroux & Donard, 1997; David Amouroux et al., 2001). Laboratory experiments using synthetic sea water and selenoamino acids as the main precursors over inorganic Se species, demonstrated that DMSe, DMSeS and DMDSe were produced under light and dark conditions, (Amouroux et al., 2000). The same study suggested that the production of DMSe would have a specific precursor, most probably a dimethylselenonium compound. The authors suggested that the production of DMSeS and DMDSe would be the result of abiotic reactions in the presence of seleno-methionine in the extracellular medium. Thereby, the presence of DMSeS in Lake Kinneret seems to be the consequence of having organically bound Se species (i.e. precursors) and sub-millimolar concentrations of S in the water and H_2S accumulation at hypolimnion (Ginzburg et al., 1999; Knossow et al., 2015).

The thermocline zone presented the highest levels of turbidity (Table Art.1.SI 3) of the water column, presumably due to the presence of dead particulate organic matter (detritus) and the presence of bacteria, which is also enriched in Se. Stability studies (Fig. Art.1.SI 7) have shown that at depths close to thermocline (~20-25m) DMSe concentrations are higher after stocking the samples more than 15 days, which may explain the predominance of DMSe of Sep 2016 samples.

In summary, hypolimnetic anoxia developed during stratification and caused mostly by biological oxygen consuming processes. Such anoxia affected considerably Selenium

distribution, causing the complete reduction of Se(VI) to reduced Se species and, partial reduction of Se(IV) with end product as Se(0). Elemental Se can remain in suspension in the colloidal form for a certain period of time (Buchs et al., 2013). However, due to organic matter or other particulates, Se(0) colloids will form aggregates and settle to the sediments, a process that is an important sink for Se. The higher concentration of Red.Se compared to previous studies (Nishri, Brenner, et al., 1999) may be due to an extended period of reducing conditions at hypolimnion. The decrease of T.Se could be a consequence of the partial but not total Se re-oxidation during holomixis periods as it happened in the lake two decades ago.

4. Biogeochemical implication

During the 3 years of this study, the lake dynamics were the main driver for Se speciation fluctuations. The observed Schematic overview of Se biogeochemical cycle in Lake Kinneret. Abbreviations: selenate (Se(VI)), selenite (Se(IV)), organic Se (Org.Se), reduced Se pool (Red.Se), dimethylselenide (DMSe), dimethyl selenide sulphide (DMSeS) and dimethyl diselenide (DMDSe). is summarized in Figure Art.1.6. Considering the increase in electric conductivity and decrease in total lake volume over the study period, an increase of T.Se would be expected. However, the decrease of dissolved T.Se indicates either the loss of Se by sink into the sediments or high volatilization and emission rates to the atmosphere.

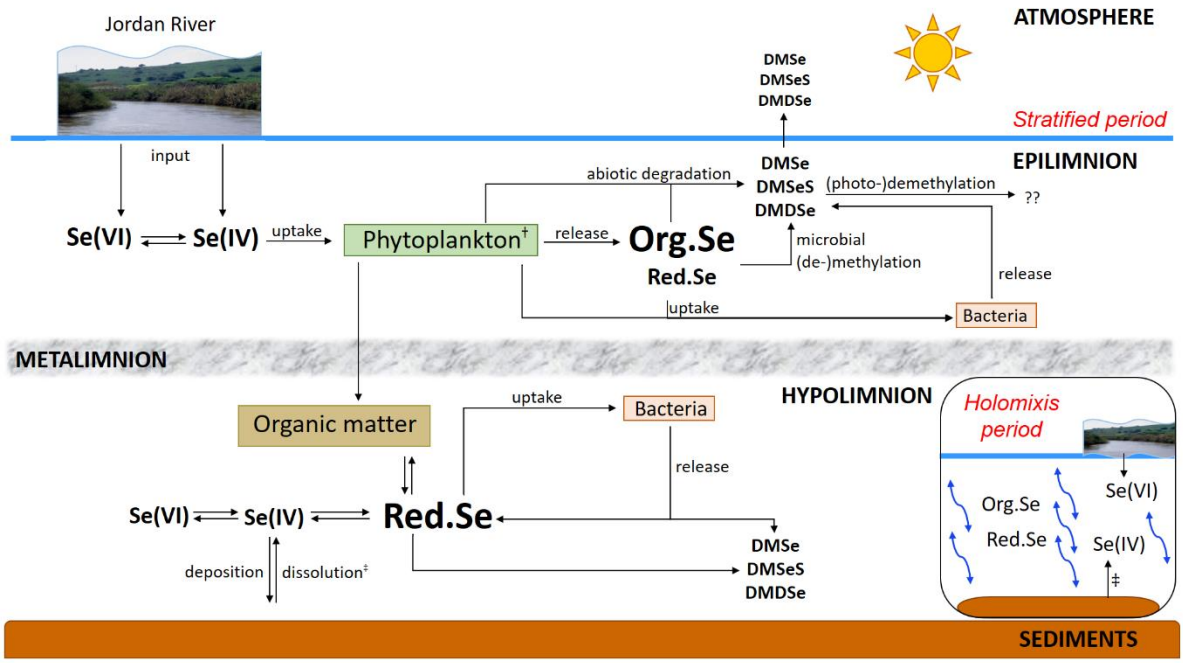

Figure Art.1.5. Schematic overview of Se biogeochemical cycle in Lake Kinneret. Abbreviations: selenate (Se(VI)), selenite (Se(IV)), organic Se (Org.Se), reduced Se pool (Red.Se), dimethylselenide (DMSe), dimethyl selenide sulphide (DMSeS) and dimethyl

diselenide (DMDSe). [†]Phytoplankton species are detailed at Fig. 3 [‡]Dissolution occurred mainly during holomixis period.

The annual pattern for Se oxyanions is similar to the one previously observed by Nishri et al., (1999). However, selenate concentration is not as high as reported by these authors. Additionally, Red.Se concentration is tripled nowadays, suggesting either that natural conditions have changed or that this is related to differences of method performance.

Questions such as the potential instability of some compounds was not investigated previously, therefore we cannot completely discard a difference between both methods. However, if natural conditions are responsible for the change, we suggest that more reducing conditions in the hypolimnion during stratified periods, especially in low water level drought years, are the main mechanism responsible for more elevated levels of Red.Se.

For the first time, epilimnetic production of organic Se compound(s), "Org.Se" (potentially an organoselenonium metabolite or methylated Se-amino acid forms to be identified), can be statistically correlated Chl-a and relate it to specific phytoplankton taxa information from Lake Kinneret database (Fig. Art.1.5). Our *in situ* observations suggest that Org.Se is directly released to the water by phytoplankton, probably by the main species: Dinophyta (*Peridinium gatunense*) and Cyanophyta (*Aphanizomenon ovalisporum* and *Cylindrospermopsis raciborskii*) (Zohary, 2004; Zohary et al., 2014b); but also with a lesser contribution of minor phytoplankton species in the lake. Once released, Org.Se may be either uptaken by bacteria present close to metalimnion, or abiotically transformed into volatile compounds close to the surface (Fig. Art.1.6). Photo-degradation may enhance Org.Se decomposition, but also volatile Se compounds degradation. Org.Se could also undergo fast uptake by bacteria associated with the production of volatile Se that has been observed with higher rates close to metalimnion. Our calculated estimates indicate that the production of volatile Se close to the surface and emission to the atmosphere can be a significant pathway for selenium removal in the lake that was not considered in previous studies.

The increase of turbidity in September and November near the thermocline zone is an indicator of higher solid particulate matter, which also includes, dead organic matter sinking through the water column. The maximum production of TVSe close to metalimnion coincides each year with the end of summer and the increase of turbidity at metalimnion; therefore, we

suggest that volatile Se formation is strongly related to the microbial turnover in the water column.

In Lake Kinneret, the presence of sub-millimolar concentrations of sulfur explains the high extent of DMSeS versus DMDSe and DMSe, in contrast with studies in other environments with lesser prevalence of sulfur (Table Art.1.2).

Our data demonstrates that Org.Se production happens primarily in the epilimnion, while the reduction of selenate to elemental Se or other reduced species is a key process in the anoxic hypolimnion. The intense activity of sulfate reducing bacteria during anoxic hypolimnetic periods contribute to the reduction of Se oxyanions. Therefore, reduced species predominantly insoluble, such as elemental Se(0), can be scavenged and sink to sediments. This is probably the major process removing Se from the hypolimnion.

The higher concentrations of Red.Se pool compared with previous studies together with the T.Se concentration decrease observed during this work probably indicate more reducing conditions in the hypolimnion of the lake during drought years with low water levels. The deepening of the thermocline occurring in fall transports nutrients and Se from hypolimnion to epilimnion. The sinking of Se into the sediments is then followed by incomplete regeneration during holomixis.

In conclusion, after observing a decrease of total Se ca. during this study and the non-negligible increase of Red.Se compared to previous study by Nishri et al. (1999), such biogeochemical scenario may be of increasing importance under dryer hydrological and warming climatic conditions in the near future. Lakes located in arid regions like Lake Kinneret will most probably suffer a decrease of water inflow and elevated impacts of human activities nearby. Additionally, climate change will most probably affect not only algae blooms but also water temperature, and could have an impact on stratification, nutrients availability and redox conditions, and phytoplankton population. So, the evolution of total Se and Se speciation will potentially be subjected to changes in the next years.

Acknowledgements

This work was supported by the Israeli Water Authority. The financial support of UPPA and IPREM supporting A. Romero–Rama Doctoral fellowship is acknowledged. The contributions of the Aquitaine Region (AQUITRACES project n° 20131206001-13010973) and ANR IA RSNR (AMORAD project n°ANR-11-RSNR-0002) for equipment funding are also acknowledged.

Supporting information

Title: Biogeochemistry of Selenium compounds in the water column of the warm, monomictic, Lake Kinneret

Authors: Andrea Romero-Rama, Maïté Bueno, Emmanuel Tessier, Yaron Be'eri-Shlevin, Assaf Sukenik, Tamar Zohary, David Amouroux

Manuscript:

Number of Figures: 5

Number of Tables: 3

Supporting information:

Number of Figures SI: 5

Number of Tables SI: 6

SUPPLEMENTARY INFORMATION FIGURE Art1.SI 1

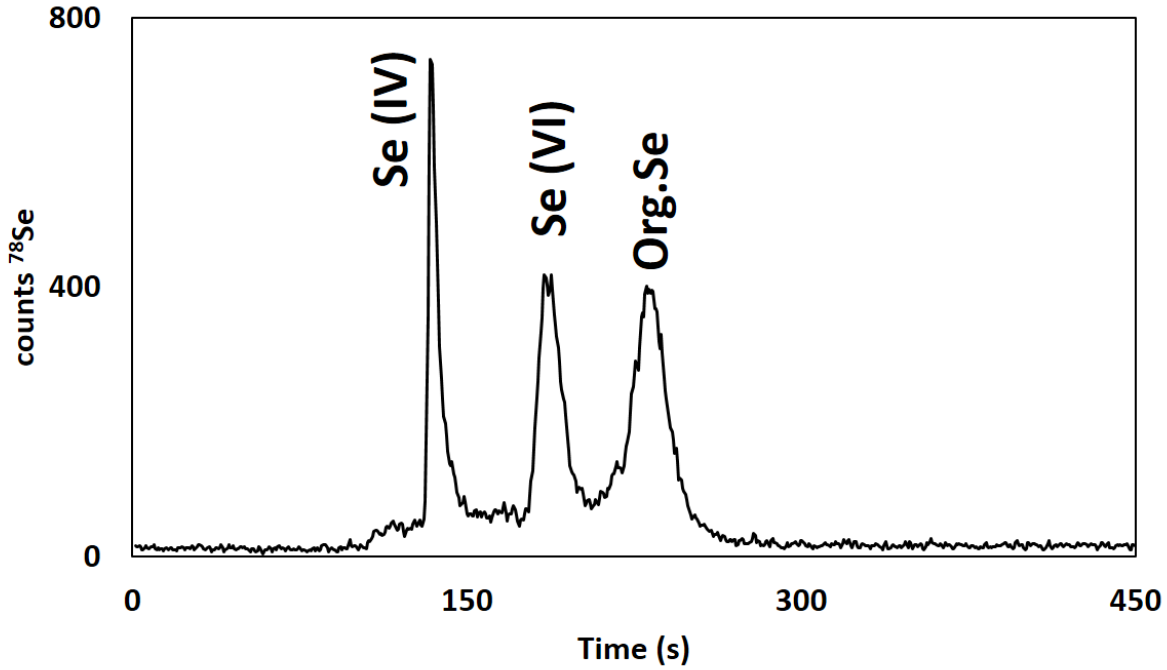

Figure Art.1.SI 1. Example of a chromatograph for April 2016 sample at 3m depth. The sample volume injected was 200µL. Concentration of compounds was: 43 ± 5, 45 ± 5 and 57 ±7 ng Se L^{-1} for Se(IV), Se(VI) and Org.Se respectively.

SUPPLEMENTARY INFORMATION FIGURE Art.1.SI 2

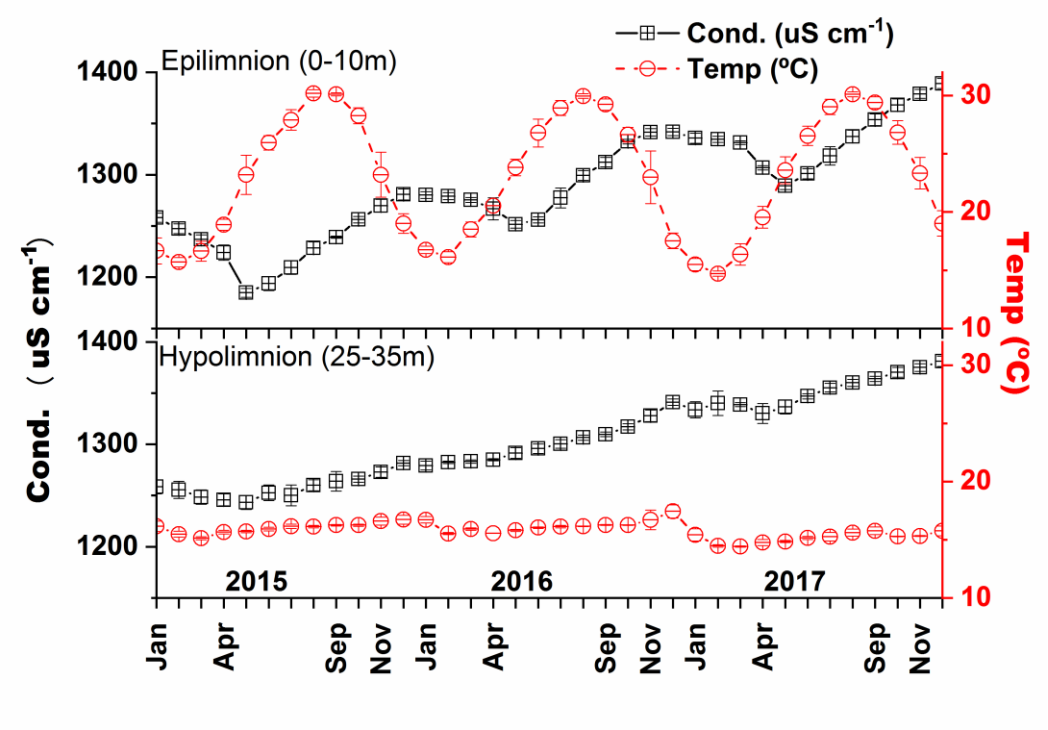

Figure Art.2.SI 2. Temporal variation as depth integrated values for conductivity (µS cm^{-1}, black squares) and Temperature (ºC red circles). Upper panel: epilimnion (0-10m) and lower panel: hypolimnion (25-35m).

SUPPLEMENTARY INFORMATION FIGURE Art.1.SI 3

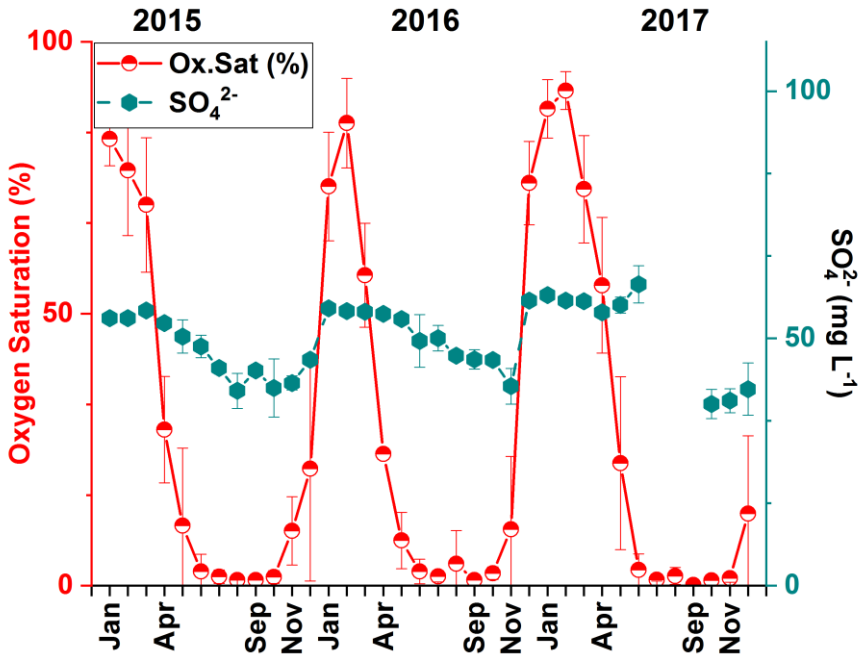

Figure Art.1.SI 3. Hypolimnetic (25-35m of depth) temporal evolution of depth integrated values of oxygen saturation (%),red half circles with solid line and sulfate (mg L-1), hexagon symbols cyan dashed line.

SUPPLEMENTARY INFORMATION FIGURE Art1.SI 4

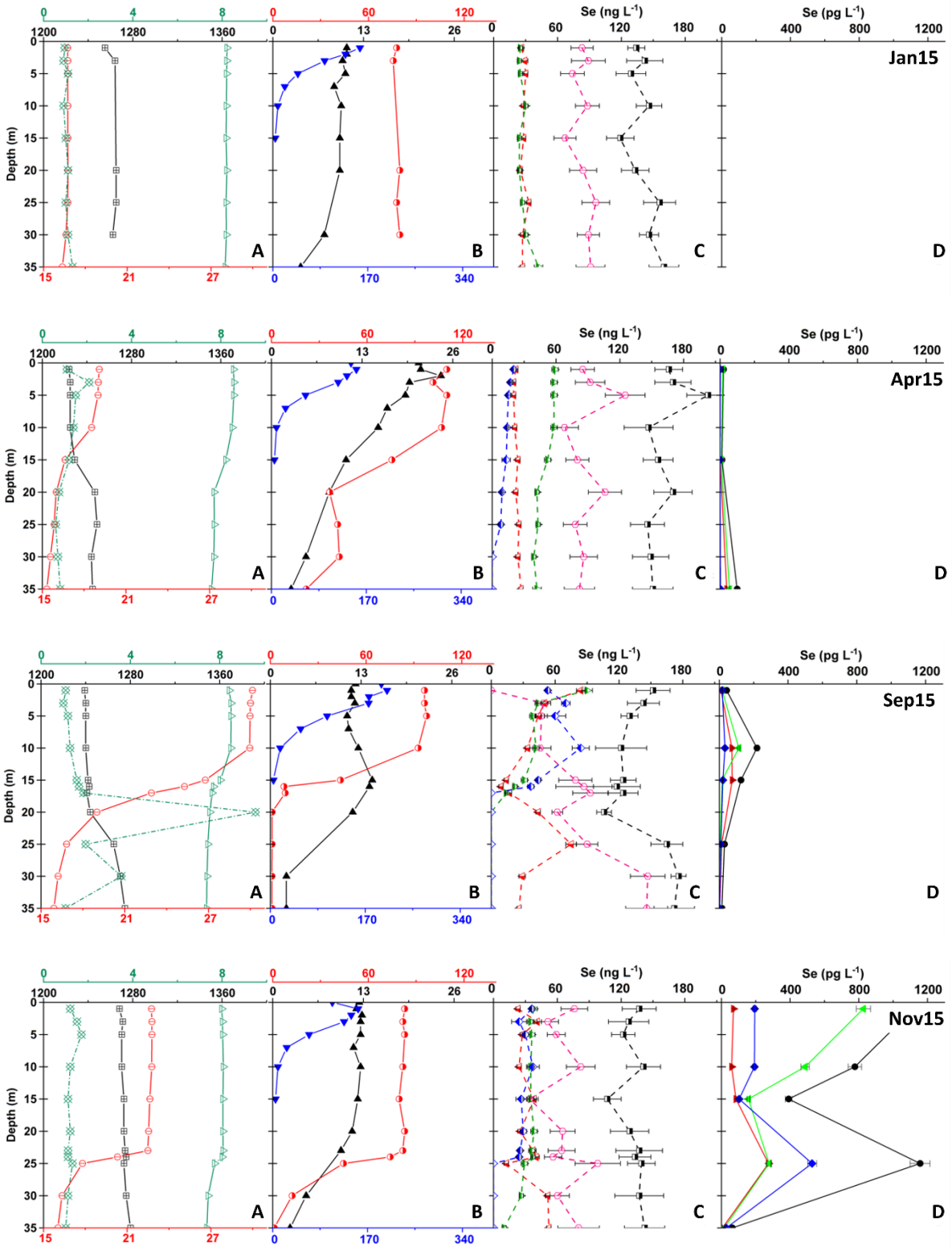

SUPPLEMENTARY INFORMATION FIGURE Art1.SI 4 (Continued)

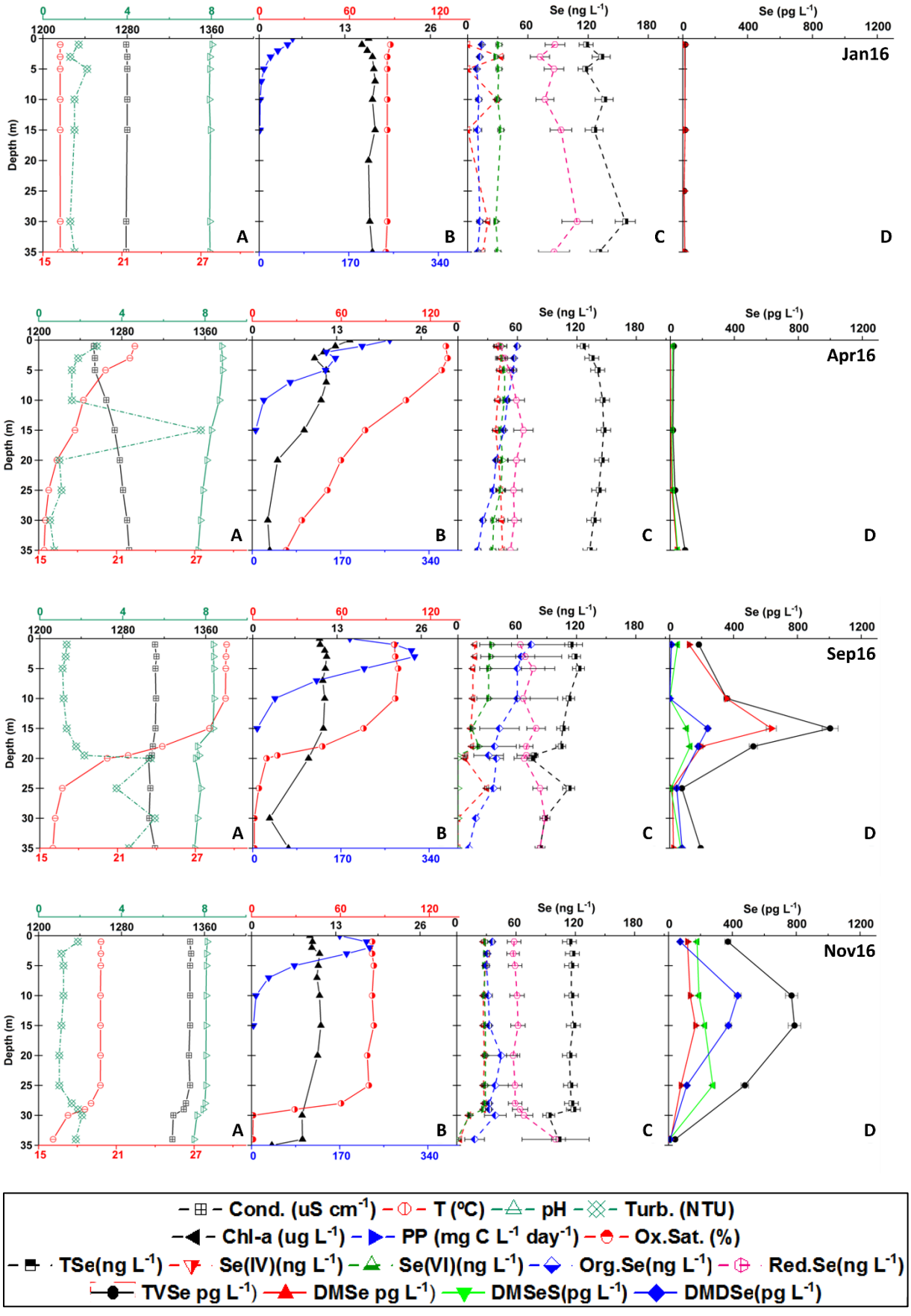

SUPPLEMENTARY INFORMATION FIGURE Art.1.SI 4 (Continued)

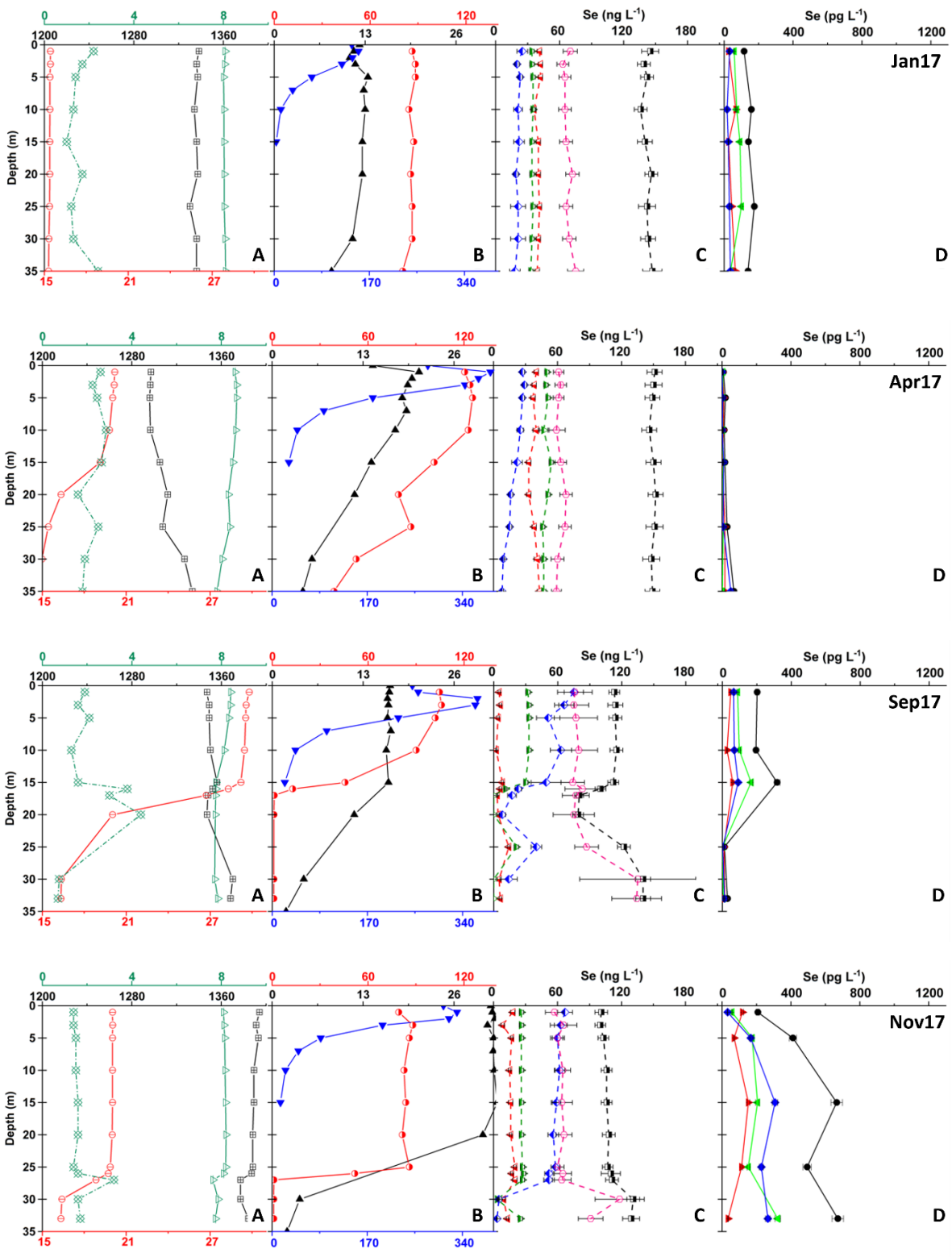

Figure Art.1.SI 4. Depth profiles for 2015-2017. A: Conductivity (µS cm^{-1}), Temperature (ºC), pH and Turbidity (NTU). B: Chl-a (µg L^{-1}), PP (mg C L^{-1} day^{-1}), oxygen saturation (%).C: TSe, Se(IV), Se(VI), Org.Se and Red.Se (ng L^{-1}). D: TVSe, DMSe, DMSeS and DMDSe in pg L^{-1}. Data presented by row corresponds to Se sampling campaigns for January, April, September and November of years 2015, 2016 and 2017 respectively.

SUPPLEMENTARY INFORMATION FIGURE Art.1.SI 5

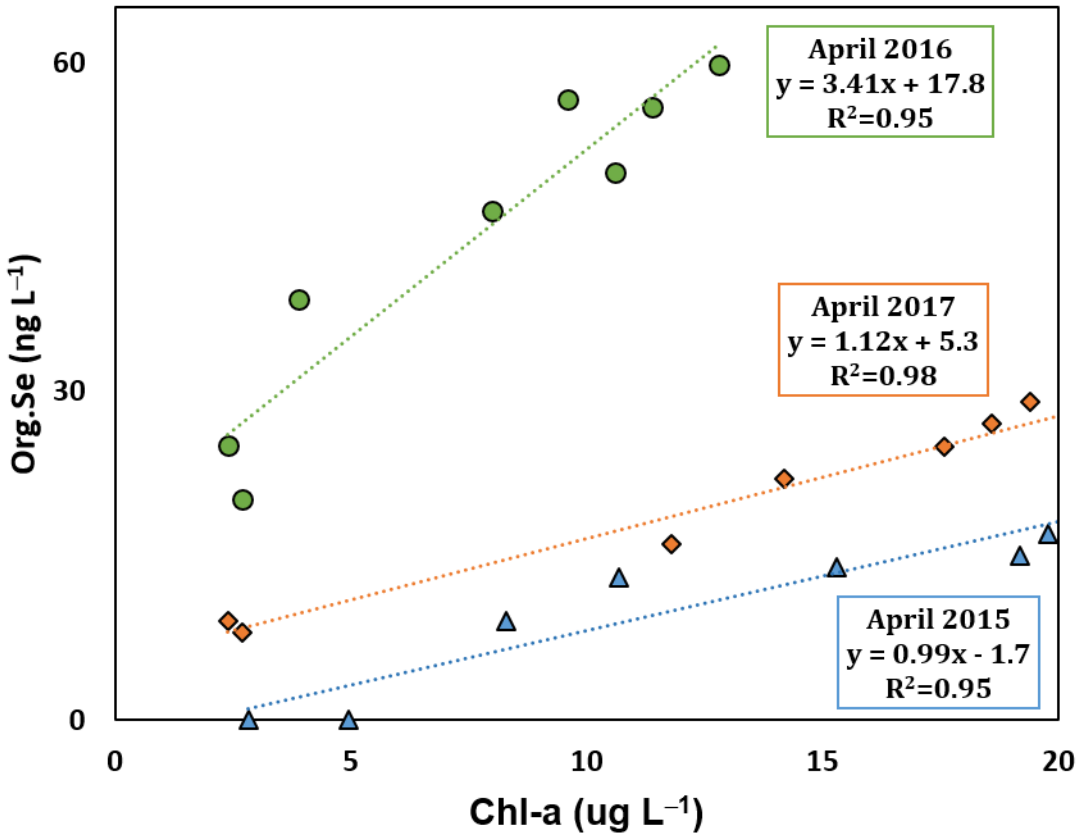

Fig. Art.1.SI 5. Linear correlation between Org.Se (ng L^{-}) vs Chl-a (µg L^{-1}) measured in the water column (1-35m depth) in spring period (April). Raw data can be found in Tables SI 4 and SI 5. Pearson correlation values were: R^2=0.946 in April 2015 (n=7) (blue triangle), R^2=0.947 in April 2016 (n=8) (green circle) and R^2=0.983 in April 2017 (n=8) (orange diamond).

SUPPLEMENTARY INFORMATION TABLE Art.1.SI 1

Table Art.1.SI 1. Epilimnion depth integrated average concentrations (0-10 m) and confidence interval for non-volatile and volatile dissolved Se (total dissolved Se (T.Se), Se(IV), Se(VI), organic Se (Org.Se) and reduced Se pool (Red.Se) in ng L^{-1}; total volatile Se (TVSe) in pg L^{-1}) and, for the main physicochemical parameters (monthly means if n>1): % of oxygen saturation (Ox. Sat), pH, temperature (T), conductivity (Cond.) and turbidity (Turb). <LOD: below detection limit.

Month	T.Se	Se(IV)	Se(VI)	Org.Se	Red. Se	TVSe	Ox. Sat	pH	T	Cond.	Turb.
	(ng Se L^{-1})					(pg Se L^{-1})	(%)		(ºC)	(µS cm^{-1})	(NTU)
Jan15	137 ± 13	29 ± 5	26 ± 2	<LOD	82 ± 14	n.d.	87 ± 13	8.14 ± 0.14	16.7 ± 1.1	1258 ± 5	1.1 ± 0.2
Apr15	175 ± 19	21 ± 4	58 ± 3	16 ± 2	96 ± 19	15 ± 1	94 ± 16	8.53 ± 0.07	18.9 ± 0.5	1224 ± 7	1.7 ± 0.2
Sep15	135 ± 15	51 ± 3	51 ± 3	67 ± 7	38 ± 16	122 ± 6	96	8.48 ± 0.02	30.1 ± 0.1	1239 ± 1	1.2 ± 0.1
Nov15	131 ± 15	28 ± 2	36 ± 3	32 ± 4	67 ± 15	965 ± 48	82 ± 5	8.12 ± 0.17	23.2 ± 1.9	1270 ± 6	1.2 ± 0.3
Jan16	125 ± 8	16 ± 3	30 ± 3	11 ± 2	80 ± 9	14 ± 1	78 ± 10	7.94 ± 0.12	16.8 ± 0.3	1280 ± 3	1.7 ± 0.6
Apr16	138 ± 7	41 ± 3	46 ± 5	55 ± 1	51 ± 9	19 ± 1	112	8.71 ± 0.11	20.5	1267 ± 11	1.9
Sep16	117 ± 6	16 ± 2	32 ± 2	64 ± 42	67 ± 7	260 ± 13	96 ± 4	8.35 ± 0.12	29.2 ± 0.5	1312 ± 5	1.2 ± 0.1
Nov16	116 ± 7	29 ± 2	28 ± 2	32 ± 3	59 ± 8	551 ± 28	85 ± 3	8.20 ± 0.08	23.0 ± 2.3	1342 ± 4	1.3 ± 0.2
Jan17	141 ± 6	40 ± 2	35 ± 2	22 ± 3	66 ± 7	134 ± 7	89 ± 5	8.10 ± 0.18	15.5 ± 0.5	1336 ± 5	1.7 ± 0.5

Table Art.1.SI 1. (Continued)

Month	T.Se	Se(IV)	Se(VI)	Org.Se	Red. Se	TVSe	Ox. Sat	pH	T	Cond.	Turb.
Apr17	149 ± 7	39 ± 2	49 ± 3	27 ± 2	61 ± 8	14 ± 1	121 ± 8	8.59 ± 0.03	19.5 ± 0.9	1307 ± 2	3.0 ± 0.4
Sep17	114 ± 6	4 ± 1	33 ± 2	62 ± 10	77 ± 6	198 ± 10	91 ± 10	8.30 ± 0.12	29.4 ± 0.5	1354 ± 6	1.5 ± 0.2
Nov17	103 ± 5	15 ± 1	26 ± 2	63 ± 6	62 ± 6	455 ± 23	93 ± 6	8.23 ± 0.10	23.3 ± 1.4	1379 ± 4	1.6 ± 0.2

SUPPLEMENTARY INFORMATION TABLE Art.1.SI 2

Table Art.1.SI 2. Hypolimnion depth integrated average concentrations (25-35 m) and confidence interval for non-volatile dissolved Se species and total volatile Se (total dissolved Se (T.Se), Se(IV), Se(VI), organic Se (Org.Se) and reduced Se pool (Red.Se) in ng L^{-1}; total volatile Se (TVSe) in pg L^{-1}) and, for the main physicochemical parameters (monthly means): % of oxygen saturation (Ox. Sat), pH, temperature (T), conductivity (Cond.) and turbidity (Turb). <LOD: below detection limit, n.d. = no data.

Month	T.Se	Se(IV)	Se(VI)	Org.Se	Red. Se	TVSe	Ox. Sat.	pH	T	Cond.	Turb.
	(µg Se L^{-1})					(pg L-1)	(%)		(ºC)	(µS cm^{-1})	(NTU)
Jan15	152 ± 12	29 ± 5	32 ± 3	<LoD	91 ± 13	n.d.	82 ± 5	8.00 ± 0.12	16.1 ± 0.4	1258 ± 7	4.1 ± 6.1
Apr15	149 ± 17	25 ± 5	41 ± 3	8 ± 2	83 ± 18	54 ± 3	29 ± 10	7.70 ± 0.16	15.7 ± 0.1	1246 ± 6	0.9 ± 0.3
Sep15	172 ± 12	40 ± 3	5 ± 1	8 ± 2	128 ± 13	22 ± 1	1 ± 0	7.47 ± 0.05	16.3 ± 0.1	1264 ± 10	1.7 ± 1.3
Nov15	139 ± 20	42 ± 2	23 ± 2	8 ± 2	75 ± 20	610 ± 30	10 ± 6	7.47 ± 0.05	16.6 ± 0.3	1273 ± 5	1.9 ± 1.5
Jan16	147 ± 14	17 ± 4	29 ± 3	11 ± 3	101 ± 15	10 ± 1	73 ± 10	7.89 ± 0.11	16.7 ± 0.3	1279 ± 4	1.9 ± 1.2
Apr16	137 ± 7	44 ± 4	38 ± 3	27 ± 3	56 ± 9	61 ± 3	24	7.72 ± 0.09	15.6	1285 ± 1	0.9 ± 0.1
Sep16	93 ± 5	10 ± 1	2 ± 0.4	21 ± 2	81 ± 5	135 ± 7	1 ± 0	7.52 ± 0.04	16.3 ± 0.0	1310 ± 2	3.1 ± 1.4
Nov16	107 ± 12	18 ± 3	18 ± 2	32 ± 15	71 ± 13	259 ± 13	10 ± 13	7.77 ± 0.02	16.7 ± 0.8	1328 ± 6	2.7 ± 0.8
Jan17	144 ± 8	40 ± 2	34 ± 2	20 ± 7	70 ± 8	156 ± 8	88 ± 5	8.09 ± 0.15	15.4 ± 0.5	1334 ± 8	1.6 ± 0.3
Apr17	149 ± 8	41 ± 3	47 ± 2	10 ± 1	62 ± 8	49 ± 2	55 ± 12	8.09 ± 0.32	14.8 ± 0.3	1330 ± 10	2.0 ± 0.9
Sep17	134 ± 7	8 ± 2	8 ± 1	20 ± 6	118 ± 7	21 ± 1	0 ± 1	7.85 ± 0.08	15.8 ± 0.3	1364 ± 3	5.5 ± 3.7
Nov17	122 ± 7	14 ± 1	18 ± 1	26 ± 2	89 ± 7	583 ± 29	1 ± 1	7.75 ± 0.30	15.3 ± 0.0	1375 ± 4	5.4 ± 6.0

SUPPLEMENTARY INFORMATION TABLE Art.1.SI 3

Table Art.1.SI 3. Physicochemical parameters raw measurements. Data includes: temperature (T, ºC), pH, Conductivity (Cond.), sulfate concentration, dissolved oxygen (DO), % of oxygen saturation and turbidity (Turb.). n.d.: no data

Date	Code	Depth (m)	T (ºC)	pH	Cond. (mS cm^{-1})	SO_4^{-2}	DO	Ox. Sat.	Turb. (NTU)
						mg L^{-1}		(%)	
11/01/2015	Jan15	1	16.7	8.22	1255	56	7.5	78%	0.95
11/01/2015	Jan15	3	16.7	8.21	1264	55	7.3	76%	0.9
11/01/2015	Jan15	5	16.7	8.2	1265	54	n.d.	n.d.	1.1
11/01/2015	Jan15	10	16.7	8.19	1265	54	n.d.	n.d.	0.9
11/01/2015	Jan15	15	16.7	8.18	1262	54	n.d.	n.d.	1
11/01/2015	Jan15	20	16.7	8.21	1262	54	7.7	80%	1.1
11/01/2015	Jan15	25	16.7	8.18	1267	54	7.5	78%	1
11/01/2015	Jan15	30	16.6	8.19	1265	54	7.7	80%	1.1
11/01/2015	Jan15	35	16.3	8.14	1250	53	n.d.	n.d.	1.3
19/04/2015	Apr15	1	19.1	8.57	1224	54	10.2	110%	1.1
19/04/2015	Apr15	3	19.0	8.59	1225	54	9.4	101%	2.1
19/04/2015	Apr15	5	19.0	8.58	1225	54	10.2	110%	1.5
19/04/2015	Apr15	10	18.5	8.51	1225	54	9.9	107%	1.4
19/04/2015	Apr15	15	16.6	8.23	1229	52	7.3	76%	1.2
19/04/2015	Apr15	20	16.0	7.7	1247	53	3.6	36%	0.75
19/04/2015	Apr15	25	15.9	7.71	1249	53	4.1	42%	0.6
19/04/2015	Apr15	30	15.6	7.69	1244	53	4.2	43%	0.7
19/04/2015	Apr15	35	15.3	7.59	1245	53	2.2	22%	0.8
06/09/2015	Sep15	1	30.1	8.43	1239	55	7.3	97%	1.1
06/09/2015	Sep15	3	30.0	8.51	1240	55	7.3	97%	1
06/09/2015	Sep15	5	30.0	8.51	1240	55	7.4	98%	1.2
06/09/2015	Sep15	10	29.9	8.5	1240	55	7	93%	1.3

SUPPLEMENTARY INFORMATION TABLE Art.1.SI 3 (Continued)

Table Art.1.SI 3. (Continued)

Date	Code	Depth (m)	T (ºC)	pH	Cond. (mS cm^{-1})	SO_4^{-2} (mg L^{-1})	DO (mg L^{-1})	Ox. Sat. (%)	Turb. (NTU)
06/09/2015	Sep15	15	26.8	8.03	1242	55	3.5	44%	1.6
06/09/2015	Sep15	16	25.3	7.73	1243	55	0.7	8%	1.7
06/09/2015	Sep15	17	22.9	7.66	1241	55	0.8	9%	1.9
06/09/2015	Sep15	20	19.0	7.56	1244	53	0.1	1%	9.6
06/09/2015	Sep15	25	16.8	7.47	1265	49	0.1	1%	2
06/09/2015	Sep15	30	16.2	7.43	1271	42	0.1	1%	3.6
06/09/2015	Sep15	35	15.9	7.41	1275	41	0.1	1%	1.1
16/11/2015	Nov15	1	22.8	7.99	1268	55	7.1	83%	1.2
16/11/2015	Nov15	3	22.8	8.02	1271	55	7	82%	1.5
16/11/2015	Nov15	5	22.8	8.03	1270	55	7.1	83%	1.7
16/11/2015	Nov15	10	22.8	8.06	1270	55	7	82%	1.2
16/11/2015	Nov15	15	22.6	8.04	1272	55	6.8	79%	1.1
16/11/2015	Nov15	20	22.5	8.04	1272	56	7.1	83%	1.2
16/11/2015	Nov15	23	22.5	8.05	1273	55	7	82%	1.1
16/11/2015	Nov15	24	20.3	8.01	1274	57	6.7	74%	1.1
16/11/2015	Nov15	25	17.8	7.67	1272	54	4.2	44%	1.3
16/11/2015	Nov15	30	16.3	7.38	1274	54	1.2	12%	1.1
16/11/2015	Nov15	35	16.0	7.32	1278	39	0.1	1%	1
25/01/2016	Jan16	1	16.3	8.03	1279	56	8.6	87%	1.7
25/01/2016	Jan16	3	16.3	7.92	1280	56	8.4	85%	1.3
25/01/2016	Jan16	5	16.3	7.92	1280	56	8.4	85%	2.1
25/01/2016	Jan16	10	16.3	7.9	1280	56	8.4	85%	1.5
25/01/2016	Jan16	15	16.3	7.95	1280	56	8.4	85%	1.5
25/01/2016	Jan16	30	16.3	7.92	1279	56	8.4	85%	1.3
25/01/2016	Jan16	35	16.3	7.93	1279	56	8.3	84%	1.5

SUPPLEMENTARY INFORMATION TABLE Art.1.SI 3 (Continued)

Table Art.1.SI 3. (Continued)

Date	Code	Depth (m)	T (ºC)	pH	Cond. (mS cm^{-1})	SO_4^{-2} (mg L^{-1})	DO (mg L^{-1})	Ox. Sat. (%)	Turb. (NTU)
17/04/2016	Apr16	1	22.4	8.8	1253	56	11.4	130%	2.8
17/04/2016	Apr16	3	22.0	8.84	1254	55	11.5	132%	1.9
17/04/2016	Apr16	5	20.1	8.84	1254	55	11.6	128%	1.6
17/04/2016	Apr16	10	18.4	8.69	1265	55	9.8	104%	1.6
17/04/2016	Apr16	15	17.8	8.3	1273	54	7.2	76%	7.8
17/04/2016	Apr16	20	16.4	8.09	1278	55	5.9	60%	1
17/04/2016	Apr16	25	15.8	7.9	1281	55	5	51%	1.1
17/04/2016	Apr16	30	15.5	n.d.	1285	55	3.3	33%	0.55
17/04/2016	Apr16	35	15.4	7.67	1287	55	2.3	23%	0.75
15/09/2016	Sep16	1	29.4	8.36	1311	58	7.4	96%	1.3
15/09/2016	Sep16	3	29.4	8.38	1313	58	7.4	96%	1.3
15/09/2016	Sep16	5	29.3	8.39	1312	58	7.6	98%	1.1
15/09/2016	Sep16	10	29.3	8.40	1312	58	7.4	96%	1.2
15/09/2016	Sep16	15	28.1	8.36	1312	58	5.9	75%	1.3
15/09/2016	Sep16	18	24.4	7.61	1309	57	4.0	47%	1.8
15/09/2016	Sep16	19.5	21.8	7.68	1308	58	1.5	17%	2.2
15/09/2016	Sep16	20	20.2	7.51	1305	54	0.9	9%	5.4
15/09/2016	Sep16	25	16.7	7.77	1307	54	0.4	4%	3.7
15/09/2016	Sep16	30	16.2	7.60	1306	42	0.1	1%	5.6
15/09/2016	Sep16	35	16.0	7.48	1311	40	0.1	1%	4.3
27/11/2016	Nov16	1	19.8	8.13	1346	59	7.4	81%	1.9
27/11/2016	Nov16	3	19.8	8.1	1347	59	7.4	81%	1.1
27/11/2016	Nov16	5	19.8	8.09	1346	59	7.5	82%	1.2
27/11/2016	Nov16	10	19.8	8.08	1346	58	7.4	81%	1.2

SUPPLEMENTARY INFORMATION TABLE Art.1.SI 3 (Continued)

Table Art.1.SI 3. (Continued)

Date	Code	Depth (m)	T (ºC)	pH	Cond. (mS cm^{-1})	SO_4^{-2} (mg L^{-1})	DO (mg L^{-1})	Ox. Sat. (%)	Turb. (NTU)
27/11/2016	Nov16	15	19.8	8.08	1346	59	7.5	82%	1.1
27/11/2016	Nov16	20	19.8	8.07	1345	59	7.1	78%	1
27/11/2016	Nov16	25	19.8	8.07	1346	59	7.2	79%	1
27/11/2016	Nov16	28	19.0	8.02	1342	NA	5.6	60%	1.6
27/11/2016	Nov16	29	18.6	7.93	1340	NA	2.7	29%	1.9
27/11/2016	Nov16	30	17.3	7.64	1330	58	0.1	1%	2.1
27/11/2016	Nov16	34	16.1	7.49	1329	51	0.1	1%	1.8
15/01/2017	Jan17	1	15.4	8.08	1338	58	8.7	86%	2.2
15/01/2017	Jan17	3	15.4	8.06	1336	58	8.9	88%	1.7
15/01/2017	Jan17	5	15.4	8.01	1337	58	8.9	88%	1.4
15/01/2017	Jan17	10	15.4	8.03	1334	58	8.5	84%	1.3
15/01/2017	Jan17	15	15.4	8.03	1336	57	8.8	87%	1
15/01/2017	Jan17	20	15.4	8.04	1337	58	8.6	85%	1.7
15/01/2017	Jan17	25	15.4	8.04	1330	58	8.7	86%	1.2
15/01/2017	Jan17	30	15.3	8.08	1336	59	8.7	86%	1.3
15/01/2017	Jan17	35	15.3	8.1	1336	58	8.1	80%	2.4
30/04/2017	Apr17	1	20.2	8.62	1297	57	11.0	120%	2.6
30/04/2017	Apr17	3	20.1	8.68	1297	57	11.3	124%	2.3
30/04/2017	Apr17	5	20.0	8.69	1296	57	11.4	125%	2.5
30/04/2017	Apr17	10	19.8	8.65	1297	57	11.2	123%	2.9
30/04/2017	Apr17	15	19.1	8.52	1305	56	9.4	101%	2.7
30/04/2017	Apr17	20	16.3	8.32	1312	57	7.8	79%	1.6
30/04/2017	Apr17	25	15.4	8.38	1308	57	8.8	87%	2.5
30/04/2017	Apr17	30	15.0	8.04	1327	56	5.3	53%	1.9

SUPPLEMENTARY INFORMATION TABLE Art.1.SI 3 (Continued)

Table Art.1.SI 3. (Continued)

Date	Code	Depth (m)	T (ºC)	pH	Cond. (mS cm^{-1})	SO_4^{-2} (mg L^{-1})	DO (mg L^{-1})	Ox. Sat. (%)	Turb. (NTU)
30/04/2017	Apr17	35	14.7	7.81	1334	57	3.9	39%	1.8
10/09/2017	Sep17	1	29.8	8.42	1347	60	7.9	105%	1.9
10/09/2017	Sep17	3	29.6	8.4	1349	60	8	106%	1.6
10/09/2017	Sep17	5	29.5	8.33	1349	60	7.7	102%	2.1
10/09/2017	Sep17	10	29.5	8.13	1350	60	6.8	90%	1.3
10/09/2017	Sep17	15	29.2	7.76	1356	60	3.5	46%	1.6
10/09/2017	Sep17	16	28.3	7.76	1352	60	1	13%	3.8
10/09/2017	Sep17	17	26.7	7.74	1348	57	0.1	1%	3
10/09/2017	Sep17	20	20.0	7.73	1347	n.d.	0.1	1%	4.4
10/09/2017	Sep17	30	16.4	7.7	1370	n.d.	0.1	1%	0.75
10/09/2017	Sep17	33	16.3	7.84	1368	n.d.	0.1	1%	0.7
12/12/2017	Nov17	1	20.0	8.1	1394	61	7.2	79%	1.4
12/12/2017	Nov17	3	20.0	8.12	1391	61	8	88%	1.4
12/12/2017	Nov17	5	20.0	8.15	1393	61	7.8	86%	1.5
12/12/2017	Nov17	10	20.0	8.17	1389	61	7.5	82%	1.5
12/12/2017	Nov17	15	20.0	8.19	1389	61	7.6	84%	1.6
12/12/2017	Nov17	20	20.0	8.21	1388	60	7.4	81%	1.6
12/12/2017	Nov17	25	19.9	8.2	1388	n.d.	7.8	86%	1.4
12/12/2017	Nov17	26	19.7	8.1	1387	58	4.7	52%	1.6
12/12/2017	Nov17	27	18.8	7.63	1377	45	0.1	1%	3.2
12/12/2017	Nov17	30	16.4	7.86	1377	40	0.1	1%	1.6
12/12/2017	Nov17	33	16.3	7.74	1384	34	0.1	1%	1.7

SUPPLEMENTARY INFORMATION TABLE Art.1.SI 4

Table Art.1.SI 4. Raw data for dissolved T.Se, Se(IV), Se(VI) and organic Se (Org.Se) as function of depth in meters. All data is presented in ng Se L^{-1}. Red.Se was calculated as T.Se-Se(IV)-Se(VI).

Sampling Date	Code	Depth (m)	T.Se	Se(IV)	Se(VI)	Org.Se
			(ng Se L^{-1})			
11/01/2015	Jan15	1	134 ± 8	26 ± 2	25 ± 2	<LoD
11/01/2015	Jan15	3	142 ± 17	29 ± 3	24 ± 2	<LoD
11/01/2015	Jan15	5	129 ± 14	30 ± 2	25 ± 2	< LoD
11/01/2015	Jan15	10	146 ± 12	28 ± 2	30 ± 2	< LoD
11/01/2015	Jan15	15	119 ± 13	28 ± 2	24 ± 2	< LoD
11/01/2015	Jan15	20	133 ± 13	25 ± 2	24 ± 2	< LoD
11/01/2015	Jan15	25	156 ± 15	33 ± 2	27 ± 2	< LoD
11/01/2015	Jan15	30	146 ± 9	27 ± 2	30 ± 2	< LoD
11/01/2015	Jan15	35	160 ± 14	27 ± 2	42 ± 4	< LoD
19/04/2015	Apr15	1	166 ± 13	22 ± 2	59 ± 3	20 ±2
19/04/2015	Apr15	3	170 ± 17	20 ± 2	58 ± 3	17 ± 2
19/04/2015	Apr15	5	203 ± 20	20 ± 2	58 ± 3	15 ± 2
19/04/2015	Apr15	10	147 ± 23	21 ± 2	58 ± 3	14 ± 1
19/04/2015	Apr15	15	156 ± 14	24 ± 2	52 ± 3	13 ± 4
19/04/2015	Apr15	20	170 ± 18	22 ± 2	42 ± 2	9 ± 1
19/04/2015	Apr15	25	146 ± 16	25 ± 2	43 ± 2	8 ± 2
19/04/2015	Apr15	30	149 ± 17	24 ± 2	39 ± 2	< LoD
19/04/2015	Apr15	35	151 ± 19	27 ± 2	42 ± 4	< LoD
06/09/2015	Sep15	1	152 ± 16	84 ± 4	90 ± 5	53 ± 2
06/09/2015	Sep15	3	143± 15	50± 3	44 ± 3	70 ± 4
06/09/2015	Sep15	5	130 ± 8	44 ± 3	39 ± 3	60 ± 10
06/09/2015	Sep15	10	122 ± 24	34 ± 2	42 ± 3	84 ± 8
06/09/2015	Sep15	15	124 ± 12	14 ± 2	31 ± 3	44 ± 2

SUPPLEMENTARY INFORMATION TABLE Art.1.SI 4 (Continued)

Table Art.1.SI 4. (Continued)

Sampling Date	Code	Depth (m)	T.Se	Se(IV)	Se(VI)	Org.Se
					(ng Se L^{-1})	
06/09/2015	Sep15	16	118 ± 22	9 ± 2	22 ± 2	37 ± 3
06/09/2015	Sep15	17	124 ± 14	17 ± 2	14 ± 1	< LoD
06/09/2015	Sep15	20	106 ± 7	44 ± 2	< LoD	< LoD
06/09/2015	Sep15	25	165 ± 15	75 ± 5	< LoD	< LoD
06/09/2015	Sep15	30	176 ± 7	29 ± 3	< LoD	< LoD
06/09/2015	Sep15	35	172 ± 19	26 ± 2	< LoD	< LoD
16/11/2015	Nov15	1	137 ± 16	23 ± 2	38 ± 3	36 ± 2
16/11/2015	Nov15	3	127± 19	41 ± 4	35 ± 3	24 ± 7
16/11/2015	Nov15	5	122 ± 11	27 ± 2	36 ± 3	30 ± 3
16/11/2015	Nov15	10	141 ± 16	24 ± 2	35 ± 3	37 ± 6
16/11/2015	Nov15	15	107 ± 13	38 ± 4	35 ± 3	26 ± 5
16/11/2015	Nov15	20	128 ± 18	25 ± 2	38 ± 3	28 ± 3
16/11/2015	Nov15	23	137 ± 22	37 ± 3	36 ± 3	25 ± 2
16/11/2015	Nov15	24	133 ± 15	40 ± 3	37 ± 2	24 ± 2
16/11/2015	Nov15	25	139 ± 13	12 ± 2	29 ± 3	< LoD
16/11/2015	Nov15	30	137 ± 23	51 ± 2	26 ± 2	< LoD
16/11/2015	Nov15	35	142 ± 19	52 ± 2	10 ± 2	< LoD
25/01/2016	Jan16	1	118 ± 7	< LoD	31 ± 3	14 ± 1
25/01/2016	Jan16	3	133 ± 9	33 ± 3	28 ± 2	12 ± 2
25/01/2016	Jan16	5	117 ± 7	< LoD	31 ± 3	9 ± 1
25/01/2016	Jan16	10	136 ± 9	29 ± 2	30 ± 2	11 ± 3
25/01/2016	Jan16	15	126 ± 9	< LoD	33 ± 3	10 ± 4
25/01/2016	Jan16	30	157 ± 10	20 ± 2	28 ± 2	12 ± 3
25/01/2016	Jan16	35	131 ± 9	15 ± 2	30 ± 3	10 ± 1
17/04/2016	Apr16	1	126 ± 6	39 ± 3	44 ± 5	60 ± 2

SUPPLEMENTARY INFORMATION TABLE Art.1.SI 4 (Continued)

Table Art.1.SI 4. (Continued)

Sampling Date	Code	Depth (m)	T.Se	Se(IV)	Se(VI)	Org.Se
			(ng Se L^{-1})			
17/04/2016	Apr16	3	135 ± 7	43 ± 5	45 ± 5	57 ± 1
17/04/2016	Apr16	5	141 ± 7	42 ± 3	47 ± 5	56 ± 0.3
17/04/2016	Apr16	10	146 ± 7	40 ± 3	47 ± 5	50 ± 2
17/04/2016	Apr16	15	147 ± 7	38 ± 3	43 ± 5	46 ± 1
17/04/2016	Apr16	20	145 ± 7	41 ± 3	45 ± 5	38 ± 1
17/04/2016	Apr16	25	142 ± 7	43 ± 5	43 ± 4	36 ± 3
17/04/2016	Apr16	30	137 ± 7	44 ± 3	36 ± 3	25 ± 2
17/04/2016	Apr16	35	133 ± 7	45 ± 4	35 ± 3	20 ± 3
15/09/2016	Sep16	1	114 ± 6	17 ± 2	34 ± 2	74 ± 52
15/09/2016	Sep16	3	118 ± 6	17 ± 2	33 ± 2	64 ± 41
15/09/2016	Sep16	5	122 ± 6	15 ± 2	31 ± 2	60 ± 38
15/09/2016	Sep16	10	112 ± 6	15 ± 1	31 ± 2	60 ± 41
15/09/2016	Sep16	15	106 ± 6	13 ± 1	14 ± 1	42 ± 20
15/09/2016	Sep16	18	104 ± 5	14 ± 1	21 ± 1	37 ± 22
15/09/2016	Sep16	19.5	77 ± 4	8 ± 1	< LoD	31 ± 15
15/09/2016	Sep16	20	74 ± 4	7 ± 1	< LoD	39 ± 7
15/09/2016	Sep16	25	112 ± 6	29 ± 2	< LoD	36 ± 7
15/09/2016	Sep16	30	88 ± 5	< LoD	< LoD	18
15/09/2016	Sep16	35	83 ± 5	< LoD	< LoD	11
27/11/2016	Nov16	1	114 ± 7	27 ± 2	29 ± 2	36 ± 2
27/11/2016	Nov16	3	117 ± 7	31 ± 2	29 ± 2	31 ± 2
27/11/2016	Nov16	5	116 ± 7	29 ± 2	28 ± 2	30 ± 3
27/11/2016	Nov16	10	116 ± 7	27 ± 2	28 ± 2	32 ± 4
27/11/2016	Nov16	15	118 ± 7	27 ± 2	29 ± 2	33 ± 2
27/11/2016	Nov16	20	114 ± 7	28 ± 2	29 ± 2	45 ± 16

SUPPLEMENTARY INFORMATION TABLE Art.1.SI 4 (Continued)

Table Art.1.SI 4. (Continued)

Sampling Date	Code	Depth (m)	T.Se	Se(IV)	Se(VI)	Org.Se
			(ng Se L^{-1})			
27/11/2016	Nov16	25	115 ± 7	27 ± 2	29 ± 2	39 ± 13
27/11/2016	Nov16	28	116 ± 7	28 ± 2	29 ± 2	33 ± 2
27/11/2016	Nov16	29	118 ± 7	27 ± 2	27 ± 2	33 ± 2
27/11/2016	Nov16	30	93 ± 6	12 ± 1	13 ± 1	39 ± 11
27/11/2016	Nov16	34	103 ± 7	3 ± 1	< LoD	18 ± 10
15/01/2017	Jan17	1	145 ± 8	41 ± 2	34 ± 2	25 ± 5
15/01/2017	Jan17	3	139 ± 6	42 ± 2	34 ± 2	20 ± 2
15/01/2017	Jan17	5	142 ± 6	42 ± 2	35 ± 2	23 ± 2
15/01/2017	Jan17	10	136 ± 6	36 ± 2	35 ± 2	21 ± 4
15/01/2017	Jan17	15	140 ± 7	40 ± 2	34 ± 2	22 ± 5
15/01/2017	Jan17	20	146 ± 6	40 ± 2	35 ± 2	19 ± 2
15/01/2017	Jan17	25	142 ± 8	40 ± 2	35 ± 2	21 ± 7
15/01/2017	Jan17	30	143 ± 7	40 ± 2	34 ± 2	21 ± 7
15/01/2017	Jan17	35	147 ± 9	39 ± 2	33 ± 2	18 ± 5
30/04/2017	Apr17	1	151 ± 7	40 ± 2	50 ± 2	27 ± 2
30/04/2017	Apr17	3	150 ± 8	38 ± 2	49 ± 2	29 ± 2
30/04/2017	Apr17	5	149 ± 7	37 ± 2	51 ± 2	27 ± 2
30/04/2017	Apr17	10	146 ± 7	40 ± 3	47 ± 5	25 ± 3
30/04/2017	Apr17	15	150 ± 7	33 ± 2	54 ± 2	22 ± 5
30/04/2017	Apr17	20	152 ± 7	33 ± 2	51 ± 2	16 ± 2
30/04/2017	Apr17	25	151 ± 8	38 ± 2	46 ± 2	15 ± 2
30/04/2017	Apr17	30	148 ± 8	41 ± 3	47 ± 2	9 ± 1

SUPPLEMENTARY INFORMATION TABLE Art.1.SI 4 (Continued)

Table Art.1.SI 4. (Continued)

Sampling Date	Code	Depth (m)	T.Se	Se(IV)	Se(VI)	Org.Se
			(ng Se L^{-1})			
30/04/2017	Apr17	35	149 ± 7	43 ± 2	47 ± 2	8 ± 1
10/09/2017	Sep17	1	113 ± 5	5 ± 1	32 ± 2	75 ± 9
10/09/2017	Sep17	3	114 ± 7	6 ± 1	33 ± 2	66 ± 9
10/09/2017	Sep17	5	114 ± 6	4 ± 1	33 ± 2	51 ± 11
10/09/2017	Sep17	10	115 ± 6	2 ± 0.5	33 ± 2	63 ± 10
10/09/2017	Sep17	15	112 ± 5	8 ± 1	30 ± 2	49 ± 14
10/09/2017	Sep17	16	100 ± 5	6 ± 1	11 ± 1	23 ± 3
10/09/2017	Sep17	17	80 ± 4	3 ± 0.5	< LoD	17 ± 4
10/09/2017	Sep17	20	79 ± 5	4 ± 1	< LoD	8 ± 3
10/09/2017	Sep17	25	122 ± 6	14 ± 1	21 ± 2	40 ± 5
10/09/2017	Sep17	30	140 ± 7	5 ± 2	< LoD	14 ± 8
10/09/2017	Sep17	33	140 ± 7	6 ± 1	< LoD	< LoD
12/12/2017	Nov17	1	101 ± 6	18 ± 2	26 ± 2	67 ± 7
12/12/2017	Nov17	3	100 ± 5	8 ± 1	26 ± 2	63 ± 6
12/12/2017	Nov17	5	103 ± 5	17 ± 1	26 ± 2	60 ± 5
12/12/2017	Nov17	10	106 ± 5	15 ± 1	26 ± 2	62 ± 5
12/12/2017	Nov17	15	106 ± 5	16 ± 2	26 ± 2	59 ± 4
12/12/2017	Nov17	20	108 ± 6	16 ± 1	26 ± 2	56 ± 5
12/12/2017	Nov17	25	107 ± 5	20 ± 1	27 ± 2	58 ± 4
12/12/2017	Nov17	26	110 ± 9	17 ± 1	28 ± 2	52 ± 4
12/12/2017	Nov17	27	111 ± 6	20 ± 2	27 ± 2	52 ± 5
12/12/2017	Nov17	30	131 ± 6	9 ± 1	3 ± 0.4	5 ± 0.5
12/12/2017	Nov17	33	129 ± 8	13 ± 1	25 ± 2	3 ± 0.2

SUPPLEMENTARY INFORMATION TABLE Art.1.SI 5

Table Art.1.SI 5. Volatile Se speciation raw data as function of depth in meters. The table includes TVSe, DMSe, DMSeS and DMDSe concentration in pg Se L^{-1}.

Sampling Date	Code	Depth (m)	TVSe	DMSe	DMSeS	DMDSe
			(pg Se L^{-1})			
19/04/2015	Apr15	1	19 ± 0.9	< LoD	15.7 ± 0.8	1.0 ± 0.05
19/04/2015	Apr15	15	10 ± 0.5	< LoD	6.8 ± 0.3	< LoD
19/04/2015	Apr15	35	99 ± 5	38 ± 2	54 ± 3	2.2 ± 0.1
06/09/2015	Sep15	1	42 ± 2	9 ± 0.5	16 ± 0.8	17 ± 0.9
06/09/2015	Sep15	10	219 ± 11	73 ± 4	113 ± 6	33 ± 1.6
06/09/2015	Sep15	15	125 ± 6	75 ± 4	15 ± 0.8	21 ± 1
06/09/2015	Sep15	25	30 ± 1.5	13 ± 0.7	3.9 ± 0.2	8.6 ± 0.4
06/09/2015	Sep15	35	15 ± 0.8	2.5 ± 0.1	2.8 ± 0.1	1.2 ± 0.06
16/11/2015	Nov15	1	1119 ± 56	70 ± 4	827 ± 41	194 ± 10
16/11/2015	Nov15	10	777 ± 39	60 ± 3	487 ± 25	192 ± 10
16/11/2015	Nov15	15	391 ± 20	84 ± 4	157 ± 8	103 ± 5
16/11/2015	Nov15	25	1157 ± 58	275 ± 14	278 ± 14	528 ± 26
16/11/2015	Nov15	35	63 ± 3	5.5 ± 0.3	16 ± 0.8	28 ± 1.4
25/01/2016	Jan16	1	15 ± 0.7	12 ± 0.6	< LoD	< LoD
25/01/2016	Jan16	15	14 ± 0.7	14 ± 0.7	< LoD	< LoD
25/01/2016	Jan16	25	8 ± 0.4	7.3 ± 0.4	< LoD	< LoD
25/01/2016	Jan16	35	13 ± 0.6	12 ± 0.6	< LoD	< LoD
17/04/2016	Apr16	1	22 ± 1	0.6 ± 0.03	13 ± 0.6	< LoD
17/04/2016	Apr16	15	16 ± 0.8	2.5 ± 0.1	9.5 ± 0.5	< LoD
17/04/2016	Apr16	25	29 ± 1.5	9.2 ± 0.5	15 ± 0.8	< LoD
17/04/2016	Apr16	35	92 ± 5	42 ± 2	45 ± 2.3	< LoD
15/09/2016	Sep16	1	182 ± 9	121 ± 6	49 ± 2	10 ± 0.5

SUPPLEMENTARY INFORMATION TABLE Art.1.SI 5 (Continued)

Table Art.1.SI 5. (Continued)

Sampling Date	Code	Depth (m)	TVSe	DMSe	DMSeS	DMDSe
			(pg Se L^{-1})			
15/09/2016	Sep16	10	356 ± 18	356 ± 18	< LoD	< LoD
15/09/2016	Sep16	15	1005 ± 50	636 ± 31	105 ± 5	238 ± 12
15/09/2016	Sep16	18	523 ± 26	198 ± 10	127 ± 6	179 ± 9
15/09/2016	Sep16	25	76 ± 4	16 ± 0.8	6.6 ± 0.3	43 ± 2
15/09/2016	Sep16	35	193 ± 10	23 ± 1	69 ± 3	77 ± 4
27/11/2016	Nov16	1	371 ± 19	118 ± 6	179 ± 9	73 ± 4
27/11/2016	Nov16	10	771 ± 39	135 ± 7	191 ± 10	434 ± 22
27/11/2016	Nov16	15	789 ± 39	169 ± 8	226 ± 11	36 ± 19
27/11/2016	Nov16	25	478 ± 24	78 ± 4	277 ± 14	115 ± 6
27/11/2016	Nov16	34	41 ± 2	13 ± 0.6	6.1 ± 0.3	10 ± 0.5
15/01/2017	Jan17	1	115 ± 6	26 ± 1	57 ± 3	32 ± 2
15/01/2017	Jan17	10	157 ± 8	67 ± 3	73 ± 4	17 ± 0.8
15/01/2017	Jan17	15	141 ± 7	26 ± 1	91 ± 5	24 ± 1
15/01/2017	Jan17	25	174 ± 9	43 ± 2	100 ± 5	31 ± 2
15/01/2017	Jan17	35	138 ± 7	65 ± 3	37 ± 2	36 ± 2
30/04/2017	Apr17	1	6.9 ± 0.3	2.3 ± 0.1	4.6 ± 0.2	< LoD
30/04/2017	Apr17	5	19 ± 0.9	10 ± 0.5	4.4 ± 0.2	4.5 ± 0.2
30/04/2017	Apr17	10	12 ± 0.6	7 ± 0.4	4 ± 0.2	1 ± 0.05
30/04/2017	Apr17	15	16 ± 0.8	2 ± 0.1	5 ± 0.3	8.6 ± 0.4
30/04/2017	Apr17	25	29 ± 1.5	16 ± 0.8	6 ± 0.3	6.7 ± 0.3
30/04/2017	Apr17	35	68 ± 3	16 ± 0.8	2 ± 0.1	51 ± 3
10/09/2017	Sep17	1	201 ± 10	48 ± 2	88 ± 4	65 ± 3
10/09/2017	Sep17	10	194 ± 10	27 ± 1	98 ± 5	69 ± 3

SUPPLEMENTARY INFORMATION TABLE Art.1.SI 5 (Continued)

Table Art.1.SI 5. (Continued)

Sampling Date	Code	Depth (m)	TVSe	DMSe	DMSeS	DMDSe
			(pg Se L^{-1})			
10/09/2017	Sep17	15	318 ± 16	60 ± 3	167 ± 8	91 ± 5
10/09/2017	Sep17	25	12 ± 0.6	8.5 ± 0.4	1.2 ± 0.05	2 ± 0.1
10/09/2017	Sep17	33	30 ± 1	13 ± 1	4.7 ± 1	12 ± 1
12/12/2017	Nov17	1	207 ± 10	118 ± 6	57 ± 3	32 ± 2
12/12/2017	Nov17	5	411 ± 21	69 ± 3	175 ± 9	167 ± 8
12/12/2017	Nov17	15	666 ± 33	152 ± 8	206 ± 10	307 ± 15
12/12/2017	Nov17	25	494 ± 25	113 ± 6	153 ± 8	228 ± 11
12/12/2017	Nov17	33	682 ± 34	35 ± 2	324 ± 16	266 ± 13

SUPPLEMENTARY INFORMATION TABLE Art.1.SI 6

Table Art.1.SI 6. Results of stability experiment for volatile Se species carried out with additional samples of 1m and 25m depth received at November of 2016. Samples were stored in the original bottle, in the dark at 4º C. The table illustrates the variation of volatile Se speciation depending on the stocking time. The column Days indicates the days elapsed from sampling to the experiment. Samples were closed up to the day of experiment. Volatile Se data is presented in pg Se L^{-1}.

Sample	Days	DMSe	DMSSe	DMDSe	TVSe
		(pg Se L^{-1})			
1m – A	4	118 ± 6	179 ± 9	73 ± 4	372 ± 19
1m – B	18	112 ± 6	3529 ± 176	476 ± 24	4146 ± 207
1m – C	37	62 ± 3	887 ± 44	233 ± 12	1183 ± 59
25m – A	4	78 ± 4	277 ± 14	115 ± 6	478 ± 24
25m – B	18	136 ± 7	223 ± 11	83 ± 4	465 ± 23
25m – C	37	84 ± 4	314 ± 16	112 ± 6	510 ± 26

SUPPLEMENTARY INFORMATION TABLE Art1.SI 7

Table Art.1.SI 7. Stability experimental results for dissolved selenite and selenate species carried out with samples of 1, 5 25m depth from April 2016 sampling. Samples were stored in the original bottle, in the dark at 4º C. The table illustrates the variation of dissolved Se species depending on the stocking time. The column Days indicates the days elapsed from the first time the bottle was opened. Samples remained closed and stored at 4 ºC in the dark between analysis. Data is presented in ng Se L^{-1}. Samples were either stored directly from the water or adding a 0.2% (V/V) HNO_3 (indicated as acid).

Sample	Days	Se(IV)	Se(VI)
Untreated samples			
1m – A	0	40 ± 2	50 ± 2
1m – B	14	37 ± 2	51 ± 2
1m – C	29	35 ± 2	52 ± 2
5m – A	0	37 ± 2	51 ± 2
5m – B	14	33 ± 2	52 ± 2
5m – C	29	28 ± 2	52 ± 2
25m – A	0	38 ± 2	46 ± 2
25m – B	14	42 ± 2	51 ± 2
25m – C	29	39 ± 2	53 ± 3
Acidified samples			
1m – A (acid)	0	35 ± 2	51 ± 2
1m – B (acid)	29	30 ± 2	51 ± 3
5m – A (acid)	0	35 ± 2	49 ± 2
5m – B (acid)	29	33 ± 2	52 ± 3
25m – A (acid)	0	43 ± 2	43 ± 2
25m – B (acid)	29	41 ± 2	44 ± 2

5. Bibliography

Amouroux, D., & Donard, O. F. X. (1996). Maritime emission of selenium to the atmosphere in Eastern Mediterranean seas. Geophysical Research Letters, 23(14), 1777–1780. https://doi.org/10.1029/96GL01271

Amouroux, D., & Donard, O. F. X. (1997). Evasion of selenium to the atmosphere via biomethylation processes in the Gironde estuary, France. Marine Chemistry, 58(1–2), 173–188. https://doi.org/10.1016/S0304-4203(97)00033-9

Amouroux, D., Liss, P. S., Tessier, E., Hamren-Larsson, M., & Donard, O. F. X. (2001). Role of ocens as biogenic sources of selenium. Earth and Planetary Science Letters, 189(3–4), 277–283. https://doi.org/10.1016/S0012-821X(01)00370-3

Amouroux, D., Pécheyran, C., & Donard, O. F. X. (2000). Formation of volatile selenium species in synthetic seawater under light and dark experimental conditions. Applied Organometallic Chemistry, 14(5), 236–244. https://doi.org/10.1002/(SICI)1099-0739(200005)14:5<236::AID-AOC982>3.0.CO;2-U

Balistrieri, L. S., & Chao, T. T. (1987). Selenium Adsorption by Goethite1. Soil Science Society of America Journal, 51, 1145–1151. https://doi.org/10.2136/sssaj1987.03615995005100050009x

Bender, J., Gould, J. P., Vatcharapijarn, Y., & Saha, G. (1991). Uptake, transformation and fixation of Se (VI) by a mixed selenium-tolerant ecosystem. Water, Air, and Soil Pollution, 59(3–4), 359–367. https://doi.org/10.1007/BF00211843

Berman, T., Zohary, T., Nishri, A., & Sukenik, A. (2014). Lake Kinneret. Lake Kinneret, 1–15. https://doi.org/10.1007/978-94-017-8944-8. https://doi.org/10.1007/978-94-017-8944-8

Buchs, B., Evangelou, M. W. H., Winkel, L. H. E., & Lenz, M. (2013). Colloidal properties of nanoparticular biogenic selenium govern environmental fate and bioremediation effectiveness. Environmental Science & Technology, 47(5), 2401–2407. https://doi.org/10.1021/es304940s

Chasteen, T. G., & Bentley, R. (2003). Biomethylation of selenium and tellurium: microorganisms and plants. Chemical Reviews, 103(1), 1–25. https://doi.org/10.1021/cr010210+

Chau, Y. K., Wong, P. T. S., Silverberg, B. A., Luxon, P. L., & Bengert, G. A. (1976). Methylation of selenium in the aquatic environment. Science, 192(4244), 1130–1131. https://doi.org/10.1126/science.192.4244.1130

Chouhan, R., & Banerjee, M. (2010). Two cyanobacteria Hapalosiphon sp. and Gloeocapsa sp. in amelioration of selenium toxicity. J. Appl. Biosci, 36(2), 137–140.

Cole, J. J., & Caraco, N. F. (1998). Atmospheric exchange of carbon dioxide in a low-wind oligotrophic lake measured by the addition of SF6. Limnology and Oceanography, 43(4), 647–656. https://doi.org/10.4319/lo.1998.43.4.0647.

Conde, J. E., & Sanz Alaejos, M. (1997). Selenium Concentrations in Natural and Environmental Waters. Chemical Reviews, 97(6), 1979–2004. https://doi.org/10.1021/cr960100g

Cooke, T. D., & Bruland, K. W. (1987). Aquatic Chemistry of Selenium: Evidence of Biomethylation. Environmental Science and Technology, 21(12), 1214–1219. https://doi.org/10.1021/es00165a009

Cutter, G. A., & Bruland, K. W. (1984). The Marine Biogeochemistry of Selenium: A Re-Evaluation Gregory A. Cutter; Kenneth W. Bruland, 29(6), 1179–1192. https://doi.org/10.4319/lo.1984.29.6.1179.

Darrouzès, J., Bueno, M., Simon, S., Pannier, F., & Potin-Gautier, M. (2008). Advantages of hydride generation interface for selenium speciation in waters by high performance liquid chromatography-inductively coupled plasma mass spectrometry coupling. Talanta, 75(2), 362–368. https://doi.org/10.1016/j.talanta.2007.11.020

Dauthieu, M., Bueno, M., Darrouzes, J., Gilon, N., & Potin-Gautier, M. (2006). Evaluation of porous graphitic carbon stationary phase for simultaneous preconcentration and separation of organic

and inorganic selenium species in “clean” water systems. Journal of Chromatography A, 1114(1), 34–39. https://doi.org/10.1016/j.chroma.2006.02.018

Diaz, X., Johnson, W. P., Oliver, W. A., & Naftz, D. L. (2009). Volatile selenium flux from the great Salt Lake, Utah. Environmental Science and Technology, 43(1), 53–59. https://doi.org/10.1021/es801638w

Domagalski, J. L., Orem, W. H., & Eugster, H. P. (1989). Organic geochemistry and brine composition in Great Salt, Mono, and Walker Lakes. Geochimica et Cosmochimica Acta, 53(11), 2857–2872. https://doi.org/10.1016/0016-7037(89)90163-4

Duan, L., Song, J., Li, X., Yuan, H., & Xu, S. (2010). Distribution of selenium and its relationship to the eco-environment in Bohai Bay seawater. Marine Chemistry, 121(1–4), 87–99. https://doi.org/10.1016/j.marchem.2010.03.007

Eckert, W., & Conrad, R. (2007). Sulfide and methane evolution in the hypolimnion of a subtropical lake: A three-year study. Biogeochemistry, 82(1), 67–76. https://doi.org/10.1007/s10533-006-9053-3

Fan, T. W.-M. W.-M., Higashi, R. M., & Lane, A. N. (1998). Biotransformations of Selenium Oxyanion by Filamentous Cyanophyte-Dominated Mat Cultured from Agricultural Drainage Waters. Environmental Science & Technology, 32(20), 3185–3193. https://doi.org/10.1021/es9708833

Fernández-Martínez, A., & Charlet, L. (2009). Selenium environmental cycling and bioavailability : a structural chemist point of view, 81–110. https://doi.org/10.1007/s11157-009-9145-3

Ginzburg, B., Chalifa, I., Gun, J., Dor, I., Hadas, O., & Lev, O. (1998). DMS formation by dimethylsulfoniopropionate route in freshwater. Environmental Science and Technology, 32(14), 2130–2136. https://doi.org/10.1021/es9709076

Ginzburg, B., Dor, I., Chalifa, I., Hadas, O., & Lev, O. (1999). Formation of Dimethyloligosulfides in Lake Kinneret: Biogenic Formation of Inorganic Oligosulfide Intermediates under Oxic Conditions. Environmental Science & Technology, 33(4), 571–579. https://doi.org/10.1021/es980636e

Guo, L., Frankenberger, W. T., & Jury, W. A. (1999). Evaluation of simultaneous reduction and transport of selenium in saturated soil columns, 35(3), 663–669. https://doi.org/10.1029/1998WR900074

Hadas, O., & Pinkas, R. (1995). Sulfate reduction processes in sediments at different sites in Lake Kinneret, Israel. Microbial Ecology, 30(1), 55–66. https://doi.org/10.1007/BF00184513

Hambright, K. D., & Zohary, T. (1998). Lakes Hula and Agmon: destruction and creation of wetland ecosystems in northern Israel. Wetlands Ecology and Management, 6(2–3), 83–89. https://doi.org/10.1023/A:1008441015990

Harrison, P. J., Yu, P. W., Thompson, P. A., Price, N. M., & Phillips, D. J. (1988). Survey of selenium requirements in marine phytoplankton. Marine Ecology Progress Series, 47(1), 89–96. Retrieved from http://www.jstor.org/stable/24831560. Last access : Nobember 09, 2020.

Hu, H., Mylon, S. E., & Benoit, G. (2007). Volatile organic sulfur compounds in a stratified lake. Chemosphere, 67(5), 911–919. https://doi.org/10.1016/j.chemosphere.2006.11.012

Hu, M., Yang, Y., Martin, J.-M., Yin, K., & Harrison, P. J. (1997). Preferential uptake of Se(IV) over Se(VI) and the production of dissolved organic Se by marine phytoplankton. Marine Environmental Research, 44(2), 225–231. https://doi.org/https://doi.org/10.1016/S0141-1136(97)00005-6

Ivanenko, N. V. (2018). The Role of Microorganisms in Transformation of Selenium in Marine Waters. Russian Journal of Marine Biology, 44(2), 87–93. https://doi.org/10.1134/S1063074018020049

Knossow, N., Blonder, B., Eckert, W., Turchyn, A. V., Antler, G., & Kamyshny, A. (2015). Annual sulfur cycle in a warm monomictic lake with sub-millimolar sulfate concentrations. Geochemical Transactions, 16(1), 7. https://doi.org/10.1186/s12932-015-0021-5

Lanceleur, L., Tessier, E., Pienitz, R., Cloquet, C., & Amouroux, D. (2019). Cycling and atmospheric exchanges of selenium in Canadian subarctic thermokarst ponds. Biogeochemistry. https://doi.org/10.1007/s10533-019-00599-w

Lenz, M., & Lens, P. N. L. (2009). The essential toxin: The changing perception of selenium in environmental sciences. Science of the Total Environment, 407(12), 3620–3633. https://doi.org/10.1016/j.scitotenv.2008.07.056

Luxem, K. E., Vriens, B., Behra, R., & Winkel, L. H. E. (2017). Studying selenium and sulfur volatilisation by marine algae Emiliania huxleyi and Thalassiosira oceanica in culture. Environmental Chemistry, 14(4), 199–206. Retrieved from https://doi.org/10.1071/EN16184

Mason, R. P., Soerensen, A. L., Dimento, B. P., & Balcom, P. H. (2018). The Global Marine Selenium Cycle: Insights from Measurements and Modeling. Global Biogeochemical Cycles, 32(1720–1737). https://doi.org/10.1029/2018GB006029

Mcneal, J. M., & Balistrieri, L. S. (1989). Geochemistry and Occurrence of Selenium : An Overview. Selenium in Agriculture and the Environment, (23), 1–13. https://doi.org/10.2136/sssaspecpub23.c1

Measures, C. I., & Burton, J. D. (1980). The vertical distribution and oxidation states of dissolved selenium in the northeast Atlantic Ocean and their relationship to biological processes. Earth and Planetary Science Letters, 46(3), 385-396. https://doi.org/10.1016/0012-821X(80)90052-7

Mehdi, Y., Hornick, J.-L., Istasse, L., & Dufrasne, I. (2013). Selenium in the Environment, Metabolism and Involvement in Body Functions. Molecules. https://doi.org/10.3390/molecules18033292

Mortimer, C. H. (1981). The oxygen content of air-saturated fresh waters over ranges of temperature and atmospheric pressure of limnological interest. SIL Communications, 1953-1996, 22(1), 1–23. https://doi.org/10.1080/05384680.1981.11904000

Nakaguchi, Y., & Hiraki, K. (1993). Selenium (IV), selenium (VI) and organic selenium in Lake Biwa, the Yodo River and Osaka Bay. Geochemical Journal, 27(6), 367–374. https://doi.org/10.2343/geochemj.27.367

Nakamaru, Y. M., & Altansuvd, J. (2014). Speciation and bioavailability of selenium and antimony in non-flooded and wetland soils: A review. Chemosphere, 111, 366–371. https://doi.org/10.1016/j.chemosphere.2014.04.024

Nancharaiah, Y. V., & Lens, P. N. L. (2015). Ecology and biotechnology of selenium-respiring bacteria. Microbiol. Mol. Biol. Rev., 79(1), 61–80. https://doi.org/10.1128/MMBR.00037-14

NEUMANN, P. M., DE SOUZA, M. P., PICKERING, I. J., & TERRY, N. (2003). Rapid microalgal metabolism of selenate to volatile dimethylselenide. Plant, Cell & Environment, 26(6), 897–905. https://doi.org/10.1046/j.1365-3040.2003.01022.x

Nishri, A., Brenner, I. B., Hall, G. E. M., & Taylor, H. E. (1999). Temporal variations in dissolved selenium in Lake Kinneret (Israel). Aquatic Sciences, 61(3), 215–233. https://doi.org/10.1007/s000270050063

Oremland, R. S., Hollibaugh, J. T., Maest, A. S., Presser, T. S., Miller, L. G., Charles, W., & Maest, A. N. N. S. (1989). Selenate Reduction to Elemental Selenium by Anaerobic Bacteria in Sediments and Culture. Applied and Environmental Microbiology, 55(9), 2333–43.

Ostrovsky, I., Rimmer, A., Yacobi, Y. Z., Nishri, A., Sukenik, A., Hadas, O., & Zohary, T. (2013). Long-Term Changes in the Lake Kinneret Ecosystem: The Anthropogenic Factors. Climate Change and Global Warming of Inland Waters: Impacts and Mitigation for Ecosystems and Societies, (July 2016), 271–293. https://doi.org/10.1002/9781118470596.ch16

Pilon-Smits, E. A. H., & Quinn, C. F. (2010). Selenium metabolism in plants. In Cell biology of metals and nutrients (pp. 225–241). Springer. https://doi.org/10.1007/978-3-642-10613-2_10

Pokrovsky, O. S., Bueno, M., Amouroux, D., Manasypov, R. M., Shirokova, L. S., Karlsson, J., & Amouroux, D. (2018). Dissolved organic matter controls on seasonal and spatial selenium concentration variability in thaw lakes across a permafrost gradient. Environ. Sci. Technol., 52(18), acs.est.8b00918. https://doi.org/10.1021/acs.est.8b00918

Ponton, D. E., Fortin, C., & Hare, L. (2018). Organic selenium, selenate, and selenite accumulation by lake plankton and the alga Chlamydomonas reinhardtii at different pH and sulfate

concentrations. Environmental Toxicology and Chemistry, 37(8), 2112–2122. https://doi.org/10.1002/etc.4158

Rimmer, A., & Gal, G. (2003). Estimating the saline springs component in the solute and water balance of Lake Kinneret, Israel. Journal of Hydrology, 284(1–4), 228–243. https://doi.org/10.1016/j.jhydrol.2003.08.006

Rimmer, A., & Givati, A. (2014). Lake Kinneret. Lake Kinneret, 97–111. https://doi.org/10.1007/978-94-017-8944-8

Rom, M., Berger, D., Teltsch, B., & Markel, D. (2014). Material Loads from the Jordan River BT - Lake Kinneret: Ecology and Management. In T. Zohary, A. Sukenik, T. Berman, & A. Nishri (Eds.) (pp. 309–327). Dordrecht: Springer Netherlands. https://doi.org/10.1007/978-94-017-8944-8_18

Sela-Adler, M., Said-Ahmad, W., Sivan, O., Eckert, W., Kiene, R. P., & Amrani, A. (2016). Isotopic evidence for the origin of dimethylsulfide and dimethylsulfoniopropionate-like compounds in a warm, monomictic freshwater lake. Environmental Chemistry, 13(2), 340–351. https://doi.org/10.1071/EN15042

Shaked, Y., Erel, Y., & Sukenik, A. (2004). The biogeochemical cycle of iron and associated elements in Lake Kinneret. Geochimica et Cosmochimica Acta, 68(7), 1439–1451. https://doi.org/10.1016/j.gca.2003.09.018

Simmons, D. B. D., & Wallschläger, D. (2011). Release of reduced inorganic selenium species into waters by the green fresh water algae chlorella vulgaris. Environmental Science and Technology, 45(6), 2165–2171. https://doi.org/10.1021/es103337p

Sukenik, A., Zohary, T., & Markel, D. (2014). The monitoring program. In Lake Kinneret (pp. 561–575). Springer.

Tessier, E., Amouroux, D., Abril, G., Lemaire, E., & Donard, O. F. X. (2002). Formation and volatilisation of alkyl-iodides and -selenides in macrotidal estuaries. Biogeochemistry, 59(1–2), 183–206. https://doi.org/10.1023/A:1015550931365

Tessier, E., Amouroux, D., & Donard, O. F. X. (2002). Biogenic volatilization of trace elements from European estuaries. Biogeochemistry of Environmentally Important Trace Elements, 835(October 2002), 151–165. https://doi.org/10.1021/bk-2003-0835.ch012

Velinsky, D. J., & Cutter, G. A. (1990). Determination of elemental selenium and pyrite-selenium in sediments. Analytica Chimica Acta, 235, 419–425. https://doi.org/10.1016/S0003-2670(00)82102-9

Vriens, B., Behra, R., Voegelin, A., Zupanic, A., & Winkel, L. H. E. (2016). Selenium Uptake and Methylation by the Microalga Chlamydomonas reinhardtii. Environmental Science & Technology, 50(2), 711–720. https://doi.org/10.1021/acs.est.5b04169

Wen, H., & Carignan, J. (2007). Reviews on atmospheric selenium: Emissions, speciation and fate. Atmospheric Environment, 41(34), 7151–7165. https://doi.org/10.1016/j.atmosenv.2007.07.035

Weres, O., Bowman, H. R., Goldstein, A., Smith, E. C., Tsao, L., & Harnden, W. (1990). The effect of nitrate and organic matter upon mobility of selenium in groundwater and in a water treatment process. Water, Air, and Soil Pollution, 49(3), 251–272. https://doi.org/10.1007/BF00507068

Weres, O., Jaouni, A.-R. A.-R., & Tsao, L. (1989). The distribution , speciation and geochemical cycling of selenium in a sedimentary environment, Keterston Reservoir, California U.S.A. Sciences-New York, 4(6), 543–563. https://doi.org/10.1016/0883-2927(89)90066-8

Winkel, L. H. E. E., Johnson, C. A., Lenz, M., Grundl, T., Leupin, O. X., Amini, M., & Charlet, L. (2012). Environmental selenium research: From microscopic processes to global understanding. Environmental Science and Technology, 46(2), 571–579. https://doi.org/10.1021/es203434d

Winkel, L. H. E., Vriens, B., Jones, G. D., Schneider, L. S., Pilon-Smits, E., & Bañuelos, G. S. (2015). Selenium cycling across soil-plant-atmosphere interfaces: A critical review. Nutrients. https://doi.org/10.3390/nu7064199

Wrench, J. J., & Measures, C. I. (1982). Temporal variations in dissolved selenium in a coastal

ecosystem. Nature, 299(5882), 431–433. https://doi.org/10.1038/299431a0

Yacobi, Y. Z., Erez, J., & Hadas, O. (2014). Lake Kinneret. In Lake Kinneret, Ecology and Management (pp. 417–437). Springer Science+Business Media Dordrecht. https://doi.org/10.1007/978-94-017-8944-8

Zhang, Y., Zahir, Z. A., & Frankenberger, W. T. (2004). Fate of Colloidal-Particulate Elemental Selenium in Aquatic Systems. Journal of Environmental Quality, 33, 559–564. https://doi.org/10.2134/jeq2004.5590

Zohary, T. (2004). Changes to the phytoplankton assemblage of Lake Kinneret after decades of a predictable, repetitive pattern. Freshwater Biology, 49(10), 1355–1371. https://doi.org/10.1111/j.1365-2427.2004.01271.x

Zohary, T., Yacobi, Y. Z., Alster, A., Fishbein, T., Lippman, S., & Tibor, G. (2014). Lake Kinneret. Lake Kinneret, 6, 161–190. https://doi.org/10.1007/978-94-017-8944-8

Zohary, T., Yacobi, Y.Z., Alster A., Fishbein, T., Lippman, S. and Tibor, G. (2014b). Phytoplankton. Chap. 10 In: Zohary T., Sukenik A, Berman T, Nishri A. [eds] Lake Kinneret: Ecology and Management, pp. 161-190. Springer, Heidelberg. https://doi.org/10.1007/978-94-017-8944-8

4.2. Article II << Selenium speciation in waters of remote and pristine high altitude lakes from the Pyrenees (France-Spain)>>

Selenium speciation in waters of remote and pristine high altitude lakes from the Pyrenees (France-Spain)

Andrea Romero-Rama[1], Bastien Duval[1,2], Emmanuel Tessier[1], Maïté Bueno[1], Luís Ángel Fernández[2], Alberto de Diego[2], David Amouroux[1]

1 - Université de Pau et des Pays de l'Adour, E2S UPPA, CNRS, Institute of Analytical Sciences and Physical-Chemistry for the Environment and Materials - IPREM, Pau, France

2 - Department of Analytical Chemistry, University of the Basque Country, Sarriena auzoa z/g; 48940 Leioa, Basque Country, Spain

Abstract

The speciation of redox reactive and volatile selenium (Se) compounds has been barely reported in remote and pristine aquatic environments. In addition, Se cycling in remote alpine lakes, considered as sensitive ecosystems to global change, has never been investigated. This work presents an integrated investigation conducted in high altitude pristine lakes from the central - western Pyrenees. Bi-annual sampling was carried out after snowmelt (June/July) and in early fall (October) for the period 2017 – 2019. Concentrations of total dissolved Se (TDSe) in the lakes investigated ranged from 7 ± 1 to 80 ± 1 ng Se L^{-1}, being selenate ubiquitously observed in most cases (8–111% of TDSe). Selenite was in the range between <LoQ to 4 ± 1 ng Se L^{-1}, therefore a fraction of total dissolved Se is presumably in the form of reduced Se such as elemental Se and selenide. Depth profiles carried out in different lakes showed the occurrence of unidentified reduced Se fraction (Se(0 or –II)) in such natural waters, together with an inherent relationship between Se speciation and lake seasonal dynamics. This is also consistent with the production of volatile Se compounds in those lakes, with total volatile Se (TVSe) ranging from 3 ± 4 to 120 ± 20 pg Se L^{-1} . The main volatile Se compound found in sub-surface samples was dimethylselenide (DMSe, 67% of TVSe concentration), while in seasonally stratified lakes dimethyl diselenide (DMDSe) represented up to 75% of total volatile Se concentration in bottom waters. This first report of Se speciation in remote alpine lakes demonstrates that, because they are less productive environments, Se speciation in surface is barely affected by the lake seasonal cycling, excepted in stratified lakes. Total dissolved Se concentrations are strongly affected by erosion and dissolution of Se and S-rich parent bedrocks, and by atmospheric deposition when geological substrate is depleted in Se.

1. Introduction

Non-polluted high-mountain lakes are pristine ecosystems characterized by extreme environmental conditions. Due to the low Se levels in unpolluted high mountain lakes, no data exist describing Se speciation in such remote ecosystems. The existing data about Se biogeochemistry in lakes is provided by research in temperate and tropical eutrophic lakes and have been reviewed elsewhere (Sharma et al., 2014; Simmons & Wallschläger, 2005). In unpolluted fresh water, total dissolved Se concentrations are typically below 0.1 μg L^{-1} (Wallschläger & Feldmann, 2010) and Se can occur in four oxidation states: -II, 0, IV and VI (Conde & Sanz Alaejos, 1997). In well aerated and oligotrophic environments, oxyanions, particularly selenate, are expected to be the major species (Sharma et al., 2014). In western Siberian lakes, total Se concentrations range from 12 to 311 ng Se L^{-1} (Pokrovsky et al., 2018). In Canadian subarctic thermokarst ponds, total dissolved Se ranged from 18 to 67 ng Se L^{-1} (Lanceleur et al., 2019). Norwegian (Økelsrud et al., 2016), Finish (Wang et al., 1994) and Canadian (Nriagu & Wong, 1983) lakes present Se concentration from 20 to 60 ng L^{-1}. While in temperate lakes of North America, Se concentrations were much higher ranging between 200 and 500 ng L^{-1} (Brandt et al., 2017) due to pyritic shale bedrock (VillaRomero et al., 2013). Less information exists for Se speciation. Selenite was found to be the predominant species in Belgium lakes (Robberecht et al., 1983), and polluted lakes from Canada (Dominic E. Ponton & Hare, 2013) and Germany (Tanzer & Heumann, 1991). Meanwhile, selenate was found as the main species in Swedish (Lindström, 1983), Finish (Wang et al., 1994; 1995) and Israeli lakes (Nishri et al., 1999). Despite the lack of analytical procedures to identify and quantify dissolved reduced Se species, several authors have reported the presence of such Se pool in lake waters. For example in Finish lakes, the sum of selenite and selenate represented less than 20% of total Se (Wang et al., 1994; 1995) and in Lake Kinneret up to 27% of total Se was associated to reduced Se species (Nishri et al., 1999).

Few studies have focused on volatile Se species in lake waters. Total volatile Se in studied lakes presents a wide range of concentration (1 to $109 \cdot 10^3$ pg Se L^{-1}), being dimethylselenide (DMSe) the major species (≥49%) with minor contribution of dimethyl diselenide (DMDSe) (4–41%). The presence of dimethyl selenide sulphide (DMSeS) was residual (≤7%) (Lanceleur et al., 2019). Two recent studies exist in remote environments. The first focused

on Se emissions in a high mountain minerotrophic peatland (elevation 972 m a.s.l.) reporting 10 ng L^{-1} of DMSe in surface water samples. However, this location presented high total Se concentration in the order of around 0.5 to 1.5 µg Se L^{-1}. In Canadian thermokarst ponds, Lanceleur et al., (2019) found DMSe to be the main species with concentrations between <0.17 to 4.1 pg Se L^{-1}. While in European estuaries, volatile Se ranged from 22 – 8067 pg L^{-1} being DMSe the main species found (Amouroux & Donard, 1997; Tessier et al., 2002). However, no information exists for high mountain oligotrophic lakes.

Eighty two per cent of Pyrenean lakes are classified as oligotrophic (Catalan et al., 2006). Low rock weathering and limited soil development determine waters with low mineralization, not only affecting Se concentration but also major salt components and nutrients. In high mountain lakes, Se can originate either from local (geogenic) or remote sources (atmospheric transport). Leaching and weathering mobilize Se from parent rocks to the water, being soil the main source of Se in unpolluted lakes (Lenny Winkel et al., 2015). Over medium and long distances, wet and dry atmospheric deposition may be significant contributors for Se concentration in some lakes despite their limited surface area (Lenny Winkel et al., 2015; Suess et al., 2019) and ice cover during, at least, 5-6 months of the year (Gascoin et al., 2015; López-Moreno & Vicente-Serrano, 2007). Previous studies have estimated that Se wet deposition (7.4 – 20.0 Gg Se yr^{-1}) was responsible of 80% of its global atmospheric deposition and was thus dominant over its dry deposition (1.1 – 5.0 Gg Se yr^{-1}) (Blazina et al., 2017; Pan & Wang, 2015). Suess et al. (2019) studied the concentration of Se in rain samples from Pic du Midi (central Pyrenees) and determined a total Se range between 13 – 184 ng Se L^{-1}. The authors determined that the dominant source of Se in rain (54%) was the North Atlantic Ocean with a contribution of terrestrial emissions of 40% with seasonal fluctuation. The ratio between total Se and other species (*i.e*. Na or S) has been employed to assess Se origin in wet deposition (Gregory A Cutter & Church, 1986; Suess et al., 2019). Pyrenean lakes are characterized by surface frost periods comprised generally between November and April (Gascoin et al., 2015; López-Moreno & Vicente-Serrano, 2007). During these periods atmospheric exchange is limited by the ice cover and several lakes have shown oxygen depletion during these periods (Catalan et al., 2002). These prevailing winter conditions may promote Se depletion from the water column by scavenging and further sedimentation.

Indeed, laboratory experiments using anaerobic sediments from the Salton Sea demonstrated the potential of prokaryotic (i.e. microbial) mediated reactions for selenate reduction to elemental Se (VillaRomero et al., 2013). Further sinking into sediments of insoluble reduced Se species was the main process removing Se from water (Schroeder et al., 2002). In the Salton Sea, only a minor loss of Se occurred trough volatilization despite a large surface area (954 km^2) (VillaRomero et al., 2013).

In this study, we performed a three years sampling survey to investigate the seasonal variation of total Se and Se species (non-volatile and volatile) concentrations in different alpine lakes of the western Pyrenees. To this end, water samples were collected in June/July 2017–2019 (late spring – early summer) and October 2017–2018 (early fall). Additionally, samples were also taken at different depths at four lakes in 2018 and at two lakes in 2019 to perform a closer study of Se biogeochemistry in more or less stratified water column. Our results are the first data on Se speciation at ultra-trace levels in remote mountain lakes.

2. Materials and Methods

2.1. Sampling lake waters and in-situ sample treatments

All the lakes considered in this study are located in an occidental transect of the Pyrenees. A total of 71 sub-surface water samples were collected in 20 lakes during June/July and October 2017–2019. The specific locations (Fig. Art.2.1) and sampling details are summarized in Table Art.2.1. In brief, five sampling campaigns were carried out in June/July 2017 (Replim I), October 2017 (Replim II), June 2018 (Replim III), October 2018 (Replim IV) and June 2019 (Replim V). Diurnal and depth profiles from lakes Gentau and Sabocos were sampled in Replim III, IV and V. Azules diurnal and depth profiles were sampled in Replim III and IV, while Arratille profiles were sampled only in Replim III. The diurnal cycle consisted in the sampling of sub-surface samples carried out every few hours from the dawn to the sunset to evaluate the effect of light in Se speciation. Depth profiles samples were collected at different depths of the water column to evaluate the Se speciation variation among the water column.

Lakes can be divided in three sectors according to their location: Cauterets, Panticosa, and Ossau/Ayous Valleys. The majority of the studied lakes are located over granitic (GR) rocks.

The study area lays on three different geological periods: Devonian, Permo-Triassic and Cretaceous (Gleizes et al., 1998; Zwart & De Sitter, 1979) which may impact Se bedrock concentration. The geological composition of the Pyrenees has been described in detail elsewhere (Van Lith, 1968). In brief, granite rocks originated during mountain formation in the pre-Devonian geological age are found ubiquitously. Devonian sedimentary rocks consisted in limestone, marble, shale and sandstone; Permo-Triassic bedrock contains sedimentary rocks in the form of conglomerates, sandstone and red and green shales; and, the most recent formations, Cretaceous sedimentary rocks consist of limestone, and sedimentary rocks like dolomites and quartz sand.

Table Art.2.1. Site location and prevailing bedrock for Pyrenean lakes studied. Devonian sedimentary (sed.) rocks include limestone, sandstone and shale. Permo-Triassic sedimentary rocks include conglomerate, sandstone, lutite, and andesite. Cretaceous sedimentary rocks are mainly composed by carbonate rocks.

Lake name	Lake code	Prevailing bedrock	Lat., Long. (degrees)	Altitude (m a.s.l.)	Max. depth (m)	Surf. area (Ha)	Catchment (Ha)
Cauterets							
Peyregnets de Cambalès	PEY	Granite	42.832, −0.238	2493	9	1.17	15.2
Grand Lac de Cambalès	CAM	Granite	42.830, −0.225	2344	15	3.46	179.7
Petite Opale	OPA	Devonian sed. rocks + Granite	42.828, −0.218	2290	6¤	0.64	129.3
Pourtet	POU	Granite	42.843, −0.203	2403	13	5.95	48.7
Nère	NER	Granite	42.835, −0.203	2304	12	2.91	94.8
Paradis†‡	PAR	Devonian sed. rocks + Granite	42.849, −0.160	1620	3	0.43	25.4
Badète	BAD	Devonian sed. rocks + Granite	42.794, −0.182	2341	7	6.97	79.9

Table Art.2.1. (Continued)

Lake name	Lake code	Prevailing bedrock	Lat., Long. (degrees)	Altitude (m a.s.l.)	Max. depth (m)	Surf. area (Ha)	Catchment (Ha)
Arratille	ARA	Devonian sed. rocks + Granite	42.801, −0.175	2256	12	5.87	296.4
Panticosa							
Bachimaña Bajo‡	BAC	Granite	42.781, −0.227	2178	13¤	3.08	1470.1
Baños de Panticosa	PAN	Granite	42.759, −0.237	1620	15	5.50	3229
Azul Superior	AZU	Devonian sed. rocks + Granite	42.790, −0.246	2420	8	3.89	151.4
Pecico	PEC	Devonian sed. rocks + Granite	42.799, −0.225	2460	9¤	0.91	167.5
Arnales	ARN	Granite	42.774, −0.244	2320	9	2.60	93.5
Ordicuso	ORD	Devonian sed. rocks + Granite	42.757, −0.248	2100	3	0.37	14.9
Coanga	COA	Granite	42.777, −0.220	2304	5	0.58	27.9

Table Art.2.1. (Continued)

Lake name	Lake code	Prevailing bedrock	Lat., Long. (degrees)	Altitude (m a.s.l.)	Max. depth (m)	Surf. area (Ha)	Catchment (Ha)
Xuans	XUA	Granite	42.777, −0.209	2600	15	2.97	41.3
Sabocos	SAB	Devonian + Cretaceous sed. rocks	42.693, −0.257	1900	25	9.56	231.7
Ayous							
Gentau	GEN	Permo-Triassic sed. rocks	42.848, −0.487	1942	20	8.62	186.2
Bersau‡	BER	Permo-Triassic sed. rocks	42.839, −0.495	2080	35	12.82	268.2
Roumassot‡	ROU	Permo-Triassic sed. rocks	42.848, −0.479	1843	16	5.15	61.4

†Peatland. ‡Samples collected from the shore. ˣCalculated (Duval et al., in prep.)

For Bachimaña reservoir, small or remote lakes where the access was difficult, samples were collected from the shore (Table Art.2.1) using nitrile gloves, water was carefully sampled below the surface to avoid contamination. For all other lakes, samples were collected on board an inflatable rubber boat and using a non-metallic and PTFE coated sampler (5 L Go-Flo; General Oceanic). The sampler was operated with gloves for subsurface waters and fixed on a Kevlar cable for samples collected at depth. One liter of sample was immediately transferred into two 500 mL Teflon bottle with a pre-cleaned silicone tubing, following a "Winkler-type" protocol as for dissolved oxygen sampling (avoiding bubbles and head-space), and stored in the dark as fresh as possible for its subsequent purge and trap of the gaseous species. Aliquots for bulk and dissolved total Se analysis (2 x 15 mL) were collected in polypropylene Falcon tubes and acidified with 150 µL (1% v/v) HNO_3 (69%, trace metal grade) for total Se analyses. For total dissolved Se (TDSe), samples were filtered (PVDF Sterivex filter units, 0.22µm, Millipore) prior to their acidification. In Replim I (June 2017) sampling, three replicates of each lake were collected at different points to study intra-lake variabilities without remarkable differences to highlight (RSD <12%) (Duval et al., in preparation).

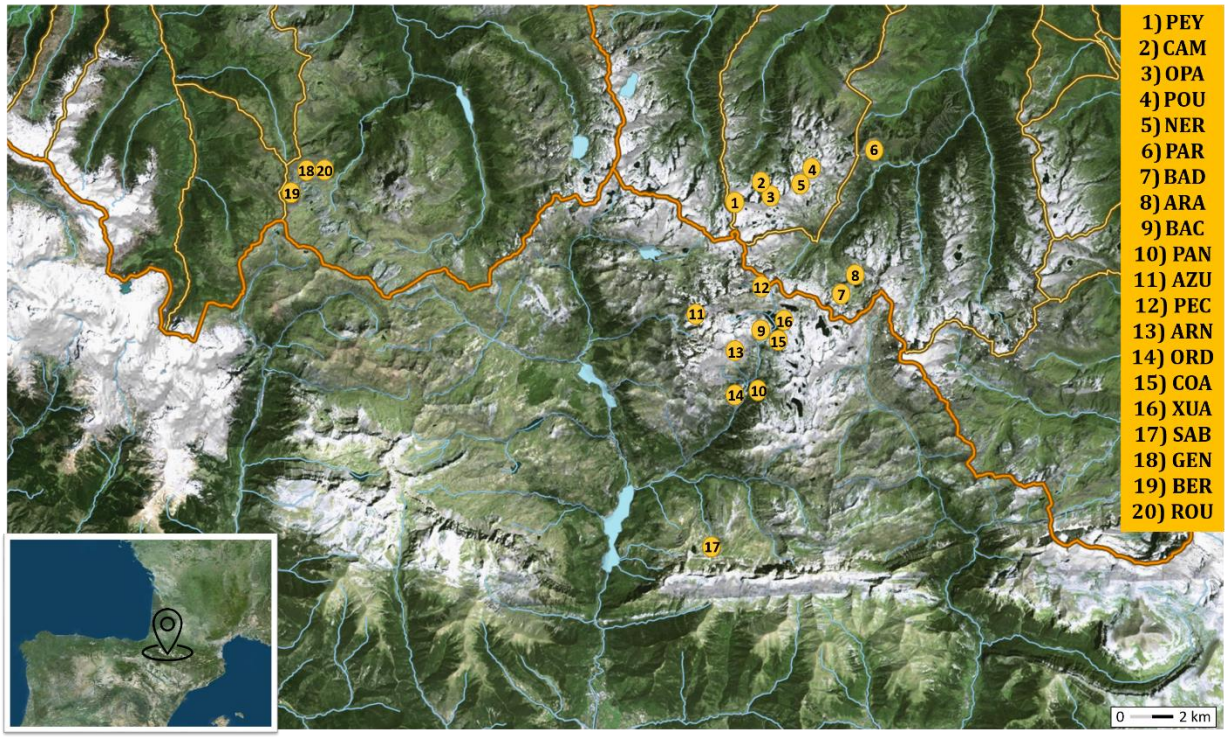

Figure Art.2.1. Geographical location of the investigated lakes. Base map obtained from Geoportail (https://www.geoportail.gouv.fr).

To study Se speciation, 50 mL water sample was filtered (PVDF Sterivex filter units, 0.22µm, Millipore) and stored without headspace in 50 mL Falcon tubes. Samples were stored as fresh as possible (4 – 10 ºC) in the field in the dark. Once in the lab all samples were stored at ca. 4 ºC in the dark until the analysis (less than two weeks). Additional samples were collected to analyze the main anions/cations, non-purgeable organic carbon (NPOC) and dissolved inorganic carbon (DIC) and were analyzed at the University of the Basque Country (Bilbao). Depth profiles ($3 \leq n \leq 6$) were treated following the same protocols detailed here and all procedures were conducted trying minimize exposition of samples to daylight. More information can be found elsewhere (Duval et al., 2020 and in preparation)

The physicochemical parameters in water lakes were measured simultaneously to the sampling using a multiparametric probe YSI EXO2 (temperature, conductivity, pH, redox potential, dissolved oxygen and chlorophyll).

2.2. Total Se analysis

Bulk total Se (TSe Bulk) was determined in unfiltered bulk samples (15 mL) after digestion with 300 µL HNO_3 (69%, tracepure grade) and 150 µL HCl (37%, tracepur grade) in sealed tubes and incubated for 3 h at 90 °C in a hot block (DIGIPREP, SCP Science). The dilution factor was corrected by weighting samples before and after the digestion.

Total Se concentrations were measured in bulk (TSe Bulk) and filtered (TDSe) samples with an Agilent 7900x Series inductively coupled plasma mass spectrometer (ICP-MS) system (Agilent Technologies, Tokyo, Japan) equipped with an octopole reaction cell, concentric nebulizer and a Scott double pass spray chamber cooled to 2 °C similar to the method used by Pokrovsky et al., (2018). Argon-based polyatomic interferences were reduced by using H_2 as cell gas at a flow rate of 5 mL min^{-1}. The parameters settings were as follow: Ar plasma gas flow, 15 $Lmin^{-1}$; Ar auxiliary gas flow, 0.86 L min^{-1}; Ar nebulizer gas flow, 1–1.1 L min^{-1}; radio frequency (RF) forward power, 1550W. Acquisition parameters consisted in 10 replicates with 50 sweeps/replicate and integration time of 2s per isotope; m/z monitored ratios were 77 and 78. External calibration was performed. Limits of quantification (based on ^{78}Se) were between 0.7 – 2.1 ng Se L^{-1}. Typical analytical precision was <12% in the range of dozen ng Se L^{-1} (relative standard deviation, 10 replicates).

2.3. Dissolved non-volatile Se speciation analysis

Chromatographic separation was carried out with an Agilent 1200 HPLC pump hyphenated to ICP-MS. Most samples were analyzed using a porous graphitic carbon stationary phase (Thermo Hypercarb column 10 cm × 4.6 mm i.d) with a formic acid mobile phase (240 mmol L^{-1}, 1% methanol and pH 2.4 adjusted with ammonia), delivered at 1 mL min^{-1} flow rate. Standard addition was used for quantification. Quantification limits (LoQ) were 3.6 and 2.2 ng Se L^{-1} for selenite and selenate respectively for 300 µl injected volumes. Exceptionally samples of October 2017 were analyzed using the mixed-mode column OmniPac PAX-500 (Thermo, 25 cm x 4 mm i.d.) with a 20 mmol L^{-1} ammonium nitrate mobile phase containing 2% methanol at pH 8.0 (adjusted with ammonia), delivered at 1 ml min^{-1} flow rate. In this case, LoQ was 21.1 and 22.3 ng Se L^{-1} for Se(IV) and Se(VI) respectively for 100 µl injected volumes. Duplicates of all samples were injected obtaining a relative standard deviation below 10%, except for some samples close to the LoQ for which rsd range was up to 15%. Chromatographic methods allowed the detection of selenite, selenate and selenomethionine. However, only selenate and eventually selenite were detected. The operationally defined, reduced Se fraction (Red.Se), was then calculated by subtraction of species concentrations from the total dissolved Se concentration. This fraction is used to estimate the contribution of Se(-II) and elemental Se species in water samples.

2.4. Dissolved gaseous Se speciation analysis

Dissolved gaseous Se species were purged and trapped within the day of sampling in the field lab set in a mountain hut. This allowed the pre-concentration of dissolved gaseous Se compounds and the preservation of their speciation as described by Lanceleur et al. (2019). Samples (2x500 mL) were purged with pure N_2 (500 mL min^{-1}) for 45 min. The resulting water vapor during the purge was removed from the gas stream in a moisture trap maintained at –20 °C. The gas stream was then carried through a volatile Se compounds trap (glass tube packed with Carbotrap sorbent). After the purge, the glass columns were tightly closed with Teflon lined plugs and stored in the dark at 4 °C in a sealed double PE bag until analysis. In the laboratory, samples were analyzed within a week after sampling using a cryogenic GC-ICP/MS set-up. Samples were thermo-desorbed from carbotraps at 250 ºC for 2 minutes under He flow (100 mL min^{-1}). Samples were flushed and trapped on the head of a Cryo GC column submerged in liquid N_2, prior to GC elution on Chromosorb SP2100 (Amouroux et al., 1998). Quantification was obtained by external calibration. The limits of quantification were between 1.3 – 3.8 pg Se L^{-1} for DMSe and DMSeS and between 1.3 – 5.4 pg Se L^{-1} for DMDSe.

Thermodesorption efficiency was controlled by carrying out two consecutive analyses of the same carbotrap column. TVSe content was determined as the sum of DMSe, DMSeS and DMDSe concentrations.

2.5. Data processing and statistics

For statistical treatment a value of one half the quantification limit was assigned to selenite and selenate concentrations in samples that did not contain quantifiable species level. Reduced Se concentration was estimated as the difference between TDSe and the species quantified:

$$[\text{Red.Se}] = [\text{TDSe}] - [\text{Se(IV)}] - [\text{Se(VI)}]$$

The limit of quantification of Red.Se was calculated as the square root of the sum of the squares of TDSe, Se(IV) and Se(VI) limits of quantification. Therefore the estimated LoQ of reduced Se fraction was 4.5 ng Se L^{-1}.

All sample sets were tested for normality using the Saphiro-Wilk test. Normally distributed samples were compared using parametric test such as 2-tail t-test. In the other cases, non-parametric Mann-Whitney test was carried out. When difference was statistically significant (2-tail test) samples were subsequently tested for the corresponding 1-tail test. These analyses were carried out using Origin 8 (Origin Lab Corporation).

3. Results

3.1. Biogeochemical characteristics of lake waters and relation to total Se concentrations

Lakes presented water temperature ranging from 2 to 19 ºC (Duval et al. 2020, in preparation) and subsurface samples were always oxygenated (>70% of oxygen saturation). Some of the parameters measured, such as fluoride (F^-), bromide (Br^-), nitrites (NO_2^-) or phosphates (PO_4^{3-}); were frequently below the LoQ (Table Art.2.SI 1). Because of this, conductivity ranged between 5 and 130 µS cm^{-1} which is indicative of waters with very low minerals and ionic content. Dissolved organic matter (0.6 to 4.6 mg L^{-1}) and nitrate (<0.065 to 1.16 mg L^{-1}) can be used as indicators of phytoplankton productivity (Camarero et al., 2009; Duval et al. 2020, in prep.). Sulphate (<0.21 mg L^{-1} and 7.56 mg L^{-1}) was the main anion found in waters and it was correlated to weathering and lixiviation processes (Duval et al. 2020, in prep.).

Nitrate and Sulphate: the nitrate median concentration of sub-surface samples (n=71) was 0.46 mg L^{-1}. Median value in June samples (0.56 mg L^{-1}) was almost the double than in October (0.29 mg L^{-1}). The highest nitrate values were found at Azul Superior (June 2019, 1.16 mg L^{-1}),

Badète (June 2018, 1.13 mg L^{-1}) and Bachimaña (June, 2019, 1.08 mg L^{-1}) (Table Art.2.SI 1). Sulphate median values (n=71) was 1.59 mg L^{-1}. Median value found in October (1.59 mg L^{-1}) was slightly higher than in June (1.36 mg L^{-1}). Since sulphate is related to weathering processes, probably the increase of concentration after summer is due to evaporation. The highest sulphate concentration was observed in Azul Superior with values of 7.56 mg L^{-1} (October 2017), 6.78 (October 2018) and 6.51 mg L^{-1} (June 2017) and Badète with a maximum of 5.4 mg L^{-1} in June 2018 (Table Art.2.SI 1). No appreciable global seasonal variations for nitrate (2-tail t-test, t=0.512, p=0.60) or sulphate (2-tail t-test, t=-0.891, p=0.38) was statistically found between June (n=44) and October (n=27). Depth profile data for nitrate and sulfate is presented in Table Art.2.SI 3.

Total Selenium: Total Se bulk concentrations were usually low and ranged from 12 ± 2 to 89 ± 9 ng Se L^{-1} while dissolved Se ranged between 7 ± 1 and 80 ± 9 ng Se L^{-1} (Table Art.2.SI 2). In general, for each of the lakes and all sampling dates taken together, no statistically significant difference was found between bulk and filtered Se concentrations. These results indicate that most of the Se in the lakes is in the dissolved or colloidal phase and not linked to particulate organic matter or other suspended mineral particles. The highest TDSe concentrations were found at Badète and Azul Superior, which are lakes presenting the highest sulphate concentration in this study. Total dissolved Se concentration ranges were similar to those reported in Siberian lakes and rivers (20–100 ng Se L^{-1}) (Pokrovsky et al., 2018) and Norwegian lakes (20–60 ng Se L^{-1}) (Økelsrud et al., 2016). Low concentrations, below 200 ng Se L^{-1}, are expected in remote unpolluted freshwater systems (Luoma & Rainbow, 2008).

The average dissolved Se concentration found was 20 ± 7 ng Se L^{-1} for lakes located at the granitic core (n=37), 52 ± 16 ng Se L^{-1} for Devonian core lakes (n=15), 12 ± 1 ng Se L^{-1} at lakes located over Permo-triasic bedrock (n=9) and 15 ± 2 ng Se L^{-1} for lake Sabocos (n=3) (Cretaceous prevailing bedrock). All sets of data proved a normal distribution using the Shapiro-Wilk test and were therefore tested using 1-tail t-test. The t-test (α=0.05) results showed that the average concentration of TSe Bulk and TDSe found in Devonian prevailing parent rock lakes was significantly higher than for other lakes (Table Art.2.SI 2). Our results do not showed any relationship between lake surface area and total Se concentration. In previous studies in thermokarst ponds, the same independency between total Se concentration and surface area was observed (Pokrovsky et al., 2018), which indicated that water residence time had no effect on Se biogeochemical cycle. In addition, TDSe did not

correlate with DOC, which means that Se is not incorporated or bound to organic matter, contrary to the observations at Siberian ponds (Pokrovsky et al., 2018).

During the period of study, no seasonal variations were found for TSe bulk nor for TDSe concentration at any group of lakes (Figure Art.2.2A). In both seasons, average concentrations of TSe Bulk and TDSe varied depending on rock composition, in the order Devonian>Granitic>Permo-Triassic>Cretaceous. In June, average TDSe values were 58 ± 19, 21 ± 8, 14 ± 3 and 12 ± 1 ng Se L^{-1}; in October TDSe averages were 44 ± 7, 20 ± 5, 15 (n=1) and 12 ± 1 ng Se L^{-1} for groups of lakes located over Devonian, Granitic, Permo-Triassic and Cretaceous rocks (Fig Art.2.2B).

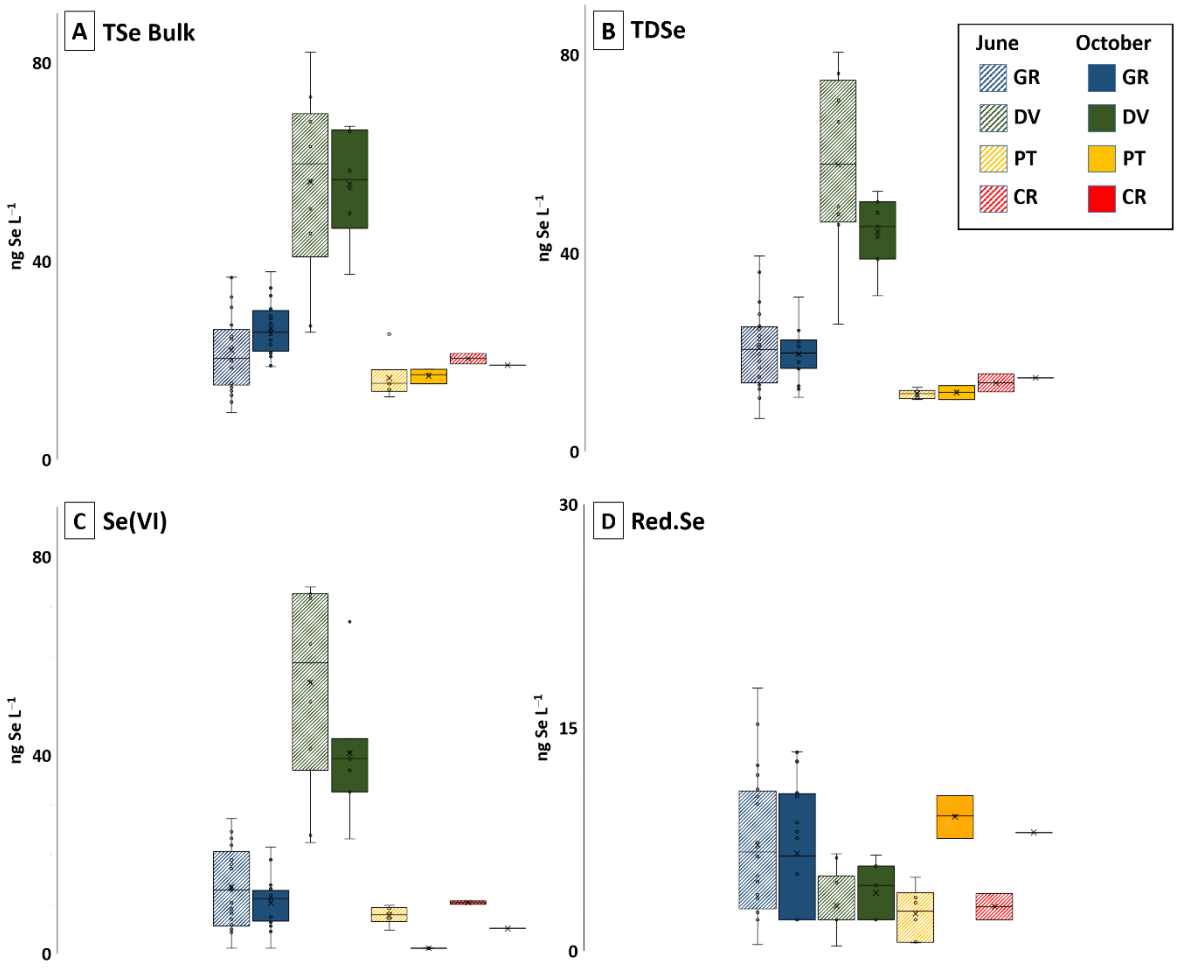

Figure Art.2.2. Seasonal variations between June (diagonal lines pattern) and October (single colour) in sub-surface water samples of A) Total Se bulk, B) Total dissolved Se, C) Se(VI) and D) Reduced Se fraction expressed in ng Se L^{-1}. Lakes are grouped by parent rock type: GR=Granite (blue), DV=Devonian (green), PT=Permo-Triassic (yellow) and CR=Cretaceous (red). Circles show the raw data, presented in Table Art.2.SI 2.

3.2. Selenium speciation in lake waters and study of seasonal variations

In terms of speciation, selenate was most often the only species detected which was in agreement with the measurement of redox potential and pH taken *in situ* (Table Art.2.SI 1, from Duval et al., in prep.). However, total dissolved Se was significantly greater than selenate concentration (1-tail t-test, n=71, t=1.987, $p<0.05$), which represented in average 63 ± 28 % of TDSe. This suggests that other species coexist at extremely low concentration. This may be the case of selenite, which was typically below the limit of quantification (2.2 – 22.3 ng Se L^{-1}); and reduced Se (LoQ = 4.5 ng Se L^{-1}). Pyrenean lakes are usually oligotrophic due to low salt and nutrient contents (Catalan et al., 2006). Therefore, the presence of organic selenide was not expected. Depending on physicochemical conditions of the waters, selenate could be potentially reduced to selenite and elemental Se(0). Considering the redox potential observed in lake waters, in the range between 36 to 271 mV and, pH in the range from 5.6 to 8.5, elemental Se should be thermodynamically stable in most lakes. An estimation of reduced Se fraction including Se(0) was done (Table Art.2.SI 2) and is presented in Figure Art2.2D. For Red.Se calculation, if selenite concentration was below the LoQ, it was set up as one-half of the quantification limit. The results indicate the presence of either selenite at concentration below the LoQ, Se(0) and/or Se(-II) in several lakes in both seasons. No statistical variation has been found among seasons for Red.Se estimated fraction, which is mainly due to the low concentration of this Se fraction.

For selenate, the results of statistical test concluded that only for permo-triassic core the seasonal variations are significant. The average values with the error expressed as the standard deviation of each lake group were for June: 13 ± 8 (n=26), 55 ± 20 (n=10), 8 ± 2 and 10 ± 0.5 ng Se L^{-1} for granitic, devonian, permo-triassic and cretaceous groups respectively. After summer, selenate values were slightly lower: 10 ± 5 (n=16), 40 ± 13 (n=7), <LoQ (n=3) and 5 (n=1) ng Se L^{-1} respectively, following the same trend as total dissolved Se. However, the difference was not enough to be considered statistically significant. Bibliographic data for Se speciation in lakes is scarce, especially in remote lakes. Existing publications in other environments report selenate concentrations in the range of 4 – 17 ng Se L^{-1} in Finish lakes (Wang et al., 1995; Wang et al., 1994). Despite the similarities in Se(VI) concentration values, in Finish lakes it represented between 6 to 12% of total Se, while most of Se present was linked to organic matter. However, those Finish lakes were impacted by selenium supplemented fertilization; meanwhile Pyrenean lakes receive very limited amounts of nutrients.

Total Volatile Se ranged from 2.6 ± 0.4 – 119 ± 18 pg Se L^{-1} with an exceptionally high value observed in September 2017 at Ordicuso (484 ± 72 pg Se L^{-1}) without remarkable intra-lake seasonal variations (Fig. Art.2.3A and Table Art.2.SI 2). The main species found in all lakes was DMSe, representing in average 67% of the TVSe detected. Previous studies in remote arctic thermokarst ponds reported DMSe as the only gaseous Se species detected (Lanceleur et al., 2019). The low concentrations of TDSe and sulfate seem to limit the production of dimethyldiselenide (DMDSe) or dimethyl selenyl sulfide (DMSeS) (Fig. Art.2.3) observed in other environments, such as minerotrophic peatlands or estuarine and marine systems (Amouroux & Donard, 1997; Tessier et al., 2002; Vriens et al., 2014).

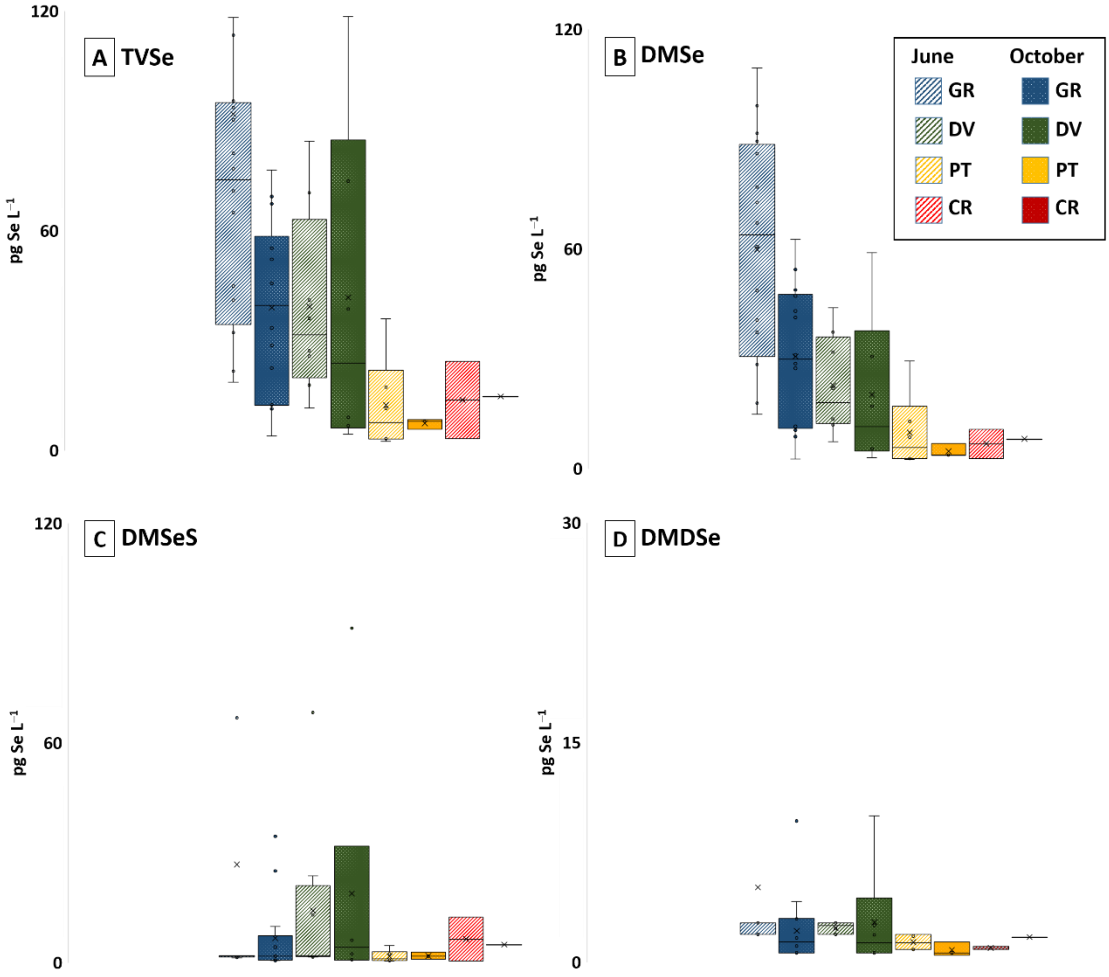

Figure Art.2.3. Seasonal variations between June (diagonal lines pattern) and October (dotted pattern) in sub-surface water samples of A) Total volatile Se, B) dimethylselenide (DMSe), C) dimethylselenide sulphide (DMSeS) and D) dimethyl diselenide expressed in pg Se L^{-1}. Lakes are grouped by parent rock type: GR=Granite (blue), DV=Devonian (green), PT=Permo-Triassic (yellow) and CR=Cretaceous (red). Full data is presented in Table Art.2.SI 2.

Total volatile Se concentration showed similar range values for granitic and devonian lakes, despite the differences in total Se levels. In June samples, just after the ice-cover melting, no accumulation was observed. The limited nutrient supplement and biological activity of Pyrenean lakes seems to be limiting total volatile Se production.

3.3. Dynamic of Se speciation in the water column and production of volatile Se compounds

During the samplings of 2018 and 2019, depth profiles were carried out in four lakes: Arratille (ARA) and Azules (AZU) (Devonian), Gentau (GEN) (Permo-Triassic) and Sabocos (SAB) (Cretaceous). Gentau and Sabocos are affected by stratification, showing complete seasonal oxygen depletion below 12m (GEN) and 15m (SAB) (Fig. Art.2.4 and Fig. Art.2.SI 1).

Gentau. In Gentau, the stratification is reflected by oxygen depletion that begins between 6 – 8 m. Temperature also drops after summer at the same depth. Nitrate showed higher concentration in June; after summer it was depleted except for small spot observed in the bottom and sulfate concentration was extremely low (<LoQ – 0.7 mg L^{-1}). Conductivity was higher at the bottom, showing an increase at the sediment-water interface in all seasons (Table Art.2.SI 3). Meanwhile, pH decreased in general with depth (Duval et al., 2020). Total dissolved Se concentration, in the range between 10 ± 1 – 23 ± 2 ng Se L^{-1}, was similar to total Se bulk (14 ± 1 – 24 ± 3 ng Se L^{-1}), indicating that most of the Se present in the water column is in the dissolved (or colloidal) phase.

Selenite concentration was in all cases below the LoQ (3.6 ng Se L^{-1}). In June, selenate concentration and proportion decreased both with depth, which indicates the presence of reduced Se species in the dissolved phase. The presence of Red. Se was substantiated (10 ± 3 – 13 ± 3 ng Se L^{-1}) in October 2018, because Se(VI) concentration was below the LoQ (2.2) in the whole water column. Total volatile Se concentration was higher (9 ± 1 – 96 ± 14 pg Se L^{-1}) in June 2018, while in the same period of 2019, concentration of volatile species was close or below the quantification limit. In June 2018, the main species detected in the photic zone was DMSe, with concentration ranging from 7 ± 1 to 19 ± 3 pg Se L^{-1}. However, at the sediment–water interface DMDSe was predominant showing a concentration of 73 ± 11 pg Se L^{-1}.

Sabocos. In Sabocos, thermo- and redox-clines exhibited a somehow less marked stratification of the water column. The temperature gradient was observed in both seasons; however, the water column was relatively oxygenated (>10%) except at the bottom where saturation was

below 2%, 5% and 7% for Replim III, IV and V respectively. Nitrate concentration ranged from 155 to 790 · µg L^{-1} and was higher in June. After summer, a nitrate depletion was observed in the photic zone that is coincident with an increase of the conductivity below 10 m depth and sulfate concentration oscillated between 2.3 – 3.3 mg L^{-1}. Total bulk and dissolved Se concentrations were similar, in the range between 12 ± 1 to 24 ± 2 ng Se L^{-1}. Selenite was below the LoQ in all samples, while selenate was found ubiquitously in the water column. The unique perturbation observed in the water column for Se(VI) was observed in October 2018. Despite an oxygen saturation above 70%, Se(VI) depletion was observed in the photic zone together with nitrate depletion. This is probably a direct evidence of selenate uptake by microorganisms as suggested elsewhere (Duan et al., 2010; Harrison et al., 1988). As observed in Gentau, the highest volatile Se species concentration (9 ± 1 – 80 ± 12 pg Se L^{-1}) was quantified in June of 2018 in Sabocos. The main species at the surface was DMSe, with a non-negligible presence of DMSeS. Close to the water–sediment interface, similar concentration of DMSe and DMDSe were found (34 – 36 pg Se L^{-1}).

Dissimilatory reduction of selenate occurs under suboxic or anoxic conditions producing insoluble elemental Se and/or reduced soluble selenides (Nancharaiah & Lens, 2015). Reducing conditions in bottom waters slows re-oxidation processes, and is the reason why selenate concentration decreased with depth. Luxem et al., (2017) experiments in marine algae indicated that soluble organic selenides would be transformed into degradation volatile Se products by either photodegradation or biomethylation. Our findings seem to indicate similar processes occurring in Gentau, Arratille and Sabocos even if volatile Se production is very limited. In the water column of such oligotrophic aquatic systems, volatile production seems to be favored under reducing conditions and most probably driven by bacterial processes. This production may occur most of the year at depth, but concentration levels of TVSe are probably enhanced in spring time after the ice coverage period preserving such compounds from volatilization and photodegradation. Meanwhile, in sub-surface waters, volatilization and/photodegradation seems to control TVSe amount.

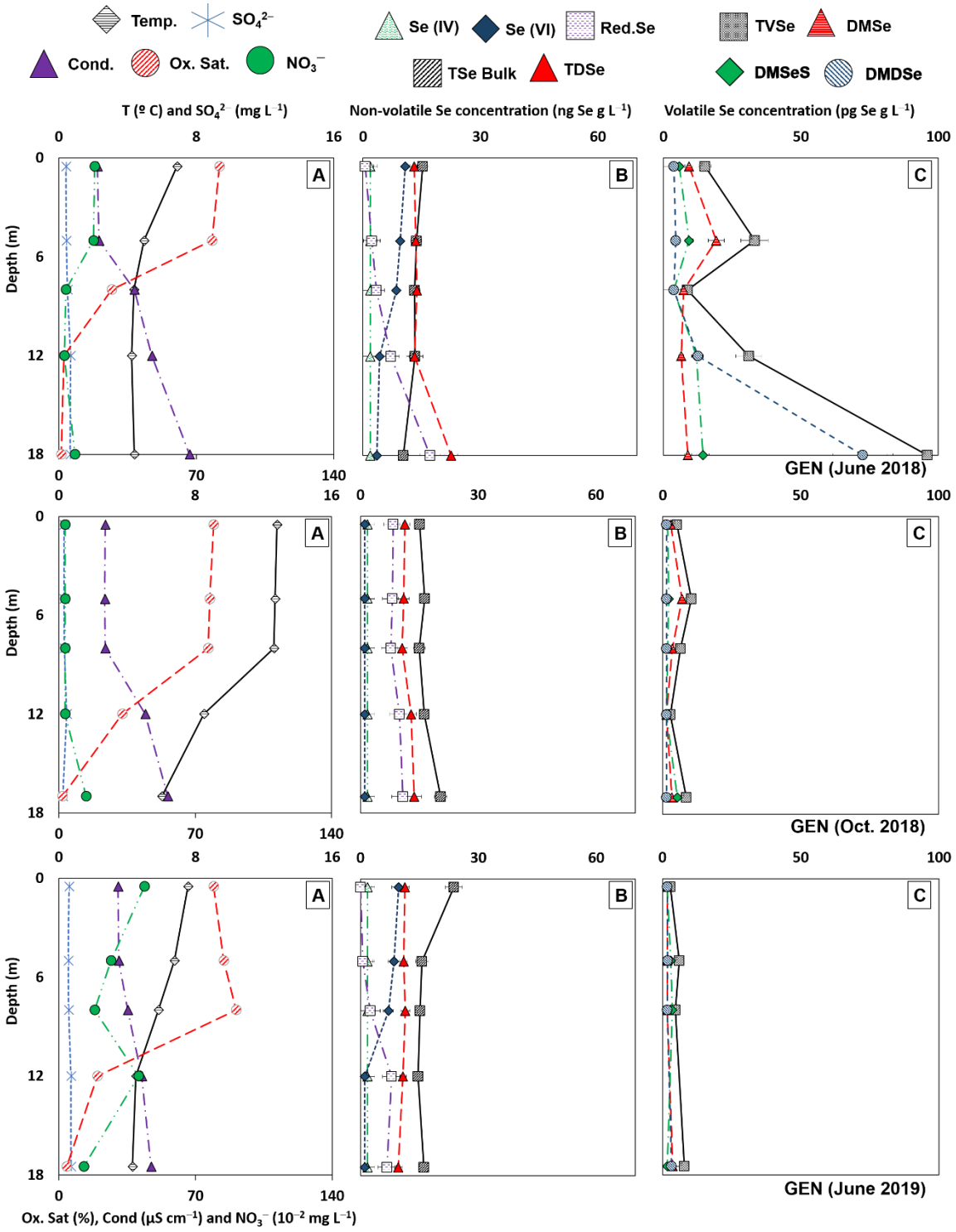
Temp.
SO_4^{2-}
Cond.
Ox. Sat.
NO_3^-
Se (IV)
Se (VI)
Red.Se
TSe Bulk
TDSe
TVSe
DMSe
DMSeS
DMDSe
T (º C) and SO_4^{2-} (mg L^{-1})
Non-volatile Se concentration (ng Se g L^{-1})
Volatile Se concentration (pg Se g L^{-1})
Depth (m)
A
B
C
GEN (June 2018)
GEN (Oct. 2018)
GEN (June 2019)
Ox. Sat (%), Cond (µS cm^{-1}) and NO_3^- (10^{-2} mg L^{-1})

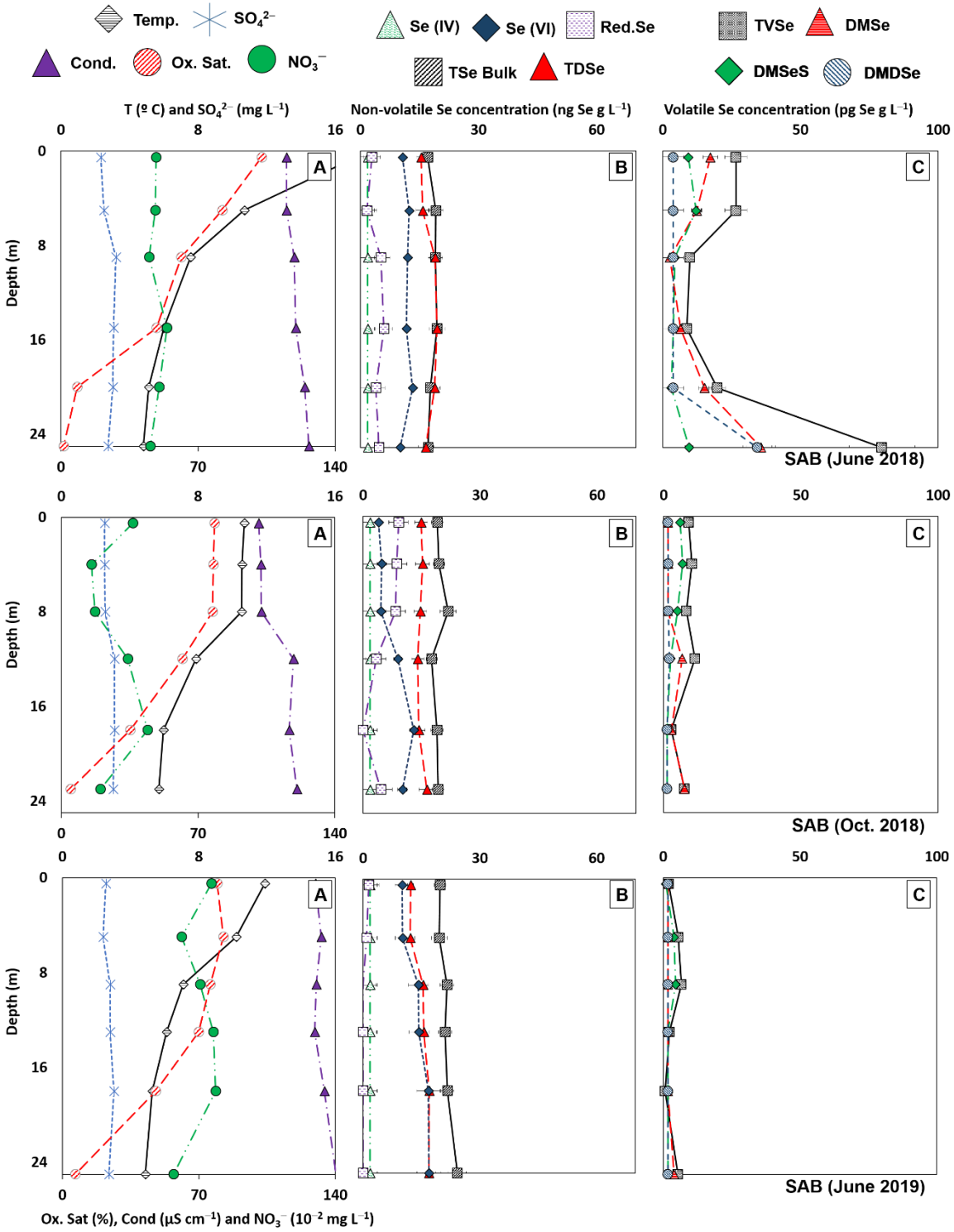

Figure Art.2.4. Depth profiles obtained from lakes Gentau (Permo-triassic bedrock) and Sabocos (Cretaceous bedrock). Figure A contains data about temperature (º C) and SO_4^{2-} (mg L^{-1}) (top axis); Conductivity (Cond.; µS cm^{-1}), oxygen saturation (Ox. Sat.) expressed in percentage and NO_3^- (10^{-2} mg L^{-1}) (bottom axis). Figure B contains the non-volatile Se speciation and total Se data including: TSe Bulk, Total dissolved Se (TDSe), selenite (Se (IV)), selenate (Se (VI)) and calculated reduced Se (Red.Se) expressed in ng Se L^{-1}. Figure C

represents dissolved volatile Se including: dimethylselenide (DMSe), dimethyl diselenide (DMDSe), dimethyl selenide sulphide (DMSeS) and total volatile Se (TVSe) in pg L^{-1}.

Additional lakes studied for Se compounds distribution with depth were Arratille (ARA) in June 2018 and Azules (AZU) in June and October 2018 (Fig. Art.2.SI 1). Oxygen and temperature depth profiles (Fig. Art.2.SI 1), demonstrate that Arratille exhibited an oxygen depletion only at the bottom water sample, while Azules, with a maximum depth of around 7 m, had a well-mixed water column. In both lakes, total Se concentration did not change along the water column and the main species was selenate. Selenite was below the LoQ, most probably due to low productivity and oxidizing conditions of the water column. In Arratille, the concentration of DMSe was higher under suboxic conditions. While in Azules, the peak of DMSe was spotted at 4 m and it was coincident with the maximum nitrate concentration. In Arratille and Azules, other volatile Se species were close or below the quantification limits.

Diurnal cycle measurements did not show significant variability along the day for total Se, nor for speciation (data not shown). The results indicated a low reactivity of the system for Se species, thus our measurements were quite representative of the season.

3.4. Sources of Selenium in alpine lake waters: bedrocks leaching/erosion versus wet depositions inputs

To understand the main geochemical factors affecting the distribution of Se in lakes a correlation matrix using the concentrations of TDSe, Se(VI) and TVSe against the main anions (NO_3^- and SO_4^{2-}), non-purgeable organic carbon (NPOC) and dissolved inorganic carbon (DIC) was made (Figure Art.2.5).

Among major anions and considering all lakes and sampling dates, Pearson's coefficient shows positive correlations between total dissolved Se and sulfate in both June (R^2=0.74, P<0.01) and October samples (R^2=0.77, P<0.01) (Fig. Art.2.5C). Sulfate's origin mainly depends on the geological substrate. In the western Pyrenees region, shales formed during the Devonian geological period is the main source of SO_4^{2-} (Van Lith, 1968). However, at low concentration atmospheric inputs become significant (Duval et al., in prep.). Among the other parameters, only nitrate was found to be partially correlated with TDSe in June (R^2=0.41, P<0.01). However, the nitrate concentration range was very small, so, the differences were minimal among seasons.

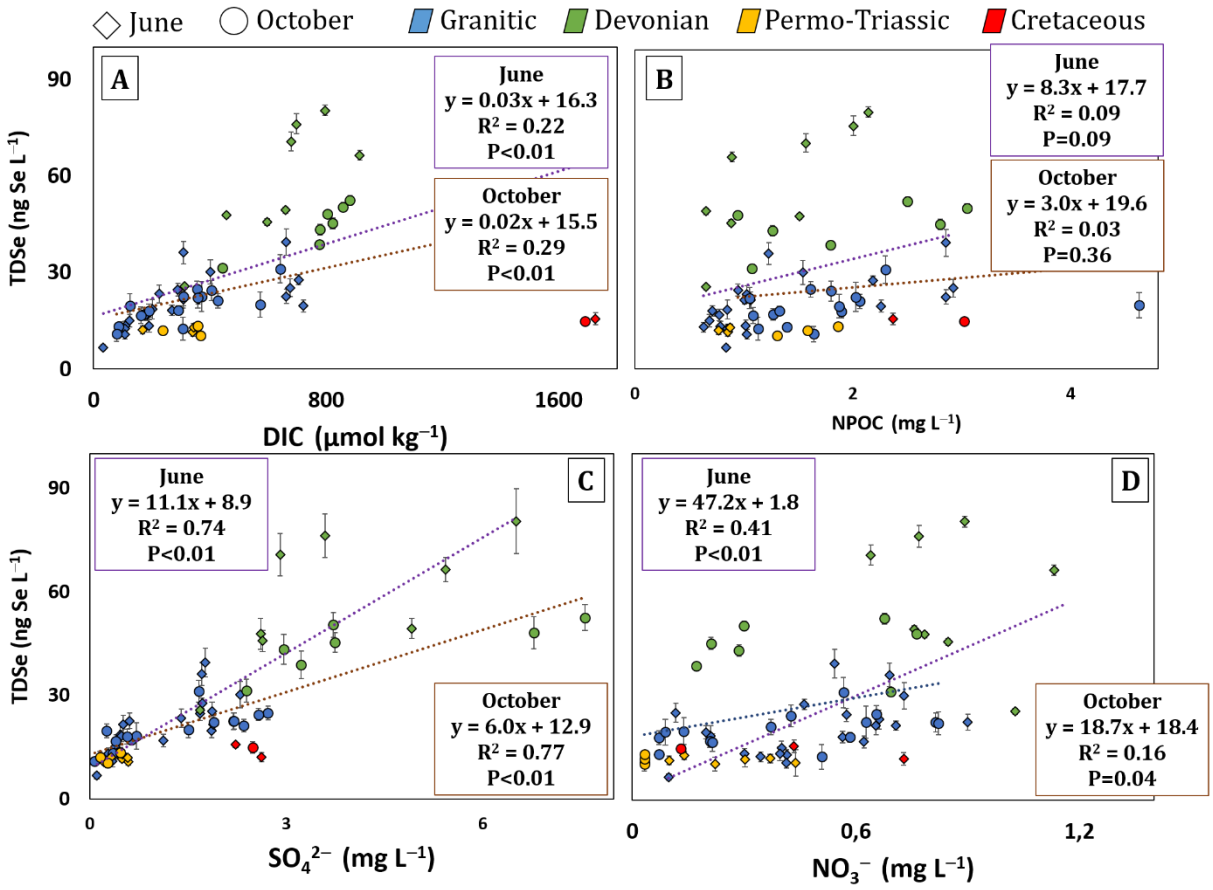

Figure Art.2.5. Correlation plots between TDSe and parameters measured: A) dissolved inorganic carbon (DIC), B) non-purgable organic carbon (NPOC), C) sulfate (SO_4^{2-}) and D) nitrate (NO_3^-). Data corresponds to June (diamond icons) and October (round icon). Samples are grouped by parent rock type: granitic (blue), devonian (green), permo-triassic (yellow) and cretaceous (red). Dotted lines represent the correlation for June (purple) and October (brown) samples.

For TVSe, any clear trend was observed, most probably because of the extremely low concentration of gaseous Se species in most lakes. In addition, the short life-time and rapid degradation of volatile Se compounds in the photic zone make difficult to establish correlation trends.

Because the investigated lakes have a limited watershed size, main Se inputs are suggested to be related to the geochemistry of the prevailing bedrocks through dissolution and erosion pathways; and direct atmospheric inputs. Wet atmospheric Se inputs at the Pic du Midi high altitude station, very close to our study sites (20 to 40 km), have been shown to be under the influence of prevailing marine air masses transported over the North Atlantic Ocean (Suess et

al., 2019). Thus, both rain and snow events and snowmelt in spring are potentially significant inputs of Se to these high altitude and remote lakes. To evaluate the contribution of geogenic versus atmospheric Se sources, the molar ratio of Se/S measured in lake waters in this study was compared with Se/S ratios calculated for different rock types using a standard database (no data available for local bedrocks) (Table Art.2.2) (Reimann & De Caritat, 1998). Molar Se/S ratios measured in lake waters were also compared with Se/S ratios in wet deposition at the Pic du Midi (calculated from Suess et al., 2019) and Adour Watershed (calculated from Roulier et al., 2020, submitted) (Table Art.2.5). The average molar ratio Se/S in Pyrenean lakes was in the range $(0.76 - 4.1) \cdot 10^{-5}$ (Table Art.2.2). Therefore, Se to S molar ratios do not allow to discriminate major sources for Se in those lakes. However, Se depletion observed in waters demonstrates that either sulfate are more efficiently solubilized from bedrocks than Se, or that Se is more efficiently lost from lakes waters than sulfate through either volatilization and/or precipitation/scavenging. Taking into account that the concentration of SO_4^{-2} in lakes is higher than concentrations found in rainwaters (Roulier et al., 2020, submitted), it could indicate because of their similarities that selenium originated also from bedrock erosion and dissolution processes, at least in lakes presenting the highest sulfate and selenate concentrations (*i.e.* lakes located over devonian sedimentary rocks containing shales).

An estimation of Se input from wet deposition was calculated using the average annual Se flux in Adour watershed (50 ± 20 µg Se m^{-2} yr^{-1}, Roulier et al., 2020, submitted). The estimation considered the surface area and volume of each lake to compare the input of Se from wet deposition with the stock of Se at each lake. The lake volume data was obtained from Duval et al., (2020) and the results are presented in Table Art.2.SI 4. We found that Se provided from wet deposition would account for 12 to 100% (median value of 40%) of Se lake stock. Thus wet depositions through rain or snow events and during snowmelt period is a non-negligible source of selenium in such alpine Pyrenean lakes, that can be counterbalanced by Se-enriched geological substrate.

The emission of volatile Se compounds could then contribute to lower the extent of Se in surface lake waters, mainly in the form of DMSe. Our measurements were used to estimate Se gaseous output from lake water to the atmosphere, but as they corresponded only to two months of the year the variability of TVSe concentrations was not well constrained. However, due to the low TVSe concentrations and low seasonal variability observed before and after summer, together with the low surface area of most lakes (Table Art.2.1) low volatilization fluxes are expected.

Table Art.2.2. Molar ratio of Selenium vs Sulfur concentrations in lake water compared to molar Se/S ratio in bedrock and in wet deposition. An average has been done classifying the lakes by bedrock type. The associated error correspond to the standard deviation between lakes (i.e. inter-lake variability).

Lake waters (by main bedrock type)	**Se/S molar ratio (x10^{-5})**	**Reference**
12 Lakes, Granitic bedrock (n=42)	3.4 ± 1.7	This study
4 Lakes, Devonian bedrock (n=17)	1.8 ± 0.5	
3 Lakes, Permo-triassic bedrock (n=9)	4.1 ± 1.9	
1 Lake, Cretaceous bedrock (n=3)	0.76	
Rock type	**Se/S molar ratio (x10^{-5})**	
Gabbro, basalt	5.41	(Reimann & De Caritat, 1998)
Gabbro, granodiorite	10.1	
Sandstone	2.03	
Shale, schist	11.1	
Limestone	2.03	
Bulk Deposition Adour watershed	**Se/S molar ratio (x10^{-5})**	
Gamarde forest (Landes)	5.1 ± 0.5	(Roulier et al., 2020, submitted)
Ance forest (Pyrénées Atlantiques)	7.3 ± 0.7	
Losse forest (Landes)	5.5 ± 0.5	
Wet deposition Pic du Midi, Pyrenees	**Se/S molar ratio (x10^{-5})**	
Bulk	6.8 ± 4.0	(Suess et al, 2019)
Wet-only	7.3 ± 9.9	

A rough estimation of Se emission was carried out similarly to (Lanceleur et al., 2019) using the model of Cole & Caraco (1998) and considering that atmospheric exchange occurs during 6 months, while during winter ice covering prevents volatilization. Results are presented in Table Art.2.SI 4. The annual Se emission of Se was compared with the estimated total Se stock in the corresponding lake. Selenium emission was calculated considering windspeeds of 3 and 10 m s $^{-1}$. The results indicated that annual Se emission from lakes to the atmosphere may represent between 0.7 and 27% of Se stock, with median values of 3% (wind: 3 m s^{-1}) and 10% (wind: 10 m s^{-1}).

Considering the data from Roulier et al., (2020, submitted), the daily Se input from wet deposition was calculated to be around 137 ng Se day^{-1} m^{-2}. This value is similar to the daily emission reported at thermokarst ponds (1–97 ng Se day^{-1} m^{-2}) (Lanceleur et al., 2019). Taking these results, wet deposition is an important source of Se to Pyrenees lakes, while volatilization seems a very limited removal pathway in small and oligotrophic Pyrenean lakes.

4. Conclusions

In general, Pyrenean lakes showed similar total Se bulk and dissolved concentration, in the low range of the ng Se L^{-1} in most lakes. Total dissolved Se was in the range between 7 – 80 ng Se L^{-1} and, on average, 63% was in the form of selenate in subsurface samples. The extremely low Se concentration in alpine lakes limited the detection of other Se species. Selenite, which was generally close or below the limit of quantification, could represent between 3 and 84% of total dissolved Se. Meanwhile, volatile Se speciation was limited to the production of DMSe and annual Se emission was estimated to be between 3 and 10% of Se stock, thus volalization did not appear to represent an important removal pathway for Se in Pyrenees lakes.

We did not find significant seasonal variations neither for total Se concentrations nor its species for surface waters. We also observed steady TDSe concentration in the water column, while reduced Se proportion increased with depth together with oxygen depletion as a result of microbial reduction that may promote Se scavenging, precipitation and further sedimentation.

Our estimations indicates that the 60% of total Se in western Pyrenean lakes originates from geogenic sources, while a 40% is derived from wet deposition. Therefore, the atmospheric input is an important source of Se to remote Pyrenean lakes. This work proved a first assessment of Se speciation in Alpine lakes and better constrained Se geochemical background in natural waters from a temperate watershed (Adour River).

Acknowledgements

This work is a contribution to the REPLIM-OPCC project and has been partially supported (65%) by the FEDER funds through the INTERREG V-A Spain-France-Andorra (POCTEFA 2014-2020) (REPLIM project, ref. EFA056/15). A. Romero–Rama thanks the UPPA and IPREM for her PhD grant (Sciences Doctoral School, UPPA). The contributions of the Aquitaine Region

(AQUITRACES project n° 20131206001-13010973) and ANR IA RSNR (AMORAD project n°ANR-11-RSNR-0002) for equipment funding are also acknowledged.

Supporting information

Title: Selenium speciation in waters of remote and pristine high altitude lakes from the Pyrenees (France-Spain)

Authors: Andrea Romero-Rama, Bastien Duval, Emmanuel Tessier, Maïté Bueno, Luís Ángel Fernández, Alberto de Diego, David Amouroux

Manuscript:

Number of Figures: 5

Number of Tables: 2

Supporting information:

Number of Figures SI: 1

Number of Tables SI: 4

Supplementary information Figure SI 1

Figure Art.2.SI 1. Depth profiles obtained from lakes Gentau (Permo-Triassic bedrock), Sabocos (Cretaceous bedrock), Arratille and Azules (Devonian core). Figure Art2.SI 1A contains data about temperature (º C) and SO_4^{2-} (mg L^{-1}) (top axis); Conductivity (Cond.; µS cm^{-1}), oxygen saturation (Ox. Sat.) expressed in percentage and NO_3^- (10^{-2} mg L^{-1}) (bottom axis). Figure Art2.SI 1B contains the non-volatile Se speciation and total Se data including: TSe Bulk, Total dissolved Se (TDSe), selenite (Se (IV)), selenate (Se (VI)) and reduced Se (Red.Se) expressed in ng Se L^{-1}. Figure Art2.SI 1C represents the dissolved volatile Se including: dimethylselenide (DMSe), dimethyl diselenide (DMDSe), dimethyl selenide sulphide (DMSeS) and total volatile Se (TVSe) in pg L^{-1}.

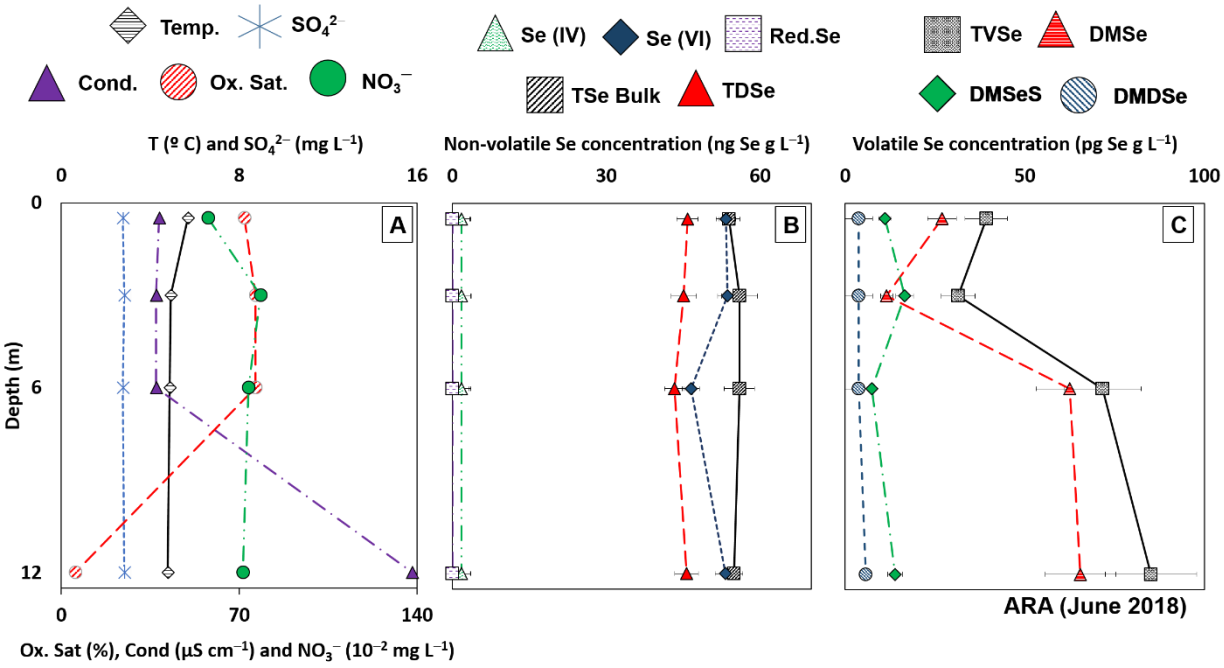

Figure Art.2.SI 1. (Continued)

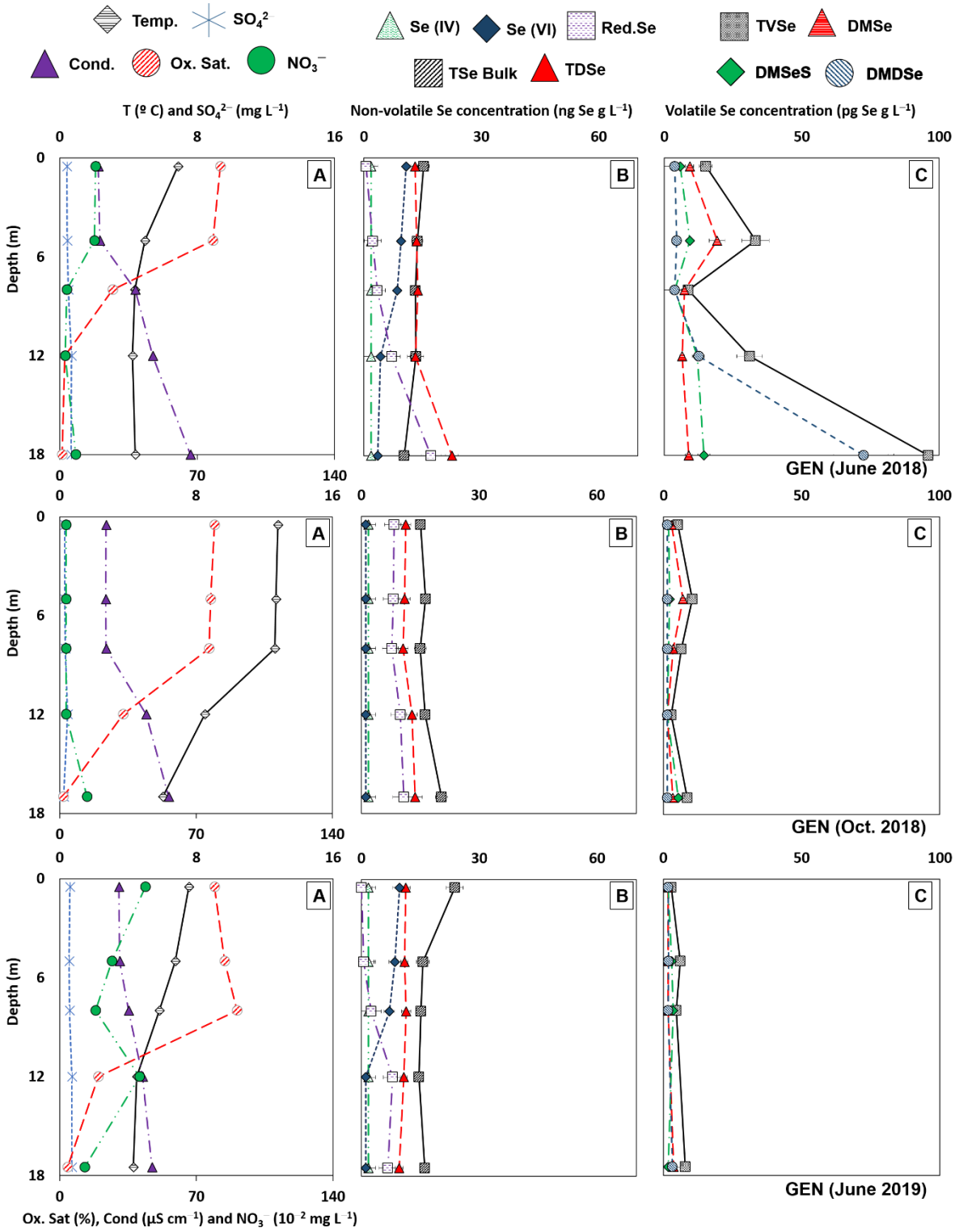

Figure Art2.SI 1. (Continued)

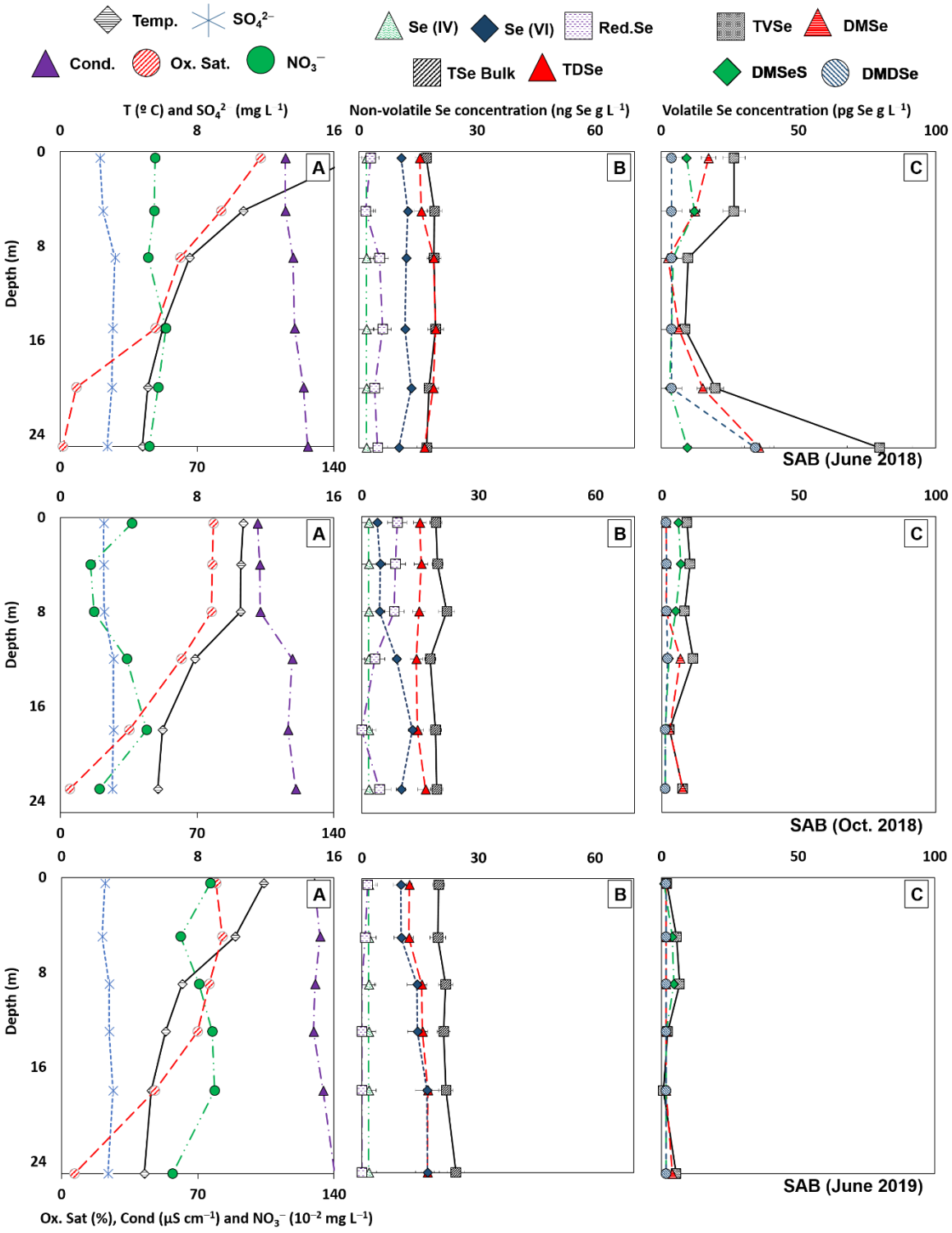

Figure Art2.SI 1. (Continued)

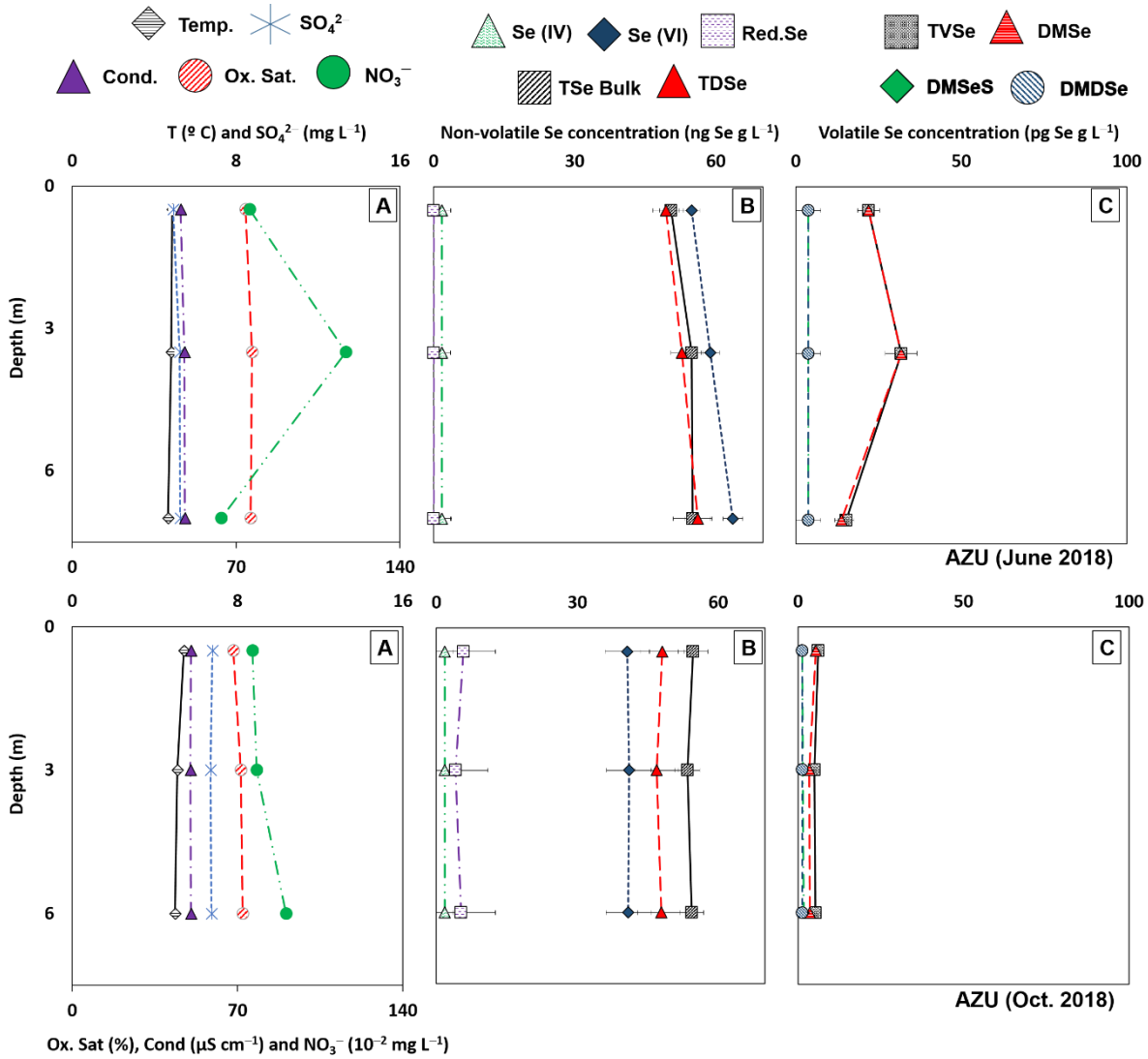

Supplementary information Table Art.2.SI 1

Table Art2.SI 1. Raw data for sub-surface samples of main anions (Cl^-, NO_3^-, SO_4^{2-}), main physicochemical parameters (conductivity (Cond.), redox potential (pE), oxygen saturation (Ox. Sat.), dissolved oxygen (DO), chlorophyll† (Chl), non-purgable organic carbon (NPOC) and dissolved inorganic carbon (DIC). LoQ for measured anions was in the range: $(3–15)\cdot10^{-2}$ mg L^{-1} for Cl^-, $(4–47)\cdot10^{-2}$ mg L^{-1} for NO^{3-} and $(12–99)\cdot10^{-2}$ mg L^{-1} SO_4^{2-}.

Lake	Cl^-	NO_3^-	SO_4^{2-}	T	Cond.	pH	pE	Ox. Sat.	DO	Chl	NPOC	DIC
	10^{-2} mg L^{-1}			(º C)	(µS cm^{-1})		(mV)	(%)	(mg L^{-1})	(µg L^{-1})	(mg C L^{-1})	(µmol kg^{-1})
Granite core												
June 2017												
Pey	15.6	41.4	28.3	5.5	17.2	6.7	208	77.2	9.7	-7.4	0.6	92
Cam	17.1	40.1	38.8	8.7	8.0	6.4	160	79.7	9.3	-7.7	0.7	124
Opa	15.6	65.4	51.2	-	-	-	-	-	-	-	1.1	308
Pou	22.8	39.7	42.6	9.5	11.9	6.9	202	78.1	8.9	-6.0	1.0	190
Ner	15.8	30.1	37.6	11.1	7.3	6.6	119	77.7	8.5	-6.7	0.8	109
Arn	16.9	66.2	139.6	8.4	17.8	7.1	122	79.5	9.3	-6.2	1.0	225
Coa	14.7	21.0	46.9	7.1	23.3	7.5	97	78.9	9.5	-6.9	0.9	202
Xua	19.7	90.0	60.7	4.6	12.5	6.3	110	71.2	9.2	-7.1	2.9	663
Par	48.9	54.3	176.4	10.6	40.8	6.8	118	88.2	9.8	-3.2	2.9	663
Ord	18.0	11.7	186.5	18.3	61.4	8.2	157	98.5	9.3	-4.6	2.9	676
Pan	33.3	73.0	229.5	10.3	27.4	7.5	195	73.4	8.2	-6.0	1.5	402
Bac	23.3	69.0	171.2	-	-	-	-	-	-	-	1.2	310

Table Art.2.SI 1 (Continued)

Lake	Cl^-	NO_3^-	SO_4^{2-}	T	Cond.	pH	pE	Ox. Sat.	DO	Chl	NPOC	DIC
	10^{-2} mg L^{-1}			(º C)	(µS cm^{-1})		(mV)	(%)	(mg L^{-1})	(µg L^{-1})	(mg C L^{-1})	(µmol kg^{-1})
June 2018												
Pey	6.9	9.8	<LoQ	6.4	15.8	6.9	36	83.5	10.3	0.0	0.8	33
Cam	12.7	34.5	34.5	2.4	5.4	6.0	172	70.8	9.7	-0.1	0.9	108
Opa	16.6	56.5	48.6	3.3	14.9	6.8	91	73.5	9.8	-0.1	0.7	267
Arn	18.9	62.2	112.6	7.5	13.1	6.6	200	76.7	9.2	0.0	0.8	184
Coa	24.4	41.4	34.5	10.1	6.9	6.4	169	76.2	8.6	-0.1	1.0	108
Par	49.8	46.2	171.4	-	-	-	-	-	-	-	2.2	705
Ord	20.2	19.8	186.2	17.5	57.0	7.4	97	75.5	7.2	0.1	2.3	722
Pan	27.4	70.8	188.3	11.2	27.7	6.5	176	80.4	8.8	0.0	1.0	359
Bac	16.1	57.4	168.3	12.45	25.2	7.2	129	81.4	8.7	0.0	0.9	290
June 2019												
Arn	10.4	78.7	127.2	-	-	-	-	-	-	-	-	-
Coa	11.8	56.4	38.9	-	-	-	-	-	-	-	-	-
Ord	18.7	38.0	159.4	-	-	-	-	-	-	-	-	-
Pan	36.0	54.7	270.2	-	-	-	-	-	-	-	-	-
Bac	13.3	108.1	132.5	-	-	-	-	-	-	-	-	-

Table Art.2.SI 1 (Continued)

Lake	Cl^-	NO_3^-	SO_4^{2-}	T	Cond.	pH	pE	Ox. Sat.	DO	Chl	NPOC	DIC
	10^{-2} mg L^{-1}			(º C)	(µS cm^{-1})		(mV)	(%)	(mg L^{-1})	(µg L^{-1})	(mg C L^{-1})	(µmol kg^{-1})
October 2017												
Pey	16.9	7.1	34.8	9.57	7.0	7.1	108	74.7	8.5	-5.3	1.4	87
Cam	19.4	20.9	63.2	9.71	13.5	7.2	121	76.6	8.7	-6.5	1.3	172
Opa	15.9	58.4	71.3	9.89	24.6	7.5	141	80.9	9.2	-7.0	1.3	291
Arn	18.8	65.5	271.8	10.19	31.0	7.3	117	76.0	8.5	-6.0	1.6	356
Coa	19.7	7.1	57.1	11.08	14.6	7.3	81	81.1	9.0	-6.8	1.9	190
Bac	33.3	42.6	257.2	10.71	51.4	7.3	114	62.3	6.9	-6.8	1.8	406
Pan	17.8	37.2	235.0	11.12	36.2	6.7	146	80.2	8.9	-6.1	2.1	427
October 2018												
Pey	14.5	<LoQ	<LoQ	6.81	4.5	6.4	151	69.4	8.5	4.4	1.6	79
Cam	18.1	<LoQ	<LoQ	8.47	10.2	6.1	222	73.2	8.6	6.4	1.1	162
Opa	17.5	50.8	47.9	5.9	17.1	6.8	127	74.2	9.3	6.7	1.1	307
Arn	20.6	81.4	219.3	7.41	19.7	5.6	221	74.2	8.9	1.1	-	309
Coa	25.1	<LoQ	<LoQ	6.18	7.2	5.6	163	73.7	9.1	2.9	1.9	125
Par	68.4	56.7	166.3	9.53	34.4	7.2	240	83.9	9.6	1.7	2.3	642
Ord	39.3	<LoQ	150.4	9.32	47.9	7.3	225	75.0	8.6	3.7	4.6	573
Pan	67.5	62.7	220.3	9.87	24.9	5.8	193	75.9	8.6	1.8	2.0	372
Bac	22.3	82.2	189.4	8.97	32.1	7.1	207	74.3	8.6	5.9	1.1	358

Table Art.2.SI 1 (Continued)

Lake	Cl^-	NO_3^-	SO_4^{2-}	T	Cond.	pH	pE	Ox. Sat.	DO	Chl	NPOC	DIC
	10^{-2} mg L^{-1}			(º C)	(µS cm^{-1})		(mV)	(%)	(mg L^{-1})	(µg L^{-1})	(mg C L^{-1})	(µmol kg^{-1})
Devonian core												
June 2017												
Bad	20.4	76.9	358.8	-	-	-	-	-	-	-	2.0	697
Ara	19.7	64.1	290.4	9.53	46.1	7.6	271	81.5	9.3	-6.0	1.6	680
Azu	20.0	89.2	651.1	8.22	58.1	7.0	131	82.2	9.6	-6.3	2.1	797
Pec	17.8	78.5	260.8	8.84	35.6	7.8	198	81.6	9.5	-8.0	1.5	457
June 2018												
Bad	18.5	113.2	543.4	5.89	33.8	6.4	207	79.4	9.9	0.1	0.9	915
Ara	26.5	84.7	263.7	5.86	37.8	6.7	176	78.1	9.8	-0.1	0.9	597
Azu	18.3	75.7	491.3	4.87	46.3	7.0	149	73.9	9.5	-0.1	0.7	661
Pec	16.8	102.8	168.0	4.33	21.0	7.0	149	76.6	10.0	-0.1	0.7	314
June 2019												
Azu	11.2	116.5	501.8	-	-	-	-	-	-	-	-	-
Pec	9.7	69.3	77.4	-	-	-	-	-	-	-	-	-
October 2017												
Bad	20.4	30.0	371.7	9.72	66.9	8.4	46	79.2	9.1	-8.1	3.1	858
Ara	14.9	21.1	374.5	9.85	65.1	8.5	80	84.4	9.6	-7.1	2.8	822
Azu	16.5	67.7	755.8	8.77	72.5	8.1	102	80.3	9.3	-7.3	2.5	882

Table Art.2.SI 1 (Continued)

Lake	Cl^-	NO_3^-	SO_4^{2-}	T	Cond.	pH	pE	Ox. Sat.	DO	Chl	NPOC	DIC
	10^{-2} mg L^{-1}			(º C)	(µS cm^{-1})		(mV)	(%)	(mg L^{-1})	(µg L^{-1})	(mg C L^{-1})	(µmol kg^{-1})
October 2018												
Bad	14.9	28.6	296.0	5.33	45.0	7.7	136	72.0	9.1	7.5	1.3	779
Ara	15.3	<LoQ	322.5	8.32	49.9	7.4	170	75.7	8.9	1.2	1.8	777
Azu	16.0	76.3	677.6	5.39	50.2	7.6	110	68.2	8.6	0.1	0.9	803
Pec	18.5	69.3	238.8	8.13	35.0	7.2	216	75.2	8.9	0.6	1.1	444
Permo-Triassic core												
June 2018												
Gen	24.5	9.9	48.9	6.89	20.3	6.7	269	82.0	10.0	0.2	0.9	341
Ber	23.2	37.0	32.1	-	-	-	-	-	-	-	0.8	168
Rou	29.5	13.9	50.4	-	-	-	-	-	-	-	0.9	345
June 2019												
Gen	32.2	43.9	58.8	7.17	30.0	7.5	234	85.3	10.3	-0.1	-	-
Ber	23.5	22.2	21.6	2.14	9.2	7.1	206	76.5	10.5	-0.6	-	-
Rou	26.4	30.3	57.6	12.69	34.0	8.2	234	89.9	9.5	-0.4	-	-
October 2018												
Gen	29.9	<LoQ	27.0	12.63	23.8	-	166	79.8	8.5	6.8	1.3	368
Ber	30.7	<LoQ	15.7	12.09	15.0	7.3	38	80.5	8.7	0.6	1.6	237
Rou	28.7	<LoQ	46.6	13.38	25.3	7.6	36	83.1	8.7	4.3	1.9	359

Table Art.2.SI 1 (Continued)

Lake	Cl^-	NO_3^-	SO_4^{2-}	T	Cond.	pH	pE	Ox. Sat.	DO	Chl	NPOC	DIC
	10^{-2} mg L^{-1}			(º C)	(µS cm^{-1})		(mV)	(%)	(mg L^{-1})	(µg L^{-1})	(mg C L^{-1})	(µmol kg^{-1})
Cretaceous core												
June 2018												
Sab	20.2	43.4	222.7	16.65	130.2	8.0	37	86.8	8.5	0.3	2.4	1727
June 2019												
Sab	14.7	72.9	-	12.47	141.1	7.5	212	80.0	8.5	-0.4	-	-
October 2018												
Sab	22.5	<LoQ	248.4	10.42	99.8	8.5	188	79.4	8.9	5.1	3.0	1691

†The apparatus was not calibrated to measure chlorophyll at Pyrenean lake conditions, a random unit was obtained.

Supplementary information Table SI 2

Table Art.2.SI 2. Sub-surface concentrations of total bulk (TSe Bulk), filtered (TDSe) and volatile (TVSe) selenium, and of its species: selenite (Se(IV)), selenate (Se(VI)), and calculated Red.Se (TDSe − Se(IV) − Se(VI)); dimethylselenide (DMSe), dimethyl selenide sulphide (DMSeS) and dimethyl diselenide (DMDSe). Values are grouped by lake (italic) and prevailing bedrock is indicated in parenthesis. Average value for each lake is indicated in bold. n.s. means no sample and values under the limit of quantification are indicated as <LoQ. Values are presented either in ng Se L^{-1} (for non-volatile Se species) or pg Se L^{-1} (for volatile Se data) ± the associated error. The associated error correspond to the confidence interval except for June 2017 where the error has been calculated to cumulate the three replicated (n=3) points sampled.

Year	Month	TSe Bulk	TDSe	Se(IV)	Se(VI)	Red.Se	TVSe	DMSe	DMSeS	DMDSe
		ng Se L^{-1}					pg Se L^{-1}			
Peyregnets de Cambalès (Granite)										
2017	June	12 ± 2	13 ± 2	<LoQ	7.5 ± 0.7	<LoQ	81 ± 12	77 ± 12	<LoQ	<LoQ
2017	October	21 ± 3	13 ± 1	<LoQ	<LoQ	<LoQ	34 ± 5	31 ± 5	<LoQ	<LoQ
2018	June	9.5 ± 0.9	6.7 ± 0.8	<LoQ	<LoQ	<LoQ	19 ± 3	15 ± 2	<LoQ	<LoQ
2018	October	19 ± 1	11 ± 1	<LoQ	<LoQ	8 ± 2	12 ± 2	11 ± 2	<LoQ	<LoQ
Average		**15 ± 5**	**11 ± 3**	**<LoQ**	**<LoQ**	**<LoQ**	**36 ± 31**	**34 ± 30**	**<LoQ**	**<LoQ**

Table Art.2.SI 2. (Continued)

Year	Month	TSe Bulk	TDSe	Se(IV)	Se(VI)	Red.Se	TVSe	DMSe	DMSeS	DMDSe
		ng Se L^{-1}					pg Se L^{-1}			
Grand Lac de Cambalès (Granite)										
2017	June	15 ± 3	15 ± 2	<LoQ	8 ± 2	5 ± 4	45 ± 7	41 ± 6	<LoQ	<LoQ
2017	October	23 ± 2	17 ± 1	<LoQ	<LoQ	<LoQ	52 ± 8	49 ± 7	<LoQ	<LoQ
2018	June	15 ± 1	13 ± 1	<LoQ	10 ± 0.6	<LoQ	41 ± 6	37 ± 6	<LoQ	<LoQ
2018	October	19 ± 1	17 ±2	<LoQ	6.3 ± 0.7	9 ± 3	4.0 ± 0.6	2.6 ± 0.4	<LoQ	<LoQ
Average		**18 ± 4**	**15 ± 2**	**<LoQ**	**9 ± 2**	**<LoQ**	**36 ± 22**	**32 ± 20**	**<LoQ**	**<LoQ**
Petite Opale (Devonian sedimentary rocks + granite)										
2017	June	19 ± 3	22 ± 3	<LoQ	13 ± 1	7 ± 4	90 ± 14	86 ± 13	<LoQ	<LoQ
2017	October	25 ± 3	18 ± 4	<LoQ	<LoQ	<LoQ	77 ± 12	63 ± 10	4.3 ± 0.6	10 ± 1
2018	June	20 ± 1	18 ± 2	<LoQ	17 ± 1	<LoQ	22 ± 3	18 ± 3	<LoQ	<LoQ
2018	October	21 ± 2	13 ± 1	<LoQ	5.6 ± 0.7	5 ± 2	12 ± 2	11 ± 2	1.3 ± 0.2	<LoQ
Average		**22 ± 3**	**18 ± 4**	**<LoQ**	**12 ± 5**	**<LoQ**	**50 ± 39**	**44 ± 36**	**<LoQ**	**<LoQ**
Pourtet (Granite)										
2017	June	14 ± 2	13 ± 2	<LoQ	4.3 ± 0.6	7 ± 3	22 ± 3	18 ± 3	<LoQ	<LoQ
Nère (Granite)										
2017	June	13 ± 1	13 ± 2	<LoQ	4.3 ± 0.8	7 ± 3	65 ± 10	61 ± 9	<LoQ	<LoQ

Table Art.2.SI 2. (Continued)

Year	Month	TSe Bulk	TDSe	Se(IV)	Se(VI)	Red.Se	TVSe	DMSe	DMSeS	DMDSe
		ng Se L^{-1}					pg Se L^{-1}			
Arnales (Granite)										
2017	June	25 ± 2	23 ± 3	<LoQ	19 ± 3	<LoQ	77 ± 12	73 ± 11	<LoQ	<LoQ
2017	October	38 ± 5	25 ± 2	<LoQ	<LoQ	<LoQ	46 ± 7	43 ± 7	<LoQ	<LoQ
2018	June	19 ± 1	17 ± 2	<LoQ	12.8 ± 0.4	<LoQ	32 ± 5	29 ± 4	<LoQ	<LoQ
2018	October	27 ± 2	22 ± 2	<LoQ	13 ± 2	8 ± 3	56 ± 8	54 ± 8	<LoQ	<LoQ
2019	June	25 ± 3	n.s.	<LoQ	23 ± 4	–	n.s.	n.s.	n.s.	n.s.
Average		**25 ± 8**	**21 ± 4**	**<LoQ**	**18 ± 5**	**<LoQ**	**53 ± 19**	**50 ± 19**	**<LoQ**	**<LoQ**
Coanga (Granite)										
2017	June	19 ± 2	19 ± 3	<LoQ	4.9 ± 0.6	12 ± 4	114 ± 17	110 ± 16	<LoQ	<LoQ
2017	October	26 ± 3	18 ± 2	<LoQ	<LoQ	<LoQ	55 ± 8	47 ± 7	4.9 ± 0.7	3.1 ± 0.5
2018	June	12 ± 1	11 ± 1	<LoQ	4.3 ± 0.1	5 ± 2	71 ± 11	67 ± 10	<LoQ	<LoQ
2018	October	25 ± 2	20 ± 2	<LoQ	4.5 ± 0.5	13 ± 3	29 ± 4	27 ± 4	<LoQ	<LoQ
2019	June	15 ± 1	n.s.	<LoQ	5 ± 1	–	n.s.	n.s.	n.s.	n.s.
Average		**20 ± 7**	**17 ± 4**	**<LoQ**	**6 ± 3**	**8 ± 6**	**67 ± 36**	**63 ± 35**	**<LoQ**	**<LoQ**
Xuans (Granite)										
2017	June	20 ± 3	23 ± 2	<LoQ	9 ± 2	12 ± 4	94 ± 14	90 ± 13	<LoQ	<LoQ

Table Art.2.SI 2. (Continued)

Year	Month	TSe Bulk	TDSe	Se(IV)	Se(VI)	Red.Se	TVSe	DMSe	DMSeS	DMDSe
		ng Se L^{-1}					pg Se L^{-1}			
Paradis (Devonian sedimentary rocks + Granite)										
2017	June	37 ± 3	40 ± 4	<LoQ	22.4 ± 4	15 ± 5	n.s.	n.s.	n.s.	n.s.
2018	June	37 ± 2	28 ± 1	<LoQ	27 ± 2	<LoQ	n.s.	n.s.	n.s.	n.s.
2018	October	35 ± 2	31 ± 3	<LoQ	19 ± 2	10 ± 4	n.s.	n.s.	n.s.	n.s.
Average		**36 ± 1**	**33 ± 6**	**<LoQ**	**23 ± 4**	**8 ± 9**	**–**	**–**	**–**	**–**
Ordicuso (Devonian sedimentary rocks + Granite)										
2017	June	31 ± 2	25 ± 3	<LoQ	5.8 ± 0.9	18 ± 4	484 ± 73	99 ± 15	339 ± 51	46 ± 7
2018	June	24 ± 2	20 ± 2	<LoQ	7.0 ± 0.2	11 ± 3	n.s.	n.s.	n.s.	n.s.
2018	October	24 ± 2	20 ± 2	<LoQ	7.5 ± 0.9	11 ± 3	11 ± 2	9 ± 1	2.0 ± 0.3	<LoQ
2019	June	25 ± 2	n.s.	<LoQ	18 ± 3	–	n.s.	n.s.	n.s.	n.s.
Average		**27 ± 4**	**22 ± 3**	**<LoQ**	**10 ± 5**	**13 ± 4**	**248 ± 334**	**54 ± 64**	**170 ± 238**	**23 ± 32**
Baños de Panticosa (Granite)										
2017	June	31 ± 2	30 ± 4	<LoQ	18 ± 2	10 ± 4	118 ± 17	49 ± 7	67 ± 10	<LoQ
2017	October	30 ± 7	21 ± 2	<LoQ	<LoQ	<LoQ	67 ± 10	29 ± 4	35 ± 5	4.1 ± 0.6
2018	June	23 ± 2	22 ± 1	<LoQ	13.4 ± 0.4	6 ± 2	n.s.	n.s.	n.s.	n.s.
2018	October	29 ± 2	23 ± 2	<LoQ	7.4 ± 0.9	13 ± 3	n.s.	n.s.	n.s.	n.s.
2019	June	20 ± 1	n.s.	<LoQ	25 ± 4	–	n.s.	n.s.	n.s.	n.s.
Average		**27 ± 5**	**24 ± 4**	**<LoQ**	**15 ± 7**	**7 ± 6**	**93 ± 36**	**39 ± 14**	**51 ± 23**	**<LoQ**

Table Art.2.SI 2. (Continued)

Year	Month	TSe Bulk	TDSe	Se(IV)	Se(VI)	Red.Se	TVSe	DMSe	DMSeS	DMDSe
		ng Se L^{-1}					pg Se L^{-1}			
Bachimaña Bajo (Granite)										
2017	June	33 ± 3	36 ± 3	<LoQ	22 ± 4	13 ± 5	n.s.	n.s.	n.s.	n.s.
2017	October	33 ± 3	24 ± 2	<LoQ	<LoQ	<LoQ	69 ± 10	41 ± 6	25 ± 4	3.0 ± 0.4
2018	June	24 ± 2	25 ± 2	<LoQ	19.4 ± 0.6	<LoQ	95 ± 14	92 ± 14	<LoQ	<LoQ
2018	October	28 ± 2	22 ± 3	<LoQ	7.7 ± 0.9	13 ± 3	22 ± 3	12 ± 1	10 ± 2	1.1 ± 0.2
2019	June	27 ± 3	n.s.	<LoQ	24 ± 4	–	n.s.	n.s.	n.s.	n.s.
Average		**29 ± 4**	**27 ± 6**	**<LoQ**	**17 ± 7**	**8 ± 6**	**62 ± 37**	**48 ± 40**	**12 ± 12**	**<LoQ**
Badète (Devonian sedimentary rocks + Granite)										
2017	June	68 ± 5	76 ± 6	2 ± 2	74 ± 8	<LoQ	12 ± 2	7 ± 1	<LoQ	<LoQ
2017	October	66 ± 5	50 ± 4	<LoQ	43 ± 3	<LoQ	74 ± 11	59 ± 9	12 ± 2	2.5 ± 0.4
2018	June	82 ± 5	66 ± 3	<LoQ	73 ± 4	<LoQ	18 ± 3	14 ± 2	<LoQ	<LoQ
2018	October	50 ± 3	43 ± 4	<LoQ	37 ± 4	5 ± 6	9 ± 1	6.0 ± 0.9	2.3 ± 0.4	<LoQ
Average		**67 ± 13**	**59 ± 15**	**<LoQ**	**57 ± 19**	**<LoQ**	**28 ± 31**	**22 ± 25**	**5 ± 5**	**<LoQ**

Table Art.2.SI 2. (Continued)

Year	Month	TSe Bulk	TDSe	Se(IV)	Se(VI)	Red.Se	TVSe	DMSe	DMSeS	DMDSe
		ng Se L^{-1}					pg Se L^{-1}			
Arratille (Devonian sedimentary rocks + Granite)										
2017	June	63 ± 5	71 ± 6	<LoQ	63 ± 7	7 ± 8	85 ± 13	14 ± 2	68 ± 10	<LoQ
2017	October	58 ± 4	45 ± 3	<LoQ	39 ± 3	<LoQ	119 ± 17	17 ± 3	91 ± 14	10 ± 1
2018	June	56 ± 3	46 ± 3	<LoQ	51 ± 2	<LoQ	27 ± 4	12 ± 2	13 ± 2	<LoQ
2018	October	n.s.	39 ± 4	<LoQ	33 ± 4	<LoQ	4.4 ± 0.7	3.0 ± 0.5	<LoQ	<LoQ
Average		**59 ± 4**	**50 ± 14**	**<LoQ**	**46 ± 13**	**<LoQ**	**59 ± 52**	**11 ± 6**	**43 ± 44**	**<LoQ**
Azul Superior (Devonian sedimentary rocks + Granite)										
2017	June	73 ± 8	81 ± 9	2.5 ± 0.3	72 ± 9	6 ± 12	70 ± 11	44 ± 7	24 ± 4	<LoQ
2017	October	67 ± 4	53 ± 4	<LoQ	67 ± 5	<LoQ	39 ± 6	31 ± 5	6 ± 0.9	1.9 ± 0.3
2018	June	51 ± 2	49 ± 3	<LoQ	55 ± 2	<LoQ	26 ± 4	22 ± 3	<LoQ	<LoQ
2018	October	55 ± 3	48 ± 5	<LoQ	41 ± 5	6 ± 7	7 ± 1	5.4 ± 0.8	<LoQ	<LoQ
2019	June	69 ± 5	n.s.	4 ± 1	73 ± 13	–	n.s.	n.s.	n.s.	n.s.
Average		**63 ± 10**	**58 ± 15**	**<LoQ**	**61 ± 14**	**<LoQ**	**35 ± 27**	**26 ± 16**	**8 ± 11**	**<LoQ**

Table Art.2.SI 2. (Continued)

Year	Month	TSe Bulk	TDSe	Se(IV)	Se(VI)	Red.Se	TVSe	DMSe	DMSeS	DMDSe
		ng Se L^{-1}					pg Se L^{-1}			
Pecico (Devonian sedimentary rocks + Granite)										
2017	June	46 ± 4	48 ± 5	2 ± 2	41 ± 4	5 ± 6	36 ± 5	32 ± 5	<LoQ	<LoQ
2018	June	27 ± 2	26 ± 1	<LoQ	23.9 ± 0.8	<LoQ	41 ± 6	37 ± 6	<LoQ	<LoQ
2018	October	37 ± 2	31 ± 3	<LoQ	23 ± 3	6 ± 5	n.s.	n.s.	n.s.	n.s.
2019	June	26 ± 2	n.s.	<LoQ	22 ± 4	–	n.s.	n.s.	n.s.	n.s.
Average		**34 ± 9**	**35 ± 12**	**<LoQ**	**28 ± 9**	**<LoQ**	**39 ± 4**	**35 ± 4**	**<LoQ**	**<LoQ**
Gentau (Permo-Triassic sedimentary rocks)										
2018	June	13 ± 1	11.5 ± 0.8	<LoQ	9.2 ± 0.3	<LoQ	17 ± 3	13 ± 2	2.4 ± 0.4	<LoQ
2018	October	15 ± 1	10 ± 1	<LoQ	<LoQ	8 ± 2	9 ± 1	7 ± 1	<LoQ	<LoQ
2019	June	14 ± 1	11 ± 1	<LoQ	10 ± 2	<LoQ	2.6 ± 0.4	2.6 ± 0.4	<LoQ	<LoQ
Average		**14 ± 1**	**11 ± 1**	**<LoQ**	**7 ± 5**	**<LoQ**	**9 ± 7**	**8 ± 5**	**5 ± 1**	**<LoQ**
Bersau (Permo-Triassic sedimentary rocks)										
2018	June	15 ± 1	12 ± 1	<LoQ	7.1 ± 0.3	<LoQ	12 ± 2	9 ± 1	1.2 ± 0.2	<LoQ
2018	October	17 ± 2	12 ± 2	<LoQ	<LoQ	9 ± 3	8 ± 1	3.7 ± 0.6	2.8 ± 0.4	1.4 ± 0.2
2019	June	16 ± 2	10.5 ± 0.8	<LoQ	8 ± 1	<LoQ	3.2 ± 0.5	2.8 ± 0.4	<LoQ	<LoQ
Average		**16 ± 1**	**12 ± 1**	**<LoQ**	**5 ± 4**	**<LoQ**	**8 ± 4**	**5 ± 3**	**3 ± 2**	**1.4 ± 0.5**

Table Art.2.SI 2. (Continued)

Year	Month	TSe Bulk	TDSe	Se(IV)	Se(VI)	Red.Se	TVSe	DMSe	DMSeS	DMDSe
		ng Se L^{-1}					pg Se L^{-1}			
Roumassot (Permo-Triassic sedimentary rocks)										
2018	June	25 ± 2	13 ± 1	<LoQ	7.5 ± 0.3	<LoQ	36 ± 5	29 ± 4	4.7 ± 0.7	<LoQ
2018	October	18 ± 2	13 ± 1	<LoQ	<LoQ	10 ± 3	5.8 ± 0.9	3.6 ± 0.5	1.8 ± 0.3	<LoQ
2019	June	15 ± 2	11.9 ± 0.9	2.2 ± 0.7	4.7 ± 0.8	5 ± 1	3.6 ± 0.5	3.0 ± 0.5	<LoQ	<LoQ
Average		**20 ± 5**	**13 ± 1**	**<LoQ**	**5 ± 3**	**6 ± 4**	**15 ± 18**	**12 ± 15**	**2 ± 2**	**<LoQ**
Sabocos (Devonian + Cretaceous sedimentary rocks)										
2018	June	21 ± 2	15.6 ± 0.7	<LoQ	10 ± 0.3	<LoQ	24.3 ± 4	11 ± 2	12 ± 2	1.1 ± 0.2
2018	October	19 ± 2	15 ± 2	<LoQ	5.1 ± 0.6	8 ± 2	15 ± 2	8 ± 1	4.9 ± 0.7	1.7 ± 0.3
2019	June	19 ± 1	12 ± 1	<LoQ	11 ± 2	<LoQ	3.2 ± 0.5	2.8 ± 0.4	<LoQ	<LoQ
Average		**20 ± 1**	**14 ± 2**	**<LoQ**	**9 ± 3**	**<LoQ**	**14 ± 11**	**7 ± 4**	**6 ± 6**	**1.2 ± 0.4**

Supplementary information Table Art.2.SI 3

Table Art.2.SI 3. Depth profiles raw data for Arratille (ARA), Azules (AZU), Gentau (GEN) and Sabocos (SAB). Data shown corresponds to non-gaseous dissolved total Se bulk (TSe Bulk), TSe filtered (TDSe) and Se speciation: selenate (Se(VI)) and the Red.Se (calculated as TSe>0.22 – Se(IV) – Se(VI), selenite was in all cases <LoQ; and gaseous Se speciation as total volatile Se. dimethylselenide (DMSe), dimethyl selenide sulphide (DMSeS) and dimethyl diselenide (DMDSe). n.s. means no sample and values under the limit of quantification are indicated as <LoQ. Values are presented either in ng Se L^{-1} (for non-volatile Se species) or pg Se L^{-1} (for volatile Se data) ± the associated error. The associated error correspond to the confidence interval. Parameters shown are temperature (Temp.). conductivity (Cond.). oxygen saturation (Ox. Sat.). dissolved oxygen (DO). nitrate (NO_3^-) and sulfate (SO_4^{2-}). Se(IV) was in all cases <LoQ.

Depth (m)	TSe Bulk	TDSe	Se(VI)	Red.Se	TVSe	DMSe	DMSeS	DMDSe	T (º C)	Cond. (µS cm^{-1})	Ox. Sat. (%)	DO (mg L^{-1})	NO_3^-	SO_4^{2-}
	(ng Se L^{-1})				(pg Se L^{-1})								(10^{-2} mg L^{-1})	
Arratille (Devonian sedimentary rocks + Granite)														
June 2018														
0.5	54 ± 2	46 ± 2	53 ± 2	<LoQ	39 ± 6	27 ± 4	11 ± 2	<LoQ	5.7	38	72	9.0	58	275
3	56 ± 4	45 ± 3	54 ± 2	<LoQ	32 ± 5	12 ± 2	17 ± 3	<LoQ	4.9	37	76	9.8	78	282
6	56 ± 3	43 ± 2	47 ± 2	<LoQ	72 ± 11	63 ± 10	7 ± 1	<LoQ	4.9	37	76	9.8	74	275
12	55 ± 2	46 ± 2	53 ± 2	<LoQ	85 ± 13	66 ± 10	14 ± 2	6 ± 1	4.8	138	5	0.7	71	283

Table Art.2.SI 3. (Continued)

Depth (m)	TSe Bulk	TDSe	Se(VI)	Red.Se	TVSe	DMSe	DMSeS	DMDSe	T	Cond.	Ox. Sat.	DO	NO_3^-	SO_4^{2-}
	(ng Se L^{-1})				(pg Se L^{-1})				(º C)	(µS cm^{-1})	(%)	(mg L^{-1})	(10^{-2} mg L^{-1})	
Azul Superior (Devonian sedimentary rocks + Granite)														
June 2018														
0.5	51 ± 3	49 ± 3	55 ± 2	<LoQ	22 ± 3	22 ± 3	<LoQ	<LoQ	4.9	46	74	9.5	76	491
3.5	55 ± 2	53 ± 2	59 ± 2	<LoQ	32 ± 5	32 ± 5	<LoQ	<LoQ	4.8	47	77	9.8	117	523
7	55 ± 4	56 ± 3	64 ± 2	<LoQ	15 ± 2	14 ± 2	1.5 ± 0.2	<LoQ	4.7	48	76	9.8	64	526
O18														
0.5	55 ± 3	48 ± 5	41 ± 5	6 ± 7	6 ± 1	5 ± 1	<LoQ	<LoQ	5.4	50	68	8.6	76	678
3	54 ± 3	47 ± 5	41 ± 5	<LoQ	5 ± 1	<LoQ	<LoQ	<LoQ	5.1	50	71	9.1	78	670
6	54 ± 3	48 ± 5	41 ± 5	5 ± 7	5 ± 1	<LoQ	<LoQ	<LoQ	5.0	50	72	9.2	91	674
Gentau (Permo-Triassic sedimentary rocks)														
June 2018														
0.5	15 ± 1	13 ± 1	11 ± 0.4	<LoQ	15 ± 2	9 ± 1	6 ± 1	<LoQ	6.9	20	82	10.0	<LoQ	<LoQ
5	14 ± 1	13 ± 1	9.5 ± 0.4	<LoQ	33 ± 5	19 ± 3	9 ± 1	4.5 ± 0.7	5.0	20	78	10.0	<LoQ	<LoQ
8	13 ± 1	14 ± 1	8.5 ± 0.3	<LoQ	9 ± 1	7 ± 1	1.3 ± 0.2	<LoQ	4.4	38	27	3.5	<LoQ	<LoQ
12	13 ± 2	13 ± 1	4.2 ± 0.1	7 ± 2	31 ± 5	6 ± 1	12 ± 2	13 ± 2	4.2	47	3	0.3	<LoQ	<LoQ
18	10 ± 1	23 ± 2	3.5 ± 0.1	17 ± 2	96 ± 14	9 ± 1	14 ± 2	73 ± 11	4.4	67	1	0.2	<LoQ	<LoQ

Table Art.2.SI 3. (Continued)

Depth (m)	TSe Bulk	TDSe	Se(VI)	Red.Se	TVSe	DMSe	DMSeS	DMDSe	T (º C)	Cond. (µS cm⁻¹)	Ox. Sat. (%)	DO (mg L⁻¹)	NO_3^-	SO_4^{2-}
	(ng Se L⁻¹)				(pg Se L⁻¹)								(10^{-2} mg L⁻¹)	
October 2018														
0.5	15 ± 1	11 ± 1	<LoQ	8 ± 2	5 ± 1	3 ± 0.4	1.7 ± 0.3	<LoQ	12.8	24	79	8.4	<LoQ	<LoQ
5	16 ± 1	11 ± 1	<LoQ	8 ± 3	10 ± 2	7 ± 1	2.2 ± 0.3	<LoQ	12.7	24	78	8.2	<LoQ	<LoQ
8	15 ± 2	11 ± 1	<LoQ	8 ± 2	6 ± 1	3.5 ± 0.5	1.7 ± 0.3	<LoQ	12.6	24	77	8.1	<LoQ	<LoQ
12	16 ± 1	13 ± 1	<LoQ	10 ± 3	2.8 ± 0.4	<LoQ	<LoQ	<LoQ	8.5	44	33	3.8	<LoQ	<LoQ
17	21 ± 2	14 ± 2	<LoQ	11 ± 3	9 ± 1	3.3 ± 0.5	5 ± 1	<LoQ	6.0	56	2	0.2	<LoQ	<LoQ
June 2019														
0.5	24 ± 2	11 ± 1	10 ± 2	<LoQ	3 ± 0.4	1.5 ± 0.2	1.3 ± 0.2	<LoQ	7.6	30	79	9.5	44	<LoQ
5	16 ± 2	11 ± 1	9 ± 2	<LoQ	6 ± 1	1.3 ± 0.2	3.0 ± 0.4	2 ± 0.3	6.8	31	85	10.3	27	<LoQ
8	15 ± 1	11 ± 1	7 ± 1	<LoQ	5 ± 1	1.1 ± 0.2	3.6 ± 0.5	<LoQ	5.8	35	91	11.4	18	<LoQ
12	15 ± 1	11 ± 1	<LoQ	8 ± 2	n.s.	n.s.	n.s.	n.s.	4.5	43	20	2.6	41	<LoQ
17.5	16 ± 1	10 ± 1	<LoQ	7 ± 2	8 ± 1	3.7 ± 0.6	0.8 ± 0.1	3.3 ± 0.5	4.3	47	4	0.5	<LoQ	<LoQ

Table Art.2.SI 3. (Continued)

Depth (m)	TSe Bulk	TDSe	Se(VI)	Red.Se	TVSe	DMSe	DMSeS	DMDSe	T	Cond.	Ox. Sat.	DO	NO3–	SO42–
	(ng Se L^{-1})				(pg Se L^{-1})				(º C)	(µS cm^{-1})	(%)	(mg L^{-1})	(10^{-2} mg L^{-1})	
Sabocos (Devonian + Cretaceous sedimentary rocks)														
June 2018														
0.5	17 ± 1	15 ± 1	11 ± 1	<LoQ	26 ± 4	17 ± 3	9 ± 1	<LoQ	17.2	115	102	9.8	49	233
5	19 ± 2	16 ± 2	12 ± 1	<LoQ	26 ± 4	12 ± 2	12 ± 2	2 ± 1	10.7	115	82	9.1	48	251
9	19 ± 2	19 ± 1	12 ± 1	5 ± 2	10 ± 2	3 ± 1	4 ± 1	3 ± 0.4	7.6	119	61	7.3	45	321
15	19 ± 2	19 ± 1	12 ± 1	6 ± 2	9 ± 1	7 ± 1	2 ± 1	<LoQ	6.0	120	49	6.1	54	307
20	18 ± 1	19 ± 1	13 ± 1	<LoQ	20 ± 3	15 ± 2	3 ± 1	1 ± 1	5.1	124	8	1.1	50	302
25	17 ± 1	17 ± 2	10 ± 1	5 ± 3	80 ± 12	36 ± 5	10 ± 1	34 ± 5	4.8	127	1	0.2	46	274
October 2018														
0.5	19 ± 2	15 ± 2	4 ± 1	9 ± 2	9 ± 1	1.5 ± 0.2	6 ± 0.9	1.6 ± 0.2	10.7	101	78	8.7	37	254
4	20 ± 1	15 ± 2	5 ± 1	9 ± 3	10 ± 2	1.7 ± 0.3	7 ± 1	1.7 ± 0.3	10.6	102	78	8.7	<LoQ	254
8	22 ± 2	15 ± 2	4.5 ± 1	8 ± 2	8 ± 1	1.5 ± 0.2	5.1 ± 0.8	1.7 ± 0.3	10.5	102	77	8.6	<LoQ	255
12	18 ± 1	14 ± 2	9 ± 1	<LoQ	11 ± 2	7 ± 1	2.5 ± 0.4	2.1 ± 0.3	7.9	119	62	7.4	34	310
18	19 ± 2	14 ± 2	13 ± 1	<LoQ	3 ± 1	2.8 ± 0.4	<LoQ	<LoQ	6.0	117	35	4.4	44	310
23	19 ± 2	16 ± 2	10 ± 1	5 ± 3	8 ± 1	8 ± 1	<LoQ	<LoQ	5.7	121	5	0.6	<LoQ	303

Table Art.2.SI 3. (Continued)

Depth (m)	TSe Bulk	TDSe	Se(VI)	Red.Se	TVSe	DMSe	DMSeS	DMDSe	T (º C)	Cond. (µS cm⁻¹)	Ox. Sat. (%)	DO (mg L⁻¹)	NO_3^-	SO_4^{2-}
	(ng Se L⁻¹)				(pg Se L⁻¹)								(10^{-2} mg L⁻¹)	
June 19														
0.5	20 ± 2	12 ± 1	10 ± 2	<LoQ	1.9 ± 0.3	0.9 ± 0.1	1 ± 0.2	<LoQ	11.9	130	79	8.6	77	255
5	20 ± 2	12 ± 1	10 ± 2	<LoQ	5.5 ± 0.8	0.6 ± 0.1	4 ± 0.6	0.9 ± 0.1	10.2	133	83	9.3	61	240
9	22 ± 2	15 ± 1	14 ± 3	<LoQ	6.7 ± 1	1.2 ± 0.2	4.6 ± 0.7	0.9 ± 0.1	7.1	130	76	9.2	71	279
13	21 ± 2	16 ± 1	14 ± 3	<LoQ	2.3 ± 0.3	1.5 ± 0.2	0.3 ± 0	0.5 ± 0.1	6.1	129	70	8.7	78	280
18	22 ± 2	17 ± 1	17 ± 3	<LoQ	0.8 ± 0.1	0.8 ± 0.1	<LoQ	<LoQ	5.3	134	50	6.1	79	302
25	24 ± 2	17 ± 2	17 ± 3	<LoQ	5.3 ± 0.8	3.9 ± 0.6	0.8 ± 0.1	0.6 ± 0.1	4.9	140	7	0.9	57	273

Supplementary information Table Art.2.SI 4

Table Art.2.SI 4. Estimated fluxes for Se wet deposition (with data from Roulier et al., (2020, submitted)) and Se emission using the model of (Cole & Caraco, 1998) for windspeeds of 3 and 10 m · s^{-1}. Selenium input and emission is presented as µg Se · $year^{-1}$ and as % of selenium stock in the corresponding lake. The data has been calculated considering an ice-covering period of 6 months.

Lake	Surface (m^2)	Volume (m^3)	Stock Se (µg Se)	Input Se (µg Se yr^{-1})	Input Se (%)	Se emitted wind: 3 m s^{-1} (µg Se yr^{-1})	Se emitted wind: 3 m s^{-1} (%)	Se emitted wind: 10 m s^{-1} (µg Se yr^{-1})	Se emitted wind: 10 m s^{-1} (%)
PEY	11700	52987	580941	587116	101	34037	5,9	126303	22
CAM	34600	208745	3204132	1736259	54	100395	3,1	372543	12
OPA	6400	25788	454579	321158	71	-	-	-	-
POU	59500	387705	5207681	2985763	57	113665	2,2	421784	8
NER	29100	178522	2391054	1460264	61	170923	7,1	634255	27
PAR	4300	16570	542846	215778	40	-	-	-	-
BAD	69700	243990	14418356	3497608	24	-	-	-	-
ARA	58700	264307	13259174	2945619	22	436444	3,3	1619539	12
BAC	30800	193335	5193036	1545572	30	-	-	-	-
PAN	55000	470072	11220284	2759949	25	-	-	-	-
AZU	38900	273527	15756053	1952037	12	-	-	-	-
PEC	9100	38954	1362496	456646	34	27996	2,1	103887	8
ARN	26000	84579	1732217	1304703	75	119503	6,9	443446	26

Table Art.2.SI 4 (Continued)

Lake	Surface (m^2)	Volume (m^3)	Stock Se (µg Se)	Input Se (µg Se yr^{-1})	Input Se (%)	Se emitted wind: 3 m s^{-1} (µg Se yr^{-1})	Se emitted wind: 3 m s^{-1} (%)	Se emitted wind: 10 m s^{-1} (µg Se yr^{-1})	Se emitted wind: 10 m s^{-1} (%)
ORD	3700	14171	306474	185669	61	-	-	-	-
COA	5800	23208	389512	291049	75	-	-	-	-
XUA	29700	183875	4146432	1490373	36	210889	5,1	782559	19
SAB	95600	1183798	18049219	4797294	27	132298	0,7	490925	3
GEN	86200	993736	10913773	4325593	40	68930	0,6	255784	2
BER	128200	2266475	27288689	6433191	24	61990	0,2	230030	1
ROU	51500	424200	5387816	2584316	48	23184	0,4	86031	2
min	3700	14171	306474	185669	**12%**	23184	**0,2%**	86031	**0,8%**
max	128200	2266475	27288689	6433191	**101%**	436444	**7,1%**	1619539	**26,5%**
median	32700	201040	4669734	1640915	**40%**	107030	**3%**	397163	**10%**

5. Bibliography

Amouroux, D., & Donard, O. F. X. (1997). Evasion of selenium to the atmosphere via biomethylation processes in the Gironde estuary, France. Marine Chemistry, 58(1–2), 173–188. https://doi.org/10.1016/S0304-4203(97)00033-9

Amouroux, D., Tessier, E., Pécheyran, C., Donard, O. F. X., & Amouroux E. AU3 - Pecheyran, C. AU4 - Donard, O.F.X., D. A.-T. (1998). Sampling and probing volatile metal(loid) species in natural waters by in-situ purge and cryogenic trapping followed by gas chromatography and inductively coupled plasma mass specitrometry (P-CT-GC-ICP/MS). Analytica Chimica Acta, 377(2–3), 241–254. https://doi.org/10.1016/S0003-2670(98)00425-5

Atkinson, R., Aschmann, S. M., Hasegawa, D., Thompson-Eagle, E. T., & Frankenberger Jr, W. T. (1990). Kinetics of the atmospherically important reactions of dimethyl selenide. Environmental Science & Technology, 24(9), 1326–1332. https://doi.org/10.1021/es00079a005

Blazina, T., Läderach, A., Jones, G. D., Sodemann, H., Wernli, H., Kirchner, J. W., & Winkel, L. H. E. E. (2017). Marine Primary Productivity as a Potential Indirect Source of Selenium and Other Trace Elements in Atmospheric Deposition. Environmental Science and Technology, 51(1), 108–118. https://doi.org/10.1021/acs.est.6b03063

Brandt, J. E., Bernhardt, E. S., Dwyer, G. S., & Di Giulio, R. T. (2017). Selenium Ecotoxicology in Freshwater Lakes Receiving Coal Combustion Residual Effluents: A North Carolina Example. Environmental Science & Technology, 51(4), 2418–2426. https://doi.org/10.1021/acs.est.6b05353

Camarero, L., Rogora, M., Mosello, R., Anderson, N. J., Barbieri, A., Botev, I., … Lotter, A. F. (2009). Regionalisation of chemical variability in European mountain lakes. Freshwater Biology, 54(12), 2452–2469. https://doi.org/10.1111/j.1365-2427.2009.02296.x

Catalan, J., Camarero, L., Felip, M., Pla, S., Ventura, M., Buchaca, T., … Casamayor, E. O. (2006). High mountain lakes: extreme habitats and witnesses of environmental changes. Limnetica, 25(1–2), 551–584.

Catalan, J., Ventura, M., Brancelj, A., Granados, I., Thies, H., Nickus, U., … Stuchlík, E. (2002). Seasonal ecosystem variability in remote mountain lakes: implications for detecting climatic signals in sediment records. Journal of Paleolimnology, 28(1), 25–46. https://doi.org/10.1023/A:1020315817235

Cole, J. J., & Caraco, N. F. (1998). Atmospheric exchange of carbon dioxide in a low-wind oligotrophic lake measured by the addition of SF6. Limnology and Oceanography, 43(4), 647–656. https://doi.org/10.4319/lo.1998.43.4.0647.

Conde, J. E., & Sanz Alaejos, M. (1997). Selenium Concentrations in Natural and Environmental Waters. Chemical Reviews, 97(6), 1979–2004. https://doi.org/10.1021/cr960100g

Cutter, G. A., & Church, T. M. (1986). Selenium in western Atlantic precipitation. Nature, 322(6081), 720. https://doi.org/10.1038/322720a0

Duan, L., Song, J., Li, X., Yuan, H., & Xu, S. (2010). Distribution of selenium and its relationship to the eco-environment in Bohai Bay seawater. Marine Chemistry, 121(1–4), 87–99. https://doi.org/10.1016/j.marchem.2010.03.007

Duval, B., Amouroux, D., & De Diego, A. (2020, in preparation). Ecodynamics of metals and metalloids in Pyrenean lakes in relation to climate change and anthropogenic pressure. Universite de Pau et des Pays de l'Adour and Euskal Herriko Unibertsitatea.

Feinberg, A., Stenke, A., Peter, T., & Winkel, L. H. E. (2020). Constraining Atmospheric Selenium Emissions Using Observations, Global Modeling, and Bayesian Inference. Environmental Science & Technology, 54(12), 7146–7155. https://doi.org/10.1021/acs.est.0c01408

Gascoin, S., Hagolle, O., Huc, M., Jarlan, L., Dejoux, J.-F., Szczypta, C., … Sánchez, R. (2015). A snow cover climatology for the Pyrenees from MODIS snow products. Hydrology and Earth System Sciences, European Geosciences Union, 2015, ⟨hal-01218966⟩. https://doi.org/10.5194/hess-19-2337-2015

Gleizes, G., Leblanc, D., Santana, V., Olivier, P., & Bouchez, J. L. (1998). Sigmoidal structures featuring dextral shear during emplacement of the Hercynian granite complex of Cauterets–Panticosa

(Pyrenees). Journal of Structural Geology, 20(9), 1229–1245. https://doi.org/https://doi.org/10.1016/S0191-8141(98)00060-1

Harrison, P. J., Yu, P. W., Thompson, P. A., Price, N. M., & Phillips, D. J. (1988). Survey of selenium requirements in marine phytoplankton. Marine Ecology Progress Series, 47(1), 89–96. Retrieved from http://www.jstor.org/stable/24831560

Lanceleur, L., Tessier, E., Bueno, M., Pienitz, R., Bouchard, F., Cloquet, C., & Amouroux, D. (2019). Cycling and atmospheric exchanges of selenium in Canadian subarctic thermokarst ponds. Biogeochemistry, 145(1-2), 193-211. https://doi.org/10.1007/s10533-019-00599-w

Lindström, K. (1983). Selenium as a growth factor for plankton algae in laboratory experiments and in some Swedish lakes. Forest Water Ecosystems, 13(1–2), 35–47. https://doi.org/10.1007/BF00008655

López-Moreno, J. I., & Vicente-Serrano, S. M. (2007). Atmospheric circulation influence on the interannual variability of snow pack in the Spanish Pyrenees during the second half of the 20th century. Hydrology Research, 38(1), 33–44. https://doi.org/10.2166/nh.2007.030

Luoma, S. N., & Rainbow, P. S. (2008). Metal contamination in aquatic environments: science and lateral management. Cambridge university press.

Luxem, K. E., Vriens, B., Behra, R., & Winkel, L. H. E. (2017). Studying selenium and sulfur volatilisation by marine algae Emiliania huxleyi and Thalassiosira oceanica in culture. Environmental Chemistry, 14(4), 199–206. Retrieved from https://doi.org/10.1071/EN16184

Mason, R. P., Soerensen, A. L., Dimento, B. P., & Balcom, P. H. (2018). The Global Marine Selenium Cycle: Insights from Measurements and Modeling. Global Biogeochemical Cycles, 32(1720–1737). https://doi.org/10.1029/2018GB006029

Nancharaiah, Y. V., & Lens, P. N. L. (2015). Ecology and biotechnology of selenium-respiring bacteria. Microbiol. Mol. Biol. Rev., 79(1), 61–80. https://doi.org/10.1128/MMBR.00037-14

Nishri, A., Brenner, I. B., Hall, G. E. M., & Taylor, H. E. (1999). Temporal variations in dissolved selenium in Lake Kinneret (Israel). Aquatic Sciences, 61(3), 215–233. https://doi.org/10.1007/s000270050063

Nriagu, J. O., & Wong, H. K. (1983). Selenium pollution of lakes near the smelters at Sudbury, Ontario. Nature, 301(5895), 55.

Økelsrud, A., Lydersen, E., & Fjeld, E. (2016). Biomagnification of mercury and selenium in two lakes in southern Norway. Science of the Total Environment, 566, 596–607. https://doi.org/10.1016/j.scitotenv.2016.05.109

Pan, Y. P., & Wang, Y. S. (2015). Atmospheric wet and dry deposition of trace elements at 10 sites in Northern China, 951–972. https://doi.org/10.5194/acp-15-951-2015

Pokrovsky, O. S., Bueno, M., Amouroux, D., Manasypov, R. M., Shirokova, L. S., Karlsson, J., & Amouroux, D. (2018). Dissolved organic matter controls on seasonal and spatial selenium concentration variability in thaw lakes across a permafrost gradient. Environ. Sci. Technol., 52(18), acs.est.8b00918. https://doi.org/10.1021/acs.est.8b00918

Ponton, D. E., & Hare, L. (2013). Relating selenium concentrations in a planktivore to selenium speciation in lakewater. Environmental Pollution, 176, 254–260. https://doi.org/10.1016/j.envpol.2013.01.032

Reimann, C., & De Caritat, P. (1998). Chemical elements in the environment: factsheets for the geochemist and environmental scientist. Springer Science & Business Media.

Robberecht, H., Van Grieken, R., Van Sprundel, M., Berghe, D. Vanden, & Deelstra, H. (1983). Selenium in environmental and drinking waters of Belgium. Science of the Total Environment, 26(2), 163–172. https://doi.org/10.1016/0048-9697(83)90109-2

Roulier, M., Bueno, M., Coppin, F., Nicolas, M., Thiry, Y., Rigal, F., … Pannier, F. (2020, submitted). Atmospheric iodine, selenium and caesium wet depositions in France: spatial and seasonal variations.

Schroeder, R. A., Orem, W. H., & Kharaka, Y. K. (2002). Chemical evolution of the Salton Sea, California: nutrient and selenium dynamics BT - The Salton Sea: Proceedings of the Salton Sea Symposium, held in Desert Hot Springs, California, 13–14 January 2000. In D. A. Barnum, J. F. Elder, D. Stephens, & M. Friend (Eds.) (pp. 23–45). Dordrecht: Springer Netherlands. https://doi.org/10.1007/978-94-017-3459-2_2

Sharma, V. K., McDonald, T. J., Sohn, M., Anquandah, G. A. K., Pettine, M., & Zboril, R. (2014).

Biogeochemistry of selenium. A review. Environmental Chemistry Letters, 13(1), 49–58. https://doi.org/10.1007/s10311-014-0487-x

Simmons, D. B. D., & Wallschläger, D. (2005). A critical review of the biogeochemistry and ecotoxicology of selenium in lotic and lentic environments. Environmental Toxicology and Chemistry, 24(6), 1331–1343. https://doi.org/10.1897/04-176R.1

Suess, E., Aemisegger, F., Sonke, J. E., Sprenger, M., Wernli, H., & Winkel, L. H. E. (2019). Marine versus Continental Sources of Iodine and Selenium in Rainfall at Two European High-Altitude Locations. Environmental Science and Technology, 53(4), 1905–1917. https://doi.org/10.1021/acs.est.8b05533

Tanzer, D., & Heumann, K. G. (1991). Determination of Dissolved Selenium Species in Environmental Water Samples Using Isotope Dilution Mass Spectrometry. Analytical Chemistry, 63(18), 1984–1989. https://doi.org/10.1021/ac00018a016

Tessier, E., Amouroux, D., & Donard, O. F. X. (2002). Biogenic volatilization of trace elements from European estuaries. Biogeochemistry of Environmentally Important Trace Elements, 835(October 2002), 151–165. https://doi.org/10.1021/bk-2003-0835.ch012

Van Lith, J. G. J. (1968). Geology of the Spanish part of the Gavarnie Nappe (Pyrenees) and its underlying sediments near Bielsa (Province of Huesca) (Vol. 10). Utrecht University.

VillaRomero, J. F., Kausch, M., & Pallud, C. (2013). Selenate reduction and adsorption in littoral sediments from a hypersaline California lake, the Salton Sea. Hydrobiologia, 709(1), 129–142. https://doi.org/10.1007/s10750-013-1443-7

Vriens, B., Ammann, A. A., Hagendorfer, H., Lenz, M., Berg, M., & Winkel, L. H. E. (2014). Quantification of methylated selenium, sulfur, and arsenic in the environment. PLoS ONE, 9(7). https://doi.org/10.1371/journal.pone.0102906

Wallschläger, D., & Feldmann, J. (2010). Formation, occurrence, significance, and analysis of organoselenium and organotellurium compounds in the environment. Met Ions Life Sci, 7, 319–364. https://doi.org/10.1039/BK9781847551771-00319

Wang, D., Alfthan, G., & Aro, A. (1994). Determination of Total Selenium and Dissolved Selenium Species in Natural Waters by Fluorometry. Environmental Science and Technology, 28(3), 383–387. https://doi.org/10.1021/es00052a007

Wang, D., Alfthan, G., Aro, A., Lahermo, P., & Väänänen, P. (1994). The impact of selenium fertilisation on the distribution of selenium in rivers in Finland. Agriculture, Ecosystems and Environment, 50(2), 133–149. https://doi.org/10.1016/0167-8809(94)90132-5

Wang, D., Alfthan, G., Aro, A., Mäkelä, A., Knuuttila, S., & Hammar, T. (1995). The impact of selenium supplemented fertilization on selenium in lake ecosystems in Finland. Agriculture, Ecosystems and Environment, 54(1–2), 137–148. https://doi.org/10.1016/0167-8809(94)00574-X

Winkel, L. H. E., Vriens, B., Jones, G. D., Schneider, L. S., Pilon-Smits, E., & Bañuelos, G. S. (2015). Selenium cycling across soil-plant-atmosphere interfaces: A critical review. Nutrients. https://doi.org/10.3390/nu7064199

Zwart, H. J., & De Sitter, L. U. (1979). The geology of the Central Pyrenees.

3.3. Article III << DISTRIBUTION OF SELENIUM AND ITS COMPOUNDS IN WATERS OF THE ADOUR RIVER ESTUARY (BAY OF BISCAY, FRANCE)>>

DISTRIBUTION OF SELENIUM AND ITS COMPOUNDS IN WATERS OF THE ADOUR RIVER ESTUARY (BAY OF BISCAY, FRANCE)

Authors: Andrea Romero-Rama, Maïté Bueno, Emmanuel Tessier, Laurent Lanceleur, Sandrine Veloso, Jonathan Deborde and David Amouroux

Université de Pau et des Pays de l'Adour, E2S UPPA, CNRS, IPREM, Institut des Sciences Analytiques et de Physico-chimie pour l'Environnement et les matériaux, Pau, France

Abstract

The fate of selenium (Se) and its compounds during estuarine land to ocean transfer has been barely documented and investigated. In this sense, Se speciation was studied in the Adour estuarine waters (Bay of Biscay) following a seasonal sampling along with biogeochemical and physico-chemical parameters. Sub-surface water samples were collected at low tide in May and September 2017 and in January 2018. Twelve different sampling points were selected to characterise upstream waters coming from Adour River and Nive River, industrial and urban effluent waters, and downstream estuarine waters. Additionally, one tidal cycle sampling was conducted on September 2018. In all water samples total bulk and dissolved Se (TDSe) were determined together with dissolved Se compounds such as selenite (Se(IV)) and selenate (Se(VI)). Reduced Se fraction (Se(0), Se(-II) and organic Se forms) was obtained subtracting the inorganic fraction (Se(IV)+Se(VI)) to the TDSe. Volatile Se species (Total volatile Se - TVSe) such as DMSe, DMSSe and DMDSe were also determined for the first time together with non-volatile species. Concentration range for TDSe varied from 71 to 771 ng Se L^{-1}. Se(VI) was the main species (50% of TDSe in average); while Se(IV) and reduced Se fraction represented, in average, 11% and 42% of TDSe. TVSe ranged from 51 to 2757 pg Se L^{-1}. Reduced species (volatile compounds and reduced fraction) presented higher concentration in late summer conditions (September 2017) compared to spring and winter while Se(VI) concentrations were higher in winter flood conditions (January 2018) . Our results confirm that Se cycling and species distribution are largely regulated by upstream anthropogenic pressure and seasonal biogeochemical settings. A large fraction of the Se upstream input to the estuary is driven by anthropogenic contributions such as agricultural and livestock farmlands runoff together with nitrogen inputs. Furthermore, Se speciation exhibits increasing production of reduced and volatile compounds during warmer productive periods in the downstream section of the estuary.

1. Introduction

Selenium is a trace element that can exist in several oxidation states (VI, selenate; IV, selenite, 0, elemental Se; –II, selenide), forming both organic and inorganic species. For decades, selenium speciation has been a subject of interest in aquatic systems due to its complex biogeochemical reactivity and the wide range of Se species having specific interactions with living organisms. The constant nutrient renewal and high biological activity make estuarine systems sites of special interest for Se speciation studies (Measures & Burton, 1978; Tessier et al., 2002).

The input of dissolved Se to estuaries and, afterwards to the ocean, most typically results from riverine discharge and the dissolution of suspended and sedimentary selenium particles (Cutter & San Diego-McGlone, 1990). The model of Mason et al., (2018), indicates an annual rivers to ocean Se input of 113 Mmol yr^{-1}, of which 30% in the form of particulate Se. Estuaries are semi-enclosed mixing zones for fresh and saline waters. The typical wide salinity range of estuarine systems is due to tidal influence and riverine discharge volume. Therefore, daily and seasonal variations of Se concentration and speciation is likely expected in estuaries. Furthermore, the shallowness of these areas, commonly below 100 m of depth, promotes the interaction between surface and bottom waters. Thus, intense physical, chemical and biological interactions, together with an impact of industrial and municipal wastewater sources may occur (Cochran & Brook, 2014). Total selenium concentration and speciation vary from one estuary to another, and thus requires further investigations. Total Se ranged from 48 – 358 ng Se L^{-1} in San Francisco Bay (Cutter, 1989), from 58 to 190 ng Se L^{-1} in Rhône (France) (Guan & Martin, 1991) from 68 to 392 ng Se L^{-1} in Zhujiang, China (Yao et al., 2006), from 47 to 95 ng Se L^{-1} in Erhjen and Kaoping estuaries (Taiwan) (Hung & Shy, 1995). In general, total dissolved Se showed conservative behavior except in Erjhen and Zhujiang estuaries that received polluted waters.

In respect to Se speciation, high variability is found between previously investigated sites. Seasonal variability of species proportion was observed in San Francisco Bay (Cutter, 1989). In there, selenite (Se(IV)) represented a maximum of 23% of total Se in spring, while in September this ratio increased to around 40%. Selenate (Se(VI)) proportion also varied depending on season and salinity, representing 82% of total Se at low salinity in spring, compared to 49% at high salinity. In September Se(VI) accounted for 48% at low salinity and decreased to 33% with increasing salinity. Cutter (1989) observed that the presence of

reduced Se fraction correlated with higher chlorophyll-*a* and primary productivity indicators. In Erhjen estuary, selenite was the main species (62 – 71% of total Se) (Hung & Shy, 1995), high concentration of selenite was associated to anthropogenic inputs, mainly urban wastewater effluents and industrial effluents from metal recycling companies (Hung & Shy, 1995). The presence of Se(IV) and more reduced Se species (calculated Red.Se), such as Se(0) and selenides, that represented between <5 and 40% of total Se; was consistent with reducing conditions in the estuary due to insufficient oxygenation that limited oxidation to selenate (Hung & Shy, 1995). At Changjiang estuary, conservative behavior of inorganic Se species was observed during winter contrary to summer (Chang et al., 2016). This happened because of selenite sorption into suspended particulate matter. Therefore, Se(IV) removal rate in Changjiang estuary was strictly linked to seasonal variations. Yao & Zhang (2005) observed at Bohai Bay that selenite was the dominant species during spring; meanwhile, selenate was predominant in autumn. Selenite decrease was associated to phytoplankton uptake during summer period.

Therefore, the input of Se in estuarine systems depends on riverine discharge but it can be affected by industrial or urban wastewaters. In general, total Se behavior is conservative in non-polluted systems, but speciation changes are driven by several factors. Main processes driving Se transformations and resulting speciation alongside an estuary include water redox conditions, being well aerated waters conducive to oxidation; temperature, affecting selenite sorption into particles (Söderlund et al., 2016); and seasonal biological cycles that can potentially increase reduced Se species.

Volatile Se speciation in estuaries has been barely reported. Methylated volatile Se species in aquatic systems are released to the atmosphere as the result of biomethylation processes carried out by microorganisms (bacteria and algae) (Amouroux & Donard, 1997; 2001; Wen & Carignan, 2007). In European estuaries the range of total volatile Se (TVSe) reported values is between 22 – 8067 pg Se L^{-1} (Amouroux & Donard, 1997; Tessier et al., 2002). Dimethylselenide (DMSe) contributed to more than 70 % of total volatile Se, followed by dimethyl selenide sulphide (DMSeS) in the range between 4 – 23 % of TVSe (Amouroux & Donard, 1997; Lanceleur et al., 2019; Tessier et al., 2002a; Tessier et al., 2002b). Typically, two more species have eventually been detected in estuaries, dimethyldiselenide (DMDSe) and methyl selenol (MeSeH), at levels generally close or below the detection limit (Amouroux & Donard, 1997; Amouroux et al., 2001; Wen & Carignan, 2007). The mechanisms producing volatile Se species have been studied in synthetic coastal seawaters. Laboratory experiments

have shown that microbial processes in natural aquatic sediments or marine waters are able to produce DMSeS from selenium containing amino acids (Amouroux et al., 2000; Chasteen & Bentley, 2003). Meanwhile, DMSe is most probably produced by nucleophilic displacement from a selenonium ($DMSe^{+}$–R), similar to the production of dimethylsulphide (DMS) from dimethylsulfopropionate (DMSP) (Amouroux et al., 2001). Studies of Se volatilization fluxes in European estuaries suggest that volatilization is an efficient removal pathway for Se. Moreover, the emission of volatile Se species from estuaries may contribute significantly to the remobilization of Se in the atmosphere (Tessier et al., 2002).

In this work, we intend to complete a new dataset on total Se and Se compounds speciation in estuarine waters (Adour estuary), and we combine for the first time non-volatile and volatile Se species determination in such critical environment. In order to observe a wider variability of the speciation results we investigated the influence of both seasonal and water bodies characteristics. The simultaneous study of non-volatile and volatile Se compounds was conducted together with hydrogeochemical parameters and regarding especially the type of water (estuarine, riverine, industrial and urban effluents). This study aims to better constrain the potential sources and factors controlling total Se level and Se compounds occurrence in estuarine waters with special emphasis on the respective distribution of dissolved inorganic, reduced, organic and volatile forms.

2. Materials and Methods

2.1. Study area and field sampling

Adour estuary is located in the SW of France. It receives water from the Adour River (16,900 km^2 river watershed, Agence de l'eau Adour-Garonne, 2014). Adour River's watershed is characterized by heavy population and industrial density nearby (Point, 2004). Adour River watershed is composed by forest, urban, agricultural and industrial areas with a population of around one million habitants. Adour watershed is characterized by oceanic and mountain climate (Adour Institution, 2014), thus rain events are frequent and river flow increases due to snow-melting during spring. The annual rainfall report for Bayonne shows that July is the driest month of the year while maximum precipitation occurs in the period from October to December (fr.climate-data.org). It is necessary to remark that rainy events occurred during September 2017 and January 2018 samplings, resulting in high turbidity, especially in January when intense rainfalls occurred during the month. Adour River receives water from many tributaries, at the river end-member it receives water from the Nive River (1000 km^2 river

watershed, (Adour Institution, 2016)). The Nive R. goes through farm and habited areas as well, however with relatively low population (~100,000 habitants, (FNAB, 2015)) compared to the Adour watershed region.

A total of 36 samples were collected in 12 points in three sample campaigns: May, 2017 (n=12), September, 2017 (n=12) and January-February 2018 (n=12) to study spatial and seasonal variations. Sampling points are detailed in Table Art.3.1 and Figure Art.3.1. Adour riverine discharge averaged 200, 108 and 643 $m^3 s^{-1}$ in May, September and January sampling campaigns. Nive riverine discharge averaged 11.4, 19.4 and 85.5 $m^3 s^{-1}$ in May, September and January respectively (Deborde, 2019). Tidal coefficients were between 78 and 83 in May, in the range between 80 and 97 in September and from 93 to 109 in January (Veloso, in preparation). Sample collection was carried out at the lowest tide possible to study Se input to the estuary. Physicochemical parameters including temperature, pH, conductivity, oxygen saturation and salinity were measured using a multi-parametric probe (HANNA Instruments® HI-9829) and data concerning nutrients (N, P, Si), sulphates and dissolved organic carbon (DOC) were obtained from simultaneous samples as detailed elsewhere (Deborde, 2019).

Figure Art.3.1. Adour estuary sampling sites: in yellow Adour River (ST1 and ST2) and Nive River (ST3 and ST4), in blue estuarine stations (STA, STB, STC and STD), in pink urban (ST6 and ST9) and industrial stations located at Aritxague (ST7) and Maharin (ST8) streams. Map from https://www.geoportail.gouv.fr/.

Table Art.3.1. Sampling description including dates, decimal GPS coordinates and water type per sampling station.

Station	Sampling Dates (DD/MM/YYYY)	Sampling time	water type	Lat.	Long.	Details
ST 1	09/05/2017 20/09/2017 01/02/2018	13h00 12h00 11h45	upstream	43,500	-1,298	Salt intrusion limit of Adour River
ST 2	09/05/2017 20/09/2017 01/02/2018	15h50 11h15 10h20	upstream	43,413	-1,462	Adour River
ST 3	09/05/2017 20/09/2017 01/02/2018	12h00 13h20 13h30	upstream	43,413	-1,463	Salt intrusion limit for Nive River
ST 4	09/05/2017 20/09/2017 01/02/2018	8h45 9h50 9h00	upstream	43,478	-1,472	Nive River
ST 6	11/05/2017 19/09/2017 31/01/2018	14h30 12h30 11h30	urban	43,487	-1,453	Sampling at 2m of the Saint-Frédéric WWTP† outlet
ST 7	11/05/2017 19/09/2017 31/01/2018	12h30 10h50 9h30	urban + industrial	43,501	-1,492	Aritxague stream
ST 8	11/05/2017 19/09/2017 31/01/2018	11h20 9h45 8h30	urban + industrial	43,504	-1,495	Maharin stream
ST 9	11/05/2017 19/09/2017 31/01/2018	10h00 11h45 10h30	urban	43,512	-1,489	Sampling point after the Saint-Bernard WWTP
ST A	10/05/2017 18/09/2017 30/01/2018	9h15 9h50 9h00	downstream	43,495	-1,475	Adour and Nive confluence

Table Art.3.1. (Continued)

Station	Sampling Dates (DD/MM/YYYY)	Sampling time	water type	Lat.	Long.	Details
ST B	10/05/2017 18/09/2017 30/01/2018	10h00 11h15 9h35	downstream	43,504	-1,492	Adour & Aritxague + Maharin confluence‡
ST C	10/05/2017 18/09/2017 30/01/2018	11h20 10h45 10h20	downstream	43,514	-1,492	Site close to Saint-Bernard WWTP outlet‡
ST D	10/05/2017 18/09/2017 30/01/2018	11h50 9h50 10h50	downstream	43,527	-1,503	Adour River before entering the Sea‡

†WWTP: wastewater treatment plant. ‡Samples collected using a boat located at the center of the river.

A first group of four sampling points that were located at or close to each main river end-members is referred to as “upstream waters”. Stations 1 and 2 were located at Adour River, and ST3 and ST4 at Nive River. ST1 and ST3 were located at the salt intrusion limit of each river (Table Art.3.1). A second group consisted of four sampling points within the estuarine systems but directly located at the outlet channel of industrial effluents and urban wastewater treatment plants (WWTP) and will be distinguished as “effluent waters”. Two streams (Aritxague, ST7 and Maharin, ST8) passing through industrialized and urban areas were sampled to study Se speciation as influenced by urban and industrial activities. Two more sampling points were established at the outlet of depuration stations of the Urban disctrict: Saint Frédéric (ST6) and Saint Bernard (ST9). Finally, the downstream section of the estuary was sampled at and identified as “downstream waters”. It consists in a group of four sampling points located along the urban, industrial and harbor areas (ST A, B, C and D) located just upstream to the estuary mouth.

Using nitrile gloves, sub-surface water samples were collected by hand in upstream and effluent waters and at ST A. At stations ST B, C and D sub-surface samples were collected on board a boat and using a non-metallic and PTFE coated sampler (5 L Go-Flo; General Oceanic). When using the Go-Flo, the sampler was operated with gloves and water was transferred to sample containers using a pre-cleaned silicone tube. For volatile Se speciation, one liter of sample was collected in two 500 mL Teflon bottles avoiding bubbles and head-space, the

sample was immediately stored in the dark and transported to the lab as soon as possible (less than 4 hours). In the lab, samples were stored in the dark at 4 ºC for subsequent purge and trap of gaseous species carried out within the day. This allowed the pre-concentration of dissolved gaseous Se compounds and the preservation of their speciation as described by Lanceleur et al. (2019). Aliquots for bulk Se analysis were collected in 50 mL polypropylene Falcon tubes and acidified with 500 µL (1% v/v) HNO_3 (69%, trace metal grade). Aliquots for total dissolved Se and Se speciation analyses were collected in 125 mL polyethylene bottles without head-space and stored in the dark as fresh as possible. Those samples were transported as fast as possible to the lab, filtrated (0.45 µm, PVDF, Durapore) and separated in aliquots (2x50 mL Falcon tubes) within the same day for further analyses of total dissolved Se and Se speciation. Samples for total dissolved Se were acidified using the same protocol than for total Se bulk, filtered samples will therefore contain Se in the dissolved phase and colloidal Se particles below 0.45µm size. For Se speciation samples were stored avoiding the presence of head-space. The analysis of the samples was carried out within two weeks from the sampling date. Such storage conditions and time were tested for stability in a previous study.

An additional sampling was carried out in September 2018 close to station B, right after the confluence of Adour and Nive rivers (Figure Art.3.1.) for the study of Se concentration and speciation variations during a tidal cycle.

2.2. Total Se analysis

Total Se content was determined in bulk and filtered waters (0.45 µm). Unfiltered bulk samples (45 mL) were digested with HNO_3 (1.0 mL) and HCl (0.5 mL) in sealed tubes and incubated for 3 h at 90 °C in a hot block (DIGIPREP, SCP Science). Digested samples were adjusted to a final volume of 50 mL after digestion and filtered (0.45 µm) prior to the analysis.

Total Se concentrations were measured with an Agilent 7900x Series inductively coupled plasma mass spectrometer (ICP-MS) system (Agilent Technologies, Tokyo, Japan) equipped with an octopole reaction cell, concentric nebulizer and a Scott double pass spray chamber cooled to 2 °C similar to the method used by Pokrovsky et al., (2018). Argon-based polyatomic interferences were reduced by using H_2 as cell gas at a flow rate of 5 mL min^{-1}. The parameters settings were as follow: Ar plasma gas flow, 15 L min^{-1}; Ar auxiliary gas flow, 0.86 L min^{-1}; Ar nebulizer gas flow, 1–1.1 L min^{-1}; radio frequency (RF) forward power, 1550 W. Acquisition parameters consisted in 10 replicates with 50 sweeps/replicate and integration time of 2 s

per isotope; m/z monitored mass were 77 and 78. External calibration was performed. Limits of quantification (based on ^{78}Se) were between 0.7 – 2.1 ng Se L^{-1}. Typical analytical precision was <5% (relative standard deviation, 10 replicates). Samples containing salinity >1 PSU were diluted up to ten times to avoid instrumental interferences or problems related to salt precipitation. For these diluted samples, LoQ was then increased up to 11 ng Se L^{-1} with the corresponding increase on the associated error up to a 14%.

2.3. Dissolved non-volatile Se speciation analysis

Chromatographic separation was carried with an Agilent 1200 HPLC pump hyphenated to ICP-MS. Most samples were analyzed using a porous graphitic carbon stationary phase (Thermo Hypercarb column 10 cm × 4.6 mm i.d) with a formic acid mobile phase (240 mmol L^{-1}, 1% methanol and pH 2.4 adjusted with ammonia), delivered at 1 mL min^{-1} flow rate. Standard addition was used for species quantification. Quantification limits (LoQ) were 3.6 – 7.1 ng Se L^{-1} for selenite and from 2.2 to 10.0 ng Se L^{-1} for selenite and selenate respectively for 300 µl injected volumes. Exceptionally samples of September 2017 were analyzed using the mixed-mode column OmniPac PAX-500 (Thermo, 25 cm x 4 mm i.d.) with a 20 mmol L^{-1} ammonium nitrate mobile phase containing 2% methanol at pH 8.0 (adjusted with ammonia), delivered at 1 ml min^{-1} flow rate. In this case, LoQ was 15.2 – 30.3 ng Se L^{-1} for selenite and 2.2 – 21.4 ng Se L^{-1} for Se(IV) and Se(VI) respectively. Duplicates of all samples were injected obtaining a relative standard deviation below 10%, except for some samples close to the LoQ for which rsd range was up to 15%. Due to high conductivity, samples at ST C and D of September required a tenfold dilution. The consequent the increase on quantification limits up to 30 ng Se L^{-1} for selenate and 21 ng Se L^{-1} for selenite, prevented detection and quantification of selenite and selenate. Chromatographic methods allowed the separation of selenite, selenate and selenomethionine and only selenate and selenite were detected. The operationally defined, reduced Se fraction (Red.Se), was then calculated by subtraction of species concentrations from the total dissolved Se concentration (Red.Se = TDSe – Se(IV) – Se(VI)). This fraction was used to estimate the contribution of Se(-II) and colloidal elemental Se (Se(0)) species to TDSe in water samples.

2.4. Volatile Se speciation analysis

Samples were purged with pure N_2 (500 mL min^{-1}) for 45 min. The resulting water vapor during the purge was condensed in a moisture trap maintained at –20 °C. The gas stream was then carried through a carbotrap column. After the purge, the glass columns were closed and

stored in the dark at 4 °C in a sealed double bag until analysis. In the laboratory, samples were analyzed using a GC-ICP/MS. Samples were thermo-desorbed from carbotraps at 250 ºC for 2 minutes under He flow (100 mL min^{-1}). Samples were flushed and trapped on the head of a Cryo GC column submerged in liquid N_2, prior to GC elution on Chromosorb SP2100 (Amouroux et al., 1998). An external calibration was carried out. The limits of quantification were between 1.3 – 3.8 pg Se L^{-1} for DMSe and DMSeS and, between 1.3 – 5.4 pg Se L^{-1} for DMDSe. Thermodesorption efficiency was controlled by carrying out two consecutive analyses of the same carbotrap column. Analysis of purge blanks were performed to estimate the efficiency of the sample treatment procedure. TVSe was determined as the sum of DMSe, DMSeS and DMDSe.

2.5. Statistical data treatment

For statistical treatment, a value of one half the quantification limit was assigned to selenite and selenate concentration in samples that did not contain quantifiable species level.

All sample sets were tested for normality using the Saphiro-Wilk test. Normally distributed samples were compared using parametric test such as t-test. In the other cases, non-parametric Mann-Whitney test was carried out. 2-tail tests were used to study significant differences among values, while 1-tail test was subsequently applied to statistically confirm if one value was significantly higher or not than other. These analyses were carried out using Origin 8 (Origin Lab Corporation).

3. Results

3.1. Hydro-biogeochemical characteristics, total Se and Se compounds in different types of estuarine waters

Water temperature was similar in all stations in May and September, in the range between 15 to 17 ºC; meanwhile in January temperature was lower in all stations, being in the range between 8 to 11 ºC. Due to inherent delay during sampling, some stations were sampled slightly after the low tide and exhibited higher salinity. Conductivity ranged from 0.15 ± 0.1 to 0.35 ± 0.1 mS cm^{-1} at Adour and Nive stations (ST 1, 2, 3 & 4), from 1.1 ± 0.4 to 2.1 ± 1.3 mS cm^{-1} at stations 6, 7, 8 and 9, and from 0.4 ± 0.04 to 13 ± 4 mS cm^{-1} at downstream stations (ST A, B, C and D) (Table Art.3.1). Nitrates, with a medium value of 118 µmol L^{-1} for the three sampling campaigns, represented more than 90% of inorganic nitrogen concentration (122 µmol L^{-1}).

Table Art.3.2. Raw data for parameters: temperature (temp.), dissolved oxygen (DO), conductivity (Cond.), nitrates (NO_3^-), phosphates (PO_4^{3-}), sulfates (SO_4^{2-}), dissolved organic carbon (DOC) and chlorophyll a (Chl-a).

Station	Temp.	DO	Cond.	NO_3^-	PO_4^{3-}	SO_4^{2-}	DOC	Chl-a
	(°C)	(mg L^{-1})	(mS cm^{-1})	(µmol L^{-1})	(µmol L^{-1})	(mmol L^{-1})	(mg L^{-1})	(µg L^{-1})
May 2017								
1	15.2	9.6	0.2	120	0.5	0.2	1.1	2.22
2	15.5	7.4	0.3	135	0.7	0.3	4.1	2.95
3	15.2	7.0	0.2	60	0.4	0.3	2.5	1.85
4	17.3	8.0	0.4	66	0.5	0.3	0.3	1.11
A	14.8	7.0	10.0	100	0.6	7.9	5.5	3.32
B	14.6	7.3	17.0	101	0.8	10.8	5.8	1.39
C	15.0	No data	9.9	118	0.9	7.7	4.9	1.11
D	14.9	No data	15.2	104	0.9	9.4	5.0	1.39
7	17.5	8.2	2.6	85	0.3	1.1	18.0	1.9
8	17.8	10.8	2.8	143	0.6	1.8	20.6	3.1
6	16.3	9.5	0.2	249	1.1	0.5	4.9	5.5
9	13.9	9.7	2.9	43	0.6	2.6	8.5	8.9

Table Art.3.2. (Continued)

Station	Temp. (°C)	DO (mg L^{-1})	Cond. (mS cm^{-1})	NO_3^- (µmol L^{-1})	PO_4^{3-} (µmol L^{-1})	SO_4^{2-} (mmol L^{-1})	DOC (mg L^{-1})	Chl-a (µg L^{-1})
September 2017								
1	16.2	7.7	0.4	124	0.8	0.5	2.1	1.51
2	16.5	7.7	0.5	119	1.0	0.5	2.3	1.92
3	14.9	9.9	0.3	65	0.4	0.4	1.1	1.08
4	15.0	8.6	0.2	70	0.4	0.4	1.0	1.33
A	15.2	8.3	2.1	405	13.3	3.0	1.5	1.66
B	16.8	7.7	2.2	98	0.3	0.9	2.2	1.85
C	17.2	7.5	8.9	128	0.8	10.4	1.9	1.11
D	17.9	7.1	18.2	95	0.1	21.2	1.7	1.11
7	17.7	7.7	0.9	112	1.1	0.8	3.6	9.2
8	15.3	6.9	2.0	102	1.4	1.8	3.6	2.8
6	20.8	7.0	3.5	75	0.9	1.4	5.8	2.2
9	15.6	8.5	0.8	78	0.9	0.7	6.2	4.6

Table Art.3.2. (Continued)

Station	Temp. (°C)	DO (mg L^{-1})	Cond. (mS cm^{-1})	NO_3^- (µmol L^{-1})	PO_4^{3-} (µmol L^{-1})	SO_4^{2-} (mmol L^{-1})	DOC (mg L^{-1})	Chl-a (µg L^{-1})
January 2018								
1	8.7	9.9	0.4	144	0.3	0.2	1.5	1.01
2	8.5	10.8	0.4	199	0.5	0.3	2.3	1.94
3	9.6	11.3	0.3	68	0.4	0.1	0.7	1.02
4	9.2	11.4	0.3	No data	No data	0.1	0.6	0.40
A	8.3	10.3	0.4	184	0.5	0.2	3.0	1.11
B	8.2	10.4	0.4	202	0.6	0.3	3.3	1.39
C	8.2	10.3	0.4	424	0.5	0.3	3.3	1.85
D	8.2	10.4	0.5	198	0.4	0.3	3.0	1.66
7	9.9	9.4	0.8	125	0.2	0.7	3.2	1.5
8	10.6	9.0	1.28	415	0.6	1.1	3.3	0.9
6	14.7	7.6	1.7	304	59.5	1.2	4.1	1.6
9	7.9	10.7	0.8	107	1.6	0.5	11.2	1.1

Phosphate highest concentration was found at ST 6 in January 2018 (60 µmol L^{-1}), because of the proximity to the WWTP outlet; however in general, values were <1.2 µmol L^{-1}. The ratio N/P was in the range between 68 to 298, thus phosphorus was the limiting nutrient in the estuary (Deborde, 2019). Dissolved organic carbon (DOC) showed median values of 1.3, 3.2 and 5.3 mg L^{-1} at upstream, downstream and industrial effluent waters respectively. Stations of effluent waters group presented slightly higher temperature and dissolved organic carbon (DOC) than other stations (see Table Art.3.2). Meanwhile, pH and oxygen saturation rates were below the values at other stations at the same season (Deborde, 2019). Chl-a concentration was in the range from 0.4 to 3.0 µg L^{-1} in upstream waters, from 1.1 to 3.3 µg L^{-1} in downstream waters and in the range from 0.9 to 9.2 µg L^{-1} in effluent waters (Table Art.3.2).

Total Selenium in waters: As previously highlighted, different Se total concentrations and species distribution patterns are expected depending on water body types: upstream waters, effluents and downstream waters. In average, 91% of Se was in the dissolved phase. Using the non-parametrical Mann-Whitney statistical test, bulk and dissolved total Se concentrations were compared. Considering all samples, no statistical differences were found between total Se bulk and dissolved Se, however at industrial effluents a difference of up to 189 ng Se L^{-1} was found, which indicates the presence of particulate Se. Data for total Se bulk can be found at Table Art.3.3.

Adour and Nive Rivers upstream waters showed an average TDSe of 118 ± 42 ng Se L^{-1}. Adour River total Se content (123 – 200 ng L^{-1}) was however significantly higher than Nive River (71 – 96 ng L^{-1}) (MW 2–tail test (α=0.05): Z=2.8, P<0.03) (Table Art.3.3). This difference may be directly linked to two factors. First, the size of each basin, being Adour (~16,900 km^2) larger than Nive basin (~1,000 km^2). Second, the different land use of each basin. A simple linear regression estimation of TDSe vs nitrate concentrations showed the strong dependence between Se concentration arriving to the estuary and the potential land-use in each watershed (R^2=0.91, P<0.01) (Figure Art.3.2). A recent study of trace elements inputs in French agricultural soils demonstrated that Se input to soil is directly related to mineral fertilizers and, in a lesser extent, to effluents from animal breeding and intensive livestock (Belon et al., 2012). Adour River runs through agricultural and livestock farm areas, which is thus consistent with higher nitrate and Se concentrations. Nive river runs mainly through forested areas, therefore, the input of Se is expected to be lower as Se water extractability from forest

soils has been shown to be lower compared to agricultural ones due both to higher pH and addition of phosphates by fertilizers for the latter (Di Tullo, 2015; Nakamaru et al., 2006). In addition, Figure Art.3.2 clearly shows the differences between both river systems. Nive upstream samples corresponding to the lowest range of TDSe and nitrate concentrations, showed very low dispersion among seasons; while Adour samples with higher concentrations of both nitrate and TDSe, presented higher dispersion, associated to higher riverine discharge in January. It would be expected to find a similar correlation with phosphates. However, the role of phosphorus as limiting nutrient (Deborde, 2019) and its rapid uptake in river and estuarine waters may explain the lack of correlation. To better elucidate Se origin, the molar concentrations and Se/N ratio at Adour and Nive rivers were compared to data obtained from Pyrenean lakes and rainwaters (Roulier et al., submitted 2020). The results, presented in Table Art.3.SI 1, show first that mean TDSe concentration is higher in Adour (1.81 nM) and Nive (1.06 nM) rivers than in headwaters of the basin (Pyrenees lakes, 0.26 nM) and rainwaters (0.60 nM). Therefore, an additional Se input is required to explain the enrichment found in both rivers. Nitrate concentration observed at Adour and Nive rivers was 5 to 20 times higher than the ones observed at Pyrenean lakes and rainwaters. The molar ratio Se/N found in rivers was thus lower than values calculated in headwaters and rain. Therefore, it is clearly possible that the addition of Se containing fertilizers can increase the input of Se in the river water of the Adour (and Nive) watershed.

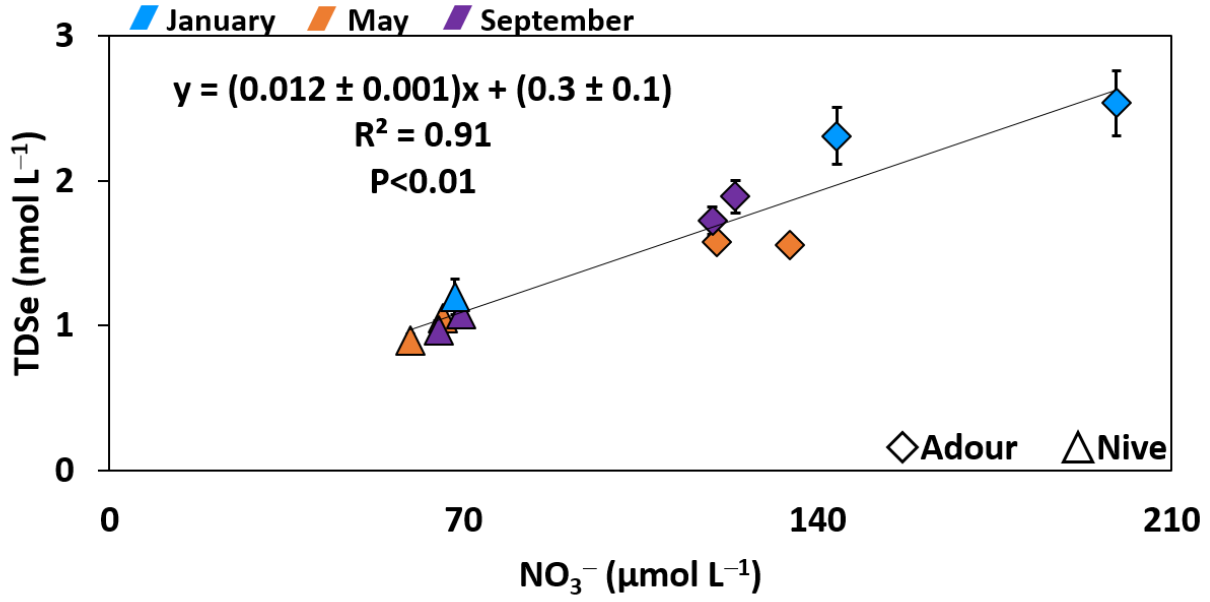

Figure Art.3.2. Correlation between Nitrate (x axis, µmol L^{-1}) and Total dissolved Se (TDSe, y axis, nmol L^{-1}) concentrations for Adour (diamond) and Nive (triangle) upstream stations.

Samples correspond to May 2017 (orange), September 2017 (purple) and January 2018 (blue).

Selenium speciation in waters: Concerning non-volatile Se speciation, selenite concentration was in average 20 ± 7 and 9 ± 7 ng Se L^{-1}, selenate was 72 ± 36 and 36 ± 18 ng Se L^{-1} and Red.Se averaged 62 ± 7 and 39 ± 15 ng Se L^{-1} for Adour and Nive upstream samples, respectively. Despite the differences in concentration values, similar species distribution pattern was found in both rivers. At Adour R., selenite represented 13% of TDSe, while selenate was 47% and reduced Se 40%. For Nive R., the percentages were 11, 43 and 46% for Se(IV), Se(VI) and Red.Se respectively. No additional compounds were detected with the applied speciation method. Total volatile Se averaged 139 ± 46 pg Se L^{-1} in Adour River upstream samples and detected species were DMSe (67%), DMSeS (29%) and DMDSe (4%). For Nive River upstream samples, TVSe concentration averaged 93 ± 25 pg Se L^{-1}, and was composed of 55% DMSe, 42% DMSeS and 3% DMDSe (Table Art.3.4).

For downstream estuarine waters (ST A, B, C & D), TDSe concentration averaged 139 ± 49 ng Se L^{-1} within the range 78 – 208 ng Se L^{-1} (Table Art.3.3). No significant differences were found downstream stations sampled at low tide and upstream waters described above. This result confirms that the main input of Se to the downstream estuary is dominantly influenced by the Adour River with a non-negligible contribution of Nive River corresponding to their respective riverine discharge. At downstream waters, selenite concentration averaged 15 ± 5 (11% of TDSe) ng Se L^{-1}, selenate 57± 45 (41%) ng Se L^{-1} and Red.Se averaged 67 ± 33 (48%) ng Se L^{-1}. Therefore, half of Se present at downstream estuary was a pool of unidentified species for all seasons. The presence of reduced and/or colloidal Se species is mainly related to the aquatic biological activity, as well as for the production of volatile compounds. Total volatile Se concentration was significantly higher in downstream waters than in river waters (MW 1-tail test (α=0.05): Z=2.6, P<0.01), , with a TVSe concentration of 319 ± 251 pg Se L^{-1}, being DMSeS the main species (67%), followed by DMSe (32%) and a minor contribution of DMDSe (<4%) (Table Art.3.4). These results also show that DMSeS sources increase within estuarine water while DMSe extent is less variable compared to upstream waters.

Table Art.3.3. Selenium speciation concentration ranges at different estuaries, including data obtained in this study. Data includes: total Bulk and dissolved Se (TDSe), selenite, selenate and estimated reduced Se (Red.Se) concentrations; Data in ng L^{-1}. The error correspond to the standard deviation of the samples.

Site	TSe Bulk	TDSe	Se(IV)	Se(VI)	Red.Se	References
San Francisco Bay		48 – 358	16 – 133	<1 – 218	<1 – 196	(Cutter, 1989; Cutter & San Diego-McGlone, 1990)
Chesapeake Bay, USA		71 – 151	43 – 136	15 – 28		(Takayanagi & Wong, 1984)
KrKa, Croatia		9 – 204				(Seyler & Martin, 1991)
Rhône, France		58 – 190	5 - 76	23 – 92		(Guan & Martin, 1991)
Kaoping, Taiwan		47 – 95	<5 – 22	13 – 67	5 - 50	(Hung & Shy, 1995)
Erhjen, Taiwan		63 – 83	<5 – 75	<5 – 24	<5□40	
Zhujiang, China		63 – 392	22 – 225	47 – 257		(Yao et al., 2006)
Changjiang, China		28 – 375	25 – 90	42 – 76		(Wu et al., 2014) (Chang et al., 2016)
Adour R.	135 – 245	123 – 200	11 – 31	44 – 123	54 – 71	
Nive R.	71 – 134	71 – 96	1 – 19	17 – 60	26 – 63	
Downstream waters	85 – 269	78 – 208	9 – 2	<LoQ – 120	39 – 150	This study
Urban effluents	176 – 430	126 – 345	<LoQ – 31	48 – 228	<LoQ – 108	
Industrial effluents	380 – 859	365 – 670	13 – 49	236 – 602	<LoQ – 146	
Adour estuary average (n=36)	**232 ± 184**	**205 ± 153**	**17 ± 10**	**125 ± 141**	**91 ± 62**	**This study**

Table Art.3.4. Volatile Se speciation range data by water type from this study and literature data for other study sites. Data is given in pg Se L^{-1} with error expressed for the average values as the standard deviation between all samples (n=36). Data for volatile speciation for other study sites is given as % of TVSe and includes dimethylselenide (DMSe), dimethyl selenide sulphide (DMSeS) and dimethyldiselenide (DMDSe).

Site	TVSe	DMSe	DMSeS	DMDSe	Reference
	(pg Se L^{-1})				
Adour R.	83 – 208	46 – 141	14 – 59	<LoQ – 8	
Nive R.	50 – 120	21 – 102	13 – 91	<LoQ – 7	
Downstream waters	92 – 775	57 – 177	20 – 675	3 – 32	This study
Urban effluents	204 – 2646	97 – 693	46 – 1669	8 – 20	
Industrial effluents	436 – 2212	83 – 360	80 – 2066	36 – 69	
Site	**TVSe (pg Se L^{-1})**	**DMSe (%)**	**DMSeS (%)**	**DMDSe (%)**	**Reference**
Adour estuary average (n=36)	**436 ± 565**	**51 ± 22**	**46 ± 24**	**4 ± 3**	**This study**
Rhine estuary	37 – 2,423	*73%*	*23%*	*4%*	(Tessier et al., 2002)
Scheldt estuary	51 – 8,067	*84%*	*12%*	*4%*	
Gironde estuary	22 – 1,351	*82%*	*13%*	*5%*	(Amouroux & Donard, 1997; Tessier et al., 2002)
Seine estuary	317 – 4,855	*94%*	*4%*	*3%*	(Lanceleur et al., 2019)
Arcachon Bay	30 – 426	*81%*	*14%*	*5%*	(Lanceleur et al., 2019)
Norway Bay	12 – 156	*79%*	*21%*	*n.d.*	

n.d.: not detected

Samples from tributaries impacted by industrial effluents averaged TDSe concentration of 495 ± 140 ng Se L^{-1} (ST 7 and ST 8) while waters directly influenced by urban wastewater treatment plants averaged 218 ± 76 ng Se L^{-1} (ST 6 and ST 9), TDSe concentration is thus significantly higher (MW 1-tail test (α=0.05): Z=3.7, P<0.01) at these stations compared to upstream and downstream stations. Despite elevated Se concentration, the limited flow of these small tributaries or effluents did not significantly impacted Se concentration of estuarine waters considering their respective water discharge (Point, 2004). At urban and industrial locations the main species detected was always selenate and the presence of selenite was residual representing <10% of TDSe. Urban WWTP samples showed 138 ± 62 (63%), 18 ± 11 (8%), and 95 ± 75 (43%) ng Se L^{-1} for Se(VI), Se(IV) and Red.Se respectively. Industrial effluents averaged 388 ± 147 (78%), 27 ± 13 (5%) and 142 ± 112 (29%) ng Se L^{-1} for selenate, selenite and reduced Se species (Table Art.3.3). Such stations exhibited also important levels of volatile Se species. Effluent waters presented high variability in TVSe concentration in the range 204 – 2646 pg Se L^{-1}. Total volatile Se concentration was significantly higher at urban and industrial stations than in upstream and downstream stations (MW 1-tail test (α=0.05): Z=-3.8, P<0.001). Those stations are characterized by high dissolved organic matter linked to the presence of bacteria and hydrophilic microbes (Deborde, 2019). The overall conditions of effluent waters may possibly promote the microbial production of volatile Se compounds as shown in other estuarine systems (David Amouroux & Donard, 1997).

Total dissolved Se concentration range at Adour estuary is similar to other European estuaries (see Table Art.3.3). Concentrations reported for the Rhône estuary (France) were 58 – 190 ng L^{-1} for total Se, 5 – 76 ng Se L^{-1} for selenite and, 23 – 92 ng Se L^{-1} for selenate (Guan & Martin, 1991). Estuarine waters from the San Francisco Bay (USA) are well recognized for their elevated Se content due to Se-rich soil erosion and industrial inputs (GA Cutter, 1989). In this estuarine system, total dissolved Se concentration was reported in the range 48 – 358 ng Se L^{-1}, while selenite ranged from 16 to 133 ng Se L^{-1}, and Se(VI) from <1 to 218 ng Se L^{-1} (Cutter, 1989; Cutter & San Diego-McGlone, 1990). For volatile Se there is even less information. Lanceleur et al. (2019) reviewed the existing data for European estuaries. Concentrations of total volatile Se compounds at European estuaries ranged from 22 to 8,067 pg Se L^{-1} (detailed data in Table Art.3.4) for the estuarine systems: Seine, Scheldt, Rhine and Gironde. At such systems, more than 80% of TVSe corresponds to DMSe. While the Adour estuary has similar TVSe concentrations than other European systems, the percentage of species is somehow

different (Table Art.3.4). In average, at upstream waters, 61% of TVSe was detected as DMSe and DMSeS represented 36%. At downstream waters, the main species was DMSeS (54%) followed by DMSe (46%). In effluent waters group, TVSe was composed of 45% of DMSe and 48% of DMSeS. In all samples, DMDSe represented less the 13% of TVSe.

In conclusion, important spatial variations of TDSe concentration exist at Adour estuary. Adour R. showed higher TDSe concentration than the Nive River, which is further reflected in downstream waters, showing intermediate concentrations as compared to both river systems. Industrial and urban effluent waters presented the highest TDSe concentration, however due to low riverine discharge the effect on estuarine waters is negligible. Speciation studies have shown that an important fraction of dissolved Se remains unidentified, either as colloidal Se(0) or reduced Se species. The proportion of reduced Se pool increased close to the ocean, most probably due to higher and more autotrophic biological activity favoring Se uptake and reduction. A similar trend was observed for TVSe, presenting higher concentration at downstream than in upstream waters. The concentration of volatile Se was similar to other estuaries; however, in the Adour estuary higher proportion of DMSeS was observed compared to other systems. The highest volatile Se compounds concentrations observed at urban and industrial waters is most probably associated to higher TDSe concentration and the presence of higher dissolved organic carbon, and higher biomethylation rates due to phytoplankton and bacteria populations.

The differences found between Se and nitrate concentration and their molar ratio in both Adour and Nive rivers compared to the headwaters of the basin and rainwaters, seem to be related to the use of Se containing fertilizers and animal effluents in French soils (Belon et al., 2012). Therefore, anthropogenic inputs are a source of Se to estuarine waters and to the Atlantic Ocean.

3.2. Non volatile and volatile dissolved Se speciation among different seasons in different estuarine water bodies

In all stations total bulk and dissolved Se as well as selenate concentrations showed maximum values in January compared to May and September sampling. Total dissolved Se concentration in upstream waters averaged 124 ± 1, 143 ± 9, 191 ± 13 ng Se L^{-1} at Adour River and 77 ± 8, 81 ± 6, 95 ± 1 ng Se L^{-1} at Nive River for May, September and January, respectively. Total dissolved Se in downstream waters averaged 95 ± 7, 127 ± 41 and 196 ± 13 ng Se L^{-1} for May, September and January respectively (Fig. Art.3.3, Table Art.3.5). Concentration in

downstream waters was indeed highly influenced by Adour R. Se content. Due to rainy events, occurring more frequently during winter–spring seasons (https://fr.climate-data.org); riverine discharge was higher in January. A similar behavior was observed in San Francisco Bay with higher Se concentration in winter, when river discharge was also higher, thus implying a close relationship to watershed runoff.

Samples from Adour R. showed minimum TDSe (124 ± 1 ng Se L^{-1}) concentration in May, with composition of 36% of Se(VI), 14% of Se(IV) and 50% of Red.Se fraction. In September TDSe increased to 143 ± 9 ng Se L^{-1} with 36% of Se(VI), 20% of Se(IV) and 44% of Red.Se. January presented the highest TDSe concentration (191 ± 13 ng Se L^{-1}) composed of 62% of selenate, 7% of selenite and 31% of Red.Se species. Nive River showed the same trend of TDSe according to sampling period (Fig. Art.3.3). However, the proportion of selenite was only 3% in May. In downstream waters, analyses of samples of stations C and D in September were below the LoQ due to higher salinity, thus a focus is done for May and January samples. Selenite represented 15 % of TDSe in May and decreased to 5% in January. Meanwhile, selenate represented 39% of TDSe in May and increased to 58% in January. Estimated reduced Se fraction varied among stations and seasons without a clear trend. Urban waters showed increasing concentrations of TDSe from 190 ± 20 in May to 355 ± 105 ng Se L^{-1} in January (average values from both urban WWTP stations), therefore large standard deviation reflects the differences between industrial and urban waters. At downstream stations, selenite concentrations were similar in May and September in the range 21 – 28 ng Se L^{-1} and were lower in January. Selenate represented 46% of TDSe in May (73 ± 34 ng Se L^{-1}), and accounted for 76% and 63% at September and January.

The increase of selenite during low riverine discharge periods has been reported in other studies (Cutter & San Diego-McGlone, 1990). However, refineries effluents in which the main Se species was selenite, highly influenced the estuarine Se content in the San Francisco Bay. In the Adour estuary, effluents represent a small input of Se to the estuary; in addition, effluents are composed mainly of selenate (Fig. Art.3.3). At downstream waters the increase of selenite and the reduced Se fraction ratios from January to the end of summer (September) were coincident to the growth of phytoplankton polutations during spring and summer (Deborde, 2019). Moreover, since the water is permanently over 80% of oxygen saturation, potential microbial reduction of selenate to selenite can only be expected in a lesser extent in more reducing conditions occurring in fine sediment deposits in the estuary. A positive ?

correlation between chlorophyll-a and selenite concentrations was obtained considering all samples, with R^2=0.33 (P<0.01). Previous studies have also shown that phytoplankton such as diatoms growth can be stimulated in the presence of organic Se in laboratory cultures (Lindström, 1983). At Adour estuary, the silicate concentration decreased during spring and summer periods, which indicates the presence of diatoms as one of the main phytoplankton species at the rivermouth (Deborde, 2019), thus diatoms could be the producers of selenite and reduced Se species in the estuary. Consequently, Se transformation could be partially linked to the uptake of Se by phytoplankton, production of selenite and potentially reduced Se species and further release to the water.

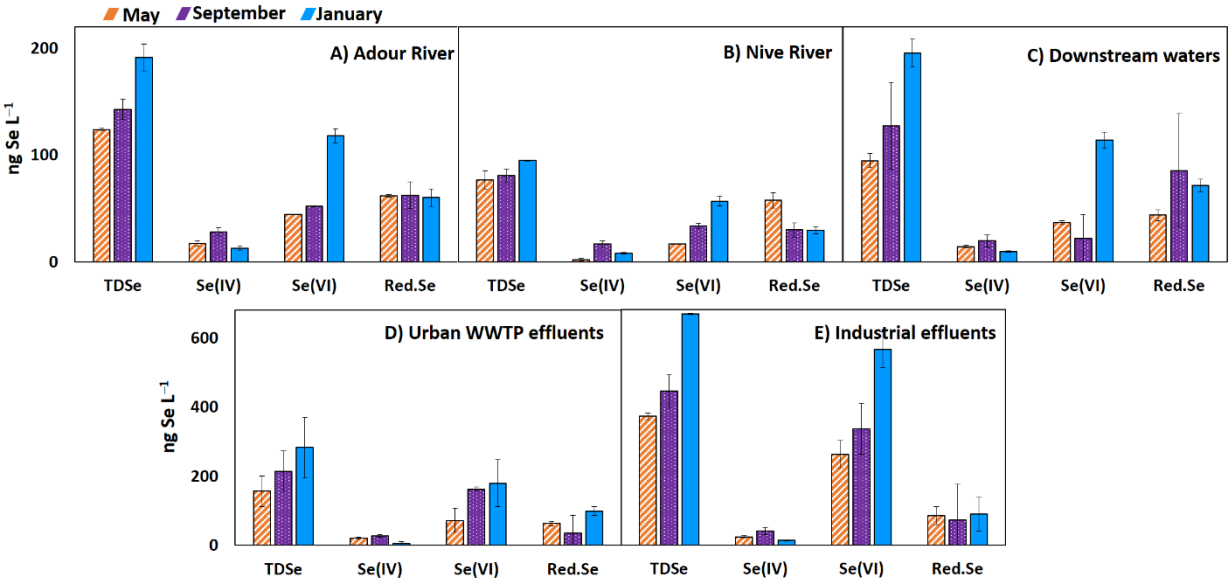

Figure Art.3.3. Seasonal variations of non-volatile dissolved Se speciation. May is represented as diagonal barred pattern (orange), September in pointed (purple) pattern and January as straight (blue) pattern. The results are expressed as the average for sampled stations at A) Adour River (n=2), B) Nive River (n=2), C) Downstream waters (n=4), D) Urban WWTP effluents (n=2) and E) Industrial effluents (n=2). The error was calculated as the standard deviation. Data presented corresponds to: total dissolved Se (TDSe), selenite (Se(IV)), selenate (SeVI)) and reduced Se (Red.Se) expressed in ng Se L^{-1}.

Volatile Se showed very different total concentrations and speciation depending on water type and season (Fig. Art.3.4). Upstream and downstream waters showed higher total volatile Se concentration during spring–summer compared to winter period as previously reported in other macrotidal estuaries (Tessier et al., 2002). At Adour River the highest concentration of TVSe was detected in September (in average 191 ± 24 pg Se L^{-1}), and DMSe was the main

species present during the period of study (Table Art.3.4). At Nive R., concentration of TVSe did not show significant seasonal variation, however if the main component was DMSe (87 ± 22 Se L^{-1}) in January, DMSeS was predominant in May, and the concentrations of both species were similar in September (Fig. Art.3.4). Dimethyl diselenide at upstream waters was not detected or close to the LoQ with no exceptions. Considering both basin characteristics, and the similar amounts of sulfate measured in both rivers, the differences of volatile Se compounds ratio suggest different biomethylation processes occurring at both basins. Our dataset is not large enough to establish a correlation between selenite and total volatile production (Fig. Art.3.SI 1), however the high rates of volatile compoundsproductivity during spring should be further investigated. Therefore, we can only suggest that the additional input of Se and other mineral from farm and livestock production (Belon et al., 2012) to the water at Adour R., may be promoting the production of DMSe in higher extents than at Nive River.

The concentration of volatile species in downstream waters was intermediary between those in upstream waters and urban and industrial effluents. Industrial effluents, containing mainly selenate (≥ 60%), showed TVSe production maximum in May with an average concentration of 625 ± 164 pg Se L^{-1} (n=4) as shown in Table Art.3.SI 1. In May, the main component was DMSeS accounting for 78% of TVSe. In September, concentrations of DMSe and DMSeS were similar and DMSe was the predominant species in January. Figure Art.3.SI 1 shows the evolution of total volatile Se versus the ratio Se(IV)/TDSe. In the plot a higher TVSe concentration in estuarine waters, especially in May is observed, thus indicating that volatile compounds formation takes place in situ at downstream waters, more markedly in spring due to higher productivity of the water.

In urban waters, TVSe concentration oscillated from 434 ± 268 – 620 ± 312 pg Se L^{-1} during spring and summer. The larger production of DMSe and, especially DMSeS in January resulted in total concentration of 1425 ± 1727 pg Se L^{-1} (Table Art.3.4). The high standard deviation indicates the differences between both stations monitored. Industrial effluents showed the highest TVSe concentration in May (1741 ± 666 pg Se L^{-1}) and similar values in September and January (501 – 520 pg Se L^{-1}). The production of volatile Se species at urban WWTP and industrial effluents was not linked to seasonal variations of physicochemical or hydrogeochemical parameters. However, industrial and urban WWTP effluents were the source of dissolved organic carbon at downstream waters (Deborde, 2019).

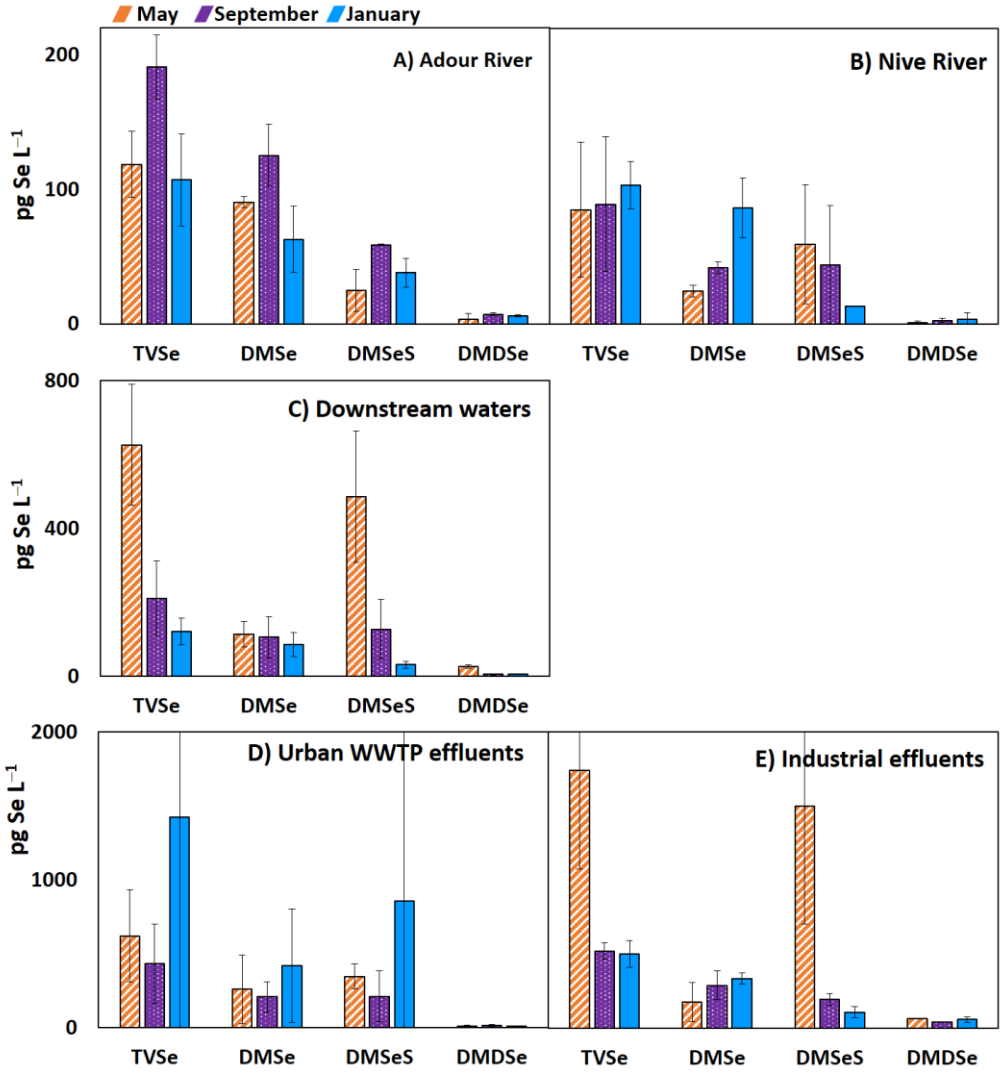

Figure Art.3.4. Seasonal variations of total volatile Se and volatile Se speciation. May is represented as diagonal barred pattern (orange), September in pointed (purple) pattern and January as straight (blue) pattern. The results are expressed as the average for sampled stations at A) Adour River (n=2), B) Nive River (n=2), C) Downstream waters (n=4), D) Urban WWTP effluents (n=2) and E) Industrial effluents (n=2). The error was calculated as the standard deviation. Data presented corresponds to: total volatile Se (TVSe), dimethylselenide (DMSe), dimethyl selenide sulphide (DMSeS) and diselenide (DMDSe) expressed as pg Se L^{-1}.

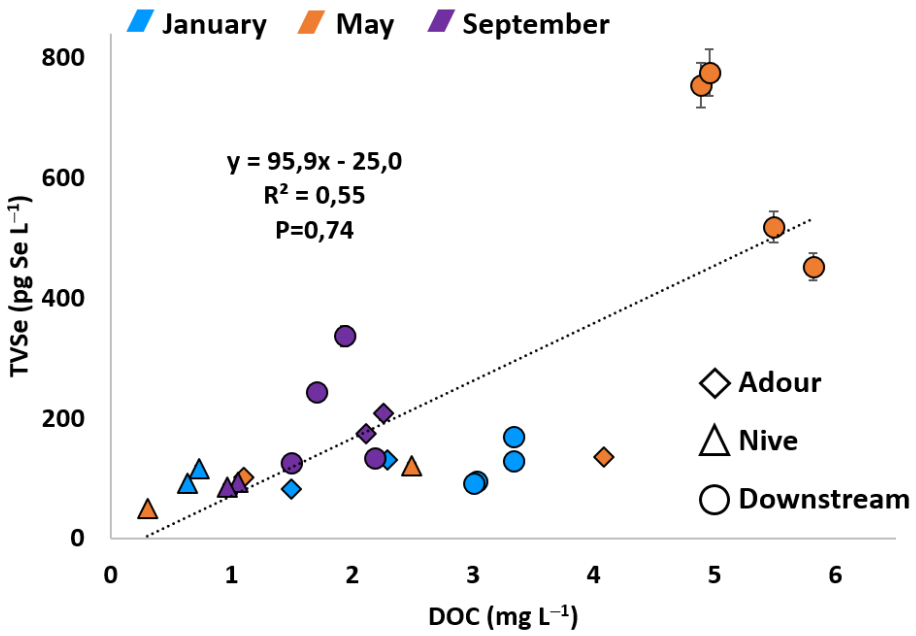

Figure Art.3.5. Total volatile Se vs dissolved organic carbon for upstream and downstream waters.

An additional study was carried out in September 2018 to examine how the tide affects Se concentration, especially in the downstream waters. The results are presented in Table Art.3.SI 2 and Figure Art.3.6. Concentration of TDSe was between 136 ± 8 and 163 ± 15 ng Se L^{-1}. Despite slightly higher TDSe concentration at low tide, in other words, higher concentration in the river water than in seawater, the variation is not enough to be statistically significant. Regarding speciation, no differences were found for selenate, which average concentration was 41 ± 6 ng Se L^{-1}. However, relative to TDSe the contribution of selenate was around 42% at salinity below 9 psu, while at higher salinity it was reduced by half (19%). Selenite contribution (in percentage) to TDSe barely changed with salinity, however its concentration increased with salinity being in the range of 24 – 63 ng Se L^{-1}. In fact, concentration at high tide are similar to those previously reported at North Atlantic Ocean (34 – 51 ng Se L^{-1}) (Measures & Burton, 1980b). Concentration of TVSe was higher at high tide (Fig. Art.3.6), varying from 102 ± 5 pg Se L^{-1} to 290 ± 15 pg Se L^{-1}. The increase of TVSe was due almost exclusively to the higher production of the mixed Se–S species DMSeS as previously documented in Atlantic oceanic waters (Amouroux et al., 2001).

Table Art.3.5. Raw data for total Se Bulk (TSe Bulk), total dissolved Se (TDSe), selenite, selenate and Reduced Se (Red.Se) expressed as ng Se L^{-1}. Data for total volatile Se (TVSe), dimethylselenide (DMSe), dimethyl selenide sulphide (DMSeS) and dimethyl diselenide (DMDSe) expressed in pg Se L^{-1}.

Station	TSe bulk	TSe diss	Se(IV)	Se(VI)	Red.Se	TVSe	DMSe	DMSeS	DMDSe
				May 2017					
ST 1	135 ± 10	125 ± 3	19 ± 2	44 ± 2	61 ± 4	101 ± 5	88 ± 4	14 ± 1	<LoQ
ST 2	149 ± 11	123 ± 4	16 ± 1	44 ± 2	63 ± 5	136 ± 7	94 ± 5	36 ± 2	6.3 ± 0.3
ST 3	84 ± 6	71 ± 3	<LoQ	17 ± 1	52 ± 3	120 ± 6	28 ± 1	91 ± 5	2.0 ± 0.1
ST 4	93 ± 6	83 ± 3	3.3 ± 0.4	17 ± 1	63 ± 3	50 ± 2	21 ± 1	28 ± 1	<LoQ
ST A	111 ± 10	87 ± 6	13 ± 2	36 ± 2	39 ± 6	519 ± 26	93 ± 5	404 ± 20	22 ± 1
ST B	117 ± 7	92 ± 4	15 ± 2	37 ± 2	40 ± 5	452 ± 23	141 ± 7	279 ± 14	32 ± 2
ST C	120 ± 10	99 ± 7	15 ± 2	35 ± 2	49 ± 8	754 ± 38	143 ± 7	584 ± 29	28 ± 1
ST D	118 ± 11	101 ± 10	15 ± 2	39 ± 2	47 ± 11	775 ± 39	75 ± 4	675 ± 34	25 ± 1
ST 7	385 ± 29	365 ± 14	26 ± 1	235 ± 11	104 ± 18	1270 ± 63	269 ± 13	937 ± 47	64 ± 3
ST 8	398 ± 28	379 ± 14	22 ± 2	290 ± 14	66 ± 20	2212 ± 111	83 ± 4	2066 ± 103	64 ± 3
ST 6	204 ± 15	126 ± 4	19 ± 1	48 ± 2	59 ± 5	841 ± 42	425 ± 21	406 ± 20	9.8 ± 0.5
ST 9	176 ± 15	188 ± 14	23 ± 5	97 ± 5	68 ± 15	400 ± 20	97 ± 5	288 ± 14	15 ± 1

Table Art.3.5. (Continued)

Station	TSe bulk	TSe diss	Se(IV)	Se(VI)	Red.Se	TVSe	DMSe	DMSeS	DMDSe
				September 2017					
ST 1	138 ± 8	149 ± 9	26 ± 2	52 ± 1	71 ± 9	174 ± 9	109 ± 5	59 ± 3	6.5 ± 0.3
ST 2	137 ± 8	136 ± 8	31 ± 2	52 ± 1	54 ± 8	208 ± 10	141 ± 7	58 ± 3	7.9 ± 0.4
ST 3	71 ± 5	77 ± 5	19 ± 1	32 ± 1	26 ± 5	93 ± 5	44 ± 2	46 ± 2	3.0 ± 0.2
ST 4	86 ± 6	85 ± 5	15 ± 1	36 ± 1	35 ± 5	86 ± 4	41 ± 2	42 ± 2	2.7 ± 0.1
ST A	85 ± 6	78 ± 5	26 ± 2	<LoQ	40 ± 12	126 ± 6	63 ± 3	60 ± 3	3.1 ± 0.2
ST B	110 ± 8	122 ± 7	23 ± 2	55 ± 1	44 ± 7	134 ± 7	61 ± 3	66 ± 3	7.7 ± 0.4
ST C	130 ± 11	133 ± 10	<LoQ	<LoQ	107 ± 21	337 ± 17	177 ± 9	154 ± 8	5.7 ± 0.3
ST D	122 ± 10	177 ± 15	<LoQ	<LoQ	150 ± 24	244 ± 12	122 ± 6	229 ± 11	4.3 ± 0.2
ST 7	427 ± 25	479 ± 25	49 ± 4	285 ± 4	146 ± 26	559 ± 28	356 ± 18	166 ± 8	36 ± 2
ST 8	380 ± 22	409 ± 21	34 ± 3	389 ± 5	<LoQ	482 ± 24	220 ± 11	222 ± 11	40 ± 2
ST 6	205 ± 11	173 ± 10	31 ± 2	167 ± 2	0 ± 10	623 ± 31	282 ± 14	333 ± 17	8.4 ± 0.4
ST 9	219 ± 13	256 ± 14	26 ± 2	158 ± 2	72 ± 14	244 ± 12	135 ± 7	89 ± 4	20 ± 1

Table Art.3.5. (Continued)

Station	TSe bulk	TSe diss	Se(IV)	Se(VI)	Red.Se	TVSe	DMSe	DMSeS	DMDSe
				January 2018					
ST 1	240 ± 13	182 ± 15	15 ± 2	113 ± 7	54 ± 17	83 ± 4	46 ± 2	30 ± 2	6.7 ± 0.3
ST 2	245 ± 12	200 ± 18	11 ± 1	123 ± 7	66 ± 19	131 ± 7	80 ± 4	46 ± 2	5.5 ± 0.3
ST 3	126 ± 6	95 ± 10	9 ± 1	54 ± 3	32 ± 10	116 ± 6	102 ± 5	14 ± 1	<LoQ
ST 4	134 ± 10	95 ± 9	8 ± 1	60 ± 4	27 ± 10	91 ± 5	71 ± 4	13 ± 1	6.9 ± 0.4
ST A	210 ± 10	177 ± 16	10 ± 1	103 ± 6	64 ± 17	95 ± 5	71 ± 4	20 ± 1	3.7 ± 0.2
ST B	237 ± 11	199 ± 17	9 ± 1	116 ± 7	74 ± 18	170 ± 9	132 ± 7	34 ± 2	4.4 ± 0.2
ST C	269 ± 12	208 ± 18	11 ± 1	120 ± 7	78 ± 19	129 ± 6	81 ± 4	43 ± 2	5.2 ± 0.3
ST D	259 ± 13	199 ± 17	9 ± 1	118 ± 7	72 ± 18	92 ± 5	57 ± 3	29 ± 1	6.3 ± 0.3
ST 7	846 ± 32	666 ± 37	15 ± 2	527 ± 29	124 ± 47	565 ± 28	360 ± 18	132 ± 7	69 ± 3
ST 8	859 ± 31	670 ± 37	13 ± 2	602 ± 33	55 ± 50	436 ± 22	309 ± 15	80 ± 4	43 ± 2
ST 6	281 ± 15	222 ± 13	<LoQ	132 ± 8	90 ± 15	2646 ± 132	693 ± 35	1669 ± 83	10 ± 1
ST 9	430 ± 20	345 ± 21	9 ± 1	228 ± 13	108 ± 25	204 ± 10	150 ± 7	46 ± 2	8.3 ± 0.4

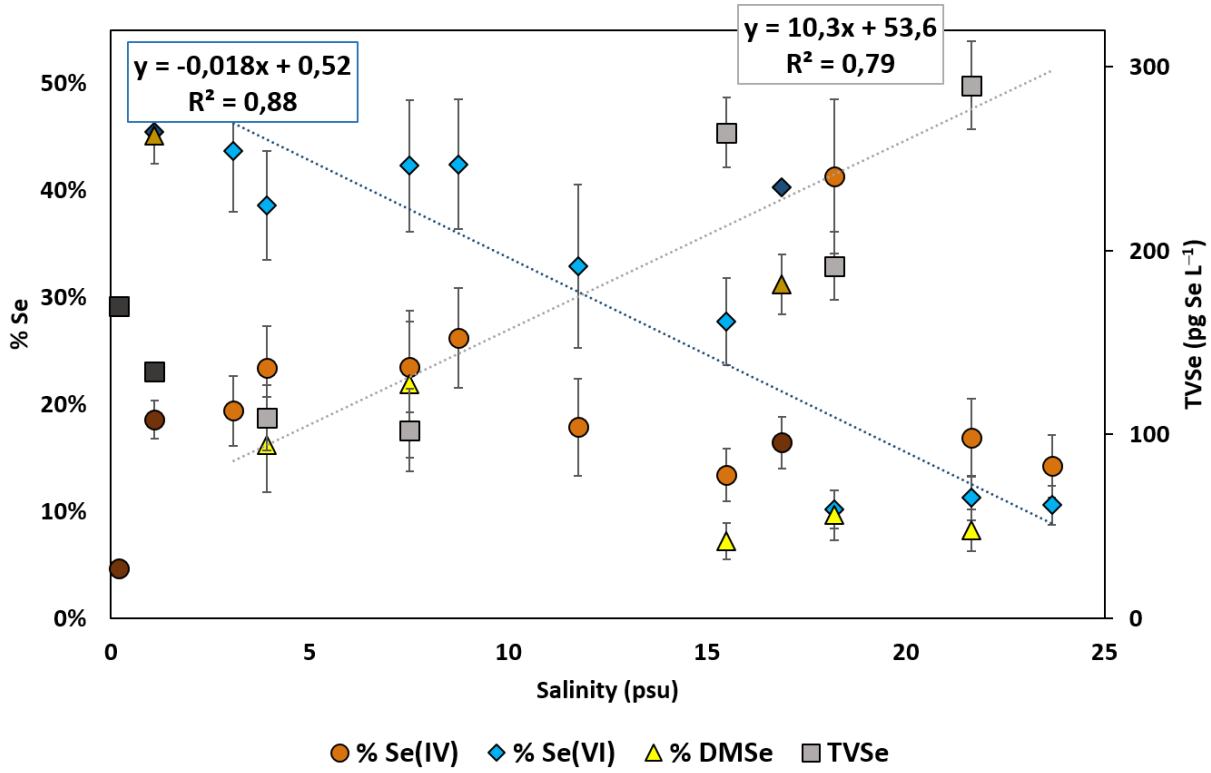

Figure Art.3.6. Percentage of Se(IV) and Se(VI) based on total dissolved Se and percentage of DMSe based on total volatile Se (left axis) as function of salinity (psu). Evolution of TVSe during the tidal cycle (right axis) expressed in pg Se L^{-1}. Pointed lines represent the linear regression obtained for salinity vs % Se(VI) (blue, y=–0.018x+0.52, R2=0.88, P=–0.11) and for salinity versus TVSe concentration (grey, y=10.3x+53.6, R2=0.79, P=0.89). The light colors represents the tidal cycle samples while the darkest marks have been used to indicate other samplings carried out at the same geographical point (station B).

The hydrodynamics of the Adour estuary, in particular short residence time (hours/day) for freshwater and particles, limit the potential formation of high turbidity zone compared to other macrotidal estuaries (Point, 2004). The observations at Gironde macrotidal estuarine system indicate that residence times of particles was enough to efficiently degrade organic matter and produce volatile Se species (Amouroux & Donard, 1997). At Adour estuary, reduced Se fraction had a higher contribution in oceanic waters than in freshwaters. In addition, processes linked to volatile production, which are degradation products of organoselenium compounds, seem to be more effective at oceanic waters as well.

4. Conclusion

In the actual context of increasing livestock and farm production to fulfill population needs, this study highlighted some critical results assessing the impact of such activities on Se input to watershed and estuarine transport. Our study demonstrated the influence of land-use on the amount of Se arriving to the Adour estuary. Comparing our results to other European estuarine systems, concentrations of total dissolved Se were similar in the Adour estuary as well as inorganic Se species proportions. Total volatile Se concentrations were also in the same range of values than those reported in other estuarine systems and were dependent on dissolved organic carbon. Interestingly, the predominance of DMSeS over DMSe, contrary to the results reported for other estuarine systems, suggests that short residence times promote the production of volatile species in downstream marine waters compared to upstream freshwaters.

Important spatial and seasonal variations were reported among the different water types with higher TDSe and TVSe occurring in waters impacted by effluents from urban and industrial wastewaters treatment. Seasonal variations resulted in higher Se concentration entering the estuary in winter, more markedly from Adour River than the Nive R., and mostly due to higher riverine discharge and selenate runoff from watersheds. Indeed, upstream waters entering the estuary are enriched in Se compared to background Se sources, such as remote headwaters and wet deposition. The elevated content of dissolved nitrate seems to indicate that agricultural and livestock farmlands are a major Se source for the estuary. Despite the high concentration of TDSe in effluents, downstream waters were not affected, and downstream TDSe concentration was the result of Adour and Nive mixing inputs.

While selenate proportion was especially higher in winter (64% of TDSe), selenite was linked to biological activity during spring and summer periods, mainly from microbial oxidation pathways of reduced Se. Indeed, unidentified Se species composed around 40% of TDSe, presumably in the form of colloidal elemental Se and other reduced species. Water redox conditions suggest that colloidal elemental Se can be a major compound of the reduced Se pool, but the occurrence of reduced and probably organically bound Se should not be discarded and further research is needed in order to identify the composition of the reduced Se fraction.

Acknowledgements

The author acknowledges the financial support of the Doctoral School (ED 211), the Université de Pau and Pays de l'Adour and the Institut des Sciences Analytiques et de Physico-chimie pour l'Environnement et les Matériaux (IPREM) given as a pre-doctoral fellowship.

The Micropolit research program « État et évolution de la qualité du milieu littoral Sud Aquitain » is co-financed by the European Union and l'Agence de l'Eau Adour Garonne. Europe is involved in Nouvelle Aquitaine with the European Regional Development Funds.

The contributions of the Aquitaine Region (AQUITRACES project n° 20131206001-13010973) and ANR IA RSNR (AMORAD project n°ANR-11-RSNR-0002) for equipment funding are acknowledged

Supplementary Information

Title: Distribution of Selenium and its compounds in waters of the Adour River estuary (Bay of Biscay, France)

Authors: Andrea Romero-Rama, Maïté Bueno, Emmanuel Tessier, Laurent Lanceleur, Sandrine Veloso, Jonathan Deborde and David Amouroux

Manuscript:

Number of Figures: 6

Number of Tables: 5

Supporting information:

Number of Figures SI: 1

Number of Tables SI: 2

Supplementary information Figure Art.3.SI 1

Figure Art.3.SI 1. Seasonal relationship between the selenite/TDSe ratio (in percentage) vs total volatile Se concentration.

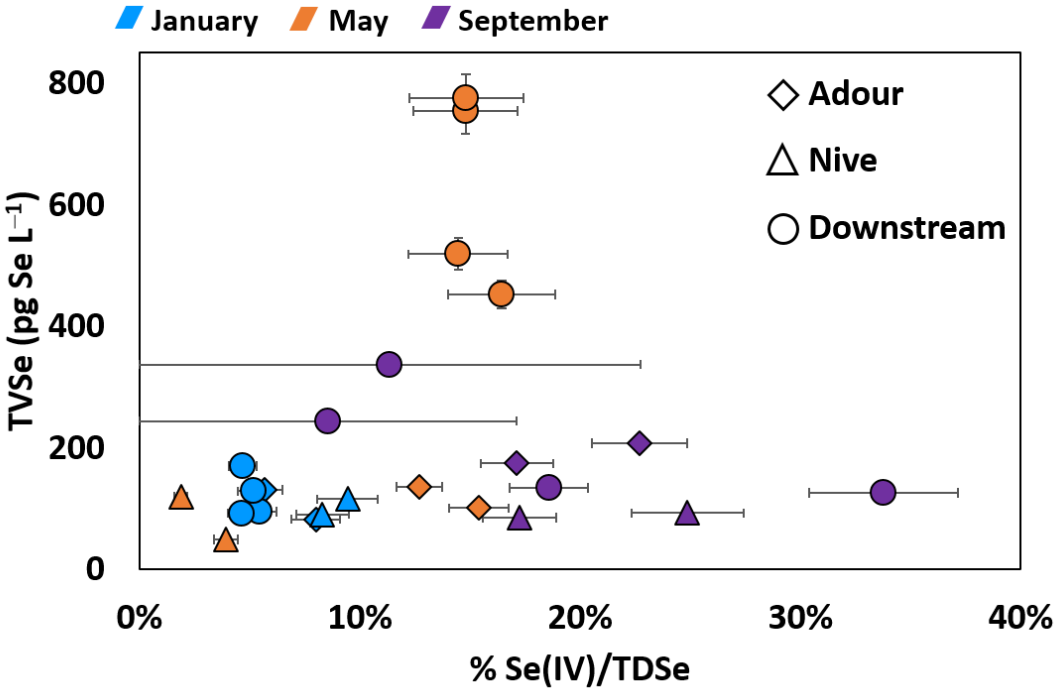

Supplementary information Table Art.3.SI 1

Table Art.3.SI 1. Raw data for Figure Art.3.2 graphic. Total dissolved Se (TDSe) with the corresponding error expressed in nmol L^{-1} and nitrate concentration in µmol L^{-1} for Adour River (ST 1 and 2) and Nive River (ST 3 and 4). Mean values for TDSe, nitrate concentration and Se/N molar ratio are presented for Adour and Nive rivers, western Pyrenean lakes (headwaters of the basin) and rainwaters of nearby areas.

Year	Month	Station	TDSe (nM)	NO_3^- (µM)	Se/N (10^{-5})	Reference
2017	May	ST 1	1.58 ± 0.04	120	1.32	this study
2017	May	ST 2	1.56 ± 0.05	135	1.16	
2017	May	ST 3	0.90 ± 0.04	60	1.51	
2017	May	ST 4	1.05 ± 0.04	66	1.59	
2017	September	ST1	1.89 ± 0.11	124	1.53	
2017	September	ST2	1.72 ± 0.10	119	1.45	
2017	September	ST3	0.97 ± 0.06	65	1.49	
2017	September	ST4	1.08 ± 0.06	70	1.55	
2018	January	ST1	2.31 ± 0.20	144	1.61	
2018	January	ST2	2.54 ± 0.22	199	1.27	
2018	January	ST3	1.20 ± 0.12	68	1.76	
2018	January	ST4	1.21 ± 0.12	no data	no data	
Adour R. (mean)			1.81	129	1.38	this study
Nive R. (mean)			1.06	66	1.55	this study
Western Pyrenees (mean)			0.26	6.9	4.49	Duval et al. (in prep.)
Rainwaters (SW France, annual mean)			0.60	13.6	4.45	Roulier et al. (submitted, 2020)

Supplementary information Table Art.3.SI 2

Table Art.3.SI 2. Data for the 4th sampling campaign carried out in September 2018 and focused on the tidal effect in Se concentration. The percentage of Se(IV) and Se(VI) is based on TDSe.

Sample	Time	Salinity (psu)	T (º C)	DO (%)	TSe Bulk (ng Se L^{-1})	TDSe (ng Se L^{-1})	Se(IV) (ng Se L^{-1})	Se(VI) (ng Se L^{-1})	Se(IV) (%)	Se(VI) (%)	TVSe (pg Se L^{-1})	DMSe (pg Se L^{-1})	DMSeS (pg Se L^{-1})	DMDSe (pg Se L^{-1})
T0	8h20	21.7	19.2	83	135 ± 19	138 ± 20	63 ± 6	44 ± 5	17 ± 4	11 ± 2	290 ± 15	24 ± 1	245 ± 12	15 ± 1
T1	9h21	23.7	19.2	84	134 ± 20	148 ± 19	35 ± 3	28 ± 3	14 ± 3	11 ± 2	–	–	–	–
T2	10h20	15.5	20.1	80	146 ± 22	163 ± 15	38 ± 3	39 ± 4	13 ± 2	28 ± 4	264 ± 13	19 ± 1	230 ± 12	10 ± 1
T3	11h20	11.8	20.7	81	143 ± 18	155 ± 31	33 ± 3	48 ± 5	18 ± 5	33 ± 8	–	–	–	–
T4	12h17	7.5	21.4	83	132 ± 16	154 ± 13	25 ± 2	37 ± 4	24 ± 4	42 ± 6	102 ± 5	22 ± 1	73 ± 4	6.5 ± 0.3
T5	13h22	3.1	22.1	91	153 ± 21	152 ± 8	24 ± 2	44 ± 4	19 ± 3	44 ± 6	–	–	–	–
T6	14h24	3.9	22.1	88	144 ± 20	136 ± 8	36 ± 3	43 ± 4	23 ± 4	39 ± 5	109 ± 5	18 ± 1	78 ± 4	12 ± 1
T7	15h20	8.7	21.5	89	122 ± 16	146 ± 12	42 ± 4	42 ± 4	26 ± 5	42 ± 6	–	–	–	–
T8	16h20	18.2	20.0	91	134 ± 20	153 ± 11	52 ± 5	41 ± 4	41 ± 7	10 ± 2	192 ± 10	18 ± 1	157 ± 8	12 ± 1

5. Bibiliography

Adour, I. (2014). Gestion du fleuve Adour et de ses affluents de leur source à l'embouchure - Institution Adour. Retrieved from www.institution-adour.fr. Last access October 20, 2020.

Adour, I. (2016). Schéma d'Aménagement et de Gestion des Eaux SAGE adour aval. Retrieved from www.sage-adouraval.fr. Last access October 22, 2020.

Agence de l'eau Adour-Garonne. (2014). Retrieved from http://www.eau-adour-garonne.fr. Last access October 20, 2020.

Amouroux, D., & Donard, O. F. X. (1997). Evasion of selenium to the atmosphere via biomethylation processes in the Gironde estuary, France. Marine Chemistry, 58(1–2), 173–188. https://doi.org/10.1016/S0304-4203(97)00033-9

Amouroux, D., Liss, P. S., Tessier, E., Hamren-Larsson, M., & Donard, O. F. X. (2001). Role of ocens as biogenic sources of selenium. Earth and Planetary Science Letters, 189(3–4), 277–283. https://doi.org/10.1016/S0012-821X(01)00370-3

Amouroux, D., Pécheyran, C., & Donard, O. F. X. (2000). Formation of volatile selenium species in synthetic seawater under light and dark experimental conditions. Applied Organometallic Chemistry, 14(5), 236–244. https://doi.org/10.1002/(SICI)1099-0739(200005)14:5<236::AID-AOC982>3.0.CO;2-U

Amouroux, D., Tessier, E., Pécheyran, C., Donard, O. F. X., & Amouroux E. AU3 - Pecheyran, C. AU4 - Donard, O.F.X., D. A.-T. (1998). Sampling and probing volatile metal(loid) species in natural waters by in-situ purge and cryogenic trapping followed by gas chromatography and inductively coupled plasma mass specitrometry (P-CT-GC-ICP/MS). Analytica Chimica Acta, 377(2–3), 241–254. https://doi.org/10.1016/S0003-2670(98)00425-5

Belon, E., Boisson, M., Deportes, I. Z., Eglin, T. K., Feix, I., Bispo, A. O., … Guellier, C. R. (2012). An inventory of trace elements inputs to French agricultural soils. Science of The Total Environment, 439, 87–95. https://doi.org/https://doi.org/10.1016/j.scitotenv.2012.09.011

Chang, Y., Zhang, J., Qu, J., Zhang, G., Zhang, A., & Zhang, R. (2016). The behavior of dissolved inorganic selenium in the Changjiang Estuary. Journal of Marine Systems, 154, 110–121. https://doi.org/10.1016/j.jmarsys.2015.01.008

Chasteen, T. G., & Bentley, R. (2003). Biomethylation of selenium and tellurium: microorganisms and plants. Chemical Reviews, 103(1), 1–25. https://doi.org/10.1021/cr010210+

Climate-data.org (n.d.). Retrieved October 20, 2020, from https://fr.climate-data.org/

Cochran, J. K., & Brook, S. (2014). Estuaries, 1–4. https://doi.org/10.1016/B978-0-12-409548-9.09151-X

Cutter, G. (1989). The Estuarine Behaviour of Selenium in San Francisco Bay, 13–34. https://doi.org/10.1016/0272-7714(89)90038-3

Cutter, G. A., & Cutter, L. S. (2004). Selenium biogeochemistry in the San Francisco Bay estuary: Changes in water column behavior. Estuarine, Coastal and Shelf Science, 61(3), 463–476. https://doi.org/10.1016/j.ecss.2004.06.011

Cutter, G. A., & San Diego-McGlone, M. L. C. (1990). Temporal variability of selenium fluxes in San Francisco Bay. Science of the Total Environment, The, 97–98(C), 235–250. https://doi.org/10.1016/0048-9697(90)90243-N

Deborde, J. (2019). Dynamique des sels nutritifs et de la matière organique dans le système fluvio-estuarien de l'Adour / golfe de Gascogne.

Di Tullo, P. (2015). Dynamique du cycle biogéochimique du sélénium en écosystèmes terrestres : rétention et réactivité dans le sol, rôle de la végétation. Retrieved from http://www.theses.fr/2015PAUU3013/document. Last access: October 09, 2020

FNAB, F. N. d'Agriculture B. (2015). Syndicat mixte du bassin versant de la Nive. Retrieved from https://www.eauetbio.org. Last access : October 17, 2020

Guan, D. M., & Martin, J. M. (1991). Selenium distribution in the Rhône delta and the Gulf of Lions. Marine Chemistry, 36(1–4), 303–316. https://doi.org/10.1016/S0304-4203(09)90068-8

Hung, J.-J., & Shy, C.-P. (1995). Speciation of Dissolved Selenium in the Kaoping and Erhjen Rivers and Estuaries, Southwestern Taiwan. Estuaries, 18(1), 234. https://doi.org/10.2307/1352633

Lanceleur, L., Tessier, E., Bueno, M., Pienitz, R., Bouchard, F., Cloquet, C., & Amouroux, D. (2019). Cycling and atmospheric exchanges of selenium in Canadian subarctic thermokarst ponds.

Biogeochemistry, 145(1-2), 193-211. https://doi.org/10.1007/s10533-019-00599-w

Lindström, K. (1983). Selenium as a growth factor for plankton algae in laboratory experiments and in some Swedish lakes. Forest Water Ecosystems, 13(1–2), 35–47. https://doi.org/10.1007/BF00008655

Measures, C. I., & Burton, J. D. (1978). Behaviour and speciation of dissolved selenium in estuarine waters. Nature, 273(5660), 293–295. https://doi.org/10.1038/273293a0

Measures, C. I., & Burton, J. D. (1980). The vertical distribution and oxidation states of dissolved selenium in the northeast Atlantic Ocean and their relationship to biological processes. Earth and Planetary Science Letters, 46(3), 385-396. https://doi.org/10.1016/0012-821X(80)90052-7

Point, D. (2004). Spéciation et biogéochimie des elements trace métalliques dans l'estuaire de l'Adour (2004). Thèse de l'Université de Pau et Pays de l'Adour.

Pokrovsky, O. S., Bueno, M., Amouroux, D., Manasypov, R. M., Shirokova, L. S., Karlsson, J., & Amouroux, D. (2018). Dissolved organic matter controls on seasonal and spatial selenium concentration variability in thaw lakes across a permafrost gradient. Environ. Sci. Technol., 52(18), acs.est.8b00918. https://doi.org/10.1021/acs.est.8b00918

Roulier, M., Bueno, M., Coppin, F., Nicolas, M., Thiry, Y., Rigal, F., … Pannier, F. (2020, submitted). Atmospheric iodine, selenium and caesium wet depositions in France: spatial and seasonal variations.

Söderlund, M., Virkanen, J., Holgersson, S., & Lehto, J. (2016). Sorption and speciation of selenium in boreal forest soil. Journal of Environmental Radioactivity, 164, 220–231. https://doi.org/10.1016/j.jenvrad.2016.08.006

Tessier, E., Amouroux, D., Abril, G., Lemaire, E., & Donard, O. F. X. (2002). Formation and volatilisation of alkyl-iodides and -selenides in macrotidal estuaries. Biogeochemistry, 59(1–2), 183–206. https://doi.org/10.1023/A:1015550931365

Tessier, E., Amouroux, D., & Donard, O. F. X. (2002). Biogenic volatilization of trace elements from European estuaries. Biogeochemistry of Environmentally Important Trace Elements, 835(October 2002), 151–165. https://doi.org/10.1021/bk-2003-0835.ch012

Veloso, S. (2020, thèse in preparation). Impact des micropolluants sur les communautés microbiennes en milieu estuarien. Université de Pay et Pays de l'Adour.

Wen, H., & Carignan, J. (2007). Reviews on atmospheric selenium: Emissions, speciation and fate. Atmospheric Environment, 41(34), 7151–7165. https://doi.org/10.1016/j.atmosenv.2007.07.035

Yao, Q. Z., & Zhang, J. (2005). The behavior of dissolved inorganic selenium in the Bohai Sea. Estuarine, Coastal and Shelf Science, 63(1–2), 333–347. https://doi.org/10.1016/j.ecss.2004.12.004

Yao, Q. Z., Zhang, J., Qin, X. G., Xiong, H., & Dong, L. X. (2006). The behavior of selenium and arsenic in the Zhujiang (Pearl River) Estuary, South China Sea. Estuarine, Coastal and Shelf Science, 67(1–2), 170–180. https://doi.org/10.1016/j.ecss.2005.11.012

General Conclusions and Perspectives

The different works carried out during this thesis had two main objectives. On the one hand, the development of an analytical methodology that would allow the simultaneous separation of reduced Se compounds and the selenite and selenate anions that are commonly found in natural aquatic systems. And on the other hand, to obtain new knowledge about the physicochemical and biological processes involved in Se biogeochemistry in different aquatic ecosystems in order to provide a better understanding of the Se aquatic cycle.

I. Analytical challenge

For analytical method development, the bibliographic study carried out reflected the need to use the HPLC technique as the most optimal solution to obtain the simultaneous separation of the maximum number of possible compounds that may be present in fresh water systems. Due to the differences in the chemical structure and the charge or not of the different species, it was decided to use a mixed stationary phase composed of a reverse phase and an anion exchange phase to achieve an efficient separation in the shortest possible time. The use of this type of stationary phases may entail a greater challenge when it comes to optimizing the parameters, since the reverse and anionic phase mechanisms respond differently when modifying the mobile phase. The detector selected was the ICP-MS because this is the most sensitive detector in the market. Obtain limits of detection in the range of low ng Se L^{-1} is critical for the method to be applied to environmental freshwater samples.

At the beginning of the study, it was decided to try to find a method that was isocratic and restrict the pH range between 6.0 and 8.5, close to natural waters to preserve speciation. During the analytical development, the composition of the mobile phase, the type of organic solvent used as well as its concentration, the use of ion pairing agent and the maximum injection volume were the parameters optimized. Subsequently, a validation of the method was carried out using a reference method and the detection and quantification limits were calculated for the species detected in real samples.

The final result of the optimization allows the separation of up to 6 selenium compounds in less than 20 minutes thanks to the use of a mobile phase composed of 20 mM NH4NO3 + 2% ipa + 1mM p-hydroxybenzoic acid at pH = 8.5 with a maximum injection volume of 300 µL, although it can be lower if the concentration of the samples allows it. The

compounds we were able to separate were methylseleninic acid, selenocystine, selenomethionine, selenite, selenate and selenocyanate, all of which have been reported in natural waters. There are two results to highlight from the optimization process. On the one hand, for the speciation of Se, the use of methanol is more common than that of isopropanol. However, our results indicated a higher plate number using isopropanol as a source of carbon. On the other hand, although the use of p-hydroxybenzoic acid as ion pairing agent produced the co-elution of the TMSe, SeCys and MeSeCys standards, it allowed to reduce the retention time of selenite and selenate by half, finally obtaining retention times of 5 and 10 minutes for each species. It had an effect on the quality of the peaks, which increased their height and reduced their broadening. This led to obtain detection limits in real samples of 1.5 ng Se L^{-1} for selenite and 3.6 ng Se L^{-1} for selenate. Thus, the final method can be applied for Se speciation in waters at the ultra-trace level.

II. Perspectives for analytical developments

The results obtained during this thesis project lead to many research perspectives in order to confirm some of the hypothesis presented here and refine the understanding of the fate of Se in the aquatic environment. From an analytical point of view, the study of Se speciation by HPLC-ICP/MS has proven to be the most powerful technique to fulfill the environmental needs in terms of limits of detection. However, this technique is not helping to identify the reduced Se pool of species that is commonly found in environmental samples. Therefore, further research should be done in order to identify which species conform this important Se fraction. To this respect, a promising option is the use of “soft ionization” in order to better asses the molecular mass and structure of reduced Se compounds. However, techniques that use soft ionization, for example, electrospray ionization coupled to mass spectrometry present in general lower sensitivity. A more promising approach seems to be the use of preconcentration techniques. The use of solid phase extraction seems a good option and has been applied to other environmental matrixes with success. In fact, both strategies could be complementary.

III. Environmental challenge

The second objective of this thesis was to improve the knowledge of the global Se cycle in freshwater systems. Thanks to the bibliographic review, three aspects that are critical for the study of the Se cycle in the aquatic environment were identified. The first aspect to take into account are the variations in the concentration of total Se and the speciation among the water column, especially if there is stratification in the medium studied. The second aspect is the study of seasonal variations, which is a fundamental aspect to be able to relate certain Se processes with the physicochemical and biological dynamics of aquatic ecosystems. The third aspect is the simultaneous study of volatile and non-volatile compounds, since volatilization can represent an important removal pathway that has not been taken into account in many studies. In the course of this thesis, three environmental studies have been carried out, each of which aims to fill a gap of knowledge to new insights of Se biogeochemistry and Se sources to freshwater systems.

The first of these studies was carried out in the eutrophic lake Kinneret (Israel). A total of twelve samplings campaigns were carried out in January, April, September and November at different depths of the water column in the period between 2015 and 2017. This lake was selected for two reasons. First, for the current understanding of its sulfur biogeochemistry. Second, because this lake is monomictic, which means that it presents stratification during certain months of the year (from spring to autumn), which generates two water layers. The surface water layer (epilimnion) is well oxygenated since it is in contact with the atmosphere, while during stratification the bottom water layer (hypolimnion) evolves from suboxic conditions in late spring to reach completely anoxic conditions during summer. This is of special interest because it was possible to study the evolution of Se speciation in the epilimnion where algae blooms occur during spring, and the processes occurring at the reducing conditions of the hypolimnion simultaneously. The results obtained by the analysis by HPLC-ICP/MS showed the presence of selenate, selenite and one or compound that could not be identified. Thanks to the results obtained, two conclusions could be drawn with respect to this compound. The first is that it elutes chromatographically with a retention time similar to that of Se amino acids, therefore we can suggest that it is most probably an organic Se compound (Org. Se). The second conclusion is that the “Org.Se” is produced exclusively in the epilimnion. In addition, this compound could be for the first time statistically correlated with chlorophyll and later related to specific phytoplankton taxa from the lake.

The presence of reduced Se compounds was also observed in the hypolimnion, with a higher incidence during the stratification periods. However, the chromatographic results indicated that they are different species since the peak reported in the epilimnion is not observed in the chromatograms. In fact, the concentration of this species was determined operationally using the formula Red.Se = TDSe - Se (IV) - Se (VI). The results were compared with a study carried out in the same lake in the 90s and it was observed that the reduced Se concentration tripled the estimated concentration in the previous study. The presence of this species was predominant in the hypolimnion during the stratification periods and subsequently reduced its concentration in winter when the water column loses its stratification and is re-oxygenated. This led to the conclusion that the hypolimnion reducing conditions that occur during the stratification period reduce selenate to insoluble elemental Se that remains as colloids in the water and further sinks to sediments. During winter, when the water column is not stratified, the concentration of this species decreases, which indicates that re-oxidation and regeneration of more oxidized species, selenite and selenate, takes place. The period between 2015 and 2017 was characterized by being a drought period, which resulted in an increase in conductivity, in other words, there was a reduction in the volume of water in the lake during the study period. However, the concentration of total Se decreased. This is indicative of re-oxidation occurring partially, and therefore the sink of elemental Se to the sediments resulted in a major process removing Se from the hypolimnion.

The study of the speciation of volatile compounds revealed the presence of DMSe, DMSeS and DMDSe. The production of DMSeS predominates in this lake over the other volatile species. This observation differs from studies conducted in other environments where the DMSe form commonly predominates. However, Lake Kinneret is characterized by sub-millimolar concentration of sulfur, which explains the large production of DMSeS. The production of total volatile Se (TVSe) coincided each year with the end of summer and the increase of turbidity at metalimnion. Therefore, we suggest that volatile Se formation is strongly related to the microbial turnover in the water column.

The results and conclusions provided by this study may be of vital importance to understand the dynamics of other lakes located in arid regions that will most likely suffer frequent periods of drought in the coming years due to climate change. Additionally, the knowledge acquired from this study will be used to constrain Se processes occurring in the other environmental studies of this thesis project.

The second study that carried out during this project was made in the oligotrophic lakes of the Pyrenees. Five sampling campaigns were carried out in the months of June/July 2017–2019 and October 2017–2018. Pyrenees lakes are ice-covered during winter, therefore the sampling carried out in June/July was set up to monitor the Se speciation after the ice and snow melting periods. The samplings carried out in October were set up to acquire information about the potential Se fluctuations during the warmest period of the year. The objective of this study was to obtain data on the concentration of total Se and the speciation of Se in these lakes and to study the existence or not of seasonal and depth variations.

The results obtained are very valuable since it is the first time that this type of monitoring has been done in high mountain lakes for Se. The results revealed that the concentrations of unfiltered and dissolved Se were similar. This means that the Se present in lakes is mostly in the dissolved phase. The content of total dissolved Se in the studied lakes was between 7 and 80 ng Se L^{-1}, and on average, 63% of this concentration was found in the form of selenate, this being the predominant compound in all the lakes. The results indicated that selenite in general is close or below the limit of detection. Therefore, and due to the redox conditions of these lakes, it is possible that selenate co-exists with extremely low concentrations of elemental Se. In general, no significant statistical variations were found between seasons for total Se nor for Se speciation. Among the water column, steady TDSe concentrations were found. However, reduced increased with depth, especially in lakes showing oxygen depletion.

The lakes were classified into several groups according to the geological substrate, obtaining four groups of lakes. The results obtained indicate that the total Se concentration is higher in those lakes that have a geological substrate formed during the Devonian period; this occurs due to the presence of shales that contain, in general, a higher concentration of sulfur and selenium that further lixiviates to the lakes. With respect to the formation of volatile compounds, it was observed that the production was low, as expected from oligotrophic lakes. The main species was DMSe. Thanks to an estimate of the flow of Se emitted into the atmosphere and the contributions by wet deposition, we were able to estimate that on average 40% of the Se input to these lakes comes from precipitation, while the other 60% has a geogenic origin. This work is a first assessment of Se speciation in Alpine lakes that provides new insights on the Se geochemical background in natural water from a temperate watershed (Adour basin).

In order to follow the course of Pyrenean waters, the last study was carried out at the Adour estuary (Bay of Biscay, France). The objective of this study was to monitor the seasonal fluctuations of total Se concentration and Se speciation to better constrain the sources of Se to the estuary and its seasonal and spatial variations. For this purpose a total of 12 sampling points were set up, 4 of them to monitor the sources of Se to the estuary were located at the main water inflows, thus Adour and Nive rivers; 4 samples to assess the impact of wastewater treatment plants and industrial effluents, and 4 to evaluate the Se content and speciation in the mouth of the estuary, defined as "downstream waters". Sub-surface samples were collected in May and September 2017 and January 2018.

The results obtained showed an enrichment of total Se in the course of the basin to respect to the concentration observed at the headwaters. Total se concentration at Adour and Nive rivers could be positively correlated with nitrate content that is derived from agricultural and livestock production at the region. Therefore, we can state that human activities in nearby areas represent an important source of Se and to the estuarine waters. In general, Adour estuarine waters presented a range of total dissolved Se and total volatile Se concentration that is similar to other European estuaries.

The dissolved Se that enters the estuary does so in the form of selenite (11–13%), selenate (43–47%) and reduced Se (40–46%). Therefore, half of the Se content found in the estuary is present as elemental Se or reduced Se species that remain unidentified. Because the main sources of water and Se in the estuary are the Adour and Nive rivers, and the residence times of water in this estuary are short, few differences are observed both in total Se content and in speciation in the estuarine "downstream waters" compared to river waters.

The production of volatile compounds did show spatial and seasonal differences. On the one hand, river waters produced less volatile species than downstream waters. Furthermore, the maximum concentration of TVSe reported in rivers occurred in September, while in downstream waters maximum TVSe concentration was observed in May. Speciation also showed differences. DMSe is the main volatile compound produced in rivers, as occurs in other estuarine sites. However, in downstream waters, the predominant compound was DMSeS. Our findings suggest that short residence times promote the production of volatile species in downstream marine waters compared to upstream freshwaters. As happened in Lake Kinneret, higher sulfate concentration at

marine waters results in different volatile Se speciation and is probably the result of different organic matter degradation processes.

Bibliography

Adour, I. (2014). Gestion du fleuve Adour et de ses affluents de leur source à l'embouchure - Institution Adour. Retrieved from www.institution-adour.fr. Last access October 20, 2020.

Adour, I. (2016). Schéma d'Aménagement et de Gestion des Eaux SAGE adour aval. Retrieved from www.sage-adouraval.fr. Last access October 22, 2020.

Afton, S., Kubachka, K., Catron, B., & Caruso, J. A. (2008). Simultaneous characterization of selenium and arsenic analytes via ion-pairing reversed phase chromatography with inductively coupled plasma and electrospray ionization ion trap mass spectrometry for detection: Applications to river water, plant extract a. Journal of Chromatography A, 1208(1), 156–163. https://doi.org/https://doi.org/10.1016/j.chroma.2008.08.077

Agence de l'eau Adour-Garonne. (2014). Retrieved from http://www.eau-adour-garonne.fr. Last access October 20, 2020.

Aiuppa, A., Dongarrà, G., Capasso, G., & Allard, P. (2000). Trace elements in the thermal groundwaters of Vulcano Island (Sicily). Journal of Volcanology and Geothermal Research, 98(1–4), 189–207. https://doi.org/10.1016/S0377-0273(99)00156-0

Alexander, J. (2015). Chapter 52 - Selenium. In G. F. Nordberg, B. A. Fowler, & M. B. T.-H. on the T. of M. (Fourth E. Nordberg (Eds.) (pp. 1175–1208). San Diego: Academic Press. https://doi.org/10.1016/B978-0-444-59453-2.00052-4

Alfthan, G., Wang, D., Aro, A., & Soveri, J. (1995). The geochemistry of selenium in groundwaters in Finland. Science of the Total Environment, 162(2–3), 93–103. https://doi.org/10.1016/0048-9697(95)04436-5

Amouroux, D., & Donard, O. F. X. (1996). Maritime emission of selenium to the atmosphere in Eastern Mediterranean seas. Geophysical Research Letters, 23(14), 1777–1780. https://doi.org/10.1029/96GL01271

Amouroux, D., & Donard, O. F. X. (1997). Evasion of selenium to the atmosphere via biomethylation processes in the Gironde estuary, France. Marine Chemistry, 58(1–2), 173–188. https://doi.org/10.1016/S0304-4203(97)00033-9

Amouroux, D., Liss, P. S., Tessier, E., Hamren-Larsson, M., & Donard, O. F. X. (2001). Role of ocens as biogenic sources of selenium. Earth and Planetary Science Letters, 189(3–4), 277–283. https://doi.org/10.1016/S0012-821X(01)00370-3

Amouroux, D., Pécheyran, C. and Donard, O.F.X. (2000), Formation of volatile selenium species in synthetic seawater under light and dark experimental conditions. Appl. Organometal. Chem., 14: 236-244. https://doi.org/10.1002/(SICI)1099-0739(200005)14:5<236::AID-AOC982>3.0.CO;2-U

Amouroux, D., Tessier, E., Pécheyran, C., Donard, O. F. X., (1998). Sampling and probing volatile metal(loid) species in natural waters by in-situ purge and cryogenic trapping followed by gas chromatography and inductively coupled plasma mass spectrometry (P-CT-GC-ICP/MS). Analytica Chimica Acta, 377(2–3), 241–254. https://doi.org/10.1016/S0003-2670(98)00425-5

Anderson, C. S. (2014). Selenium and Tellurium [Advanced Release]. Retrieved from https://www.usgs.gov/. Last access November 03, 2020.

Aono, T., Nakaguchi, Y., & Hiraki, K. (1991). Vertical profiles of dissolved selenium in the North Pacific. Geochemical Journal, 25(1), 45–55. https://doi.org/10.2343/geochemj.25.45

Aries, E., Chen, J., Collins, P., Hodges, J., & Pearson, S. (2011) "Characterisation of priority hazardous substances and priority substances in cokemaking and steelmaking effluents from UK integrated steelworks". 2nd International Conference and Exhibition Clean Technologies in the Steel Industry, Budapest.

Ashournia, M., & Aliakbar, A. (2009). Determination of selenium in natural waters by adsorptive differential pulse cathodic stripping voltammetry. Journal of Hazardous Materials, 168(1), 542–547. https://doi.org/10.1016/j.jhazmat.2009.02.070

Ashournia, M., & Aliakbar, A. (2010). Determination of Se (IV) in natural waters by adsorptive stripping voltammetry of 5-nitropiazselenol. Journal of Hazardous Materials, 174(1–3), 788–794. https://doi.org/10.1016/j.jhazmat.2009.09.121

Atkinson, R., Aschmann, S. M., Hasegawa, D., Thompson-Eagle, E. T., & Frankenberger Jr, W. T. (1990). Kinetics of the atmospherically important reactions of dimethyl selenide. Environmental Science & Technology, 24(9), 1326–1332. https://doi.org/10.1021/es00079a005

B'Hymer, C., & Caruso, J. A. (2006). Selenium speciation analysis using inductively coupled plasma-mass spectrometry. Journal of Chromatography A, 1114(1), 1–20. https://doi.org/10.1016/j.chroma.2006.02.063

Bailey, R. T. (2017). Review: Selenium contamination, fate, and reactive transport in groundwater in relation to human health. Hydrogeology Journal, 25(4), 1191–1217. https://doi.org/10.1007/s10040-016-1506-8

Balistrieri, L. S., & Chao, T. T. (1987). Selenium Adsorption by Goethite1. Soil Science Society of America Journal, 51, 1145–1151. https://doi.org/10.2136/sssaj1987.03615995005100050009x

Barnes, J. (1992). High performance liquid chromatography. John Wiley & Sons.

Barron, E., Migeot, V., Rabouan, S., Potin-Gautier, M., Séby, F., Hartemann, P., … Legube, B. (2009). The case for re-evaluating the upper limit value for selenium in drinking water in Europe. Journal of Water and Health, 7(4), 630–641. https://doi.org/10.2166/wh.2009.097

Belon, E., Boisson, M., Deportes, I. Z., Eglin, T. K., Feix, I., Bispo, A. O., … Guellier, C. R. (2012). An inventory of trace elements inputs to French agricultural soils. Science of The Total Environment, 439, 87–95. https://doi.org/https://doi.org/10.1016/j.scitotenv.2012.09.011

Bender, J., Gould, J. P., Vatcharapijarn, Y., & Saha, G. (1991). Uptake, transformation and fixation of Se (VI) by a mixed selenium-tolerant ecosystem. Water, Air, and Soil Pollution, 59(3–4), 359–367. https://doi.org/10.1007/BF00211843

Berman, T., Zohary, T., Nishri, A., & Sukenik, A. (2014). Lake Kinneret. Lake Kinneret, 1–15. https://doi.org/10.1007/978-94-017-8944-8

Bertolino, F. A., Torriero, A. A. J., Salinas, E., Olsina, R., Martinez, L. D., & Raba, J. (2006). Speciation analysis of selenium in natural water using square-wave voltammetry after preconcentration on activated carbon. Analytica Chimica Acta, 572(1), 32–38. https://doi.org/10.1016/j.aca.2006.05.021

Billen, G., Garnier, J., Ficht, A., & Cun, C. (2001). Modeling the response of water quality in the Seine River estuary to human activity in its watershed over the last 50 years. Estuaries, 24(6), 977–993. https://doi.org/10.2307/1353011

Blazina, T., Läderach, A., Jones, G. D., Sodemann, H., Wernli, H., Kirchner, J. W., & Winkel, L. H. E. E. (2017). Marine Primary Productivity as a Potential Indirect Source of Selenium and Other Trace

Elements in Atmospheric Deposition. Environmental Science and Technology, 51(1), 108–118. https://doi.org/10.1021/acs.est.6b03063

Boehrer, B., & Schultze, M. (2008). Stratification of lakes, (2006), 1–27. https://doi.org/10.1029/2006RG000210.1. Introduction.

Brandt, J. E., Bernhardt, E. S., Dwyer, G. S., & Di Giulio, R. T. (2017). Selenium Ecotoxicology in Freshwater Lakes Receiving Coal Combustion Residual Effluents: A North Carolina Example. Environmental Science & Technology, 51(4), 2418–2426. https://doi.org/10.1021/acs.est.6b05353

Bratakos, M. S., Zarifopoulos, T. F., Siskos, P. A., & Ioannou, P. V. (1988). Total selenium concentration in tap and bottled drinking water and coastal waters of Greece. Science of The Total Environment, 76(1), 49–54. https://doi.org/https://doi.org/10.1016/0048-9697(88)90282-3

Brodowska, M. S., Kurzyna-Szklarek, M., & Haliniarz, M. (2016). Selenium in the environment. Journal of Elementology, 21(4), 1173–1185. https://doi.org/10.5601/jelem.2016.21.2.1148

Buchs, B., Evangelou, M. W., Winkel, L. H., & Lenz, M. (2013). Colloidal properties of nanoparticular biogenic selenium govern environmental fate and bioremediation effectiveness. Environmental science & technology, 47(5), 2401-2407. https://doi.org/10.1021/es304940s

M. Bueno, J. Darrouzès, M. Dauthieu, S. Simon, N. Gilon, et al.. Analytical strategies for inorganic and organic selenium speciation in natural waters [Stratégies analytiques pour la spéciation du sélénium inorganique et organique dans les eaux naturelles]. Journal Europeen d'Hydrologie, 2005, 36 (2), pp.179-190. ⟨hal-01561326⟩

Cai, Y., Cabañas, M., Fernández-Turiel, J., Abalos, M., & Bayona, J. M. (1995). On-line preconcentration of selenium(IV) and selenium(VI) in aqueous matrices followed by liquid chromatography-inductively coupled plasma mass spectrometry determination. Analytica Chimica Acta, 314(3), 183–192. https://doi.org/10.1016/0003-2670(95)00274-4

Camarero, L., Rogora, M., Mosello, R., Anderson, N.J., Barbieri, A., Botev, I., Kernan, M., Kopacek, J., Korhola, A., Lotter, A.F., Muri, G., Postolache, C., Stuchlik, E., Thies, H. and Wright, R.F. (2009), Regionalisation of chemical variability in European mountain lakes. Freshwater Biology, 54: 2452-2469. https://doi.org/10.1111/j.1365-2427.2009.02296.x

Cary, L., Benabderraziq, H., Elkhattabi, J., Gourcy, L., Parmentier, M., Picot, J., … Négrel, P. (2014). Tracking selenium in the Chalk aquifer of northern France: Sr isotope constraints. Applied Geochemistry, 48, 70–82. https://doi.org/https://doi.org/10.1016/j.apgeochem.2014.07.014

Casey, R., & Siwik, P. (2000). Concentrations of selenium in surface water, sediment and fish from the McLeod, Pembina and Smoky Rivers: results of surveys from fall 1998 to fall 1999: Interim Report. Alberta Environment, Natural Resources Service, Water Management Division.

Catalan, J., Camarero, L., Felip, M., Pla, S., Ventura, M., Buchaca, T., ... & Medina-Sánchez, J. M. (2006). High mountain lakes: extreme habitats and witnesses of environmental changes. limnetica, 25(1-2), 551-584.

Catalan, J., Ventura, M., Brancelj, A. et al. Seasonal ecosystem variability in remote mountain lakes: implications for detecting climatic signals in sediment records. Journal of Paleolimnology 28, 25–46 (2002). https://doi.org/10.1023/A:1020315817235

Chandrasekaran, K., Ranjit, M., & Arunachalam, J. (2009). Determination of inorganic selenium species [Se(IV) and Se(VI)] in tube well water samples in Punjab, India. Chemical Speciation and Bioavailability, 21(1), 15–22. https://doi.org/10.3184/095422909X416405

Chang, Y., Zhang, J., Qu, J., Zhang, G., Zhang, A., & Zhang, R. (2016). The behavior of dissolved inorganic selenium in the Changjiang Estuary. Journal of Marine Systems, 154, 110–121. https://doi.org/10.1016/j.jmarsys.2015.01.008

Chapman, P. M., Adams, W. J., Brooks, M., Delos, C. G., Luoma, S. N., Maher, W. A., … Shaw, P. (2010). Ecological Assessment of Selenium in the Aquatic Environment. CRC Press. Retrieved from https://books.google.fr/books?id=lFjRBQAAQBAJ. Last access: April 17, 2020.

Chasteen, T. G., & Bentley, R. (2003). Biomethylation of selenium and tellurium: microorganisms and plants. Chemical Reviews, 103(1), 1–25. https://doi.org/10.1021/cr010210+

Chatterjee, A., & Irgolic, K. J. (1998). Behaviour of selenium compounds in FI-HG-AAS. Analytical Communications, 35(10), 337–340. https://doi.org/10.1039/A805575K

Chau, Y. K., Wong, P. T. S., Silverberg, B. A., Luxon, P. L., & Bengert, G. A. (1976). Methylation of selenium in the aquatic environment. Science, 192(4244), 1130–1131. https://doi.org/10.1126/science.192.4244.1130

Chen, Y.-W., & Belzile, N. (2010). High performance liquid chromatography coupled to atomic fluorescence spectrometry for the speciation of the hydride and chemical vapour-forming elements As, Se, Sb and Hg: A critical review. Analytica Chimica Acta, 671(1), 9–26. https://doi.org/https://doi.org/10.1016/j.aca.2010.05.011

Chen, Y.-W., Li, L., D'Ulivo, A., & Belzile, N. (2006). Extraction and determination of elemental selenium in sediments—A comparative study. Analytica Chimica Acta, 577(1), 126–133. https://doi.org/10.1016/j.aca.2006.06.020.

Chen, Y., Zhou, X.-L., Tong, J., Truong, Y., & Belzile, N. (2005). Photochemical behavior of inorganic and organic selenium compounds in various aqueous solutions. Analytica Chimica Acta, 545(2), 149–157. https://doi.org/https://doi.org/10.1016/j.aca.2005.03.033

Chouhan, R., & Banerjee, M. (2010). Two cyanobacteria Hapalosiphon sp. and Gloeocapsa sp. in amelioration of selenium toxicity. J. Appl. Biosci, 36(2), 137–140.

Climate-data.org. (n.d.). Retrieved from https://fr.climate-data.org/. Last access: October 20, 2020.

Cobo-Fernández, M.G., Palacios, M.A., Chakraborti, D. et al. On line speciation of Se(VI), Se(IV), and trimethylselenium by HPLC-microwave oven-hydride generation-atomic absorption spectrometry. Fresenius J Anal Chem 351, 438–442 (1995). https://doi.org/10.1007/BF00322915.

Cochran, J. K. (2014). Estuaries–where rivers meet the sea. Reference Module in Earth Systems and Environmental Sciences, 1–4. https://doi.org/10.1016/B978-0-12-409548-9.09151-X

Cole J. J., Caraco N. F., (1998), Atmospheric exchange of carbon dioxide in a low-wind oligotrophic lake measured by the addition of SF6, Limnology and Oceanography, 4, https://doi.org/10.4319/lo.1998.43.4.0647.

Conde, J. E., & Sanz Alaejos, M. (1997). Selenium Concentrations in Natural and Environmental Waters. Chemical Reviews, 97(6), 1979–2004. https://doi.org/10.1021/cr960100g

Cooke, T. D., & Bruland, K. W. (1987). Aquatic Chemistry of Selenium: Evidence of Biomethylation. Environmental Science and Technology, 21(12), 1214–1219. https://doi.org/10.1021/es00165a009

Coplen, T. B., Meyers, F., & Holden, N. E. (2017). Clarifying Atomic Weights: A 2016 Four-Figure Table of Standard and Conventional Atomic Weights. Journal of Chemical Education, 94(3), 311–319. https://doi.org/10.1021/acs.jchemed.6b00510

Ćurković, M., Sipos, L., Puntarić, D., Dodig-Ćurković, K., Pivac, N., & Kralik, K. (2016). Arsenic, copper, molybdenum, and selenium exposure through drinking water in rural eastern Croatia. Polish Journal of Environmental Studies, 25(3), 981–992. https://doi.org/10.15244/pjoes/61777

Cutter, G. (1978). Species determination of selenium in natural waters. Analytica Chimica Acta, 98(1), 59–66. https://doi.org/10.1016/S0003-2670(01)83238-4

Cutter, G. (1989). The Estuarine Behaviour of Selenium in San Francisco Bay, 13–34. https://doi.org/10.1016/0272-7714(89)90038-3

Cutter, G. A. (1978). Species determination of selenium in natural waters. Analytica Chimica Acta, 98(1), 59–66. https://doi.org/10.1016/S0003-2670(01)83238-4

Cutter, G. A. (1993). Metalloids in wet deposition on Bermuda: Concentrations, sources, and fluxes. Journal of Geophysical Research: Atmospheres, 98(D9), 16777–16786. https://doi.org/10.1029/93JD01689

Cutter, G.A., Bruland, Kenneth W., (1984), The marine biogeochemistry of selenium: A re-evaluation, Limnology and Oceanography, 6, https://doi.org/10.4319/lo.1984.29.6.1179.

Cutter, G. A., & Church, T. M. (1986). Selenium in western Atlantic precipitation. Nature, 322(6081), 720. https://doi.org/10.1038/322720a0

Cutter, G. A., & Cutter, L. S. (1995). Behavior of dissolved antimony, arsenic, and selenium in the Atlantic Ocean. Marine Chemistry, 49(4), 295–306. https://doi.org/10.1016/0304-4203(95)00019-N

Cutter, G. A., & Cutter, L. S. (1998). Metalloids in the high latitude North Atlantic Ocean: Sources and internal cycling. Marine Chemistry, 61(1), 25–36. https://doi.org/https://doi.org/10.1016/S0304-4203(98)00005-X

Cutter, G. A., & Cutter, L. S. (2004). Selenium biogeochemistry in the San Francisco Bay estuary: Changes in water column behavior. Estuarine, Coastal and Shelf Science, 61(3), 463–476. https://doi.org/10.1016/j.ecss.2004.06.011

Cutter, G. A., & San Diego-McGlone, M. L. C. (1990). Temporal variability of selenium fluxes in San Francisco Bay. Science of the Total Environment, The, 97–98(C), 235–250. https://doi.org/10.1016/0048-9697(90)90243-N

D'Ulivo, A., Gianfranceschi, L., Lampugnani, L., & Zamboni, R. (2002). Masking agents in the determination of selenium by hydride generation technique. Spectrochimica Acta Part B: Atomic Spectroscopy, 57(12), 2081–2094. https://doi.org/10.1016/S0584-8547(02)00166-0

D'Ulivo, A., Mester, Z., & Sturgeon, R. E. (2005). The mechanism of formation of volatile hydrides by tetrahydroborate(III) derivatization: A mass spectrometric study performed with deuterium labeled reagents. Spectrochimica Acta Part B: Atomic Spectroscopy, 60(4), 423–438. https://doi.org/10.1016/j.sab.2005.03.015

Dall'Aglio, M., Ghiara, E., & Proietti, W. (1978). New data on the hydrogeochemistry of selenium. Rend. Soc. Ital. Mineral. Petrol., 34(2), 591–604.

Darrouzès, J., Bueno, M., Lespès, G., & Potin-Gautier, M. (2005a). Operational optimisation of ICP—octopole collision/reaction cell—MS for applications to ultratrace selenium total and

speciation determination. Journal of Analytical Atomic Spectrometry, 20(2), 88–94. https://doi.org/10.1039/B410142A

Darrouzès, J., Bueno, M., Lespès, G., & Potin-Gautier, M. (2005b). Operational optimisation of ICP - Octopole collision/reaction cell - MS for applications to ultratrace selenium total and speciation determination. Journal of Analytical Atomic Spectrometry, 20(2), 88–94. https://doi.org/10.1039/b410142a

Darrouzès, J., Bueno, M., Simon, S., Pannier, F., & Potin-Gautier, M. (2008). Advantages of hydride generation interface for selenium speciation in waters by high performance liquid chromatography-inductively coupled plasma mass spectrometry coupling. Talanta, 75(2), 362–368. https://doi.org/10.1016/j.talanta.2007.11.020

Dauthieu, M., Bueno, M., Darrouzes, J., Gilon, N., & Potin-Gautier, M. (2006). Evaluation of porous graphitic carbon stationary phase for simultaneous preconcentration and separation of organic and inorganic selenium species in “clean” water systems. Journal of Chromatography A, 1114(1), 34–39. https://doi.org/10.1016/j.chroma.2006.02.018

Davis, T. Z., & Hall, J. O. (2017). Selenium. In Reproductive and Developmental Toxicology (pp. 595–605). Elsevier.

De Gregori, I., Lobos, M. G., & Pinochet, H. (2002). Selenium and its redox speciation in rainwater from sites of Valparaíso region in Chile, impacted by mining activities of copper ores. Water Research, 36(1), 115–122. https://doi.org/https://doi.org/10.1016/S0043-1354(01)00240-8

Deborde, J. (2019). Dynamique des sels nutritifs et de la matière organique dans le système fluvio-estuarien de l’Adour / golfe de Gascogne.

Delafiori, J., Ring, G., & Furey, A. (2016). Clinical applications of HPLC–ICP-MS element speciation: A review. Talanta, 153, 306–331. https://doi.org/10.1016/j.talanta.2016.02.035

Dhillon, K. S., & Dhillon, S. K. (2016). Selenium in groundwater and its contribution towards daily dietary Se intake under different hydrogeological zones of Punjab, India. Journal of Hydrology, 533, 615–626. https://doi.org/10.1016/j.jhydrol.2015.12.016

Di Tullo, P. (2015). Dynamique du cycle biogéochimique du sélénium en écosystèmes terrestres : rétention et réactivité dans le sol, rôle de la végétation. Retrieved from http://www.theses.fr/2015PAUU3013/document. Last access: October 09, 2020

Diaz, X., Johnson, W. P., Oliver, W. A., & Naftz, D. L. (2009). Volatile selenium flux from the great Salt Lake, Utah. Environmental Science and Technology, 43(1), 53–59. https://doi.org/10.1021/es801638w

do Nascimento, P. C., Jost, C. L., de Carvalho, L. M., Bohrer, D., & Koschinsky, A. (2009). Voltammetric determination of Se(IV) and Se(VI) in saline samples-Studies with seawater, hydrothermal and hemodialysis fluids. Analytica Chimica Acta, 648(2), 162–166. https://doi.org/10.1016/j.aca.2009.06.057

Domagalski, J. L., Orem, W. H., & Eugster, H. P. (1989). Organic geochemistry and brine composition in Great Salt, Mono, and Walker Lakes. Geochimica et Cosmochimica Acta, 53(11), 2857–2872. https://doi.org/https://doi.org/10.1016/0016-7037(89)90163-4

Duan, L., Song, J., Li, X., Yuan, H., & Xu, S. (2010). Distribution of selenium and its relationship to the eco-environment in Bohai Bay seawater. Marine Chemistry, 121(1–4), 87–99. https://doi.org/10.1016/j.marchem.2010.03.007

Dunhu, W., Diyang, Z., & Xiaoming, L. (1989). 1.5th-Differential polarographic determination of trace amounts of selenium(IV) and selenium(VI) in natural waters at a dropping mercury electrode. The Analyst, 114(July), 793–797. https://doi.org/10.1039/AN9891400793

Duval, B., Amouroux, D., & De Diego, A. (2020, in preparation). Ecodynamics of metals and metalloids in Pyrenean lakes in relation to climate change and anthropogenic pressure. Universite de Pau et des Pays de l'Adour and Euskal Herriko Unibertsitatea.

Eckert, W., & Conrad, R. (2007). Sulfide and methane evolution in the hypolimnion of a subtropical lake: A three-year study. Biogeochemistry, 82(1), 67–76. https://doi.org/10.1007/s10533-006-9053-3

El-Ramady, H., Abdalla, N., Alshaal, T., Domokos-Szabolcsy, É., Elhawat, N., Prokisch, J., … Shams, M. S. (2014). Selenium in soils under climate change, implication for human health. Environmental Chemistry Letters, 13(1), 1–19. https://doi.org/10.1007/s10311-014-0480-4

Etim, E. U. (2017). Occurrence and Distribution of Arsenic, Antimony and Selenium in Shallow Groundwater Systems of Ibadan Metropolis, Southwestern Nigerian. Journal of Health and Pollution, 7(13), 32–41. https://doi.org/10.5696/2156-9614-7-13.32

Fan, T. W.-M. W.-M., Higashi, R. M., & Lane, A. N. (1998). Biotransformations of Selenium Oxyanion by Filamentous Cyanophyte-Dominated Mat Cultured from Agricultural Drainage Waters. Environmental Science & Technology, 32(20), 3185–3193. https://doi.org/10.1021/es9708833

Feinberg, A., Stenke, A., Peter, T., & Winkel, L. H. E. (2020). Constraining Atmospheric Selenium Emissions Using Observations, Global Modeling, and Bayesian Inference. Environmental Science & Technology, 54(12), 7146–7155. https://doi.org/10.1021/acs.est.0c01408

Fernández-Martínez, A., & Charlet, L. (2009). Selenium environmental cycling and bioavailability : a structural chemist point of view. Reviews in Environmental Science and Bio/Technology, 8(1), 81–110. https://doi.org/10.1007/s11157-009-9145-3

Floor, G. H., Iglesías, M., Román-Ross, G., Corvini, P. F. X., & Lenz, M. (2011). Selenium speciation in acidic environmental samples: Application to acid rain-soil interaction at Mount Etna volcano. Chemosphere, 84(11), 1664–1670. https://doi.org/10.1016/j.chemosphere.2011.05.006

Floor, G. H., & Román-Ross, G. (2012). Selenium in volcanic environments: A review. Applied Geochemistry, 27(3), 517–531. https://doi.org/https://doi.org/10.1016/j.apgeochem.2011.11.010

FNAB, F. N. d'Agriculture B. (2015). Syndicat mixte du bassin versant de la Nive. Retrieved from https://www.eauetbio.org. Last access : October 17, 2020

Fordyce, F. M. (2013). Selenium Deficiency and Toxicity in the Environment. In Essentials of medical geology (pp. 375–416). Springer. https://doi.org/10.1007/978-94-007-4375-5_16

Fordyce, F. M., Johnson, C. C., Navaratna, U. R. B., Appleton, J. D., & Dissanayake, C. B. (2000). Selenium and iodine in soil, rice and drinking water in relation to endemic goitre in Sri Lanka. Science of the Total Environment, 263(1–3), 127–141. https://doi.org/10.1016/S0048-9697(00)00684-7

Fu, J., Zhang, X., Qian, S., & Zhang, L. (2012). Preconcentration and speciation of ultra-trace Se (IV) and Se (VI) in environmental water samples with nano-sized TiO2 colloid and determination by HG-AFS. Talanta, 94, 167–171. https://doi.org/10.1016/j.talanta.2012.03.012

Gallignani, M., Valero, M., Brunetto, M. R., Burguera, J. L., Burguera, M., & de Pena, Y. P. (2000). Sequential determination of Se (IV) and Se (VI) by flow injection-hydride generation-atomic absorption spectrometry with HCl/HBr microwave aided pre-reduction of Se (VI) to Se (IV). Talanta, 52(6), 1015–1024. https://doi.org/10.1016/S0039-9140(00)00438-0

Gao, S., Tanji, K. K., Peters, D. W., & Herbel, M. J. (2000). Water selenium speciation and sediment fractionation in a California flow-through wetland system. Journal of Environmental Quality, 29(4), 1275–1283. https://doi.org/10.2134/jeq2000.00472425002900040034x

Gascoin, S., Hagolle, O., Huc, M., Jarlan, L., Dejoux, J.-F., Szczypta, C., … Sánchez, R. (2015). A snow cover climatology for the Pyrenees from MODIS snow products. Hydrology and Earth System Sciences, European Geosciences Union, 2015, ⟨hal-01218966⟩. https://doi.org/10.5194/hess-19-2337-2015

Ghasemi, E., & Farahani, H. (2012). Head space solid phase microextraction based on nano-structured lead dioxide: Application to the speciation of volatile organoselenium in environmental and biological samples. Journal of Chromatography A, 1258, 16–20. https://doi.org/https://doi.org/10.1016/j.chroma.2012.08.027

Ginzburg, B., Chalifa, I., Gun, J., Dor, I., Hadas, O., & Lev, O. (1998). DMS formation by dimethylsulfoniopropionate route in freshwater. Environmental Science and Technology, 32(14), 2130–2136. https://doi.org/10.1021/es9709076

Ginzburg, B., Dor, I., Chalifa, I., Hadas, O., & Lev, O. (1999). Formation of Dimethyloligosulfides in Lake Kinneret: Biogenic Formation of Inorganic Oligosulfide Intermediates under Oxic Conditions. Environmental Science & Technology, 33(4), 571–579. https://doi.org/10.1021/es980636e

Gleizes, G., Leblanc, D., Santana, V., Olivier, P., & Bouchez, J. L. (1998). Sigmoidal structures featuring dextral shear during emplacement of the Hercynian granite complex of Cauterets–Panticosa (Pyrenees). Journal of Structural Geology, 20(9), 1229–1245. https://doi.org/https://doi.org/10.1016/S0191-8141(98)00060-1

Gómez-Ariza, J. L., Pozas, J. A., Giráldez, I., Moralesa, E., & Morales, E. (1999). Use of solid phase extraction for speciation of selenium compounds in aqueous environmental samples. Analyst, 124(1), 75–78. https://doi.org/10.1039/a805447i

Grabarczyk, M., & Korolczuk, M. (2010). Development of a simple and fast voltammetric procedure for determination of trace quantity of Se(IV) in natural lake and river water samples. Journal of Hazardous Materials, 175(1), 1007–1013. https://doi.org/https://doi.org/10.1016/j.jhazmat.2009.10.110

Grober, R., Heumann, K. G., & Großer, R. (1989). Negative Thermionen-Massenspektrometrie von Selen. Fresenius' Zeitschrift Für Analytische Chemie, 332(8), 880–883. https://doi.org/10.1007/BF00481895

Guan, D. M., & Martin, J. M. (1991). Selenium distribution in the Rhône delta and the Gulf of Lions. Marine Chemistry, 36(1–4), 303–316. https://doi.org/10.1016/S0304-4203(09)90068-8

Guerin, T., Astruc, A., & Astruc, M. (1999). Speciation of arsenic and selenium compounds by HPLC hyphenated to specific detectors: A review of the main separation techniques. Talanta, 50(1), 1–24. https://doi.org/10.1016/S0039-9140(99)00140-X

Guo, L., Frankenberger, W. T., & Jury, W. A. (1999). Evaluation of simultaneous reduction and transport of selenium in saturated soil columns, 35(3), 663–669. https://doi.org/10.1029/1998WR900074

Guo, X., Sturgeon, R. E., Mester, Z., & Gardner, G. J. (2003). UV Vapor Generation for Determination of Selenium by Heated Quartz Tube Atomic Absorption Spectrometry. Analytical Chemistry, 75(9), 2092–2099. https://doi.org/10.1021/ac020695h

Hadas, O., & Pinkas, R. (1995). Sulfate reduction processes in sediments at different sites in Lake Kinneret, Israel. Microbial Ecology, 30(1), 55–66. https://doi.org/10.1007/BF00184513

Hall, G. E. M., & Pelchat, J.-C. (1997). Analysis of geological materials for bismuth, antimony, selenium and tellurium by continuous flow hydride generation inductively coupled plasma mass spectrometry. Journal of Analytical Atomic Spectrometry, 12(1), 97–102. https://doi.org/10.1039/A605398J

Hall, J. O. (2018). Chapter 33 - Selenium. In R. C. B. T.-V. T. (Third E. Gupta (Ed.) (pp. 469–477). Academic Press. https://doi.org/https://doi.org/10.1016/B978-0-12-811410-0.00033-7

Hambright, K., Zohary, T (1998). Lakes Hula and Agmon: destruction and creation of wetland ecosystems in northern Israel. Wetlands Ecology and Management 6, 83–89. https://doi.org/10.1023/A:1008441015990

Han, F. X. (2007). Biogeochemistry of Trace Elements in Arid Environments. Springer Netherlands. Retrieved from https://books.google.fr/books?id=gwgSoKEvaPUC. Last access: November 08, 2020.

Harrison, P. J., Yu, P. W., Thompson, P. A., Price, N. M., & Phillips, D. J. (1988). Survey of selenium requirements in marine phytoplankton. Marine Ecology Progress Series, 47(1), 89–96. Retrieved from http://www.jstor.org/stable/24831560, Last access : Nobember 09, 2020.

Haygarth, P. M. (1994). Global importance and global cycling of selenium. Selenium in the Environment, 1–27. Retrieved from https://books.google.es/. Last access November 09, 2020.

Hem, J. D. (1985). Study and interpretation of the chemical characteristics of natural water (Vol. 2254). Department of the Interior, US Geological Survey.

Holden, N. E., Coplen, T. B., Böhlke, J. K., Tarbox, L. V., Benefield, J., De Laeter, J. R., … Yoneda, S. (2018). IUPAC Periodic Table of the Elements and Isotopes (IPTEI) for the Education Community (IUPAC Technical Report). Pure and Applied Chemistry, 90(12), 1833–2092. https://doi.org/10.1515/pac-2015-0703

Horne, A. J., & Goldman, C. R. (1994). Lake ecology overview. Limnology. McGraw-Hill Co, New York, USA.

Hu, H., Mylon, S. E., & Benoit, G. (2007). Volatile organic sulfur compounds in a stratified lake. Chemosphere, 67(5), 911–919. https://doi.org/10.1016/j.chemosphere.2006.11.012

Hu, M., Yang, Y., Martin, J.-M., Yin, K., & Harrison, P. J. (1997). Preferential uptake of Se(IV) over Se(VI) and the production of dissolved organic Se by marine phytoplankton. Marine Environmental Research, 44(2), 225–231. https://doi.org/10.1016/S0141-1136(97)00005-6

Hung, J.-J., & Shy, C.-P. (1995). Speciation of Dissolved Selenium in the Kaoping and Erhjen Rivers and Estuaries, Southwestern Taiwan. Estuaries, 18(1), 234. https://doi.org/10.2307/1352633

Ivanenko, N. V. (2018). The Role of Microorganisms in Transformation of Selenium in Marine Waters. Russian Journal of Marine Biology, 44(2), 87–93. https://doi.org/10.1134/S1063074018020049

Jaffe WG, Ruphael M, Mondragon MC, Cuevas MA. Estudio clínico y bioquímico en niños escolares de una zona selenífera [Clinical and biochemical study in school children of a seleniferous zone]. Arch Latinoam Nutr. 1972 Dec;22(4):595-611. Spanish. PMID: 4664553.

Jakubowski, N., Thomas, C., Stuewer, D., Dettlaff, I., & Schram, J. (1996). Speciation of inorganic selenium by inductively coupled plasma mass spectrometry with hydraulic high pressure nebulization. Journal of Analytical Atomic Spectrometry, 11(11), 1023–1029. https://doi.org/10.1039/JA9961101023

Esbaugh, A. J., Khursigara, A., & Johansen, J. (2018). Toxicity in Aquatic Environments: The Cocktail Effect. In Development and Environment (pp. 203-234). Springer, Cham. https://doi.org/10.1007/978-3-319-75935-7_9

Jiang, S., Robberecht, H., & Adams, F. (1983). Identification and determination of alkylselenide compounds in environmental air. Atmospheric Environment (1967), 17(1), 111–114. https://doi.org/10.1016/0004-6981(83)90014-8

Kennish, M. J. (2017). Practical handbook of Estuarine and Marine pollution. Practical Handbook of Estuarine and Marine Pollution. https://doi.org/10.1201/9780203742488

Kennish, M. J. (2019). Ecology of Estuaries: Volume 2: Biological Aspects. CRC Press. Retrieved from https://books.google.fr/books?id=0TSoDwAAQBAJ. Last access: November 09, 2020.

Knossow, N., Blonder, B., Eckert, W., Turchyn, A. V., Antler, G., & Kamyshny, A. (2015). Annual sulfur cycle in a warm monomictic lake with sub-millimolar sulfate concentrations. Geochemical Transactions, 16(1), 7. https://doi.org/10.1186/s12932-015-0021-5

Kotrebai, M., Birringer, M., Tyson, J. F., Block, E., & Uden, P. C. (2000). Selenium speciation in enriched and natural samples by HPLC-ICP-MS and HPLC-ESI-MS with perfluorinated carboxylic acid ion-pairing agents. Analyst, 125(1), 71–78. https://doi.org/10.1039/A906320J

Kotrebai, M., Tyson, J. F., Block, E., & Uden, P. C. (2000). High-performance liquid chromatography of selenium compounds utilizing perfluorinated carboxylic acid ion-pairing agents and inductively coupled plasma and electrospray ionization mass spectrometric detection. Journal of Chromatography A, 866(1), 51–63. https://doi.org/10.1016/S0021-9673(99)01060-2

Kovaleva, S. V, Gladyshev, V. P., & Rubinskaya, T. B. (2006). Voltammetric determination of selenosulfate ions at a mercury-film electrode. Journal of Analytical Chemistry, 61(1), 72–76. https://doi.org/10.1134/S1061934806010151

Kumar, A. R., & Riyazuddin, P. (2006). Studies on the efficiency of hydrogen selenide generation with different acid media by continuous flow hydride generation atomic absorption spectrometry. Microchimica Acta, 155(3–4), 387–396. https://doi.org/10.1007/s00604-006-0583-0

Kumar, A. R., & Riyazuddin, P. (2011). Speciation of selenium in groundwater: Seasonal variations and redox transformations. Journal of Hazardous Materials, 192(1), 263–269. https://doi.org/10.1016/j.jhazmat.2011.05.013

Kurokawa, S., & Berry, M. J. (2013). Selenium. Role of the Essential Metalloid in Health. In A. Sigel, H. Sigel, & R. K. O. Sigel (Eds.), Interrelations between Essential Metal Ions and Human Diseases (pp. 499–534). Dordrecht: Springer Netherlands. https://doi.org/10.1007/978-94-007-7500-8_16

Laborda, F., Chakraborti, D., Mir, J. M., & Castillo, J. R. (1993). Selenium speciation by high-performance liquid chromatography-fraction collection-electrothermal atomic absorption spectrometry: Optimization of critical parameters. Journal of Analytical Atomic Spectrometry, 8(4), 643–648. https://doi.org/10.1039/JA9930800643

Lahermo, P., Alfthan, G., & Wang, D. (1998). Selenium and arsenic in the environment in Finland. Journal of Environmental Pathology, Toxicology and Oncology : Official Organ of the International Society for Environmental Toxicology and Cancer, 17(3–4), 205–216.

Lanceleur, L., Tessier, E., Bueno, M., Pienitz, R., Bouchard, F., Cloquet, C., & Amouroux, D. (2019). Cycling and atmospheric exchanges of selenium in Canadian subarctic thermokarst ponds. Biogeochemistry, 145(1-2), 193-211. https://doi.org/10.1007/s10533-019-00599-w

Larsen, E. H., & Stürup, S. (1994). Carbon-enhanced inductively coupled plasma mass spectrometric detection of arsenic and selenium and its application to arsenic speciation. Journal of Analytical Atomic Spectrometry, 9(10), 1099–1105. https://doi.org/10.1039/JA9940901099

Lawson, N. M., & Mason, R. P. (2001). Concentration of Mercury, Methylmercury, Cadmium, Lead, Arsenic, and Selenium in the Rain and Stream Water of Two Contrasting Watersheds in Western Maryland. Water Research, 35(17), 4039–4052. https://doi.org/10.1016/S0043-1354(01)00140-3

LeBlanc, K. L., Kumkrong, P., Mercier, P. H. J., & Mester, Z. (2018). Selenium analysis in waters. Part 2: Speciation methods. Science of the Total Environment. https://doi.org/10.1016/j.scitotenv.2018.05.394

LeBlanc, K. L., Ruzicka, J., & Wallschläger, D. (2016). Identification of trace levels of selenomethionine and related organic selenium species in high-ionic-strength waters. Analytical and Bioanalytical Chemistry, 408(4), 1033–1042. https://doi.org/10.1007/s00216-015-9124-1

LeBlanc, K. L., Smith, M. S., & Wallschläger, D. (2012). Production and release of selenocyanate by different green freshwater algae in environmental and laboratory samples. Environmental Science and Technology, 46(11), 5867–5875. https://doi.org/10.1021/es203904e

Leblanc, K. L., & Wallschläger, D. (2016). Production and Release of Selenomethionine and Related Organic Selenium Species by Microorganisms in Natural and Industrial Waters. Environmental Science and Technology, 50(12), 6164–6171. https://doi.org/10.1021/acs.est.5b05315

Lemly, A. D. (2004). Aquatic selenium pollution is a global environmental safety issue. Ecotoxicology and Environmental Safety, 59(1), 44–56. https://doi.org/10.1016/S0147-6513(03)00095-2

Lenny Winkel, Vriens, B., Jones, G. D., Schneider, L. S., Pilon-Smits, E., & Bañuelos, G. S. (2015). Selenium cycling across soil-plant-atmosphere interfaces: A critical review. Nutrients. https://doi.org/10.3390/nu7064199

Lenz, M., Hullebusch, E. D. van, Farges, F., Nikitenko, S., Borca, C. N., Grolimund, D., & Lens, P. N. L. (2008). Selenium speciation assessed by X-ray absorption spectroscopy of sequentially extracted anaerobic biofilms. Environmental Science & Technology, 42(20), 7587–7593. https://doi.org/10.1021/es800811q

Lenz, M., & Lens, P. N. L. (2009). The essential toxin: The changing perception of selenium in environmental sciences. Science of the Total Environment, 407(12), 3620–3633. https://doi.org/10.1016/j.scitotenv.2008.07.056

Lidman, F., Bj, L., Mörth, C.-M., Björkvald, L., & Laudon, H. (2011). Selenium Dynamics in Boreal Streams : The Role of Wetlands and Changing Groundwater Tables. Environmental Science & Technology, 45(7), 2677–2683. https://doi.org/10.1021/es102885z

Lindemann, T., & Hintelmann, H. (2002). Selenium speciation by HPLC with tandem mass spectrometric detection. Analytical and Bioanalytical Chemistry, 372(3), 486–490. https://doi.org/10.1007/s00216-001-1113-x

Lindström, K. (1983). Selenium as a growth factor for plankton algae in laboratory experiments and in some Swedish lakes. In C. Forsberg & J.-Å. Johansson (Eds.), Hydrobiologia (Vol. 101, pp. 35–47). Dordrecht: Springer Netherlands. https://doi.org/10.1007/BF00008655

Long, G. L., & Winefordner, J. D. (1983). Limit of Detection: A Closer Look at the IUPAC Definition. Analytical Chemistry, 55(7), 712A–724A. https://doi.org/10.1021/ac00258a001

Long, J., & Nagaosa, Y. (2007). Determination of selenium (IV) by catalytic stripping voltammetry with an in situ plated bismuth-film electrode. Analytical Sciences, 23(11), 1343–1346. https://doi.org/10.2116/analsci.23.1343

López-Moreno, J. I., & Vicente-Serrano, S. M. (2007). Atmospheric circulation influence on the interannual variability of snow pack in the Spanish Pyrenees during the second half of the 20th century. Hydrology Research, 38(1), 33–44. https://doi.org/10.2166/nh.2007.030

Luoma, S. N., & Rainbow, P. S. (2008). Metal contamination in aquatic environments: science and lateral management. Cambridge university press.

Luxem, K. E., Vriens, B., Behra, R., & Winkel, L. H. E. (2017). Studying selenium and sulfur volatilisation by marine algae Emiliania huxleyi and Thalassiosira oceanica in culture. Environmental Chemistry, 14(4), 199–206. https://doi.org/10.1071/EN16184

Martin, A. J., Simpson, S., Fawcett, S., Wiramanaden, C. I. E. E., Pickering, I. J., Belzile, N., … Wallschläger, D. (2011). Biogeochemical mechanisms of selenium exchange between water and sediments in two contrasting lentic environments. Environmental Science and Technology, 45(7), 2605–2612. https://doi.org/10.1021/es103604p

Mason, R. P., Soerensen, A. L., Dimento, B. P., & Balcom, P. H. (2018). The Global Marine Selenium Cycle: Insights from Measurements and Modeling. Global Biogeochemical Cycles, 32(1720–1737). https://doi.org/10.1029/2018GB006029

Masscheleyn, P. H., & Patrick Jr, W. H. (1993). Biogeochemical processes affecting selenium cycling in wetlands. Environmental Toxicology and Chemistry: An International Journal, 12(12), 2235–2243. https://doi.org/10.1002/etc.5620121207

Mattsson, G., Nyholm, L., Olin, Å., & Örnemark, U. (1995). Determination of selenium in freshwaters by cathodic stripping voltammetry after UV irradiation. Talanta, 42(6), 817–825. https://doi.org/10.1016/0039-9140(95)01494-V

Mcneal, J. M., & Balistrieri, L. S. (1989). Geochemistry and Occurrence of Selenium : An Overview. Selenium in Agriculture and the Environment, (23), 1–13. https://doi.org/10.2136/sssaspecpub23.c1

Measures, C. I., & Burton, J. D. (1978). Behaviour and speciation of dissolved selenium in estuarine waters. Nature, 273(5660), 293–295. https://doi.org/10.1038/273293a0

Measures, C. I., & Burton, J. D. (1980a). Gas chromatographic method for the determination of selenite and total selenium in sea water. Analytica Chimica Acta, 120, 177–186. https://doi.org/10.1016/S0003-2670(01)84361-0

Measures, C. I., & Burton, J. D. (1980). The vertical distribution and oxidation states of dissolved selenium in the northeast Atlantic Ocean and their relationship to biological processes. Earth

and Planetary Science Letters, 46(3), 385-396. https://doi.org/10.1016/0012-821X(80)90052-7

Grant, B. C., Mangum, B. J., & Edmond, J. M. (1983). The relationship of the distribution of dissolved selenium IV and VI in three oceans to physical and biological processes. In Trace metals in sea water (pp. 73-83). Springer, Boston, MA. https://doi.org/10.1007/978-1-4757-6864-0_4

Mehdi, Y., Hornick, J.-L., Istasse, L., & Dufrasne, I. (2013). Selenium in the Environment, Metabolism and Involvement in Body Functions. Molecules. https://doi.org/10.3390/molecules18033292

Mehra, H. C., & Frankenberger, W. T. (1988). Simultaneous analysis of selenate and selenite by single-column ion chromatography. Chromatographia, 25(7), 585–588. https://doi.org/10.1007/BF02327651

Merino, I. E., Stegmann, E., Aliaga, M. E., Gomez, M., Arancibia, V., & Rojas−Romo, C. (2019). Determination of Se(IV) concentration via cathodic stripping voltammetry in the presence of Cu(II) ions and ammonium diethyl dithiophosphate. Analytica Chimica Acta, 1048, 22–30. https://doi.org/10.1016/j.aca.2018.09.061

Meyer, R. D., & Burau, R. G. (1995). The geochemistry and biogeochemistry of selenium in relation to its deficiency and toxicity in animals. In Proceedings of a national symposium: Selenium in the environment: Essential nutrient, potential toxicant. Sacramento, California (pp. 38–44).

Milley, J. E., & Chatt, A. (1987). Preconcentration and instrumental neutron activation analysis of acid rain for trace elements. Journal of Radioanalytical and Nuclear Chemistry, 110(2), 345–363. https://doi.org/10.1007/BF02035526

Mills, T. J., Mast, M. A., Thomas, J., & Keith, G. (2016). Controls on selenium distribution and mobilization in an irrigated shallow groundwater system underlain by Mancos Shale, Uncompahgre River Basin, Colorado, USA. Science of The Total Environment, 566–567, 1621–1631. https://doi.org/10.1016/j.scitotenv.2016.06.063

Montiel, A. (1981). [Determination of selenium in water by gas chromatography and electron capture].[French]. Analusis.

Moreno, M. E., Pérez-Conde, C., & Cámara, C. (2000). Speciation of inorganic selenium in environmental matrices by flow injection analysis-hydride generation-atomic fluorescence spectrometry. Comparison of off-line, pseudo on-line and on-line extraction and reduction methods. Journal of Analytical Atomic Spectrometry, 15(6), 681–686. https://doi.org/10.1039/A909590J

Moreno, M. E., Pérez-Conde, C., & Cámara, C. (2003). The effect of the presence of volatile organoselenium compounds on the determination of inorganic selenium by hydride generation. Analytical and Bioanalytical Chemistry, 375(5), 666–672. https://doi.org/10.1007/s00216-003-1774-8

Mortimer, C. H. (1981). The oxygen content of air-saturated fresh waters over ranges of temperature and atmospheric pressure of limnological interest. SIL Communications, 1953-1996, 22(1), 1–23. https://doi.org/10.1080/05384680.1981.11904000

Mosher, B. W., & Duce, R. A. (1987). A global atmospheric selenium budget. Journal of Geophysical Research: Atmospheres, 92(D11), 13289–13298. https://doi.org/10.1029/JD092iD11p13289

Najafi, N. M., Seidi, S., Alizadeh, R., & Tavakoli, H. (2010). Inorganic selenium speciation in environmental samples using selective electrodeposition coupled with electrothermal atomic absorption spectrometry. Spectrochimica Acta - Part B Atomic Spectroscopy, 65(4), 334–339. https://doi.org/10.1016/j.sab.2010.02.017

Najafi, N. M., Tavakoli, H., Abdollahzadeh, Y., & Alizadeh, R. (2012). Comparison of ultrasound-assisted emulsification and dispersive liquid-liquid microextraction methods for the speciation of inorganic selenium in environmental water samples using low density extraction solvents. Analytica Chimica Acta, 714, 82–88. https://doi.org/10.1016/j.aca.2011.11.063

Nakaguchi, Y., & Hiraki, K. (1993). Selenium (IV), selenium (VI) and organic selenium in Lake Biwa, the Yodo River and Osaka Bay. Geochemical Journal, 27(6), 367–374. https://doi.org/10.2343/geochemj.27.367

Nakamaru, Y. M., & Altansuvd, J. (2014). Speciation and bioavailability of selenium and antimony in non-flooded and wetland soils: A review. Chemosphere, 111, 366–371. https://doi.org/10.1016/j.chemosphere.2014.04.024

Nakamaru, Y., Tagami, K., & Uchida, S. (2006). Effect of phosphate addition on the sorption–desorption reaction of selenium in Japanese agricultural soils. Chemosphere, 63(1), 109–115. https://doi.org/10.1016/j.chemosphere.2005.07.046

Nancharaiah, Y. V., & Lens, P. N. L. (2015). Ecology and biotechnology of selenium-respiring bacteria. Microbiol. Mol. Biol. Rev., 79(1), 61–80. https://doi.org/10.1128/MMBR.00037-14

Naumov, A. V. (2010). Selenium and tellurium: State of the markets, the crisis, and its consequences. Metallurgist, 54(3–4), 197–200. https://doi.org/10.1007/s11015-010-9280-7

Nazarenko, I. I., & Kislova, I. V. (1978). Determination of different forms of selenium in water. Journal of analytical chemistry of the URRS. 33(9), 1429-1430.

Neue, U. D. (2007). Chromatography: Liquid | Mechanisms: Reversed Phases. In I. D. B. T.-E. of S. S. Wilson (Ed.) (pp. 1–7). Oxford: Academic Press. https://doi.org/10.1016/B0-12-226770-2/00311-2

Neumann, P. M., De Souza, M. P., Pickering, I. J., & Terry, N. (2003). Rapid microalgal metabolism of selenate to volatile dimethylselenide. Plant, Cell & Environment, 26(6), 897–905. https://doi.org/10.1046/j.1365-3040.2003.01022.x

Neve, J., Hanocq, M., & Molle, L. (1980). Nouvelles propositions pour la dètermination du sèlènium dans des eaux naturelles. International Journal of Environmental Analytical Chemistry, 8(3), 177–188. https://doi.org/10.1080/03067318008071498

Niedzielski, P. (2005). The new concept of hyphenated analytical system: Simultaneous determination of inorganic arsenic(III), arsenic(V), selenium(IV) and selenium(VI) by high performance liquid chromatography-hydride generation-(fast sequential) atomic absorption spectrometry . Analytica Chimica Acta, 551(1–2), 199–206. https://doi.org/10.1016/j.aca.2005.06.073

Niedzielski, P., Siepak, M., & Grabowski, K. (2002). Microtrace Contents of Arsenic, Antimony and Selenium in Surface Waters of Pszczewski Landscape Park as a Region Potentially Free from Anthropogenic Pressure. Polish Journal of Environmental Studies, 11(5), 547–553.

Nishri, A., Brenner, I. B., Hall, G. E. M., & Taylor, H. E. (1999). Temporal variations in dissolved selenium in Lake Kinneret (Israel). Aquatic Sciences, 61(3), 215–233. https://doi.org/10.1007/s000270050063

Nishri, A., Stiller, M., Rimmer, A., Geifman, Y., & Krom, M. (1999). Lake Kinneret (The Sea of Galilee): The effects of diversion of external salinity sources and the probable chemical composition of the internal salinity sources. Chemical Geology, 158(1–2), 37–52. https://doi.org/10.1016/S0009-2541(99)00007-8

NRC, U. S. (1983). Risk assessment in the federal government: managing the process. National Research Council, Washington DC, 11, 3.

Nriagu, J. O. (1989). A global assessment of natural sources of atmospheric trace metals. Nature, 338(6210), 47–49. https://doi.org/10.1038/338047a0

Nriagu, J. O., & Pacyna, J. M. (1988). Quantitative assessment of worldwide contamination of air, water and soils by trace metals. Nature, 333(6169), 134.

Nriagu, J. O., & Wong, H. K. (1983). Selenium pollution of lakes near the smelters at Sudbury, Ontario. Nature, 301(5895), 55.

Ohlendorf, H. M. (2003). Handbook of ecotoxicology, second edition (2nd ed.). Boca Raton, FL: Lewis Publishers. Retrieved from http://pubs.er.usgs.gov/publication/5200177

Økelsrud, A., Lydersen, E., & Fjeld, E. (2016). Biomagnification of mercury and selenium in two lakes in southern Norway. Science of the Total Environment, 566, 596–607. https://doi.org/10.1016/j.scitotenv.2016.05.109

Olivas, R. M. M., Donard, O. F. X. X., Gilon, N., & Potin-Gautier, M. (1996). Speciation of organic selenium compounds by high-performance liquid chromatography-inductively coupled plasma mass spectrometry in natural samples. J. Anal. At. Spectrom., 11(12), 1171–1176. https://doi.org/10.1039/JA9961101171

Olson, L. K., Vela, N. P., & Caruso, J. A. (1995). Hydride generation, electrothermal vaporization and liquid chromatography as sample introduction techniques for inductively coupled plasma mass spectrometry. Spectrochimica Acta Part B: Atomic Spectroscopy, 50(4–7), 355–368. https://doi.org/10.1016/0584-8547(94)00170-Z

Oram, L. L., Strawn, D. G., Marcus, M. A., Fakra, S. C., & Möller, G. (2008). Macro- and microscale investigation of selenium speciation in Blackfoot Ri+ver, Idaho sediments. Environmental Science and Technology, 42(18), 6830–6836. https://doi.org/10.1021/es7032229

Oremland, R. S., Hollibaugh, J. T., Maest, A. S., Presser, T. S., Miller, L. G., Charles, W., & Maest, A. N. N. S. (1989). Selenate Reduction to Elemental Selenium by Anaerobic Bacteria in Sediments and Culture. Applied and Environmental Microbiology, 55(9), 2333–43.

Orvini, E., & Gallorini, M. (1982). Speciation problems solved with NAA: Some actual cases for Hg, V, Cr, As and Se. Journal of Radioanalytical Chemistry, 71(1–2), 75–95. https://doi.org/10.1007/BF02516142

Ostrovsky, I., Rimmer, A., Yacobi, Y. Z., Nishri, A., Sukenik, A., Hadas, O., & Zohary, T. (2013). Long-Term Changes in the Lake Kinneret Ecosystem: The Anthropogenic Factors. Climate Change and Global Warming of Inland Waters: Impacts and Mitigation for Ecosystems and Societies, (July 2016), 271–293. https://doi.org/10.1002/9781118470596.ch16

Oyamada, N., & Ishizaki, M. (1986). Fractional determination of dissolved selenium compounds of trimethylselenonium ion, selenium (IV) and selenium (VI) in environmental water samples. Analytical Sciences, 2(4), 365–369. https://doi.org/10.2116/analsci.2.365

Palacios, Ò., & Lobinski, R. (2007). Investigation of the stability of selenoproteins during storage of human serum by size-exclusion LC-ICP-MS. Talanta, 71(4), 1813–1816. https://doi.org/10.1016/j.talanta.2006.08.018

Pan, Y. P., & Wang, Y. S. (2015). Atmospheric wet and dry deposition of trace elements at 10 sites in Northern China, 951–972. https://doi.org/10.5194/acp-15-951-2015

Panhwar, A. H., Tuzen, M., & Kazi, T. G. (2017). Ultrasonic assisted dispersive liquid-liquid microextraction method based on deep eutectic solvent for speciation, preconcentration and determination of selenium species (IV) and (VI) in water and food samples. Talanta, 175(July), 352–358. https://doi.org/10.1016/j.talanta.2017.07.063

Peachey, E., Cook, K., Castles, A., Hopley, C., & Goenaga-Infante, H. (2009). Capabilities of mixed-mode liquid chromatography coupled to inductively coupled plasma mass spectrometry for the simultaneous speciation analysis of inorganic and organically-bound selenium. Journal of Chromatography A, 1216(42), 7001–7006. https://doi.org/10.1016/j.chroma.2009.08.047

Pécheyran, C., Amouroux, D., & Donard, O. F. X. X. (1998). Field determination of volatile selenium species at ultra trace levels in environmental waters by on-line purging, cryofocusing and detection by atomic fluorescence spectroscopy. Journal of Analytical Atomic Spectrometry, 13(7), 615–621. https://doi.org/10.1039/A802246A

Pettine, M., McDonald, T. J., Sohn, M., Anquandah, G. A. K. K., Zboril, R., & Sharma, V. K. (2015). A critical review of selenium analysis in natural water samples. Trends in Environmental Analytical Chemistry, 5, 1–7. https://doi.org/10.1016/j.teac.2015.01.001

Pilon-Smits, E. A. H., & Quinn, C. F. (2010). Selenium metabolism in plants. In Cell biology of metals and nutrients (pp. 225–241). Springer. https://doi.org/10.1007/978-3-642-10613-2_10

Plant, J. A., Bone, J., Voulvoulis, N., Kinniburgh, D. G., Smedley, P. L., Fordyce, F. M., & Klinck, B. (2013). Arsenic and Selenium. Treatise on Geochemistry: Second Edition (2nd ed., Vol. 11). Elsevier Ltd. https://doi.org/10.1016/B978-0-08-095975-7.00902-5

Point, D. (2004). Spéciation et biogéochimie des elements trace métalliques dans l'estuaire de l'Adour (2004). Thèse de l'Université de Pau et Pays de l'Adour.

Pokrovsky, O. S., Bueno, M., Amouroux, D., Manasypov, R. M., Shirokova, L. S., Karlsson, J., & Amouroux, D. (2018). Dissolved organic matter controls on seasonal and spatial selenium concentration variability in thaw lakes across a permafrost gradient. Environ. Sci. Technol., 52(18), acs.est.8b00918. https://doi.org/10.1021/acs.est.8b00918

Ponton, D. E., Fortin, C., & Hare, L. (2018). Organic selenium, selenate, and selenite accumulation by lake plankton and the alga Chlamydomonas reinhardtii at different pH and sulfate concentrations. Environmental Toxicology and Chemistry, 37(8), 2112–2122. https://doi.org/10.1002/etc.4158

Ponton, D. E., & Hare, L. (2013). Relating selenium concentrations in a planktivore to selenium speciation in lakewater. Environmental Pollution, 176, 254–260. https://doi.org/10.1016/j.envpol.2013.01.032

Presser, T. S., Sylvester, M. A., & Low, W. H. (1994). Bioaccumulation of selenium from natural geologic sources in western states and its potential consequences. Environmental Management, 18(3), 423–436. https://doi.org/10.1007/BF02393871

Pyrzynska, K. (1996). Speciation analysis of some organic selenium compounds: A review. Analyst, 121(8), 77R–83R. https://doi.org/10.1039/AN996210077R

Quijano, M. A., Gutiérrez, A. M., Pérez-Conde, M. C., & Cámara, C. (1996). Determination of selenocystine, selenomethionine, selenite and selenate by high-performance liquid chromatography coupled to inductively coupled plasma mass spectrometry. Journal of Analytical Atomic Spectrometry, 11(6), 407–411. https://doi.org/10.1039/JA9961100407

Rabin, S., & Stillian, J. (1994). Practical aspects on the use of organic solvents in ion chromatography. Journal of Chromatography A, 671(1–2), 63–71. https://doi.org/10.1016/0021-9673(94)80222-X

Raptis, S. E., Kaiser, G., & Tölg, G. (1983). A Survey of selenium in the environment and a critical review of its determination at trace levels. Fresenius' Zeitschrift Für Analytische Chemie, 316(2), 105–123. https://doi.org/10.1007/BF00488176

Selenium Production, Import/Export, Use and Disposal (1997). Retrieved from https://www.atsdr.cdc.gov/toxprofiles/tp92-c5.pdf. Last access: November 09, 2020.

Reich, H. J., & Hondal, R. J. (2016). Why Nature Chose Selenium. ACS Chemical Biology, 11(4), 821–841. https://doi.org/10.1021/acschembio.6b00031

Reichardt, C. (1979). Empirical Parameters of Solvent Polarity as Linear Free-Energy Relationships. Angewandte Chemie International Edition in English, 18(2), 98–110. https://doi.org/10.1002/anie.197900981

Reichardt, C., & Welton, T. (2010). Classification of Solvents. Solvents and Solvent Effects in Organic Chemistry. https://doi.org/doi:10.1002/9783527632220.ch3

Reimann, C., & De Caritat, P. (1998). Chemical elements in the environment: factsheets for the geochemist and environmental scientist. Springer Science & Business Media. https://doi.org/10.1007/978-3-642-72016-1

Rimmer, A., & Gal, G. (2003). Estimating the saline springs component in the solute and water balance of Lake Kinneret, Israel. Journal of Hydrology, 284(1–4), 228–243. https://doi.org/10.1016/j.jhydrol.2003.08.006

Rimmer, A., & Givati, A. (2014). Lake Kinneret. Lake Kinneret, 97–111. https://doi.org/10.1007/978-94-017-8944-8

Robberecht, H., Van Grieken, R., Van Sprundel, M., Berghe, D. Vanden, & Deelstra, H. (1983). Selenium in environmental and drinking waters of Belgium. Science of the Total Environment, 26(2), 163–172. https://doi.org/10.1016/0048-9697(83)90109-2

Rom, M., Berger, D., Teltsch, B., & Markel, D. (2014). Material Loads from the Jordan River BT - Lake Kinneret: Ecology and Management. In T. Zohary, A. Sukenik, T. Berman, & A. Nishri (Eds.) (pp. 309–327). Dordrecht: Springer Netherlands. https://doi.org/10.1007/978-94-017-8944-8_18

Ross, H. B. (1984). Atmospheric selenium. atse.

Ross, H. B. (1985). An atmospheric selenium budget for the region 30° N to 90° N. Tellus B, 37B(2), 78–90. https://doi.org/10.1111/j.1600-0889.1985.tb00057.x

Roulier, M., Bueno, M., Coppin, F., Nicolas, M., Thiry, Y., Rigal, F., … Pannier, F. (2020, submitted). Atmospheric iodine, selenium and caesium wet depositions in France: spatial and seasonal variations.

Rovira, M., Giménez, J., Martínez, M., Martínez-Lladó, X., de Pablo, J., Marti, V., & Duro, L. (2008). Sorption of selenium (IV) and selenium (VI) onto natural iron oxides: goethite and hematite.

Journal of Hazardous Materials, 150(2), 279–284. https://doi.org/10.1016/j.jhazmat.2007.04.098

Rubinskaya, T. B., Kovaleva, S. V, Kulagin, E. M., & Gladyshev, V. P. (2003). Determination of selenium (IV) by stripping voltammetry at a mercury-film electrode. Journal of Analytical Chemistry, 58(2), 165–170. https://doi.org/10.1023/A:1022314323176

Saeki, K., Matsumoto, S., & Tatsukawa, R. (1995). Selenite adsorption by manganese oxides. Soil science, 160(4), 265-272.

Santos, S., Ungureanu, G., Boaventura, R., & Botelho, C. (2015). Selenium contaminated waters: An overview of analytical methods, treatment options and recent advances in sorption methods. Science of the Total Environment, 521–522(1), 246–260. https://doi.org/10.1016/j.scitotenv.2015.03.107

Saygi, K. O., Melek, E., Tuzen, M., & Soylak, M. (2006). Speciation of selenium(IV) and selenium(VI) in environmental samples by the combination of graphite furnace atomic absorption spectrometric determination and solid phase extraction on Diaion HP-2MG. Talanta, 71(3), 1375–1381. https://doi.org/10.1016/j.talanta.2006.07.008

Schroeder, R. A., Orem, W. H., & Kharaka, Y. K. (2002). Chemical evolution of the Salton Sea, California: nutrient and selenium dynamics BT - The Salton Sea: Proceedings of the Salton Sea Symposium, held in Desert Hot Springs, California, 13–14 January 2000. In D. A. Barnum, J. F. Elder, D. Stephens, & M. Friend (Eds.) (pp. 23–45). Dordrecht: Springer Netherlands. https://doi.org/10.1007/978-94-017-3459-2_2

OmniPac PAX-100 and PAX-500 Product Manual Scientific, T. (n.d.). Retrieved from https://www.thermofisher.com/. Last access: November 09, 2020.

Séby, F., Giffaut, E., & Donard, O. F. X. (1998). Review Assessing the speciation and the biogeochemical processes affecting the mobility of selenium from a geological repository of radioactive wastes to the biosphere, 193–198. https://doi.org/10.1051/analusis:1998134

Séby, F., Potin-Gautier, M., Giffaut, E., Borge, G., & Donard, O. F. X. (2001). A critical review of thermodynamic data for selenium species at 25 C. Chemical Geology, 171(3-4), 173-194. https://doi.org/10.1016/S0009-2541(00)00246-1

Sela-Adler, M., Said-Ahmad, W., Sivan, O., Eckert, W., Kiene, R. P., & Amrani, A. (2016). Isotopic evidence for the origin of dimethylsulfide and dimethylsulfoniopropionate-like compounds in a warm, monomictic freshwater lake. Environmental Chemistry, 13(2), 340–351. https://doi.org/10.1071/EN15042

Seyler, P., & Martin, J. M. (1991). Arsenic and selenium in a pristine river-estuarine system: the Krka (Yugoslavia). Marine Chemistry, 34(1–2), 137–151. https://doi.org/10.1016/0304-4203(91)90018-R

Shahid, M., Khan, N., & Khalid, S. (2018). A critical review of selenium biogeochemical behavior in soil-plant system with an inference to human health. Environmental Pollution, 234, 915–934. https://doi.org/10.1016/j.envpol.2017.12.019

Shaked, Y., Erel, Y., & Sukenik, A. (2004). The biogeochemical cycle of iron and associated elements in Lake Kinneret. Geochimica et Cosmochimica Acta, 68(7), 1439–1451. https://doi.org/https://doi.org/10.1016/j.gca.2003.09.018

Sharma, V. K., McDonald, T. J., Sohn, M., Anquandah, G. A. K., Pettine, M., & Zboril, R. (2014). Biogeochemistry of selenium. A review. Environmental Chemistry Letters, 13(1), 49–58. https://doi.org/10.1007/s10311-014-0487-x

Sherrard, J. C., Hunter, K. A., & Boyd, P. W. (2004). Selenium speciation in subantarctic and subtropical waters east of New Zealand: Trends and temporal variations. Deep-Sea Research Part I: Oceanographic Research Papers, 51(3), 491–506. https://doi.org/10.1016/j.dsr.2003.11.001

Simmons, D. B. D., & Wallschläger, D. (2005). A critical review of the biogeochemistry and ecotoxicology of selenium in lotic and lentic environments. Environmental Toxicology and Chemistry, 24(6), 1331–1343. https://doi.org/10.1897/04-176R.1

Simmons, D. B. D., & Wallschläger, D. (2011). Release of reduced inorganic selenium species into waters by the green fresh water algae chlorella vulgaris. Environmental Science and Technology, 45(6), 2165–2171. https://doi.org/10.1021/es103337p

Söderlund, M., Virkanen, J., Holgersson, S., & Lehto, J. (2016). Sorption and speciation of selenium in boreal forest soil. Journal of Environmental Radioactivity, 164, 220–231. https://doi.org/10.1016/j.jenvrad.2016.08.006

Stará, V., & Kopanica, M. (1988). Cathodic stripping voltammetry and adsorptive stripping voltammetry of selenium (IV). Analytica Chimica Acta, 208, 231–236. https://doi.org/10.1016/S0003-2670(00)80750-3

Stewart, A. R., Luoma, S. N., Elrick, K. A., Carter, J. L., & Van Der Wegen, M. (2013). Influence of estuarine processes on spatiotemporal variation in bioavailable selenium. Marine Ecology Progress Series, 492, 41–56. https://doi.org/10.3354/meps10503

Stripeikis, J., Pedro, J., Bonivardi, A., & Tudino, M. (2004). Determination of selenite and selenate in drinking water: a fully automatic on-line separation/pre-concentration system coupled to electrothermal atomic spectrometry with permanent chemical modifiers. Analytica Chimica Acta, 502(1), 99–105. https://doi.org/10.1016/j.aca.2003.09.022

Suess, E., Aemisegger, F., Sonke, J. E., Sprenger, M., Wernli, H., & Winkel, L. H. E. (2019). Marine versus Continental Sources of Iodine and Selenium in Rainfall at Two European High-Altitude Locations. Environmental Science and Technology, 53(4), 1905–1917. https://doi.org/10.1021/acs.est.8b05533

Sukenik, A., Zohary, T., & Markel, D. (2014). The monitoring program. In Lake Kinneret (pp. 561–575). Springer.

Suzuki, Y., Sugimura, Y., & Miyake, Y. (1981). The content of selenium and its chemical form in rain water and aerosol in Tokyo. Journal of the Meteorological Society of Japan. Ser. II, 59(3), 405–409. https://doi.org/10.2151/jmsj1965.59.3_405

Takayanagi, K., & Wong, G. T. F. (1984). Total selenium and selenium (IV) in the James River estuary and southern Chesapeake Bay. Estuarine, Coastal and Shelf Science, 18(1), 113–119. https://doi.org/10.1016/0272-7714(84)90010-6

Tanzer, D., & Heumann, K. G. (1991). Determination of Dissolved Selenium Species in Environmental Water Samples Using Isotope Dilution Mass Spectrometry. Analytical Chemistry, 63(18), 1984–1989. https://doi.org/10.1021/ac00018a016

Tao, G.-H., & Sturgeon, R. E. (1999). Sample nebulization for minimization of transition metal interferences with selenium hydride generation ICP-AES. Spectrochimica Acta Part B: Atomic Spectroscopy, 54(3–4), 481–489. https://doi.org/10.1016/S0584-8547(99)00003-8

Tessier, E., Amouroux, D., Abril, G., Lemaire, E., & Donard, O. F. X. (2002). Formation and volatilisation of alkyl-iodides and -selenides in macrotidal estuaries. Biogeochemistry, 59(1–2), 183–206. https://doi.org/10.1023/A:1015550931365

Tessier, E., Amouroux, D., & Donard, O. F. X. (2002). Biogenic volatilization of trace elements from European estuaries. Biogeochemistry of Environmentally Important Trace Elements, 835(October 2002), 151–165. https://doi.org/10.1021/bk-2003-0835.ch012

Thomas, C., Jakubowski, N., Stuewer, D., Klockowa, D., Emons, H., Klockow, D., & Emons, H. (1998). Speciation of organic selenium compounds by reversed-phase liquid chromatography and inductively coupled plasma mass spectrometry. Part I. Sector field instrument with low mass resolution. Journal of Analytical Atomic Spectrometry, 13(11), 1221–1226. https://doi.org/10.1039/a804349c

Thomas, R. (2013). Practical guide to ICP-MS: a tutorial for beginners. CRC press.

Thompson-Eagle, E. T., & Frankenberger, W. T. (1991). Selenium biomethylation in an Alkaline, saline environment. Water Research, 25(2), 231–240. https://doi.org/10.1016/0043-1354(91)90034-N. https://doi.org/10.1016/0043-1354(91)90034-N

Thompson-Eagle, E. T., Frankenberger, W. T., & Karlson, U. (1989). Volatilization of selenium by Alternaria alternata. Appl. Environ. Microbiol., 55(6), 1406–1413.

Tolu, J. (2012). Spéciation et mobilité du sélénium présent dans les sols à l'état de traces : contribution aux prévisions à long terme. Thèse de l'Université de Pau et Des Pays de l'Adour.

Trofast, J. (2011). The News Magazine of the International Union of Pure and Applied Chemistry (IUPAC). Chemistry International, 33(5). https://doi.org/10.1515/ci.2011.33.5.16

Di Tullo, P. (2015). Dynamique du cycle biogéochimique du sélénium en écosystèmes terrestres : réactivité dans les sols, rôle de la végétation. Thèse de l'Université de Pau et Des Pays de l'Adour.

Tuttle, M. L. W., Fahy, J. W., Elliott, J. G., Grauch, R. I., & Stillings, L. L. (2014). Contaminants from Cretaceous black shale: I. Natural weathering processes controlling contaminant cycling in Mancos Shale, southwestern United States, with emphasis on salinity and selenium. Applied Geochemistry, 46, 57–71. https://doi.org/https://doi.org/10.1016/j.apgeochem.2013.12.010

Tuzen, M., Saygi, K. O., & Soylak, M. (2006). Separation and speciation of selenium in food and water samples by the combination of magnesium hydroxide coprecipitation-graphite furnace atomic absorption spectrometric determination. Talanta, 71(1), 424–429. https://doi.org/10.1016/j.talanta.2006.04.016

Tyson, J. F., & Palmer, C. D. (2009). Simultaneous detection of selenium by atomic fluorescence and sulfur by molecular emission by flow-injection hydride generation with on-line reduction for the determination of selenate, sulfate and sulfite. Analytica Chimica Acta, 652(1), 251–258. https://doi.org/https://doi.org/10.1016/j.aca.2009.07.002

Uchida, H., Shimoishi, Y., & Toei, K. (1980). Gas chromatographic determination of selenium(-II, 0), -(IV), and -(VI) in natural waters. Environmental Science and Technology, 14(5), 541–544. https://doi.org/10.1021/es60165a007

Van Ael, E., Blust, R., & Bervoets, L. (2017). Metals in the Scheldt estuary: From environmental concentrations to bioaccumulation. Environmental Pollution, 228, 82–91. https://doi.org/https://doi.org/10.1016/j.envpol.2017.05.028

Van Lith, J. G. J. (1968). Geology of the Spanish part of the Gavarnie Nappe (Pyrenees) and its underlying sediments near Bielsa (Province of Huesca) (Vol. 10, pp. 1-64). Utrecht University.

Velinsky, D. J., & Cutter, G. A. (1990). Determination of elemental selenium and pyrite-selenium in sediments. Analytica Chimica Acta, 235, 419–425. https://doi.org/10.1016/S0003-2670(00)82102-9

Velinsky, D. J., & Cutter, G. A. (1991). Geochemistry of selenium in a coastal salt marsh. Geochimica et Cosmochimica Acta, 55(1), 179–191. https://doi.org/10.1016/0016-7037(91)90410-7

Veloso, S. (2020, thèse in preparation). Impact des micropolluants sur les communautés microbiennes en milieu estuarien. Université de Pau et Pays de l'Adour.

VillaRomero, J. F., Kausch, M., & Pallud, C. (2013). Selenate reduction and adsorption in littoral sediments from a hypersaline California lake, the Salton Sea. Hydrobiologia, 709(1), 129–142. https://doi.org/10.1007/s10750-013-1443-7

Vriens, B., Ammann, A. A., Hagendorfer, H., Lenz, M., Berg, M., & Winkel, L. H. E. (2014). Quantification of methylated selenium, sulfur, and arsenic in the environment. PLoS ONE, 9(7). https://doi.org/10.1371/journal.pone.0102906

Vriens, B., Behra, R., Voegelin, A., Zupanic, A., & Winkel, L. H. E. (2016). Selenium Uptake and Methylation by the Microalga Chlamydomonas reinhardtii. Environmental Science & Technology, 50(2), 711–720. https://doi.org/10.1021/acs.est.5b04169

Vriens, B., Lenz, M., Charlet, L., Berg, M., & Winkel, L. H. E. (2014). Natural wetland emissions of methylated trace elements. Nature Communications, 5, 3035. https://doi.org/10.1038/ncomms4035

Wallschläger, D., & Bloom, N. S. (2001). Determination of selenite, selenate and selenocyanate in waters by ion chromatography-hydride generation-atomic fluorescence spectrometry (IC-HG-AFS). Journal of Analytical Atomic Spectrometry, 16(11), 1322–1328. https://doi.org/10.1039/B103108M

Wallschläger, D., & Feldmann, J. (2010). Formation, occurrence, significance, and analysis of organoselenium and organotellurium compounds in the environment. Met Ions Life Sci, 7, 319–364. https://doi.org/10.1039/BK9781847551771-00319

Wallschläger, D., & London, J. (2004). Determination of inorganic selenium species in rain and sea waters by anion exchange chromatography-hydride generation-inductively-coupled plasma-dynamic reaction cell-mass spectrometry (AEC-HG-ICP-DRC-MS). Journal of Analytical Atomic Spectrometry, 19(9), 1119–1127. https://doi.org/10.1039/B401616E

Wang, D., Alfthan, G., & Aro, A. (1994). Determination of Total Selenium and Dissolved Selenium Species in Natural Waters by Fluorometry. Environmental Science and Technology, 28(3), 383–387. https://doi.org/10.1021/es00052a007

Wang, D., Alfthan, G., Aro, A., Lahermo, P., & Väänänen, P. (1994). The impact of selenium fertilisation on the distribution of selenium in rivers in Finland. Agriculture, Ecosystems and Environment, 50(2), 133–149. https://doi.org/10.1016/0167-8809(94)90132-5

Wang, D., Alfthan, G., Aro, A., Mäkelä, A., Knuuttila, S., & Hammar, T. (1995). The impact of selenium supplemented fertilization on selenium in lake ecosystems in Finland. Agriculture, Ecosystems and Environment, 54(1–2), 137–148. https://doi.org/10.1016/0167-8809(94)00574-X

Wang, D., Alfthan, G., Aro, A., & Soveri, J. (1993). Anthropogenic emissions of Se in Finland. Applied Geochemistry, 8, 87–93. https://doi.org/10.1016/S0883-2927(09)80017-6

Wang, Q., Liang, J., Qiu, J., & Huang, B. (2004). Online pre-reduction of selenium(vi) with a newly designed UV/TiO2 photocatalysis reduction device. Journal of Analytical Atomic Spectrometry, 19(6), 715–716. https://doi.org/10.1039/B403129F

Wang, Z., Gao, Y.-X. X., & Belzile, N. (2001). Microwave Digestion of Environmental and Natural Waters for Selenium Speciation. Analytical Chemistry, 73(19), 4711–4716. https://doi.org/10.1021/ac010330h

Wang, Z., & Gao, Y. (2001). Biogeochemical cycling of selenium in Chinese environments. Applied Geochemistry, 16(11–12), 1345–1351. https://doi.org/10.1016/S0883-2927(01)00046-4

Weeks, M. E. (1932). The Discovery of the Elements. VI. tellurium and Selenium. Journal of Chemical Education, 474–485. https://doi.org/10.1021/ed009p474

Wen, H., & Carignan, J. (2007). Reviews on atmospheric selenium: Emissions, speciation and fate. Atmospheric Environment, 41(34), 7151–7165. https://doi.org/10.1016/j.atmosenv.2007.07.035

Weres, O., Bowman, H. R., Goldstein, A., Smith, E. C., Tsao, L., & Harnden, W. (1990). The effect of nitrate and organic matter upon mobility of selenium in groundwater and in a water treatment process. Water, Air, and Soil Pollution, 49(3), 251–272. https://doi.org/10.1007/BF00507068

Weres, O., Jaouni, A.-R. A.-R., & Tsao, L. (1989). The distribution , speciation and geochemical cycling of selenium in a sedimentary environment, Keterston Reservoir, California U.S.A. Sciences-New York, 4(6), 543–563. https://doi.org/10.1016/0883-2927(89)90066-8

White, A. F., Benson, S. M., Yee, A. W., Wollenberg Jr., H. A., & Flexser, S. (1991). Groundwater contamination at the Kesterson Reservoir, California: 2. Geochemical parameters influencing selenium mobility. Water Resources Research, 27(6), 1085–1098. https://doi.org/10.1029/91WR00264

Winkel, L. H. E. E., Johnson, C. A., Lenz, M., Grundl, T., Leupin, O. X., Amini, M., & Charlet, L. (2012). Environmental selenium research: From microscopic processes to global understanding. Environmental Science and Technology, 46(2), 571–579. https://doi.org/10.1021/es203434d

Woittiez, J., & Nieuwendijk, B. (1987). Analysis of selenium in environmental and biological samples by neutron activation. Journal of Radioanalytical and Nuclear Chemistry, 110(2), 603–611. https://doi.org/10.1007/bf02035549

World Health Organization. (2011). Selenium in Drinking-water Background. WHO Press, 2, 7. https://doi.org/WHO/HSE/WSH/10.01/14

Wrench, J. J., & Measures, C. I. (1982). Temporal variations in dissolved selenium in a coastal ecosystem. Nature, 299(5882), 431–433. https://doi.org/10.1038/299431a0

Wu, X., Song, J., Wu, B., Li, T., & Li, X. (2014). Geochemical processes controlling dissolved selenium in the Changjiang (Yangtze) Estuary and its adjacent waters. Acta Oceanologica Sinica, 33(10), 19–29. https://doi.org/10.1007/s13131-014-0537-z

Yacobi, Y. Z., Erez, J., & Hadas, O. (2014). Lake Kinneret. In Lake Kinneret, Ecology and Management (pp. 417–437). Springer Science+Business Media Dordrecht. https://doi.org/10.1007/978-94-017-8944-8

YanardaĞ, R., & Orak, H. (2001). Total selenium concentration in various waters of turkey. Environmental Technology (United Kingdom), 22(2), 237–246. https://doi.org/10.1080/09593332208618303

Yang, G., Zhou, R., Yin, S., Gu, L., Yan, B., Liu, Y., & Li, X. (1989). Studies of safe maximal daily dietary selenium intake in a seleniferous area in China. I. Selenium intake and tissue selenium levels of the inhabitants. Journal of Trace Elements and Electrolytes in Health and Disease, 3(2), 77–87.

Yang, J., Conver, T. S., & Koropchak, J. A. (1996). Direct speciation of selenite and selenate with thermospray sample introduction methods. Analytical Chemistry, 68(22), 4064–4071. https://doi.org/10.1021/ac960610a

Yao, Q. Z., & Zhang, J. (2005). The behavior of dissolved inorganic selenium in the Bohai Sea. Estuarine, Coastal and Shelf Science, 63(1–2), 333–347. https://doi.org/10.1016/j.ecss.2004.12.004

Yao, Q. Z., Zhang, J., Qin, X. G., Xiong, H., & Dong, L. X. (2006). The behavior of selenium and arsenic in the Zhujiang (Pearl River) Estuary, South China Sea. Estuarine, Coastal and Shelf Science, 67(1–2), 170–180. https://doi.org/10.1016/j.ecss.2005.11.012

Yee, H. S., Measures, C. I., & Edmond, J. M. (1987). Selenium in the tributaries of the Orinoco in Venezuela. Nature, 326(6114), 686–689. https://doi.org/10.1038/326686a0

Zhang, H., Feng, X., & Larssen, T. (2014). Selenium speciation, distribution, and transport in a river catchment affected by mercury mining and smelting in Wanshan, China. Applied Geochemistry, 40, 1–10. https://doi.org/10.1016/j.apgeochem.2013.10.016

Zhang, Moore, J. N., & Frankenberger, W. T. (1999). Speciation of Soluble Selenium in Agricultural Drainage Waters and Aqueous Soil-Sediment Extracts Using Hydride Generation Atomic Absorption Spectrometry. Environmental Science & Technology, 33(10), 1652–1656. https://doi.org/10.1021/es9808649

Zhang, Y., Zahir, Z. A., & Frankenberger, W. T. (2004). Fate of Colloidal-Particulate Elemental Selenium in Aquatic Systems. Journal of Environmental Quality, 33, 559–564. https://doi.org/10.2134/jeq2004.5590

Zheng, C., Wu, L., Ma, Q., Lv, Y., & Hou, X. (2008). Temperature and nano-TiO2 controlled photochemical vapor generation for inorganic selenium speciation analysis by AFS or ICP-MS without chromatographic separation. Journal of Analytical Atomic Spectrometry, 23(4), 514–520. https://doi.org/10.1039/B713651J

Zohary, T. (2004). Changes to the phytoplankton assemblage of Lake Kinneret after decades of a predictable, repetitive pattern. Freshwater Biology, 49(10), 1355–1371. https://doi.org/10.1111/j.1365-2427.2004.01271.x

Zohary, T., Yacobi, Y. Z., Alster, A., Fishbein, T., Lippman, S., & Tibor, G. (2014). Lake Kinneret. Lake Kinneret, 6, 161–190. https://doi.org/10.1007/978-94-017-8944-8

Zwart, H. J., & De Sitter, L. U. (1979). The geology of the Central Pyrenees.